Aus dem Bereich Physiologie
Theoretische Medizin und Biowissenschaften
der Medizinischen Fakultät
der Universität des Saarlandes, Homburg/Saar

INNATE AND GLIAL CELLS ORCHESTRATE MYELIN INJURY AND REPAIR IN LPC-INDUCED DEMYELINATION MOUSE MODEL *IN VIVO*

Dissertation

zur Erlangung des Grades eines Doktors der Naturwissenschaften

der Medizinischen Fakultät
der UNIVERSITÄT DES SAARLANDES

2024

vorgelegt von: Emeline Lydie Buttigieg

geb. am: 08.03.1992 in Aix-en-Provence, France

Date of oral examination: 20.12.2024

Dean of the faculty: **Univ.-Prof. Dr. med. Matthias Hannig**

Examinants: **Prof. Dr. Frank Kirchhoff -** University of Saarland

Dr. Franck Debarbieux - University of Aix-Marseille

This project has received funding from the ARSEP foundation, grant agreement No 1248.

Eidesstattliche Erklärung

Ich erkläre hiermit an Eides statt, dass ich die vorliegende Arbeit ohne unzulässige Hilfe Dritter und ohne Benutzung anderer als der angegebenen Hilfsmittel angefertigt habe; die aus anderen Quellen direkt oder indirekt übernommenen Daten und Konzepte sind unter Angabe des Literaturzitats gekennzeichnet.
Bei der Auswahl und Auswertung folgenden Materials haben mir die nachstehend aufgeführten Personen in der jeweils beschriebenen Weise entgeltlich/unentgeltlich geholfen:

Vor- und Nachname: **Dr. Bilal El Waly** ☐ entgeltlich ■ unentgeltlich
Beitrag: **Zwei-Photonen-Bildgebung, zelluläre Quantifizierung, FACS-Sortierung und qRT-PCR (Figures 13A-B; 15; 16; 18F)**
Vor- und Nachname: **Guo Qilin** ☐ entgeltlich ■ unentgeltlich
Beitrag: **Partielle Extraktion von Ribotag-RNA zur Sequenzierung von OPCs**
Vor- und Nachname: **Dr. Scheller Anja** ☐ entgeltlich ■ unentgeltlich
Beitrag: **AxioScan.Z1 Epifluoreszenzmikroskopbetrieb**
Vor- und Nachname: **Dr. Thomas Hentrich** ☐ entgeltlich ■ unentgeltlich
Beitrag: **Bioinformatische Analyse von RiboTag-RNA-Sequenzierungsdaten (Figures 21; 22; 23; 25; 26A-D; 27; 28)**
Vor- und Nachname: **Novogene Company** ■ entgeltlich ☐ unentgeltlich
Beitrag: **Sequenzierung von Ribotag-RNA (RNA-Qualität, Bibliotheksvorbereitung und Sequenzierung)**

Weitere Personen waren an der inhaltlich-materiellen Herstellung der vorliegenden Arbeit nicht beteiligt. Insbesondere habe ich hierfür nicht die entgeltliche Hilfe eines Promotionsberaters oder anderer Personen in Anspruch genommen. Niemand hat von mir weder unmittelbar noch mittelbar geldwerte Leistungen für Arbeiten erhalten, die im Zusammenhang mit dem Inhalt der vorgelegten Dissertation stehen.
Die Arbeit wurde bisher weder im In- noch im Ausland in gleicher oder ähnlicher Form einer anderen Prüfungsbehörde vorgelegt.
Ich versichere an Eides Statt, dass ich nach bestem Wissen die reine Wahrheit gesagt und nichts verschwiegen habe.
Die Bedeutung der eidesstattlichen Erklärung und die strafrechtlichen Folgen einer unrichtigen oder unvollständigen eidesstattlichen Erklärung sind mir bekannt.

Ort, Datum

Unterschrift der/des Promovierenden

A mon fils,

TABLE OF CONTENTS

List of Abbreviation

$[Ca^{2+}]_i$	intracellular calcium concentration
20-HETE	20-hydroxyeicosatetraenoic acid
2P-LSM	two-photon laser scanning microscopy
AMPA	α-amino-3-hydroxy-5-methyl-4-isoxazolepropionic acid
anti-I	anti-inflammatory
APC	antigen-presenting cell
ApoE	apolipoprotein E
Arg1	arginase 1
Ascl1	Achaete scute homolog 1
BAFF	B cell activating factor
BBB	blood-brain barrier
BDNF	brain-derived neurotrophic factor
bFGF	basic fibroblast growth factor
BMP	bone morphogenetic protein
bp	base pair
BP	biological process
BSA	bovine serum albumin
C3	complement 3
CARS	Coherent Anti Stoke Raman Scattering
CC	cellular component
CDK	cyclin dependent kinase
cDNA	complementary DNA
CFP	cyan fluorescent protein
CNS	central nervous system
CPZ	cuprizone
CR3	complement receptor-3
Cre	Cre-DNA recombinase
CSF1	colony stimulating factor 1
CSF1R	colony stimulating factor 1 receptor
CSPG	chondroitin sulfate proteoglycans
CTL	control
CX_3CR_1	fractalkine receptor
CXC4	chemokine receptor 4
D	day post LPC-incubation
DAPI	4′,6-diamidino-2-phenylindole
DE	differential expression
DEG	differential gene expression
DNA	deoxyribonucleic acid
DTT	DL-Dithiothreitol
EAE	experimental allergic encephalomyelitis
ECM	extracellular matrix
EDTA	ethylendiamintetraacetic acid
EGFP	enhanced green fluorescent protein
FA	Formaldehyde
FAs	fatty acids
FACS	fluorescence-activated cell sorting
FC	fold change
FGF	fibroblast growth factor
GABA	gamma-aminobutyric acid
Gal-3	Galectin-3
GO	gene onthology
HA	hemagglutinin
HA-tag	hemagglutinin tag
hGFAP	human glial fibrillary acidic protein
HIFα	hypoxia inducible factor alpha
HS	horse serum
IFN	interferon
IFN-β	interferon beta
IHC	immunohistochemical

iNOS	inducible nitric oxide synthase
IP	immunoprecipitated
kb	kilobase
KEGG	kyoto encyclopedia of genes and genomes
LPC	L-α, lysophosphatidylcholine,
MAPK	mitogen-activated protein kinase
MBP	myelin basic protein
MCM	mini chromosome maintenance
MCT	monocarboxylate transporters
MDM	monocyte-derived macrophage
MF	molecular function
MHC	major histocompatibility complex
MMP	metalloproteinase
moDC	monocyte-derived dendritic cells
mOL	myelinating oligodendrocyte
mRNA	messenger ribonucleic acid
MS	multiple sclerosis
Nav	voltage-gated sodium channel
ncRNA	noncoding RNA
NCS	neural stem cell
NFIA	nuclear factor-I A
NG2	nerve/glia antigen-2
NGF	nerve growth factor
NGS	next-generation sequencing
NK	natural killer
NMDA	N-methyl-D-aspartate
NO	nitric oxid
NPC	neural progenitor cell
nRPKM	normalized Reads Per Kilobase per Million mapped reads
OL	oligodendrocyte
OPC	oligodendrocyte precursor cell
PBS	phosphate-buffered saline
PCA	principal component analysis
PCR	polymerase chain reaction
PDGFRα	platelet derived growth factor receptor α
PFA	Paraformaldehyde
PLP	proteolipid protein
PNS	peripheral nervous system
pro-I	pro-inflammatory
NCAM	polysialylated neural cell adhesion molecule
RiboTag	ribosomal Tagging
RIN	RNA Integrity Number
RNA	ribonucleic acid
RNAseq	mRNA sequencing
ROI	region of interest
ROS	reactive oxygen species
RT	room temperature
SC	spinal cord
scRNAseq	single cell mRNA sequencing
SMRT	single-molecule real-time
TAE	tris-Acetate-EDTA buffer
TCA	tricarboxylic acid cycle
TDCPP	tris (1,3-dichloro-2-propyl) phosphate
TF	transcription factor
TMEM	Theiler's murine encephalomyelitis
Treg	regulatory T cell
TrkB	tropomyosin receptor kinase B
TSP	thrombospondins
VCAM	vascular adhesion molecule
VEGF	vascular endothelial growth factor
VOI	volume of interest
VZ	ventricular zone
YFP	yellow fluorescent protein

List of Figures

List of Tables

1. ABSTRACT

Myelination of axons by mature oligodendrocytes (OLs) enables saltatory conduction and provides trophic support to maintain axonal integrity. The loss of myelin sheath observed in multiple sclerosis (MS) trigger microglia and astroglial cell activation, thereby releasing pro- and anti-inflammatory factor or signal modulating cell responses, and participating in myelin and cellular debris removal. Thus, glial cells regulate the fate of OL lineage by influencing the survival of myelinating OLs or promoting remyelination by oligodendrocyte precursor cells (OPCs). Hence, we investigated glial dynamics, signaling, and cross-talk during de- and remyelination using the lysophosphatidylcholine (LPC)-induced demyelination model in the dorsal mouse spinal cord. To this end, we combined *in vivo* longitudinal two-photon and CARS microscopies, as well as histopathological and qR-PCR analysis. Furthermore, we performed RNA sequencing using cell-specific RiboTag expression in OPCs, microglia and astrocytes to decipher their transcriptomic gene profiles.

LPC triggered rapid myelin loss through its action on mOLs following time-dependent breakdown cellular patterns, with concomitant axonal degeneration. In parallel, we observed the transient recruitment of $CD11c^+$ microglia to the lesion site, while $GFAP^+$ astrocytes were secondary recruited and sustained until complete remyelination. Conversely, $LysM^+$ innate immune cells invaded the spinal tissue in two distinct waves. Furthermore, while both microglia and infiltrating immune cells exhibited pro-inflammatory polarization consistent with the loss of OLs, the induction of anti-inflammatory microglia likely induced similar phenotypic shift in immune cells during remyelination and axon repair. Additionally, the transcriptomic analysis of glial cells revealed that OPCs, microglia, and astrocytes were rapidly proliferating in response demyelination. Moreover, OPCs seemed to engage differentiation and maturation in late demyelination while preventing axonal degeneration. In contrast, microglia behaved as antigen-presenting cells to recruit immune cells, whereas its phagocytic and lysosomal activities, as well as anti-inflammatory gene expression later supported efficient remyelination. Astroglia immediately after LPC prevented excitotoxicity by enhancing buffering functions, ensuring neurotransmission continuity. They as well exhibited a balanced inflammatory polarization, alternately promoting neuroinflammation or remyelination and CNS repair. Finally, we identified genes suggesting glial intercommunication and signaling highlighting their reciprocal regulation in de-and remyelination, in addition to their close commitment to the neuronal compartment during the whole process.

In conclusion, these data demonstrate the complexity of cellular dynamics underlying myelin injury, where de- and remyelination trigger an intricate combination of time-dependent, coordinated glial, immune, and neuronal signaling. Moreover, understanding each genetic cell activation cascade could pave the way for new therapeutic perspectives.

2. RESUME

La myélinisation des axones par les oligodendrocytes matures (mOLs) permet la conduction saltatoire et fournit un soutien trophique pour maintenir l'intégrité axonale. L'altération de la gaine myéline observée dans la Sclérose en Plaques (SEP) déclenche l'activation de la microglie et des astrocytes, libérant ainsi des facteurs pro- et anti-inflammatoires ou des signaux modulant les réponses cellulaires, et participant à l'élimination des débris cellulaires et myéliniques. Ainsi, les cellules gliales peuvent orienter le destin de la lignée oligodendrocytaire en influençant la survie des OL myélinisants, ou en favorisant la remyélinisation par les cellules progénitrice des oligodendrocytes (OPCs). De ce fait, nous avons étudié la dynamique gliale, leurs signalisations et communications durant la dé- et la remyélinisation dans un modèle de démyélinisation induite par la lysophosphatidylcholine (LPC) dans la moelle épinière dorsale de souris. Pour ce faire, nous avons combiné l'imagerie chronique biphotonique et CARS *in vivo*, et établi des analyses histopathologique et qRT-PCR. De plus, nous avons réalisé un séquençage d'ARN en utilisant la méthode RiboTag spécifiquement pour les OPCs, les microglies et les astrocytes afin de décrypter leurs expressions génétiques.

Le LPC a rapidement déclenché une lésion de la myéline *via* son action sur les mOLs, dégénérant selon des mécanismes de dégradation cellulaire dépendants du temps et en entrainant une perte axonale concomitante. En parallèle, nous avons observé le recrutement transitoire de la microgliale $CD11c^+$ au site lésionnel, tandis que les astrocytes $GFAP^+$ ont été recrutés secondairement et maintenu jusqu'à la remyélinisation complète. Inversement, les cellules immunitaires innées $LysM^+$ ont envahi le tissu spinal en deux vagues distinctes. De plus, alors que les microglies et les cellules immunitaires infiltrées présentaient une polarisation pro-inflammatoire cohérente avec la perte des mOLs, l'induction de microglies anti-inflammatoires a probablement induit un changement phénotypique similaire dans les cellules immunitaires pendant la remyélinisation et la réparation axonale. Enfin, l'analyse transcriptomique des cellules gliales a révélé que les OPCs, les microglies et les astrocytes proliféraient rapidement en réponse à la démyélinisation. En outre, les OPCs initient leur différenciation et maturation durant la phase tardive de la démyélinisation, tout en freinant la perte axonale. Les microglies, elles, ont démontré une capacité de présentation antigénique afin de recruter les cellules immunitaires périphériques, tandis que leur fonctions phagocytaires et lysosomales ainsi que l'expression de gènes anti-inflammatoires, ont promu une remyélinisation efficace. Immédiatement après le LPC, les astrocytes ont empêché l'excitotoxicité en amplifiant leurs fonctions tampon, assurant ainsi la bonne continuité de la neurotransmission. Ils ont également démontré une polarisation contrastée, promouvant alternativement la neuroinflammation ou la remyélinisation et la réparation du SNC. Enfin, nous avons identifié des gènes suggérant une intercommunication entre cellules gliales, mettant ainsi en évidence une possible régulation

réciproque dans la dé- et remyélinisation, en plus de leur soutient étroit au compartiment neuronal tout au long du processus.

En conclusion, ces données démontrent la complexité des dynamiques cellulaires sous-jacentes aux lésions de la myéline, où la dé- et la remyélinisation déclenchent une combinaison complexe et coordonnée dans le temps des signalisations gliales, immunitaires et neuronales. Enfin, la compréhension des cascades génétiques d'activation cellulaires pourrait ouvrir la voie à de nouvelles perspectives thérapeutiques.

3. ZUSAMMENFASSUNG

Die Myelinisierung von Axonen durch reife Oligodendrozyten (OLs) ermöglicht die saltatorische Erregungsleitung und bietet trophische Unterstützung zur Aufrechterhaltung der axonalen Integrität. Der Verlust der Myelinscheide, wie er bei Multipler Sklerose (MS) beobachtet wird, löst die Aktivierung von Mikroglia und Astrozyten aus, wodurch pro- und anti-inflammatorische Faktoren und/oder Signale freigesetzt werden, die Zellreaktionen modulieren und an der Beseitigung von Myelin- und Zelltrümmern beteiligt sind. Gliazellen regulieren somit das Schicksal der OL-Linie, indem sie das Überleben myelinisierender OLs beeinflussen sowie die Remyelinisierung durch Oligodendrozyten-Vorläuferzellen (OPCs) fördern. Wir haben die Dynamik, Signalgebung und Kommunikation von Gliazellen während der De- und Remyelinisierung mit Hilfe des Lysophosphatidylcholin (LPC)-induzierten Demyelinisierungsmodels im dorsalen Rückenmark der Maus untersucht durch Kombination von in vivo longitudinaler Zwei-Photonen- und CARS-Mikroskopie sowie histopathologischer und qR-PCR-Analysen untersucht. Additive RNA-Sequenzierungen, bei denen zellspezifische RiboTag-Expressionen in OPCs, Mikroglia und Astrozyten verwendet wurden, halfen transkriptionellen Genprofile zu entschlüsseln.

Ein durch LPC ausgelöster Myelinverlust der zeitabhängigen zellulären Abbauprozessen folgte und gleichzeitig mit einer axonalen Degeneration einhergingführte zu vorübergehender Rekrutierung von $CD11c^+$ Mikroglia an die Läsionsstelle, während $GFAP^+$ Astrozyten sekundär rekrutiert wurden und bis zur vollständigen Remyelinisierung erhalten blieben. Im Gegensatz dazu drangen $LysM^+$ angeborene Immunzellen in zwei verschiedenen Wellen in das Rückenmarksgewebe ein. Während sowohl Mikroglia als auch infiltrierende Immunzellen eine proinflammatorische Polarisierung zeigten, die mit dem Verlust von OLs einherging, löste die Induktion von anti-inflammatorischen Mikroglia eine ähnliche phänotypische Verschiebung in den Immunzellen während der Remyelinisierung und der Axonreparatur aus. Zusätzlich zeigte die transkriptionelle Analyse, dass OPCs, Mikroglia und Astrozyten als Reaktion auf die Demyelinisierung schnell proliferierten. Darüber hinaus differenzierten sich OPCs in der späten Phase der Demyelinisierung und reiften, während sie die axonale Degeneration verhinderten. Im Gegensatz dazu verhielten sich Mikroglia als antigen-präsentierende Zellen. Sie rekrutieren Immunzellen, während ihre phagozytischen und lysosomalen Aktivitäten sowie ihre anti-inflammatorische Genexpression später eine effiziente Remyelinisierung unterstützte. Astrocyten verhinderten unmittelbar nach LPC-Behandlung eine Exzitotoxizität durch die Verbesserung der Pufferfunktionen und stellten die Kontinuität der Neurotransmission sicher. Sie zeigten ebenfalls eine ausgewogene entzündliche Polarisierung, die abwechselnd die Neuroinflammation oder die Remyelinisierung und die Reparatur des ZNS förderte. Schließlich identifizierten wir Gene, die auf eine interzelluläre Kommunikation und Signalgebung zwischen Gliazellen hinweisen, was auf ihre gegenseitige Regulierung bei der De- und

Remyelinisierung sowie auf ihr enges Engagement im neuronalen Kompartiment während des gesamten Prozesses hindeutet.

Abschließend zeigen diese Daten die Komplexität der zellulären Dynamiken, die den Myelinschäden zugrunde liegen, wobei De- und Remyelinisierung eine komplizierte Kombination aus zeitabhängigen, koordinierten glialen, immunologischen und neuronalen Signalen auslösen. Darüber hinaus könnte das Verständnis jeder genetischen Zellaktivierungskaskade den Weg für neue therapeutische Perspektiven ebnen.

4. INTRODUCTION

4.1. Glial cells: more than a glue!

The concept of glial cells, also known as glia (derived from the ancient Greek "glía," meaning glue), was initially introduced by Rudolf Virchow in 1846 as the connective structure called "nervenkitt," which was believed to hold nervous tissue together (Somjen, 1988). Since then, our comprehension of glia has significantly evolved, encompassing a large diversity of cells present in both the central and peripheral nervous systems (CNS and PNS). In contrast to neurons, these cells do not generate electrical impulses and are categorized into four major groups: astrocytes (or astroglia), microglia, oligodendrocyte precursor cells (OPCs), and oligodendrocytes (OLs) (Kato et al., 2018).

4.1.1. Oligodendrocyte lineage

4.1.1.1. Oligodendrogenesis in the spinal cord

Oligodendrocytes (OLs) are the myelinating cells in the central nervous system (CNS). They generate from oligodendrocyte precursor cells (OPCs) and follow a highly regulated differentiation program encompassing four stages: proliferative OPCs, pre-OLs, differentiated OLs, and myelinating OLs (Bradl and Lassmann, 2010).

Developmental waves of spinal OPCs. In the developing spinal cord (SC), OPCs originate from neural stem cells (NSCs) and arise in several “waves”: The first wave takes place at embryonic day 12.5 (E12.5) in the ventral ventricular zone (VZ) at the motor neural progenitor (pMN) domain (Timsit et al., 1995; Orentas et al., 1999). By E15.5, a second wave emerges from the transdifferentiation of radial glia cells in the dorsal VZ, contributing to around 10% of the final OL population (Cai et al., 2005; Vallstedt et al., 2005). The third wave appears at post-natal day 0 (P0). Its exact origin remains elusive, but these OPCs might stem from the central canal's progenitor cells or proliferative OPCs within the parenchyma (Rowitch and Kriegstein, 2010) (**Fig. 1A, B**). Interestingly, OPCs population of the whole SC is achieved via their migration along the vasculature through the chemokine receptor 4 (CXCR4), mediating their interactions with endothelial cells (Tsai et al., 2016). However, their detachment from the vessels is timely regulated during development and relies on repulsive cues, including semaphorin 3a/6a expressed by astrocytes (Duncan and Emery, 2023). Around E18.5, the differentiation of OPCs into mature myelinating-OLs (mOLs) begins, peaking between 2 to 4 weeks and lasting up to 8 months after birth (Rivers et al., 2008). Along the maturation process, from OPCs to mOLs, these cells express specific markers. Indeed, OPCs express the proteoglycan NG2, the platelet derived growth factor receptor α (PDGFRα), the transcriptions factors Olig1/2 and Ascl1, while maturing OLs expressed the ectonucleotide

pyrophosphatase/phosphodiesterase 6 (ENPP6) and the 20 ,30 -cyclic-nucleotide 30 -phosphodiesterase (CNPase) (Poduslo and Norton, 1972; Nishiyama et al., 1999; Fancy et al., 2004). mOLs are identifiable based on their expression of myelin related-genes such as myelin basic protein (MBP), myelin regulatory factor (MYRF), and proteolipid protein (PLP) (Sobel et al., 1994; Cahoy et al., 2008) (**Fig. 1B**).

Regulation of oligodendrogenesis in the spinal cord. Oligodendrogenesis in the SC is modulated by extrinsic and intrinsic factors. A pivotal extrinsic factor is Sonic hedgehog (Shh), which is crucial for determining the fate of ventral-derived OPCs (**Fig. 1B**) Shh is expressed at the notochord and the floor plate and induces first the transcription factor Nkx.6 thereby regulating the expression of Olig2 which represses the nuclear factor-I A (NFIA) and the astrocytic fate (Okano and Temple, 2009; Dessaud et al., 2010). Conversely, dorsal-derived OPCs determination is Shh-independent due to concomitant expression of inhibitors such as bone morphogenetic proteins (BMPs) and Wnt/b-catenin (Cai et al., 2005) (**Fig. 1B**). Moreover, laminin from the extra cellular matrix (ECM) enhances OPC survival within the VZ (Relucio et al., 2012). Transcription factors, including Sox8/9 and Achaete scute homolog 1 (Ascl1 or Mash1), also play roles in modulating OL production (Stolt et al., 2003; Sugimori et al., 2008). Recently, epigenetic mechanisms have been highlighted as major contributors to OPCs differentiation. DNA methylation enhances OL differentiation by silencing transcriptional inhibitors while defect in DNA methyltransferases arrest OPCs proliferation (Huang et al., 2011; Moyon et al., 2016; Scaglione et al., 2018). Histone methylation increases during specification time and negatively regulates neuronal fate (Liu et al., 2015). Finally, microRNAs participate OPCs specification by acting on intrinsic and extrinsic transcription factor expression (Fitzpatrick et al., 2015). As an example, miRNA-7a is enriched in OPCs and determine their fate over neuronal progenitors (Zhao et al., 2012).

Unique characteristics of OPCs. Unlike many progenitor cells, OPCs in the adult CNS retain a stable cell density due to their self-renewal capacity, accounting for approximately 5-8% of the CNS's total cell population (Beiter et al., 2022). Their proliferative and differentiation abilities vary based on their location in the CNS. White matter-associated OPCs remain proliferative, supporting adult oligodendrogenesis. Meanwhile, most gray matter-associated OPCs remain immature and quiescent (Dawson et al., 2000; Dimou et al., 2008). Interestingly, the dorso-ventral origin of OPCs during development does not influence their electrical properties. They are functionally equivalent and can replace each other in populating and producing adult mOLs in non-originally assigned SC regions (Kessaris et al., 2006; Tripathi et al., 2011). However, a recent study has shown the coexistence of two transcriptionally distinct adult OPCs population within the homeostatic CNS: clusterin-expressing OPCs and Gpr17-expressing (Beiter et al., 2022). Clusterin potentially directs OPCs towards a phagocytic phenotype during injury due to its ability to amplify phagocytosis (Gaultier et al., 2009).

In contrast, Gpr17 is present in cells proliferating near the lesion site, suggesting its role in rapidly responding to damage (Ceruti et al., 2009; Viganò et al., 2016).

4.1.1.2. OPC's functions within the CNS

One of the main functions of OLs throughout the developing and adult CNS is the myelination. This particular function is addressed in 4.2 chapter.

Vascular implications and immunomodulation. The importance of the BBB in protecting and isolating CNS parenchyma is crucial to prevent pathogenic influences from the circulating blood. OPCs have been reported to support BBB tightness through the secretion of the soluble factor TGF-β1 (Seo et al., 2014) (**Fig. 1B, panel D**). OPCs can interact with pericytes, the major cell type forming the BBB, through the PDGF-BB/PDGFRα signaling to maintain BBB integrity (Kimura et al., 2020). In a mouse model of ischemia, OPCs reduced BBB leakage via increasing the expression of tight junctions-related proteins claudin-5, occludin and β-catenin (Wang et al., 2020). They also take part to angiogenesis through hypoxia inducible factor alpha (HIFα)-activated Wnt, and release of vascular endothelial growth factor (VEGF) (Yuen et al., 2014; Zhang et al., 2020). Recently, adult OLs have been described to participate in vasculature through their association with the endothelial basement membrane and vascular remodeling via the expression of metalloproteinase-9 (MMP9) (Pham et al., 2012; Palhol et al., 2023) (**Fig. 1B, panel D**). The role of OPCs in preventing CNS homeostasis disruptions also involves the immunomodulation of microglia. OPC-derived TGF-β suppresses microglia activation through CX_3CR_1 signaling which promotes their immune patrolling function (Zhang et al., 2019) (**Fig. 1B, panel E**).

Ion homeostasis, neurotransmission, plasticity. Several ions are implicated in the generation and propagation of electrical signals and the release of neurotransmitters, and their homeostasis balance is essential to prevent excitotoxicity. OPCs and OLs control the intracellular concentration of potassium (K^+) through Kir4.1 channels, clearing out the excess of K^+ (Larson et al., 2018) (**Fig. 1B, panel C**). OPCs are actively taking part in neurotransmission through the expression NG2 and FGF2, respectively involved in AMPA receptor-mediated synaptic neurotransmission and glutamatergic neurotransmission (Sakry et al., 2014; Birey et al., 2015) The expression on their postsynaptic membrane of AMPA and NMDA receptors enables to receive glutamatergic signals while $GABA_{A/B}$ receptors mediates GABAergic inputs (Fang and Bai, 2023) (**Fig. 1B, panel A**). OLs can modulate neurotransmitter release at presynaptic terminals by secreting brain-derived neurotrophic factor (BDNF) that acts via tropomyosin receptor kinase B (TrkB) (Jang et al., 2019). OPCs are also involved in the establishment of interneurons during development of brain and SC. The first wave of OPCs regulates their migration through cell-cell contact via the expression of Sema6a/6b interacting with Plxna3 receptors on interneurons. Moreover, OPCs originating from the third developmental

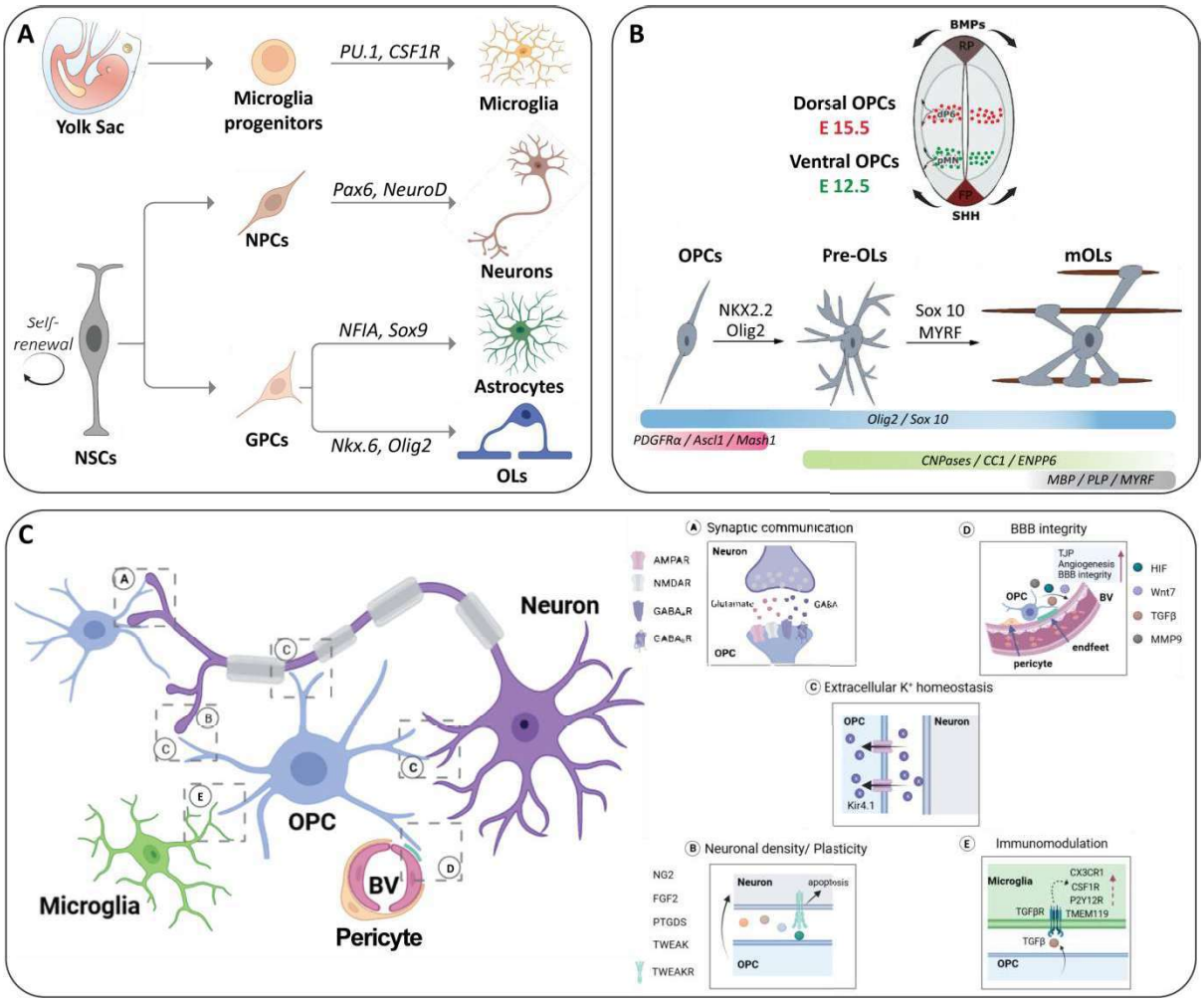

Figure 1. Spinal oligodendrocyte development and homeostatic functions

A. Origin and specification of glial cells within the CNS during embryo development. **B.** In the developing spinal cord, OPCs are generated in two waves, differentiating into immature intermediate cells (Pre-OLs) and subsequently into myelinating oligodendrocytes (mOLs) (*modified from Gacem and Nait-Oumesmar, 2021)*. **C.** Under physiological conditions, OPCs are involved in various functions. They receive neuronal inputs through specific receptors (AMPAR, NMDAR, $GABA_{A/B}R$) (A), regulate neuronal density and plasticity via diverse secreted factors (B), maintain extracellular K^+ homeostasis (C), support the integrity of the BBB (D), and modulate microglial activation through expression of TGF-β (E) (*modified from Fang and Bai, 2023)*. NSCs: Neural Stem Cells; NPCs: Neural Precursor Cells; GPCs: Glial Precursor cells; RP: Roof Plate; FP: Floor Plate.

wave control interneurons apoptosis by releasing TNF-related weak inducer of apoptosis (TWEAK) (Fang and Bai, 2023) (**Fig. 1B, panel B**).

4.1.2. Astrocytes

4.1.2.1. Origins and classification

Spinal astrocytes development. In the developing spinal cord, astrocytogenesis is achieved following four steps: specification, migration, proliferation, and functional maturation of astrocytes. Specification of radial glia progenitor cells to an astrocytic fate is initiated at E12.5 within the VZ (Deneen et al., 2006; Barry et al., 2014) (**Fig. 1A**). This gliogenic competence is acquired through the regulation of the transcription factor NFIA and Sox9 which repress neuronal fate. These specific radial glia-derived progenitor cells divide asymmetrically and constitute the first wave of astrocyte proliferation at E15-17 (Tien et al., 2012; Zarei-Kheirabadi et al., 2020). Lineage tracing studies demonstrated the poor migratory capacity of these embryonic progenitor cells along radial glia processes. At P0-3, a second proliferative wave of transient amplifying progenitors referred to as "intermediate astrocyte progenitors" (IAPs) occur. These cells lack radial glia morphology and depend on BRAF signaling (Tien et al., 2012). The maturation of astrocytes is achieved by four weeks post-nataly and is initiated by astrocytes-astrocytes contacts inhibiting their proliferation (Li et al., 2019). It consists of the acquisition of mature functional and morphological characteristics and relies on BMP and Shh signaling (Scholze et al., 2014; Gingrich et al., 2022). Mature astrocytes have a complex morphology with numerous branches and fine processes whose elaboration requires the involvement of BDNF and FGFR signaling (Kang et al., 2014; Holt et al., 2019). There are several markers expressed by mature spinal astrocytes such as Aldh1l1, GFAP, AldoC, or Aquaporin 4 (Molofsky et al., 2012).

Astrocytes classification and heterogeneity. The primary astrocyte classification relies on their morphology distinction and falls into two categories: protoplasmic or fibrous. Protoplasmic astrocytes express the calcium-binding protein S100b and are found in the grey matter in spatially segregated domains (Bushong et al., 2004; Du et al., 2021) . With their spongiform shape, they arbor a multitude of fine processes found in close contact with synapses forming the "tripartite synapses" and establishing direct vascular contacts (Reichenbach et al., 2010; Hösli et al., 2022). Fibrous astrocytes are distributed throughout the white matter and highly express GFAP (Middeldorp and Hol, 2011). In contrast to protoplasmic, fibrous astrocytes have fewer but longer and thicker processes in close relationship with the axonal compartment (Lundgaard et al., 2014; Verkhratsky et al., 2021). Interestingly, within the SC grey matter exists a subpopulation of Olig2 expressing-astrocytes derived from $Olig2^{+}$ precursor cells in the pMN and promoted by the expression of the heparin sulfate modification enzyme, Sulf2 (Ohayon et al., 2019). Finally, in both white and grey matter of adult SC, single-cell sequencing analysis revealed the existence of intermediate cells expressing neuronal genes such as PDGFRα (Wei et al., 2023).

4.1.2.2. Astroglial functional diversity

Blood Brain Barrier and vascular tone. Astrocytes are key partners of CNS vasculature and contribute to BBB formation and maintenance (**Fig. 2, panel c**). Astroglial end-feet are found in contact with endothelial cells and participate through the release of growth factors such as basic fibroblast growth factor (bFGF), glial cell line-derived neurotrophic factor (GDNF) and VEGF to promote tight junction formation (Cabezas et al, 2014). Astrocytes are in close contact with CNS vasculature and modulate blood flow circulation via secreting factors like prostaglandin E2 (PGE2) (vasodilatation) or 20-hydroxyeicosatetraenoic acid (20-HETE) (vasoconstriction) (MacVicar and Newman, 2015).

Synaptic development and functions. Astrocytes are required for synaptogenesis and support, through the secretion of diffusible molecules such as thrombospondins (TSPs) and the dual secretion of hevin and SPARC protein or cholesterol, and ensure the correct structure development and number of synapses (Christopherson et al., 2005; Kucukdereli et al., 2011) (**Fig. 2, panel f**). Astrocyte-derived cholesterol has been described with together ApoE lipoprotein to increase synaptic transmission as well as the secretion of TNF-α via amplification of the surface AMPAR expression (Mauch et al., 2001; Beattie et al., 2002). Finally, astrocytes can unsilence synapses via releasing glypicans factors (Tan et al., 2021).

CNS homeostasis and neuronal support. Astroglia is involved in the regulation of ionic, water, and neurotransmitter concentration in the extracellular space. Neuronal activity increases the amount of extracellular K^+, which is taken up by astrocytes through specialized channels Kir4.1 to prevent hyper excitability and which is eventually dispersed via gap junction-connected astrocytes (Holthoff and Witte, 2000) (**Fig. 2, panel e**). The amount of water is tightly regulated via the expression of aquaporin 4 channels at the astrocytic endfeet and the excess of water spilled into the perivascular space (Szczygielski et al., 2021) (**Fig. 2, panel e**). Their essential role in neurotransmission has long been documented. The recapture of neurotransmitters in the synaptic cleft is achieved by their expression of dedicated transporters to glutamate (GLAST and GLT-1) or GABA ($GABA_{A/B}R$) to thwart neurotoxic effects. They are both converted into glutamine and cyclically available for neurons to recapture and resynthesize active neurotransmitters (Mahmoud et al., 2019) (**Fig. 2, panel a**). Astrocytes ensure metabolic support to neurons, using the glycolysis to convert their glycogen into lactate, which is provided to neurons as energy substrate at the node of Ranvier (Hirrlinger and Nave, 2014; Kann, 2023) (**Fig. 2, panel d**).

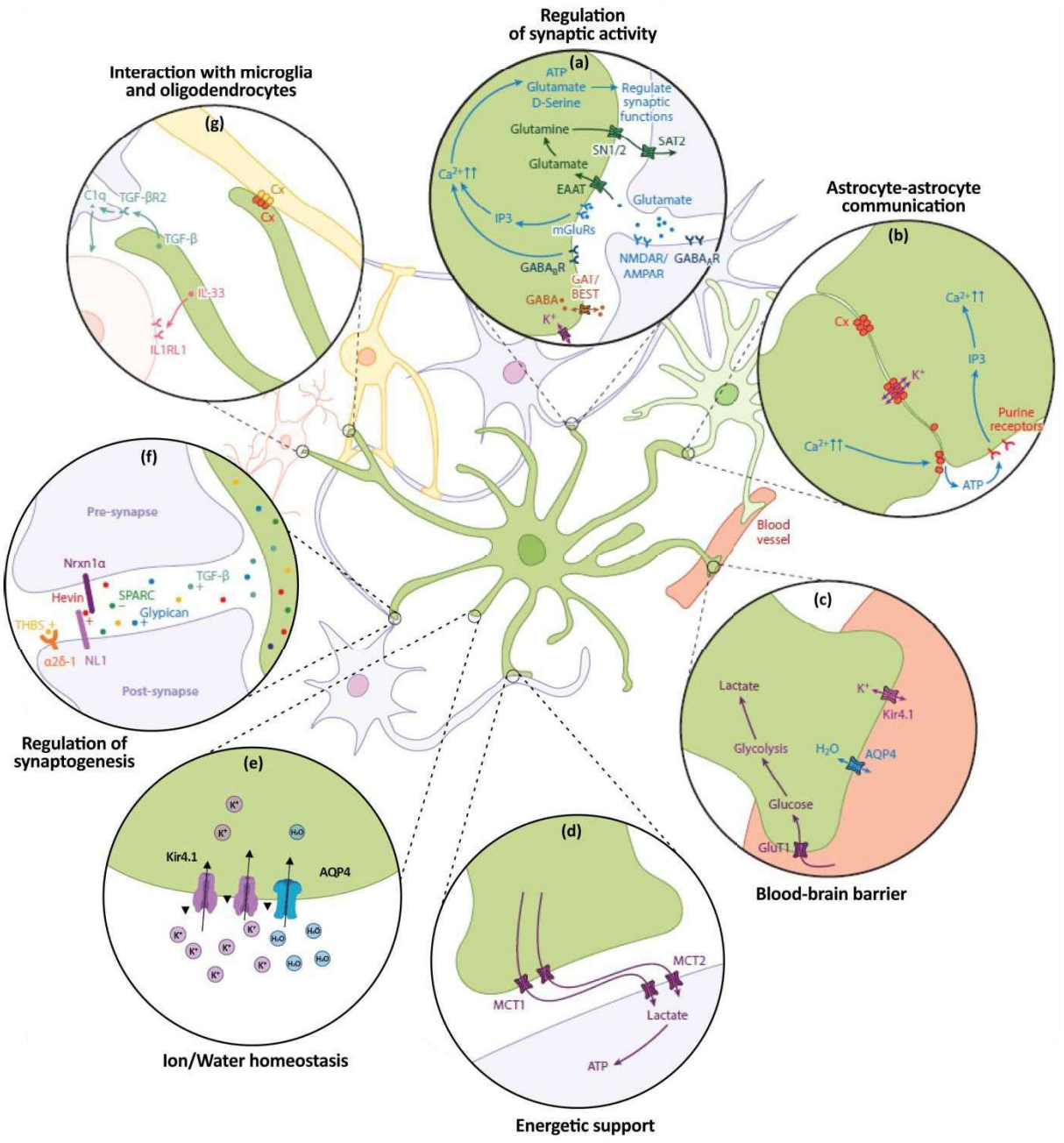

Figure 2. Physiological functions of astrocytes across the CNS

Astrocytes are tasked with a wide range of functions in the nervous system. They are regulating synaptic activity or preventing dysfunctions and death from glutamate excitotoxicity (a) and establishing constant contact with other glial cells (b, g). Astrocytes are responsible for protection and maintenance of BBB via end feet-contacts with endothelial cells (c), are in close relationship with neurons, providing energetic support (d). They ensure homeobalance of ionic and water concentrations within the extra cellular environment (e) and regulate synaptogenesis (f). *(modified from Khakh and Deneen, 2019).*

4.1.3. Microglia

4.1.3.1. The resident immune cells

Embryonic Origins and CNS expansion. Microgliocytes or microglia cells, are the specialized immune cells of the CNS. Unlike neurons and other glial cells, they do not derive from the common neural progenitor cells (NPCs). Although debated, microglia originates from erythro-myeloid progenitor cells of the yolk sac colonizing the CNS (Ginhoux et al., 2010; Schulz et al., 2012a) (**Fig. 1A**). Detected starting from E8 in the yolk sac, microglia progenitors penetrate the developing SC in two waves. At E8–E9, they colonize the neuroepithelium through the developing vasculature. The second wave at E11.5–14.5 consists of the expansion of embryonic microglia cells within the parenchyma and subsequently invading the developing CNS (Ginhoux and Prinz, 2015). Meanwhile, microglia start to differentiate from a progenitor amoeboid shape to a characteristic ramified shape with long and thin processes (Rigato et al., 2011). The microglia highly proliferate in the first post-natal week to reach a sufficient number to disperse into the whole CNS and maintain their density by self-renewal throughout life (Tambuyzer et al., 2009). The process of microgliogenesis is tightly regulated: microglia development and survival in the adult CNS require CSF-1R signaling and the transcription factor PU.1 (Beers et al., 2006; Ginhoux et al., 2010; Elmore et al., 2014).

Microglial markers. Asserting specific microglial markers appears challenging due to their mesodermal origin and the common features shared with the macrophage lineage. Indeed, both cell types express F4/80, CD68, MHCII, and CD11b (Prinz and Mildner, 2011). Even though not strictly specific, microglia can be identified based on their high expression level of CX_3CR_1 and Iba1 (Yona et al., 2013; Kolos and Korzhevskii, 2020). Recently TMEM119 and Sigle-H have been identified as specific to microglia (Konishi et al., 2017). Sigle-H labels microglia at all developmental stages and activation while TMEM119 is expressed mostly by resting adult microglia (Bennett et al., 2016; Krasemann et al., 2017).

Functional Phenotypes. Microglia functional phenotypes can be determined based on morphology: resting microglia (homeostatic) arbor ramified processes sensing the CNS environment and, once a perturbation is detected, retract their branches to an amoeboid shape (activated) with hypertrophic somata. This simplest classification does not reflect adequately the complexity of microglia activation (Paolicelli et al., 2022). Functional phenotypes refer to the immune response of microglia: M1 phenotype pro-inflammatory (pro-I) neurotoxic phenotype and M2 anti-inflammatory (anti-I) neuroprotective phenotype. M1 microglia cells are characterized by the secretion of pro-I factors, which worsen tissue damages like cytokines (IL-1, IL-6, TNF-α), reactive oxygen species (ROS), or the inducible nitric oxide synthase (iNOS) (Saha and Pahan, 2006; Smith et al., 2012; Simpson and Oliver, 2020). In contrast, the M2 phenotype releases anti-I cytokines (IL-10, IL-4, TGF-β), growth factors (BDNF), and Arginase 1 (Arg1) (Guo et al., 2022). However, this classification is heavily

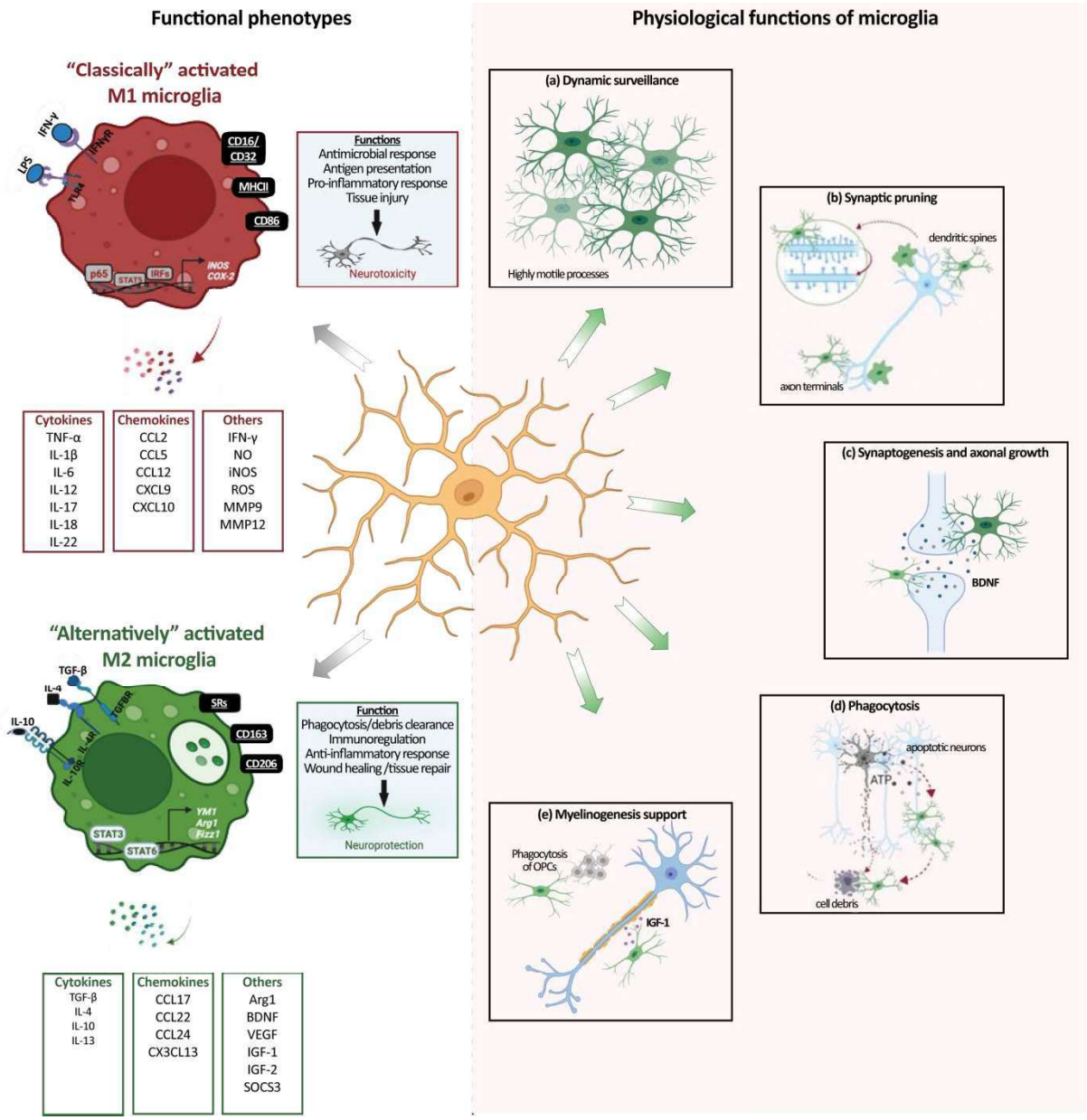

Figure 3. Heterogeneity of microglial functions and phenotypes in the nervous system

Although debated, the activation of microglia cells is referred as to "classically" activated M1 microglia and "alternatively" activated M2 microglia. M1 phenotype is neurotoxic for myelinated axons and characterized by the expression of pro-inflammatory factors. Conversely, the microglial M2 polarization is neuroprotective and pro-regenerative to myelin and neuronal compartments through the secretion of anti-inflammatory molecules (left panel, *modified from Wendimu and Hooks, 2022)*. Microglia cells are the resident immune cells of the CNS and are implicated in many key aspects of the homeostatic nervous system such as environment surveillance (a), synaptic plasticity (b) and, neurotransmission (c), phagocytosis (d) and, myelination (e) (right panel, *modified from Vecchiarelli and Simoncicova, 2021)*.

debated within the scientific community since microglial activation is not simply an 'on/off' button but rather a spectrum of activation states.

4.1.3.2. Physiological functions of microglia

Within the healthy CNS, microglia's main function as "guardian cells" is the permanent scanning of the neuroenvironment (**Fig. 3, panel a**). They can quickly respond to stimuli and accordingly adapt their phenotype, thereby exerting an essential role throughout the lifespan under healthy conditions.

Phagocytosis. Embryonic neuronal circuit formation and adult network remodeling imply apoptotic death of neurons phagocytosed by microglia cells *via* "find-me" signal recognition (CX3CL1 or sphingosine kinase 1 signaling) (Gude et al., 2008; Truman et al., 2008; Dekkers and Barde, 2013). Microglia are involved in clearing cell debris dying from programmed cell death via "efferocytosis" and preventing aberrant inflammatory reactions (Borggrewe et al., 2020) (**Fig. 3, panel d**). Microglia can also shape the CNS environment via phagocytosing viable astrocytic and neural progenitor cells (Nelson et al., 2017; VanRyzin et al., 2019).

Neurotransmission, axonogenesis, and plasticity. The idea that microglia and neurons are close communicators is sustained by the expression of various neurotransmitter receptors such as acetylcholine, glutamate (AMPA-type), or GABA ($GABA_{A/B}R$) on the membrane of microglia (Liu et al., 2016). Neuron-derived transmitters can affect microglial activation leading to their release of immunomodulatory factors in the CNS microenvironment. This bidirectional microglial–neuronal communication relies on the ability of microglia cells, based on neuronal activity, to support new spine growth (BDNF) as well as, the refinement and pruning of synapses during development and throughout adult life (Ball et al., 2022). Moreover, it has been shown that microglial processes preferentially contact myelinated axons at the node of Ranvier. The readout involves THIK-1 and these interactions are modulated by neuronal activity and K^+ release (Ronzano et al., 2021). Microglia cells may also participate in axonogenesis. They are found in close association with axons in the white matter where they orient themselves parallel to developing axonal tracks (Dalmau et al., 1998; Pont-Lezica et al., 2014) (**Fig. 3, panel c**).

4.2. (patho)Physiology of the myelin sheath

4.2.1. Principle and functions of myelination

Myelinogenesis, or myelination, is the process of generation of the myelin sheath, a multilamellar membrane isolating and protecting the axons within the nervous system. It starts around birth first in the peripheral nervous system (PNS) followed by the SC and, at last, the brain.

Myelin Sheath Composition. The myelin sheath is a lipid-rich membrane containing 70-80% of lipids and only 15-30% of proteins (Williams and Deber, 1993). The three major lipids classes

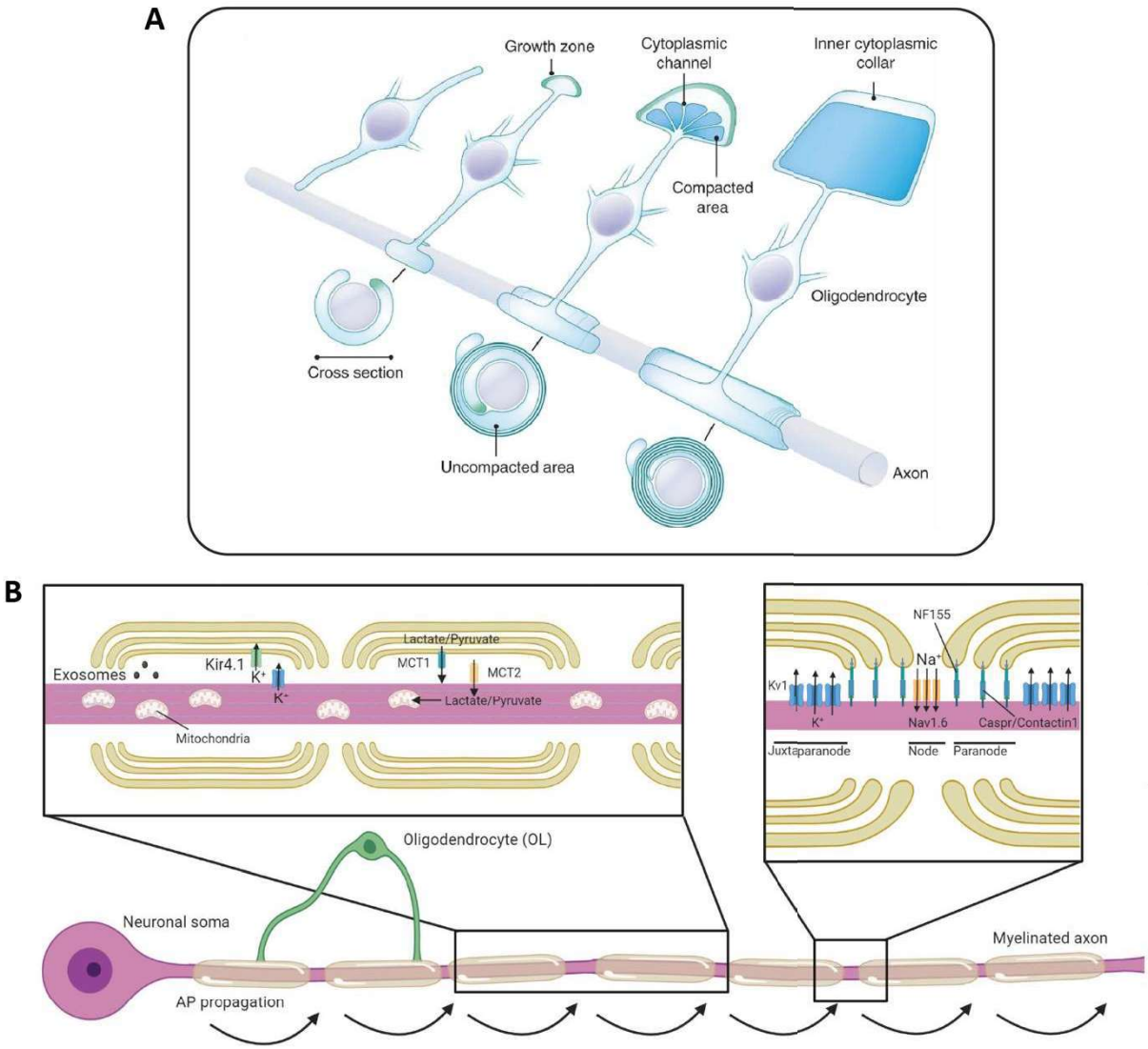

Figure 4. Myelinogenesis, saltatory nerve conduction, and axonal metabolic supply

A. The formation of the myelin sheath around axons occurs through a series of well-defined steps. A mature oligodendrocyte first selects an axon, establishes contact, and initiates the wrapping by spreading its membrane. The newly formed myelin grows both radially (more wraps) and longitudinally (longer sheath) and forms a multiple layer membrane around the axon. The compaction is initiated intracellularly, from the outermost layer toward the inner layers, and is achieved with the formation of the node of Ranvier (*modified from Chang et al., 2016)*. **B.** Although myelin sheath supports axon survival by providing lactate and pyruvate via monocarboxylate transporters (MCT1/2), it also allows saltatory nerve conduction where action potentials are generated at the nodes of Ranvier, greatly increasing conduction velocities compared to unmyelinated axons. Oligodendrocytes and axons are connected at the paranode via NF155-Caspr/Contactin1 while Na^+ and K^+ channels are involved in potential regeneration (*modified from Duncan et al., 2021)*.

involved are glycolipids (galactosylceramide), cholesterol, and phospholipids (plasmalogen, lecithin, sphingomyelin) with a 1: 2: 2 ratio (Kister and Kister, 2022). The distribution of these lipids at the membrane surface forms specific micro-domains called lipid rafts, which are involved membrane protein trafficking and signal transduction (Krämer et al., 1999; Grassi et al., 2020).

Myelinogenesis. Myelination is initiated by axon selection. Within the CNS, fully and partially myelinated axons and unmyelinated axons coexist. mOLs select axons with a diameter between 0.2 to 1 μm and, excluding immature neurons based on their expression of inhibitory cell surface molecules such as polysialylated neural cell adhesion molecule (PSA-NCAM) or class 3 semaphorins (Waxman and Bennett, 1972; Charles et al., 2000; Piaton et al., 2011). Once mOLs target an axon, the cell-cell interaction is established through beta 1 integrin signaling to ensure axonal survival and the initiation of the myelin synthesis (Câmara et al., 2009). Myelin growth is achieved by the extension of the mOL membrane with the possibility for a single mOL to myelinate 20 to 60 axons (Chong et al., 2012). Initially, OL processes encircle the axon, followed by bidirectional lateral growth to form a multilayer spiral wrapping around the axon as it elongates (Sobottka et al., 2011) (**Fig. 4A**). The entire process of myelination is temporally regulated within the lifespan of mOLs, with a "myelination window" lasting a few hours *in vivo* (Czopka et al., 2013).

Myelin biogenesis regulation. Myelin biogenesis is regulated by numerous factors. Myelin growth involves significant remodeling of the mOL cytoskeleton and cycles of actin polymerization/depolymerization at the leading edge during axonal ensheathment. Mutations in actin-related protein complexes like Arp2/3 and depolymerizing factors such as ADF/cofilin1, as well as Wiskott-Aldrich Syndrome Protein Family Verprolin-Homologous (WAVE) proteins involved in lamellipodia formation, profoundly affect myelin synthesis (Kim et al., 2006; Nawaz et al., 2015; Zuchero and Barres, 2015). The neuronal activity also regulates myelination through the modulation of intracellular Ca^{2+} concentration ($[Ca^{2+}]_i$) in mOLs. High-frequency $[Ca^{2+}]_i$ transients induced by action potentials promote myelin elongation, whereas low-frequency $[Ca^{2+}]_i$ elevation are associated with sheath shortening (Krasnow et al., 2018). Spinal OLs possess distinct intrinsic capacity based on their regional identity and form longer sheath and internodes around axons compared to the cortical mOLs (Bechler et al., 2015). Myelination induces axonal vesicular fusion where the sheath grows (heminodal non-myelinated domains), a process required for sheath elongation (Almeida et al., 2021). Myelinogenesis is achieved with the layer compaction of the newly formed myelin sheath. During this step, MBP protein participates to form the major dense lines by counteracting the repulsive negative charges on cytoplasmic leaflets (Chang et al., 2016). Together with PLP, they are the most abundant proteins in compact myelin. Studies have described their storage within mOLs and subsequent Ca^{2+}-dependent secretion triggered by neuronal signals via exosomes, which are then transported to the plasma membrane to form the sheath (Domingues et al., 2020).

Functions of the myelin sheath. While it provides evident mechanical protection to axons, one of its primary functions is the propagation of action potentials through saltatory nerve conduction, enhancing signal velocity and diffusion compared to unmyelinated fibers (Ritchie, 1982) (**Fig. 4B**). This mechanism relies on the hermetic ensheathment of the axons, the node of Ranvier, and the paranodal axon-glial junction to prevent current leakage. Nodes of Ranvier are axon segments devoid

of myelin coverage, characterized by an enrichment of voltage-gated sodium (Na_v) channels that are critical for the initiation and propagation of electric signals, as well as saltatory conduction. During development, immature nodes display Nav1.2 channels mostly replaced by Nav1.6 in adult nodes, except for a specific subset enriched with Nav1.2 and Nav1.8 (Waxman and Ritchie, 1993; Boiko et al., 2001; Arroyo et al., 2002) (**Fig. 4B**). The activity of these channels is mediated by several cytoskeletal proteins such as ankyrin G (AnkG), neurofascin (NF155 and NF186), or contactin. Deficits in these proteins result in inability of Na_v channels to cluster, defect in saltatory conduction, misattachment of the myelin at the paranode junction and incapacity to fire action potentials (Zhou et al., 1998; Boyle et al., 2001; Sherman et al., 2005). Metabolic coupling is also one of the great features of the myelin sheath. Since it isolates axons from the environment, axons depend on oligodendrocytes (OLs) for nutrient supplementation to meet their metabolic demands. OLs are connected to the subjacent axon through cytoplasmic-rich myelinic channels, facilitating the diffusion of metabolites in the periaxonal space, as observed with the expression of monocarboxylate transporters (MCT1) providing lactate and pyruvate (Lee et al., 2012) (**Fig. 4B**). They are also an excellent reservoir of glucose for neurons. Indeed, following the NMDAR activation, their sheath-surface receptors GLUT1 enable conversion of glucose into lactate via glycolysis (Saab et al., 2016). Recently, it has been shown that OLs are able to promote axonal mitochondrial ATP production by transcellular delivery of SIRT2 (NAD-dependent deacetylase sirtuin 2) via exosomes to neurons which alters acetylation of key mitochondrial proteins (Chamberlain et al., 2021). Moreover, exosomes take part in a myriad of essential neuronal functions. Their release is glutamate-dependent and involve AMPA and NMDA receptors (Frühbeis et al., 2013). Once internalized by neurons, exosomes may serve to protect them from cellular stress, contribute to axonal homeostasis by providing proteins implicated in axonal transport of vesicular cargo and cytoskeletal components, and increase firing rate (Fröhlich et al., 2014; Frühbeis et al., 2020).

4.2.2. Role of glial cells in developmental myelinogenesis

During development, glial cells participate in myelin production through their expression and release of molecules such as growth factors, cytokines, and chemokines, thereby exerting both positive and negative effects on oligodendrocyte fate.

Astrocytic control of myelination. Astrocytes communicate with OL lineage cells during myelinogenesis by releasing cytokines and growth factors. Astrocytes are the main producers of PDGF which interact with immature OPCs via their receptors PDGFRα, inducing their proliferation and migration (Richardson et al., 1988). They also release the growth factor BDNF supporting OPC maturation as well as neurotrophic factor CNTF known to act on the final step of their maturation through the Janus kinase (JAK) pathway (Cellerino et al., 1997; Nash et al., 2011). Astrocytes can

negatively affect OL fate; the expression of chemokine CXCL1 during SC development impedes PDGF signaling *via* the chemokine receptor CCR2 expressed by OPCs (Tsai et al., 2002). Beyond the differentiation and maturation of OPCs, astrocytes provide metabolic support to OLs and part of the lipids necessary for sheath production. They provide lactate to OLs through monocarboxylate transporters (MCT), used as an energy source and precursor for lipid synthesis (Rinholm et al., 2011). Astrocytes also synthesize cholesterol, later available to OLs *via* the apolipoprotein E (ApoE) and subsequently incorporated within the sheath (Saher and Stumpf, 2015).

Microglial regulation of myelinogenesis. During development and early postnatal stages, microglia support myelination. A specific transient subset of $CD11c^+$ microglia has been identified to regulate CNS myelination via IGF-1 expression. Developing amoeboid microglia phagocyte viable OPCs and thereby regulate the pool of OPCs and subsequent correct thickness of newly formed myelin sheath (Nemes-Baran et al., 2020). Moreover, an *in vitro* study demonstrated their ability to increase the expression of the myelin-specific proteins MBP and PLP in OLs (Hamilton and Rome, 1994). Microglia cells are preserving OPCs from degeneration. Microglia can induce OPCs apoptosis by orchestrating the upregulation of intrinsic NF-κB signaling through OPCs PDGFRα (Nicholas et al., 2001). Finally, microglial-derived IGF-2 was found to prevent mOLs degeneration (Nicholas et al., 2002).

4.2.3. Demyelination and myelin repair

4.2.3.1. Demyelination - chronicle of myelin injury

Causes of myelin disruption. Demyelination is a hallmark of various neurological disorders and corresponds to the pathological destruction of the protective myelin sheath surrounding axons. Several factors can lead to myelin disruption, including environmental factors, viral infections, genetic disorders, CNS auto-immunity, metabolism dysfunctions, or SC traumatic injury. Exposure to environmental toxins and pollutants like bisphenol A (BPA) and tris (1,3-dichloro-2-propyl) phosphate (TDCPP) induce myelin disruption via the alteration of myelin-specific gene expression (Khan et al., 2019; Chesnut et al., 2021). Viral infection such as coronaviruses or human immunodeficiency virus (HIV-1) cause subacute or chronic demyelinating processes, leading to myelin destruction and axonal damage (Nagashima et al., 1978; Mir et al., 2021). Viruses might also cause perturbation of OL homeostasis fostering a decrease in myelin-related gene expression and subsequent alteration of myelin lipidome (Louie et al., 2023). In the worst cases, viruses induce the necrotic death of OLs leading to an apoptotic cell death of neighboring cells (Fazakerley and Walker, 2003). Defects in myelin can be due to an inherited genetic condition. Mutations in myelin-related genes such as PLP or MAG result in flaws of nerve conduction, hypomyelination, and premature OLs

death (Griffiths et al., 1995; Roda et al., 2016). Moreover, MAG protein deficiency has been linked to the "dying back oligodendrogliopathy" affecting periaxonal OL processes (Lassmann et al., 1997). This lesion model can produce an energy deficit in OLs leading to mitochondrial damage and ultimately cell death (Bradl and Lassmann, 2010). The immune system can mistakenly target surface-exposed antigens of the myelin, primarily destroying the sheath rather than the OLs themselves. The initiation site of these autoimmune reactions is debated: the "outside-in" model sustains the theory of peripheral onset while the "inside-in" model argues in favor of primary damage to OLs and myelin causing the invasion of circulating immune cells (Lampert, 1978; Lopez et al., 2021). Finally, SC traumatic injury refers to a blunt trauma or spinal section. These types of injuries cause a direct loss of OLs via necrosis and apoptosis induced by the toxic acute environment (Almad et al., 2011).

Consequences of demyelination to axonal compartment. The consequences of demyelination extend to the axonal compartment. The myelin sheath not only insulates axons but also provides essential support and nutrients, safeguarding them from damage. Until recently, it was believed that demyelination do not alter axons which could survive unmyelinated (Smith et al., 2013). However, persisting axons exhibit a reduction of axonal transport and impaired neuronal conduction (Smith, 1994; Edgar et al., 2010). Myelin impairment induces subsequent axonal degeneration and some studies emphasize Wallerian degeneration as the involved mechanism (Dziedzic et al., 2010; El Waly et al., 2020). Moreover, chronic demyelination has been linked to a significant acceleration of axonal loss (Klistorner et al., 2022). Alternatively, myelin loss may induce neuronal cell death through defects in mitochondrial transport leading to insufficient cell ATP energy and subsequent axonal degeneration (Stys, 1998; Kiryu-Seo et al., 2010). However, the immobilization of mitochondria mediated by syntaphilin may facilitate the survival of these demyelinated axons (Ohno et al., 2014). In autoimmune diseases, the myelin sheath increases the risk of axonal degeneration in this inflammatory environment promoting OL death (Schäffner et al., 2023). Demyelination and axonal degeneration ultimately lead to SC atrophy and electrophysiological defect linked to reduce motor coordination capacity (McGavern et al., 2000). Despite the significant axonal loss, myelin impairment leads to disturbances of axonal electrical properties including slowing of internodal conduction time or conduction blockade, increased refractory period (Franssen and Straver, 2013).

4.2.3.2. Remyelination – myelin sheath regeneration

Remyelination process. Remyelination is the repair process of damaged myelin and play a crucial role in restoring spinal cord functions. It is a highly regulated mechanism influenced by the nature of the injury or disease, damage severity, and the age of occurrence. Although spontaneous remyelination can occur, it often remains incomplete or inefficient, leading to persistent neurological deficits (Gilson and Blakemore, 1993; Franklin, 2002).

Remyelination required the recruitment, proliferation, and differentiation of new OPCs on the lesion site. Several factors and cells have been identified as key regulators of this repair process. Upon activation, OPCs increase the expression of progenitors-related genes such as Olig2, NG2, and Nkx2.2 needed to further initiate their differentiation into mOLs (Chari, 2007). Their rapid proliferation is promoted by growth factors including PDGF, FGF2, or GGF2, released by neurons (Redwine and Armstrong, 1998). Olig1 is crucial for OPC differentiation as well as IGF-1 or TGF-β whose expression decrease their proliferation by inhibiting growth factors (Carson et al., 1993; McKinnon et al., 1993; Arnett et al., 2004). Differentiating OLs also accumulate intracellularly cyclin-dependent kinase inhibitor p27Kip-1 and express Lingo-1 (Durand and Raff, 2000; Mi et al., 2005). For some time, remyelination was thought to be based solely on newly differentiated mOLs. However, a recent study demonstrated that pre-existing mOLs surviving in the demyelinating lesion site are also involved in the repair process (Mezydlo et al., 2023). Additionally, it has been shown that the newly formed myelin sheath is thinner and displays shortened internode length but properly restores conduction properties (Chari, 2007). Finally, remyelinating potential declines with the age; ageing adult OPCs become less responsive to proliferating factors due to epigenetic modifications of their transcriptome notably in apelin receptor (APJ)-mediated remyelination, but also acquire extrinsic age-related modification from the substrate. To note, the neighboring glial and immune cells, which participate to create a favorable environment to remyelination become less efficient in producing pro-remyelinating cues or removing myelin debris with an alteration of their gene profiles (Neumann et al., 2019; Ito et al., 2021).

4.2.4.Neurodegeration: focus on Multiple Sclerosis disease

4.2.4.1. Multiple Sclerosis

Worldwide 2.5 million people are affected with Multiple Sclerosis (MS), thus making MS one of the most common neurodegenerative diseases (Dilokthornsakul et al., 2016). There has been an overall increase in incidence with a clear female preponderance over recent years. MS is a chronic inflammatory autoimmune disease causing myelin degeneration, axon loss, and reactive gliosis progressively impairing sensory-motor and cognitive functions in patients (Noyes and Weinstock-Guttman, 2013). This pathology is characterized by the infiltration of autoreactive perivascular immune cells (mainly macrophages, T cells, B cells, and NK cells) assaulting the myelin sheath. Symptoms are versatile and depend on demyelination plaque location in the CNS, whose precise position cannot be predicted (**Fig. 5B**). However, the exact origin of the disease has yet to be fully elucidated, although some promising hypotheses are emerging. Patients suffering from MS experience a wide range of symptoms such as neuropathic pain, vision loss, muscle spasms or weakness, ataxia,

or urinary incontinence. Regeneration of the CNS injury is poor; patients do not recover from symptoms and neurological defects ultimately leading to their death.

Etiology of MS disease. The etiology of MS remains unknown but the involvement of some risk factors on the onset of the disease has been identified: immune defect, environmental factors, or genetic predisposition.

Immune defect - The aberrant autoactivation of $CD4^+$ T cells may be the initial event of MS pathogenesis (Tsunoda and Fujinami, 2002). T helper cells (Th1 and Th17) can bind and destabilize the BBB through their surface adhesive molecules and the expression of matrix metalloproteinase (MMP) enzymes respectively. When they infiltrate CNS parenchyma, antigen-presenting cells (APCs) reactivate T cells by presenting myelin-specific proteins which induce secretion of pro-I cytokines and other factors, and ultimately, the lysis of the myelin membrane (Lazibat et al., 2018). Moreover, the intestine microbiota has been recently pointed out as influencing MS pathogenesis (Miyake et al., 2015). The dysbiosis - imbalance or disruption of micro-organisms composition and function of the microbiota – induce systemic inflammation through gut leakage triggering the activation of autoreactive $CD4^+$ T cells. It also impairs the expansion of pro-resolving cells such as regulatory T cells (Tregs), thereby predisposing patients to develop MS further (Shahi et al., 2022).

Environmental factors - Hypotheses of the mechanism behind T cell autoimmunity emphasize an intrinsic CNS abnormality, while another considers the viral origin of the antigen. (Tsunoda and Fujinami, 2002). Indeed, Epstein-Barr viruses such as Human herpesvirus 6 have been recently pointed out as contributors to the pathophysiology of MS (Bjornevik et al., 2022; Lanz et al., 2022; Voumvourakis et al., 2022). Vitamin D deficiency has been also proposed as a risk factor for the development of MS disease (Sintzel et al., 2018).

Genetic predisposition – Gene mutations have been identified as a susceptibility risk for MS. Variation in the human leukocyte antigen *HLA-DRB1*1501* is one of the most described genetic predispositions to MS. Physiologically, this gene is involved in the discrimination of self and non-self by the organism (Alcina et al., 2012). Mutations of the *Il17r* gene, involved in the expansion and survival of immune cells, have been found in patients (Zhao et al., 2022). The mutation causes the inability of the receptor to translocate to the cell membrane. However, it is uncertain if these two mutations are related to the development of the disease or solely participate to symptoms. Finally, heritability is estimated to account for 35-75% of MS cases (Westerlind et al., 2014).

Time course of myelin injury. MS is a chronic disease with a progressive course leading to permanent disabilities in patients. The time course of MS has been categorized into the following four groups (**Fig. 5A**):

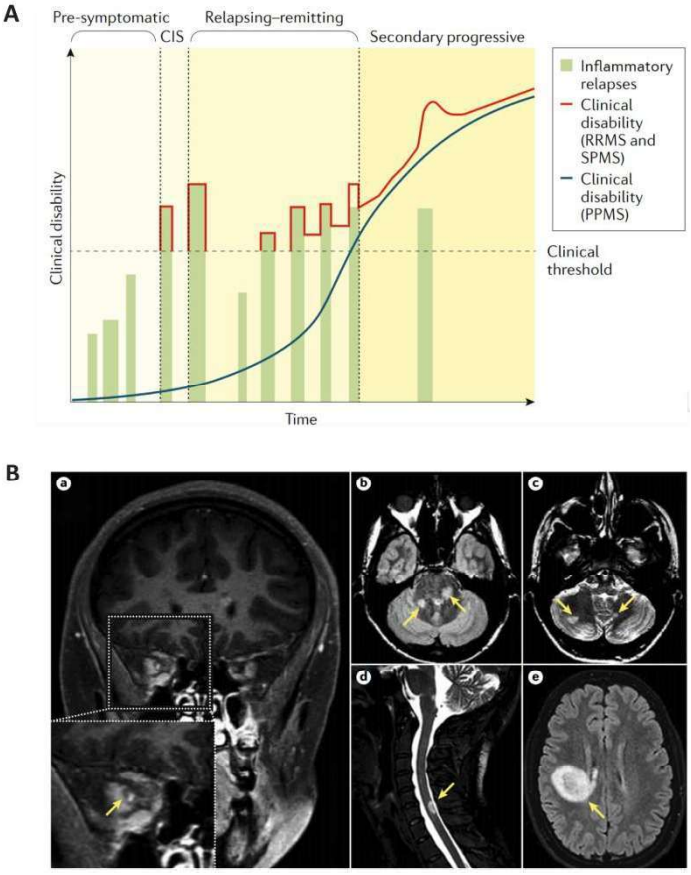

Figure 5. Clinical course of Multiple Sclerosis patients and MRI diagnosis of demyelinating events

A. The evolution of multiple sclerosis is defined by different clinical course including relapsing–remitting MS (RRMS), secondary progressive MS (SPMS) or, primary progressive MS (PPMS). Patients with RRMS suffer from random relapses without complete neurological recovery unlike patients with SPMS or PPMS, causing progressive and permanent disabilities to patients. The patients experiencing initial inflammatory demyelination, without meeting the MS diagnostic criteria, are categorized under "clinically isolated syndrome" (CIS). **B.** Patients diagnosis consists of MRI detection of focal lesions within the white matter tracts (arrows) scattered within the whole CNS: optic nerve (a), left pons and the right middle cerebellar peduncle (b), cerebellar hemispheres (c), cervical spinal cord (d) and, left cerebral hemisphere (e). (Filippi et al., 2018).

Relapsing-remitting (RRMS) – This phase is characterized by the alternate of worsening symptoms (relapse) and recovery and lasts for a day or a few weeks. In 70-80% of the patients, the disease manifests with this phase.

Primary progressive (PPMS) – This type of MS consists of a progressive aggravation of the symptoms experienced by the patients with an accumulation of disability and concerns 15% of MS cases. PPMS can alternate between active and inactive phases.

Secondary progressive (SPMS) – This phase may concern the patients initiating the disease through RRMS and correspond to a progressive aggravation of the neurologic condition.

Progressive-relapsing (PRMS) – It is estimated that 5% of the patients develop this type of MS which is the least common manifestation of the pathology. Similarly to PPMS, the symptoms and neurological outcomes gradually deteriorate and are interspersed with relapses. The deterioration is induced by neuronal loss, whereas the relapse episodes are attributed to inflammation.

Therapeutic strategies. Currently, there is no curative treatment for multiple sclerosis (MS). Therapeutic strategies, termed "disease-modifying therapy" (DMT), aim to alleviate patient symptoms and slow the progression of the disease by reducing myelin degeneration, inflammation, and relapses. Initially, acute episodes of MS were treated systemically with glucocorticoids for their potent anti-

inflammatory and immunosuppressive effects (Kieseier and Hartung, 2003). While effective, these non-specific treatments only improve the duration of relapse episodes. This led to increased interest in immunosuppressive and immunomodulatory therapeutic strategies targeting adaptive immune cells, such as T cells and B cells, during RRMS. A myriad of such therapies has been developed and is routinely used with patients. Among them, we find interferon beta (IFN-β), known to inhibit T cell proliferation and promote the release of anti-I cytokines like IL-10 or IL-4 preventing peripheral immune migration across the BBB. Glatiramer acetate effectively reduces the number of active lesions by shifting the release of pro-I to the release of anti-I cytokines, production of BDNF and induction of Tregs. Monoclonal antibody therapies are widely used to treat MS patients given their great efficacy. Their mechanisms rely on the capacity to bind and counteract specific targets involved in MS pathogenicity. Notably, the anti-TNF antibody, the anti-CD20 antibody used to deplete B cells in both RRMS and PPMS, the anti-CD52 or the anti CD25 antibodies that target an integrin expressed on T cell surface causing their lysis and prevent the expansion of autoreactive T cells by blocking their IL-2 receptor, respectively. Unfortunately, even though antigen strategies were promising based on animal studies, involving the administration of myelin autoantigens such as MBP to induce T cell tolerance, they failed in clinical trials. However, MS diagnosis as well as the evaluation of the effects of new therapeutic candidates could benefit from the development and optimization of imaging techniques such as MRI, while the emergence of transcriptomic approaches allows for the discovery of new genes involved in MS pathogenicity (Croxford and Yamamura, 2009; Talanki Manjunatha et al., 2022).

4.2.4.2. Murine models to study MS

This section is adapted from the review "Contribution of Intravital Neuroimaging to Study Animal Models of Multiple Sclerosis", Buttigieg et al., 2023).

Animal models are essential to study the pathophysiology of MS, recapitulating the events associated with the human disease with remarkable reproducibility. Thereby, they provided insights into cellular interactions and demyelination mechanisms and contributed to test potential therapies. Each model is restricted to distinct processes: the model of experimental allergic encephalomyelitis (EAE) exhibit neuroinflammation and immune system activation, toxin-induced demyelination models are relevant to decipher de- and remyelination while virus-induced models focus on axonal damages and subsequent inflammation (**Fig. 6**).

- **EAE model**

EAE models mimic the clinical symptoms of MS patients as well as the time course of the disease. EAE is based on immunizing mice by subcutaneous injection of a water-in-oil emulsion of myelin-associated peptides together with or without inactivated mycobacteria (complete or incomplete

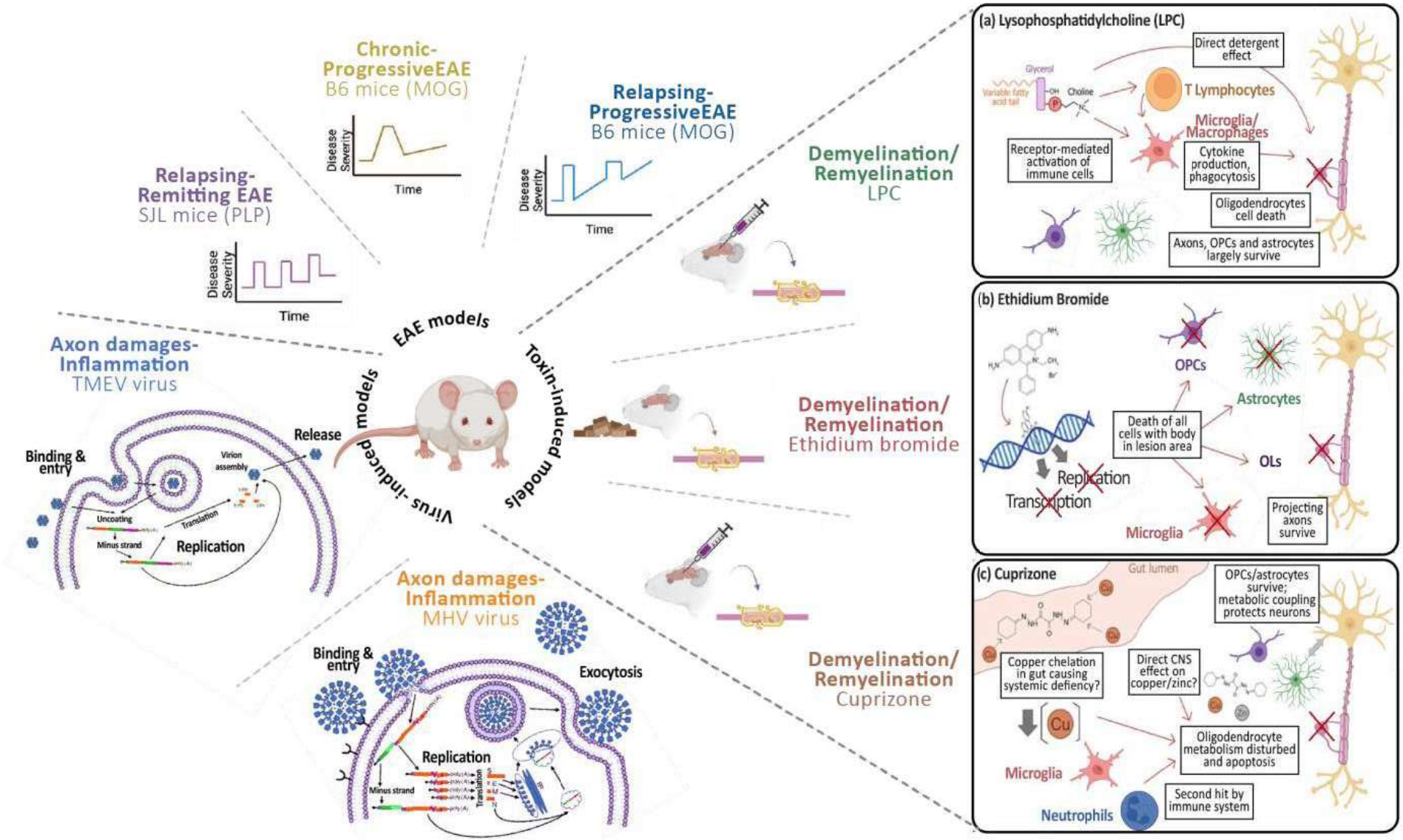
EAE models
Virus -induced models
Toxin-induced models
Chronic-ProgressiveEAE
B6 mice (MOG)
Relapsing-ProgressiveEAE
B6 mice (MOG)
Relapsing-Remitting EAE
SJL mice (PLP)
Disease Severity
Time
Axon damages-Inflammation
TMEV virus
Binding & entry
Uncoating
Translation
Minus strand
Replication
Virion assembly
Release
Axon damages-Inflammation
MHV virus
Binding & entry
Replication
Minus strand
Translation
Exocytosis
Demyelination/ Remyelination
LPC
Demyelination/ Remyelination
Ethidium bromide
Demyelination/ Remyelination
Cuprizone
(a) Lysophosphatidylcholine (LPC)
Glycerol
Variable fatty acid tail
Choline
Direct detergent effect
T Lymphocytes
Microglia/ Macrophages
Receptor-mediated activation of immune cells
Cytokine production, phagocytosis
Oligodendrocytes cell death
Axons, OPCs and astrocytes largely survive
(b) Ethidium Bromide
OPCs
Astrocytes
Death of all cells with body in lesion area
OLs
Replication
Transcription
Microglia
Projecting axons survive
(c) Cuprizone
Gut lumen
OPCs/astrocytes survive; metabolic coupling protects neurons
Copper chelation in gut causing systemic deficency?
Direct CNS effect on copper/zinc?
Cu
Zn
Oligodendrocyte metabolism disturbed and apoptosis
Microglia
Second hit by immune system
Neutrophils

Figure 6. Mouse models to study the pathophysiology of Multiple Sclerosis

A myriad of mouse models have been developed to decipher the mechanisms of the disease. The three main categories are experimental allergic encephalomyelitis (EAE), where the mouse strain, as well as the peptide used for the immunization, offer the possibility to study the time course of the disease observed in patients; the virus-induced models (TMEM and MHV) are useful to understand the viral contribution to MS etiology; the toxin-induced models where demyelination is induced through systemic or focal oligodendroglial intoxication using the lysophosphatidylcholine (LPC) (a), the ethidium bromide (b) or, the cuprizone (c) (*modified from McMurran et al., 2019; Libbey and Fujinami, 2021; Melamed et al., 2022)*.

Freund's adjuvant; CFA or IFA). The choice of the adjuvant has its relevance: IFA induces Th2 humoral response whereas CFA triggers Th1 cell-mediated immunity with microglia activation releasing pro-I cytokines or ROS leading to astrocytic activation (Billiau and Matthys, 2001; Raghavendra et al., 2004). According to the mouse strain or the immunization peptides used, EAE models may differ in terms of symptom severity and disease time course. The SJL/J mouse strain immunized with MBP or PLP peptides, allows addressing the relapsing-remitting phase of MS (Ben-Nun and Lando, 1983; McRae et al., 1992). Instead, MOG immunization instead induces a chronic and progressive form of EAE. MOG-reactive T cells are more widely observed in patients thereby making it the main EAE model to study the pathophysiology of MS (Mendel et al., 1995; Raddassi et al., 2011). Demyelination is initially triggered by the infiltration of autoreactive T cells into the CNS parenchyma, possibly activated by B cells and together attack the myelin sheath in the early stages of the disease (Fletcher et al., 2010; Pierson et al., 2014). Inoculation of naïve mice with T cells from immunized mice is enough to induce EAE-like symptoms and a pathology referred to as "passive EAE model" (Zamvil et al., 1986; Tanaka et al., 2017). However, from an imaging point of view, this model suffers from the difficulty of localizing lesion sites and their time course during EAE progression.

- **Toxin-induced models**

Lysophosphatidylcholine (LPC). The ability of LPC to produce demyelination was first described in 1972 (Hall, 1972). Due to its detergent activity, LPC solution at 1 % concentration damages the myelin sheath in white matter tracts and selectively kills most of the mature OLs by dissolving their membrane (Gregson, 1989). Their higher sensitivity is possibly due to their inability to metabolize LPC compared to other cell types (Gregson and Hall, 1973). Usually, LPC is injected into the ventral horns of SC, the corpus callosum, or the optic nerve. However, superficial incubation of LPC at the dorsal surface of the SC was proven to be valuable in differentiating demyelination-induced axonal death/degeneration from the mechanical axonal degeneration induced by needle insertion during LPC injection (El Waly et al., 2020). The loss of OLs and demyelination occurs within 2-4 days after LPC treatment and is followed by spontaneous remyelination one week later. Remyelination mainly relies on local OPCs proliferation and differentiation into new mOLs (Nait-Oumesmar et al., 1999). Although Schwann cells are usually restricted to the PNS, they also contribute to remyelination to a

certain extent, either by invading the lesioned parenchyma or by differentiation from OPCs (Blakemore, 1976; Zawadzka et al., 2010).

Ethidium Bromide. Ethidium bromide (EtBr) is a DNA intercalator that inhibits transcription and replication in the nucleus of all living cells causing their death (Waring, 1965). Unlike LPC, EtBr is not selective to OLs and causes the death of neighboring cells such as OPCs, astrocytes, and microglia. The lesion size is dose-dependent but axonal loss is minimal (Kuypers et al., 2013). Noteworthy, spontaneous remyelination is delayed compared to other animal models where demyelinated axons can still be observed six months after injection (Woodruff and Franklin, 1999). Although new OLs are generated, the remyelination largely involves Schwann cells in these lesions devoid of astrocytes, usually known to prevent their recruitment to the lesion site.

Cuprizone. While LPC and EtBr must be applied topically or injected into the tissue to induce focal lesions, cuprizone (CPZ) is instead a systemically administered drug that produces reversible demyelination in relatively predictable brain regions such as CC, hippocampus, or cerebellar cortex (Gudi et al., 2009; Koutsoudaki et al., 2009). The addition of this copper chelator to mouse chow at 0.2-0.3 % for a defined number of weeks selectively alters the homeostasis of OLs leading to their apoptotic death and subsequent loss of myelin sheath (Torkildsen et al., 2008). OLs susceptibility might be explained by mitochondrial disturbances causing their inability to support their high energetic demands for membrane synthesis (Pasquini et al., 2007; Acs et al., 2013). CPZ leads to early activation of microglia and strong astrogliosis preceding the demyelination (Gudi et al., 2009). The remyelination is achieved through migration and subsequent maturation of new OLs derived from OPCs and begins within a week after toxin arrest (Baxi et al., 2017). However, this model can be turned into a chronic-demyelinating model when CPZ treatment is extended to more than 12 weeks (Ludwin, 1980).

- **Viral-induced models**

TMEV and MHV. The growing evidence of a possible virus-triggered origin of MS brought up respective models of virus-induced demyelination to explore the potential etiology (Bjornevik et al., 2022; Lanz et al., 2022; Voumvourakis et al., 2022). Usually, mice are infected with Theiler's murine encephalomyelitis (TMEV) or Murine hepatitis (MHV) viruses. The two major subgroups of TMEV strains are GDVII (Glycine Dehydrogenase (decarboxylating) V-Type II) strains causing fatal encephalomyelitis opposite to BeAn and Daniel's TMEV strains characterized by a low virulence and then mostly used (Jarousse et al., 1998). The TMEV model can only be induced in mice and the clinical outcomes depend on the mouse strains (Owens, 2006). SLJ/V-infected mice develop a progressive-like form of MS with the persistence of viral antigen presentation by microglia and OLs (Zoecklein et al., 2003; DePaula-Silva et al., 2017). In contrast, C57BL/6J mice develop chronic MS with no inflammatory-mediated demyelination. Unlike EAE where axonal degeneration is secondary

to inflammation, in this model it precedes demyelination where the virus triggers $CD4^+$ helper and $CD8^+$ cytotoxic T cells but also activation of B cells and macrophages (Tsunoda and Fujinami, 2002; Tsunoda et al., 2003). MHV infection causes MS-like demyelination due to their ability to infect OLs and thus induce demyelination via OL death (Lampert et al., 1973; Matthews et al., 2002). These models are used to study the efficiency of the CNS immune system to clear viruses but also the ability to demyelinate while lacking T and B cells involvement and axonal loss (Das Sarma et al., 2009).

4.3. Glial and immune cells in myelin injury: a summit discussion

4.3.1. Introduction to Immune Cells

CNS has long been considered as an immune privileged organ. Indeed, parenchyma is devoid of innate and adaptive immune cells blocked by the restrictive function of the BBB. However, demyelination is known to trigger peripheral immune cell invasion into the lesion site, and their recruitment relies on secreted signaling factors from other involved cells. Moreover, immune cells are not functionally equivalents and each of them induces a specific response.

Immune cell diversity. The cells composing CNS peripheral immunity are various arising from innate or adaptive immune system. During inflammatory demyelination, the innate immune response is mostly mediated by myelomonoytic cells such as monocytes with their derived cells, granulocytes like neutrophils, and natural killer (NK) cells, while the adaptive immune response comprises T cells and derivative subsets, and B cells (**Fig. 7**). Upon demyelination, CNS immune privilege is revoked due to BBB destabilization. Circulating monocytes penetrate the parenchyma via diapedesis mechanism and preferentially at leptomeningeal microvessels (Reijerkerk et al., 2006; Haghayegh Jahromi et al., 2017). Once in the parenchyma, they differentiate into monocyte-derived dendritic cells (moDC) or monocyte-derived macrophages (MDM). moDC are characterized by the expression of CD11c and MHC-II and they are involved in the reactivation and immuno-modulation of T cells but also the release of pro-and anti-I cytokines (Zanna et al., 2021). MDM cells are found in the parenchyma in the acute phase of demyelination and are described as potential regulators of microglia inflammatory phenotype (Yamasaki et al., 2014; Greenhalgh et al., 2018). Inflammation itself is sufficient to trigger NK cell activation. Their phenotypes depend on their polarity which can enhance or improve inflammation outcomes through direct cell-killing cytotoxic activity and releasing of cytokines and growth factors (Morandi et al., 2008). The involvement of adaptive immunity via T cells is critical during CNS inflammation. Effector T cells regroup $CD4^+$ and $CD8^+$ T cells - also called cytotoxic T cells – that are respectively activated through antigen presentation by major histocompatibility complex (MHC) class II and MHC class I, respectively. In response to an inflammatory environment, $CD4^+$ T cells can differentiate into helper T cells (Th1, Th2, and Th17

cells) characterized by the expression of pro-I factors and cytotoxic properties, or Tregs defined as inflammatory pro-resolving cells (Fletcher et al., 2010; Arbour and Prat, 2015). Finally, B cells are involved in demyelination but their role is still unclear. Two different subsets of B cells with opposite inflammatory phenotypes exist: a subset releasing pro-I cytokines and a regulatory anti-I B cells subset (Cencioni et al., 2021). However, these adaptive immune cells in pathogenic demyelinating disease are crucial, cause their selective depletion revokes inflammatory activity (de Sèze et al., 2023).

4.3.2. Immune cells reactivity in de- and remyelination

In the context of demyelination and remyelination, innate and adaptive immune components play pivotal roles in orchestrating both pro- and anti-I responses. These immune responses are mediated by a complex interplay of cytokines and signals that influence their interactions with glial cells. Thus, balancing inflammatory signals is critical to determining lesion fate (Setzu et al., 2006; McMurran et al., 2016).

Innate immune cells activity. Demyelination triggers the infiltration of innate immune cells into the spinal parenchyma and MDMs are abundantly found in inflammatory lesions (van der Valk and De Groot, 2000). These macrophages describe two polarization phenotypes: classically activated M1 macrophages with cytotoxic and pro-I properties, and alternatively activated M2 macrophages known as pro-resolving cells. M1 macrophages release pro-I factors such as IL-1β, TNF-α, IL-6, and chemokines like CCL2 and CXCL10, which collectively promote inflammation and enhance myelin degeneration. Conversely, M2 macrophages participate in promoting tissue repair by decreasing the pro-I adaptive response via the expression of TGF-β and IL-10 but also myelin clearance with the expression of the integrin CD163 (Mayo et al., 2012; Vogel et al., 2013). However, M1 macrophages outnumber the M2 counterparts during demyelination, pointing out their deleterious effect on lesion fate. Finally, innate neutrophils have dual role in inflammatory demyelination. Their recruitment or persistence worsen myelin injury via secretion of ROS or IL-1β and the antigen presentation to T cells while they participate to enhance remyelination through CXCR2 signaling pathway (De Bondt et al., 2020; Khaw et al., 2020).

Innate and adaptive crosstalk. Crosstalk between innate and adaptive immune cells plays a crucial role in regulating immune responses in the myelin injury context. Indeed, innate immune cells release IL-1β and TNF-α to recruit and activate adaptive T cells and B cells at demyelination site (Miron and Franklin, 2014). Moreover, they can activate T cells via MHC class II leading to their differentiation into effector T cells including Th1, Th2, and Th17. In turn, cells can release cytokines, such as IL-2, IFN-γ, or IL-17 to modulate innate immune cell functions (Mayo et al., 2012). On the other hand,

innate NK cells possess the capacity to balance CNS inflammation through their ability to suppress myelin-reactive Th17 cells thereby contributing to a better inflammatory outcome (Hao et al., 2010).

Adaptive immune cells in demyelinating disease. Adaptive immune system plays an important role in the development of MS disease. The diversity of involved cells as well as the complexity of their interactions complicates the precise understanding of the pathogenic mechanism. However, inflammatory demyelination involves peripheral myelin-specific autoreactive $CD4^+$ and $CD8^+$ T cells. The inflammation triggers the endothelial expression of adhesion molecules (ICAM-1 and VCAM-1) that interact with integrin ligands (LFA-1 and VLA-4) and mediate the infiltration of these T cells within the parenchyma (Larochelle et al., 2011). Inflammation is sustained by the expression of pro-I cytokines from differentiated $CD4^+$ T cells. Th17 cells release the pro-I interleukins IL-17, IL-21, IL-9, IL-22, and TNF-α mediating the onset of pathogenic inflammatory demyelination (Harrington et al., 2005; Komiyama et al., 2006). IL-17 is critical to regulating local tissue inflammation as it induces macrophagic expression of IL-1β and TNF-α while sustaining astroglial activation through the enhancement of pro-I transcriptional programs (Jovanovic et al., 1998; Kang et al., 2010). On the other hand, Th1 cells release pro-I IFN-γ inducing microglia priming toward a neurotoxic M1 phenotype, which appears to be resistant to further IL-10 anti-I modulation needed for tissue repair (Hemmerich et al., 2022). Th1 and Th17 both produced GM-CSF considered critical for CNS inflammation and microglial activation (Codarri et al., 2013). Interestingly, Th2 cells release IL-4 known to reduce TLR-induced pro-I cytokines production of microglia cells and promote phagocytosis and oligodendrogenesis (Butovsky et al., 2006; Yi et al., 2020; Zuiderwijk-Sick et al., 2021). The recruitment of $CD8^+$ T cells enhances inflammation by releasing IL-17 but also exerts a detrimental influence on axonal survival and OLs (Bitsch et al., 2000; Arbour and Prat, 2015). Indeed, these cells damage axons via releasing lytic enzymes such as granzyme B or perforin and promote OLs death by disrupting their association with glial cells (Mars et al., 2011). Even if CNS infiltration of adaptive immune cells is correlated with a poor outcome, the involvement of Tregs cells promotes tissue repair and remyelination suppressing effector T-cell responses and microglial activation (Marshall et al., 2003; McIntyre et al., 2020). Indeed, these cells release anti-I cytokines such as IL-10, TGF-β, or the immunosuppressive cytokine IL-35, thus downregulating pro-I polarization of glial cells and subsequent inflammation (Wei et al., 2017; Roncarolo et al., 2018).

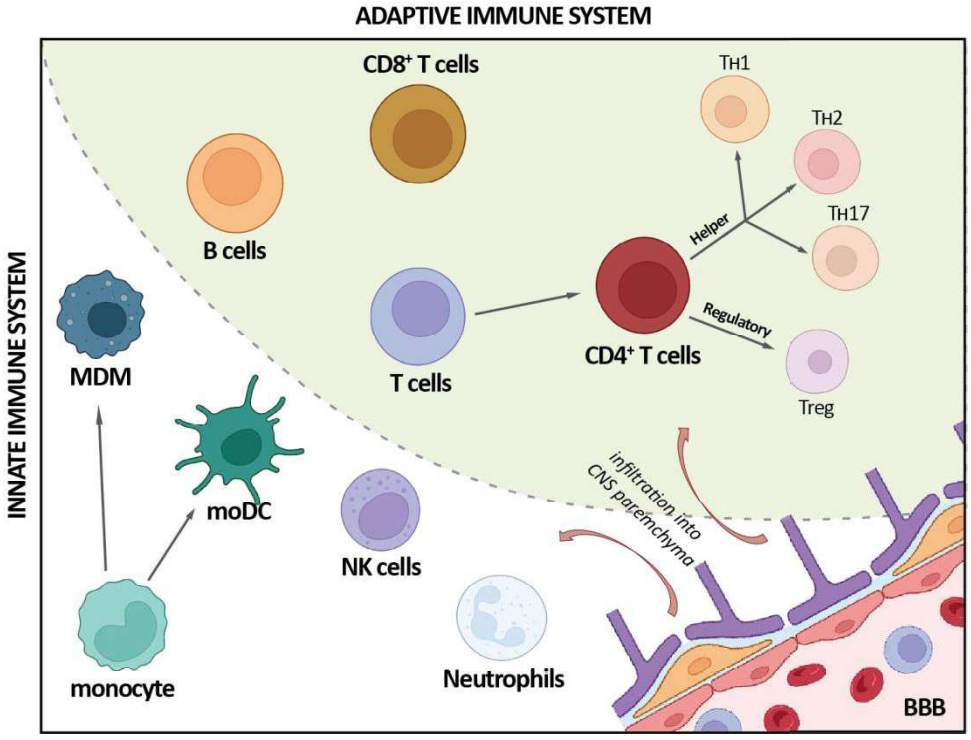

Figure 7. Repertoire of peripheral immune cells involved in myelin injury

Demyelinating events are characterized by peripheral immune infiltration, involving innate immune cells (monocytes and derived MDM and moDC, NK cells and neutrophils) and adaptive immune cells with T cells and B cells. MDM: Monocytes Derived Cells; moDC: monocyte-derived Dendritic Cells; NK: Natural Killer; BBB: Blood-brain barrier, composed of astrocytic endfeet (purple), pericytes (yellow), and endothelial cells (light red).

4.3.3. Glial orchestration of the demyelinating lesion

4.3.3.1. Cytotoxic reactive astrocytes

"A1" astrocytes. Upon demyelination, homeostatic astrocytes rapidly become activated displaying a hypertrophic cell body with concomitant upregulation of GFAP and vimentine (Escartin et al., 2021). Activated astrocytes are often classified into two categories: neurotoxic pro-I astrocytes referred to as A1 astrocytes and regenerative anti-I astrocytes referred to as A2 astrocytes (Clarke et al., 2018; Traiffort et al., 2020). Although this classification is controversial and does not reflect the wide range of phenotypic activations, we'll refer here to this nomenclature for simplicity. A1 astrocytes are characterized by the expression of complement 3 (C3) and release of pro-I cytokines such as TNF-α or IL-6 and oxidative stress-related cues exasperating the inflammatory environment and demyelination (Clarke et al., 2018). The occurrence of a such phenotype has been linked to the pivotal role of Notch signaling and the transducer/activator of transcription 3 (Stat3), but also through an upregulation of NF-κB signaling triggered by external factors such as CNS neuroinflammatory clues like IL-1β, TNF-α, IL-17, or ROS or intrinsic activation of sphingolipids signaling (Chandel et al.,

2000; Qian et al., 2007; Qian et al., 2019). Indeed, reactive astrocytes increase their expression the ceramide-derived sphingolipid LacCer as well as sphingolipid receptor S1PR1 linked to NF-κB activation and subsequent cytokine production, microglial activation, and pro-I innate immune cells recruitment (Mayo et al., 2014; Rothhammer et al., 2017; Linnerbauer et al., 2020). The inhibition of NF-κB signaling in reactive astrocyte promoted the protection the myelin component and improved remyelination (Brambilla et al., 2014). These astrocytes display also an upregulation of their interferon gamma (IFN-γ) signaling pathway involved as well in pro-I chemokines secretion (Ding et al., 2015).

Neurotoxic activity. A1 reactive astrocytes are described as neurotoxic. Accordingly, astrocytes release the fibroblast growth factor 9 (FGF9) which participates in impeding differentiation of mOLs and axon ensheathment and further expression of pro-I chemokines CCL2 and CCL7 (Lindner et al., 2015) (**Fig. 8, panel 11**). Demyelination triggers astrocytic production of nitric oxide (NO) through NF-κB signaling impairing their homeostatic function of neurotransmitter buffering (Bezzi et al., 2001; Calabrese et al., 2007). A1 astrocytes decrease their expression of glutamate transporters GLAST and GLT-1 leading to excessive glutamate concentration and excitotoxicity-mediated neuronal death (Rose et al., 2017) (**Fig. 8, panel 10**). Moreover, NO production might also be stimulated by the activation of neurotrophin receptor TrkB on astrocytes under inflammatory demyelinating conditions and is detrimental to neuronal survival (Colombo et al., 2012). In line with this, the reduction of astrocytic Kir4.1 channel expression increases the extracellular K^+ and participates in neuronal loss (Tong et al., 2014) (**Fig. 8, panel 10**).

Reactive astrocytes, OL fate, and remyelination. Reactive Astrocytes are able to act in the lesion environment via releasing ECM molecules thereby influencing OLs fate and remyelination. Inflammation induces the expression of fibronectin by astrocytes, which is found to accumulate around active demyelinating lesions and form aggregates that repress remyelination due to the impairment of OPC differentiation (van Schaik et al., 2022). Moreover, the astroglial N-cadherin-mediated interactions with OPCs are, impaired as well, therefore leading to their poor migration capacity to repopulate the lesion for remyelination (Schnädelbach et al., 2000) (**Fig. 8, panel 11**). Reactive astrocytes found at the border side of the lesion produced chondroitin sulfate proteoglycans (CSPG) as well as Anosmin-1, known to restrain migration/differentiation of OPCs and process outgrowth (Lau et al., 2012; Clemente et al., 2013; Pendleton et al., 2013). At the onset of demyelination, astrocytes release high levels of CXCL10 chemokine. Although the mechanism does not perturb OPCs maturation, astrocyte-derived CXCL10 impairs myelination (Nash et al., 2011). Moreover, astrocyte-derived TNF-α, CD38, endothelin-1, and Fas ligand (FasL) impair OLs survival and induce apoptosis of OLs, worsening demyelination (Li et al., 2002; Valentin-Torres et al., 2018; Langley et al., 2021). Finally, demyelination decreases astrocytes-OLs communication through

connexin signaling, therefore impacting metabolic support of OLs and myelination. Down-regulation of astrocytic Cx47 impairs the coupling with OLs and inhibits remyelination (Markoullis et al., 2014).

BBB disruption and immune cell signaling. Under physiological conditions, astrocytes are involved in the maintenance of BBB integrity. Demyelination and neuroinflammation induce loss of astrocytic end-feet around small vessels leading to increased BBB permeability and subsequent immune cell invasion (Correale and Farez, 2015). Reactive astrocytes express the pro-I cytokine IL-1β, which activates the expression of HIF-1 and VEGF-A. These in turn decrease the proteins involved in endothelial tight junctions ending up in BBB disruption (Argaw et al., 2006; Argaw et al., 2009) (**Fig. 8, panel 8**). Astrocytes are actively taking part in the recruitment of immune cells. They express the vascular adhesion molecule-1 (VCAM-1) and mediate T cells infiltration into the parenchyma (Gimenez et al., 2004). Moreover, in EAE astrocytes were found to highly express the CCL2 chemokine mediating the recruitment of monocytes and T cells (Huang et al., 2001; Kim et al., 2014) (**Fig. 8, panel 5**). IFN-γ and TNF-α enhance the expression of major histocompatibility complex class II HLA-DR, which enables astrocytes to recruit myelin-specific cytolytic $CD4^+$ T lymphocytes (Weber et al., 1994). Furthermore, the NF-κB activation in reactive astrocytes induces the expression of interleukins (IL-12, IL-23, IL-15) driving the $CD4^+$ T cells differentiation into a pro-I phenotype such as Th1 and Th17 but also regulates the $CD8^+$ T cells cytotoxic-mediated activity (Brambilla et al., 2014; Correale and Farez, 2015) (**Fig. 8, panel 7**). Astrocytes govern B cells expansion and activation via the expression of the B cell activating factor (BAFF) especially within the lesion site (Krumbholz et al., 2005) (**Fig. 8, panel 6**).

Astroglial signaling to microglia cells. Reactive astrocytes are able to induce pro-I activation of microglia cells during demyelination through the expression of diverse factors. This dialog is crucial for the reciprocal regulation during demyelination and later to promote tissue repair and remyelination. Activated astrocytes secrete GM-CSF, which is known to trigger microglia activation by modulating their transcriptional program toward a pro-I phenotype to release deleterious cytokines and chemokines (Linnerbauer et al., 2020) (**Fig. 8, panel 9**). Astrocytes-derived IL-6, a pro-I interleukin, induces microglia activation via upregulation of MHC class II and pro-inflammatory genes (Savarin et al., 2015; Garner et al., 2018). Recently, a study emphasized the putative synergy of Sigma1R-IRE1a-XBP1 signaling in astrocytes to modulate this glial cell crosstalk during inflammation and the regulation of pro-I cytokines release from microglia cells (Wheeler et al., 2019). Next to their action on T cells and OPCs, the expression of the chemokines CCL2 and CXCL10 promotes the recruitment and activation of microglia cells towards a pro-I phenotype (Tanuma et al., 2006; He et al., 2016) (**Fig. 8, panel 9**).

4.3.3.2. Pro-inflammatory microglia cells

Classically activated "M1" microglia. Although debated, microglia cells are described as classically activated during inflammatory demyelination and termed "M1" microglia. These microglia cells are involved during demyelination and exert pro-I activity, which is detrimental for OLs as well as neurons and mediates pro-I cells recruitment from the periphery with the activation of neurotoxic astrocytes (Miron et al., 2013b). They are known to express various pro-I molecules including cytokines (TNF-α, IL-1β/6, IFN-γ), chemokines (CXCL9; CXCL10, CCL5/2), matrix metalloproteinases, reactive oxygen species (iNOS, NO) and, glutamate (Benveniste, 1997). They also express specific integrins such as CD11b, CD11c or costimulatory molecules (CD36, CD45, CD47) (Colonna and Butovsky, 2017; Guo et al., 2022) (Fig. 3). Such a M1 phenotype is associated with the activity of TLR4 with the adaptor protein myeloid differentiation factor 88 (MyD88) leading to activation of pro-I pathways, NF-κB mitogen-activated protein kinases (MAPK) which induce transcription of pro-I genes (Kawai and Akira, 2007; Subhramanyam et al., 2019; Guo et al., 2022).

Impact on OL lineage, and neurons. Classically activated microglia during demyelination appear to be neurotoxic for OL lineage and myelin sheath as well as neuronal compartment. The secretion of the pro-I cytokines TNF-α and IL-β are cytotoxic for OLs but also induce myelin damage (Selmaj and Raine, 1988; Kaur et al., 2013) (**Fig. 8, panel 4**). The expression of IFN-γ induces endoplasmic reticulum stress inhibiting remyelination but also causes OLs death via apoptosis (Lin et al., 2005). Moreover, the putative mechanism by which these pro-inflammatory cytokines mediate OL death may rely on their ability to induce iNOS expression, which in turn produces NO implicated in cytolysis and Krebs' cycle arrest (Nave, 2010). Microglia cells also release NO and the stress chaperone heat shock protein 60 (HSP60) leading to OL death (Merrill et al., 1993; Li et al., 2017). Microglia-derived NO is also responsible for axonal damages. Indeed, it induces inhibition of axonal transport of synaptic vesicle precursors causing neuronal dysfunctions (Stagi et al., 2005). Moreover, IL-1β is detrimental to neurons and leads to swelling and clumping of synaptic vesicles while the excessive amount of glutamate released by activated microglia cells leads to excitotoxicity and neuronal death (Takeuchi et al., 2008; Han et al., 2017). Classically activated M1 microglia thus appears as direct mediators of axonal degeneration as well as oligodendrocyte cell death, worsening the inflammatory environment and demyelination.

Microglia signaling to astrocytes and peripheral immune cells. Due to their homeostatic functions in the CNS, microglia are capable of fast response to disturbances and of signaling to surrounding cells to induce their activation. Mice lacking IL-1β exhibited delayed activation of astrocytes in a demyelination context, highlighting the necessity of their activation before astrocytic activation (Butzkueven et al., 2002). Furthermore, pro-inflammatory cytokines IL-1α, TNF-α, and C1q secreted by microglia can polarize astrocytes towards a neurotoxic A1 phenotype, reducing their ability to

express neurotrophic factors and promoting inflammation and cellular death (Clarke et al., 2018) (**Fig. 8, panel 3**). Additionally, TNF-α and NO induce the activation of the CXCR4-dependent signaling pathway in astrocytes, increasing intracellular calcium concentration and excessive glutamate release, leading to excitotoxicity and neuronal death (Bezzi et al., 2001). Microglia cells are also critical to recruiting peripheral immune cells. They facilitate their penetrance into the parenchyma via increasing BBB permeability via matrix metalloproteinases expression (Benveniste, 1997) **(Fig. 8, panel 1**). Microglia enhance the chemotaxis of immune cells (CCL2, CCL5, CCL8) into the lesion site and in the reactivation of peripheral $CD4^+$ and $CD8^+$ T cells through the expression of MHC class II (Schetters et al., 2017; Plastini et al., 2020; Shi et al., 2023) (**Fig. 8, panel 2**). In conclusion, in addition to their pro-I phenotype, microglia cells can activate and polarize into deleterious inflammatory phenotypes worsening demyelination and lesion fate.

4.3.3.3. Influence of oligodendrocytes

It is often mistakenly thought that oligodendrocytes adopt a "neutral" phenotype during demyelination, enduring damage caused by other cells. Although they are not key players, they are also taking part in neuroinflammation. OLs are involved in BBB destabilization by disrupting the integrity of endothelial tight junctions (Niu et al., 2019). Moreover, under certain conditions, OLs participate in phagocytic function and can activate $CD4^+$ T cells (Falcão et al., 2018). Finally, like microglia and astrocytes, they display a pro-I phenotype during demyelination and secrete pro-I cytokines such as IL-1β, CCL2, IL-17, and IL-6 worsening the inflammatory environment as well as inflammasome complex components like NLRP1, NLRP3, and NLRC4 (Tzartos et al., 2008; Moyon et al., 2015; Zeis et al., 2016). OLs express versican (VCAN), an extracellular matrix proteoglycan, known to take part in inflammatory responses and immune cell responses (Gu et al., 2007; Wight et al., 2014). Finally, the expression of chemokines such as CCL2, CCL5, CCL10, and CCL3 enable OLs to control innate immune cells chemotaxis within the neuroinflammed CNS (Menten et al., 2002; Balabanov et al., 2007; Marques et al., 2013; Moyon et al., 2015).

4.3.4. Glial mediation of inflammation and remyelination

4.3.4.1. Pro-regenerative astrocytes

Pro-regenerative "A2" astrocytes. In contrast to A1 astrocytes, A2 astrocytes were found in MS lesions during remyelination emphasizing their pro-regenerative capacities (Haindl et al., 2019). NFIA governs the switch from A1 to A2 neuroprotective astrocytes, which are characterized by the expression of S100A10 (Clarke et al., 2018; Tchieu et al., 2019). These pro-regenerative astrocytes display a downregulation of the NF-κB signaling pathway to the profit of JAK/STAT3 controlling

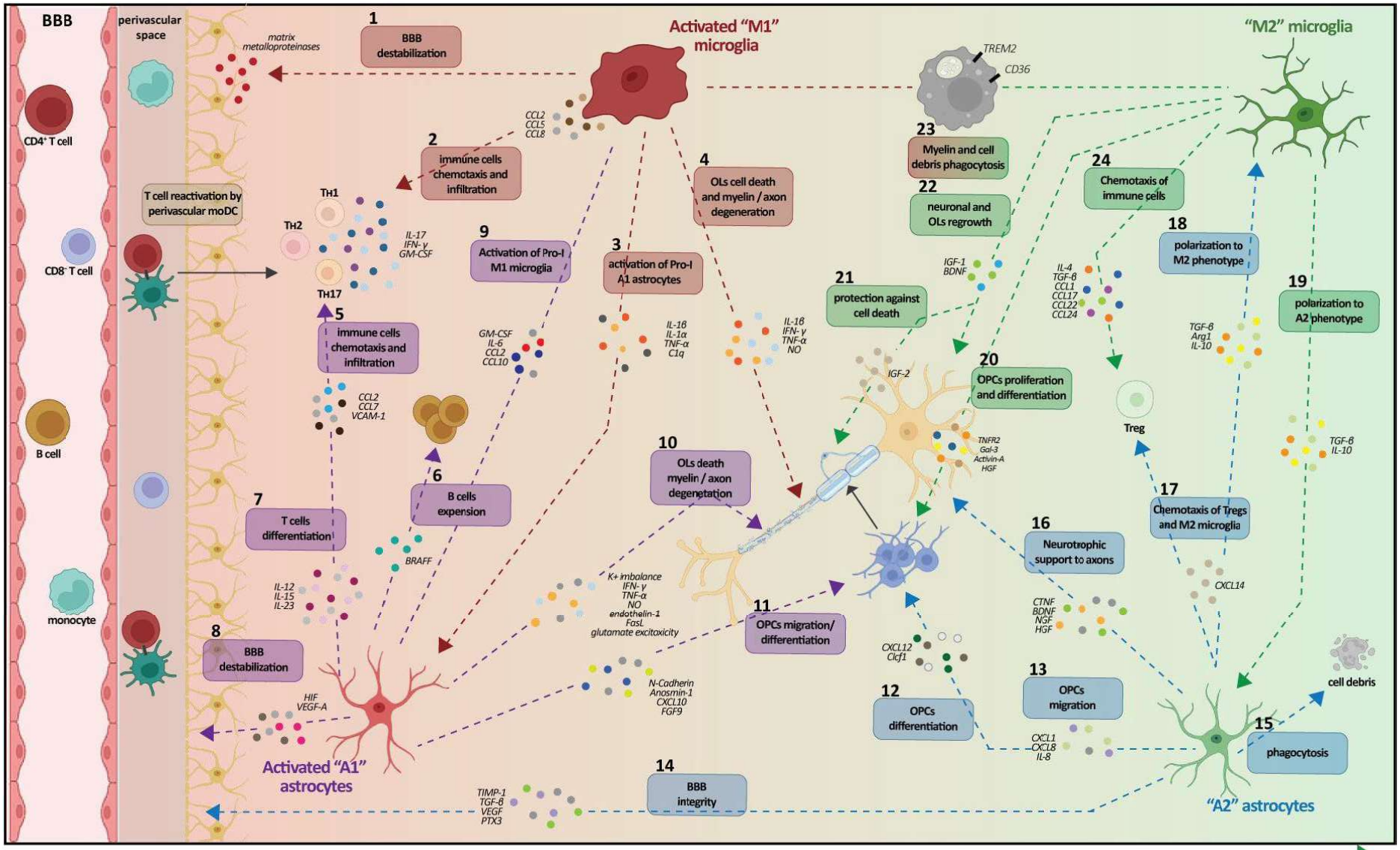
BBB
perivascular space
CD4+ T cell
CD8- T cell
B cell
monocyte
matrix metalloproteinases
1
BBB destabilization
Activated "M1" microglia
"M2" microglia
TREM2
CD36
CCL2
CCL5
CCL8
2
immune cells chemotaxis and infiltration
T cell reactivation by perivascular moDC
TH1
TH2
TH17
IL-17
IFN-γ
GM-CSF
4
OLs cell death and myelin / axon degeneration
23
Myelin and cell debris phagocytosis
22
neuronal and OLs regrowth
24
Chemotaxis of immune cells
18
polarization to M2 phenotype
19
polarization to A2 phenotype
9
Activation of Pro-I M1 microglia
3
activation of Pro-I A1 astrocytes
21
protection against cell death
IGF-1
BDNF
IL-4
TGF-β
CCL1
CCL17
CCL22
CCL24
TGF-β
Arg1
IL-10
5
immune cells chemotaxis and infiltration
GM-CSF
IL-6
CCL2
CCL10
IL-1β
IL-1α
TNF-α
C1q
IL-1β
IFN-γ
TNF-α
NO
IGF-2
20
OPCs proliferation and differentiation
Treg
TGF-β
IL-10
CCL2
CCL7
VCAM-1
6
B cells expension
10
OLs death myelin / axon degeneration
TNFR2
Gal-3
Activin-A
HGF
7
T cells differentiation
17
Chemotaxis of Tregs and M2 microglia
BRAFF
16
Neurotrophic support to axons
IL-12
IL-15
IL-23
K+ imbalance
IFN-γ
TNF-α
NO
endothelin-1
FasL
glutamate excitoxicity
11
OPCs migration/ differentiation
CXCL14
CTNF
BDNF
NGF
HGF
8
BBB destabilization
HIF
VEGF-A
N-Cadherin
Anosmin-1
CXCL10
FGF9
CXCL12
Clcf1
13
OPCs migration
cell debris
12
OPCs differentiation
15
phagocytosis
CXCL1
CXCL8
IL-8
Activated "A1" astrocytes
14
BBB integrity
"A2" astrocytes
TIMP-1
TGF-β
VEGF
PTX3
(a) DEMYELINISATION
(b) REMYELINISATION

Figure 8. Inflammatory phenotypes of microglia and astrocytes orchestrating demyelination and myelin repair

Myelin injury triggers the activation of microglia and astrocytes toward pro-inflammatory phenotypes (M1 microglia and A1 astrocytes). M1 microglia induce A1 astrocytes via expression of IL-1β, C1q, and TNF-α (3) which in turn enhance microglial M1 activation (9). Together, they recruit deleterious immune cells (2, 5, 6, 7) and promote permeabilization of the BBB (1, 8). These neurotoxic glial cells exacerbate demyelination by promoting oligodendrocytes death subsequently leading to axon degeneration (panels 4, 10) and impeding repair (11). Conversely, microglia and astrocytes acquire pro-regenerative phenotypes (M2 microglia and A2 astrocytes) characterized by anti-inflammatory gene expression, repair capacities, and enhancing remyelination. Indeed, they can stimulate each other toward these anti-inflammatory phenotypes via expression of TGF-β, IL-10, and Arg1 (18, 19). Microglia are mainly involved in phagocytosis of axon and myelin debris required for proper remyelination and may be helped by astrocytes (15, 23). With astrocytes, they are recruiting from the periphery Tregs with pro-resolving capacities (17, 24). Moreover, they promote axon repair/regrowth through neurotrophic factors (16, 22) while protecting them from death (21) as well as enhancing OPCs proliferation/differentiation and, remyelination (12, 13, 20).

immune cell infiltration, myelin protection, anti-I cytokines expression, and neuronal survival (Colombo and Farina, 2016). Indeed, they upregulate key protective genes such as prokineticin-2 (PK2), Nrf2, PTX3, SPHK1, and TM4SF1 (Neal et al., 2018). Notably, PK2 expression is known to increase antioxidant and anti-I cytokines while increasing glutamate uptake (Neal et al., 2018). They also exert immunomodulatory functions through the release of anti-I cytokines like TGF-β, Arg1, and IL-10. Astrocyte-derived TGF-β and IL-10 decrease pro-I activation of microglia (Norden et al., 2014; Recasens et al., 2019) (**Fig. 8, panel 18**). Furthermore, astrocytes can recruit Tregs and microglia cells to resolve the lesion via the expression of CXCL14 and CXCL12, respectively (**Fig. 8, panel 17**). They can also increase microglia phagocytic activity by the expression of IL-33, which indirectly promotes remyelination (Vainchtein et al., 2018).

Impact on OL lineage for remyelination. Demyelinating lesions are often devoid of OPCs. To remyelinate, OPCs have to migrate to the lesion side, and subsequently differentiate and remyelinate axons. Reactive A2 astrocytes are described as pro-regenerative with an anti-I phenotype favoring tissue repair and neuroprotection. In this sense, astrocytes attract OPCs to the inflammatory demyelinated site through the expression of chemoattractants such as CXCL1, CXCL8, and CXCL10 as well as the interleukin IL-8 (Omari et al., 2005; Moyon et al., 2015) (**Fig. 8, panel 13**). On the other hand, astrocyte-derived CNTF induces the expression of the neurotrophic factor Clcf1 promoting OPCs differentiation into mOLs (Ji-Wei et al., 2022) (**Fig. 8, panel 13**). Activated astrocytes express the receptor TNFR2, which is known to induce autocrine expression of CXCL12. This chemokine promotes OPC proliferation and differentiation for remyelination through its receptor CXCR4 (Patel et al., 2012) (**Fig. 8, panel 13**). To favor remyelination, astrocytes release TIMP-1, an inhibitor of metalloproteinase known to mediate immune infiltration, BBB breakdown, myelin impairment, and secretion of pro-I cytokines (Kieseier et al., 1999; Nygårdas and Hinkkanen, 2002) (**Fig. 8, panel 14**). Astrocytic-derived BDNF during white matter repair enhance the maturation of

OLs (Miyamoto et al., 2015). Finally, the expression of the neuroprotective factor LIF preserves mature OLs from inflammatory-mediated death and enhances their myelinogenic capacity for repair (Gard et al., 1995). Moreover, astrocytic LIF secretion is potentiated by the neuronal release of ATP, thus emphasizing the intricate relationship of astrocytes and neurons too during remyelination (Ishibashi et al., 2006).

Astrocytic-mediated phagocytosis of myelin debris. During demyelination, the engulfment of myelin debris and clearance of the environment are prerequisites for initiating proper remyelination, as they represent pro-I signals (Kopper and Gensel, 2018). For a long time, the clearance of myelin debris was ascribed solely to microglia cells. However, depletion of astrocytes has demonstrated an alteration in debris removal, highlighting their importance in this crucial step for efficient tissue repair (Skripuletz et al., 2013). Moreover, astrocytes have shown their ability to take over the phagocytosis of degraded myelin when microglia cells are dysfunctional. This compensatory mechanism relies on the expression of TAM phagocytic receptors by reactive astrocytes, which stand by to assist if microglial functions are impaired (Konishi et al., 2020). Another study has established that a specific subset of astrocytes expressing lipocalin-2 (LCN2) is competent in myelin uptake and can reduce the demyelination (Wan et al., 2022). However, the degree of astrocyte-mediated phagocytosis during demyelination is poor. Rather, the involvement of astrocytes in the phagocytosis process includes the recruitment of microglia cells to the lesion site through direct glial-glial crosstalk (Matejuk and Ransohoff, 2020) (**Fig. 8, panel 15**).

Axonal regeneration. Injured axons possess the intrinsic capacity to regrowth. As astrocytes support axonogenesis during development, reactive astrocytes are able to promote axonal regeneration. Astrocytes can form a “bridge-like structure” to physically guide axon regeneration (Zukor et al., 2013). Moreover, within the lesion site, damaged axons are contacting astrocytes secreting regrowth factors such as laminin and neurocan (White et al., 2008). As mentioned above, astrocytes secrete the neurotrophic factor CNTF, supporting regeneration through the sprouting of intact axons (Chen et al., 2022b). Besides CNTF, astrocytes can secrete a wide range of neurotrophic factors following white matter injury. This includes BDNF, nerve growth factor (NGF) and hepatocyte growth factor (HGF) promoting axon regrowth, while the expression of FGF2 enhances axon branching and sensory axon regeneration (Ikeda et al., 2001; Szebenyi et al., 2001; Lee et al., 2017; Yamane et al., 2018; Mesentier-Louro et al., 2019) (**Fig. 8, panel 16**). As in healthy conditions, astrocytes provide metabolic and energetic support for axonal repair. Astrocytes can transfer through endocytosis mitochondria to supply neurons with ATP (Hayakawa et al., 2016). They also provide lactate to preserve neuronal integrity (Jha and Morrison, 2020).

Restoration BBB integrity. One of the key criteria for tissue repair and remyelination involves restoring the integrity of the blood-brain barrier (BBB) to prevent the infiltration of peripheral

immune cells. In this regard, A2 astrocytes express TGF-B, VEG-F, and PTX3, known to reduce vascular damage and promote angiogenesis (Rodriguez-Grande et al., 2015; Rajkovic et al., 2018; Zong et al., 2020) (**Fig. 8, panel 13**).

4.3.4.2. Anti-inflammatory-like "M2" microglia

"M2" microglia. M2 microglia are referred to as an alternative state of microglial activation involved in OPC recruitment and differentiation, and characterized by anti-inflammatory properties (Traiffort et al., 2020) (Fig. 3). As described in section 2.1.3, they express the marker CD206 and anti-inflammatory cytokines such as TGF-β, IL-10, and Arg1, which are implicated in the resolution of local inflammation as well as supporting neuronal regrowth and remyelination through the expression of IGF-1 or BDNF (Miron et al., 2013b; Guo et al., 2022) (**Fig. 8, panel 22**). Moreover, M2 microglia are heavily involved in the phagocytosis of myelin debris (Tang and Le, 2016). The impairment of this property leads to a "secondary injury", which further enhance axonal damage and myelin loss (Fu et al., 2014). Indeed, the expression of miR-223 is needed for M2 polarization and efficient myelin removal by microglia cells (Galloway et al., 2019). However, this alternative activation of microglia cells cannot be reduced to a unique 'M2' phenotype, and RNA sequencing approaches have demonstrated a broad spectrum of activation states with multiple gene expression profile clusters (Hammond et al., 2019; Plemel et al., 2020). Thus, microglia cells in actively demyelinating lesions are described with a pro-I polarization but already express genes related to the M2 phenotype, increasing with remyelination and tissue repair (Locatelli et al., 2018).

Microglia-mediated phagocytosis. Clearance of the myelin debris by microglia cells is a prerequisite to promoting newly formed myelin sheath through the recruitment and differentiation of OPCs on the lesion site. Microglia are the main active phagocytic cells under myelin injury conditions. The activation of complement receptor-3 (CR3) induces structural rearrangements to enable myelin debris engulfment while the expression of the fatty acid translocase CD36 is required for myelin uptake (Reichert and Rotshenker, 2003; Grajchen et al., 2020). Moreover, the expression of Galectin-3 (Gal-3) and CX_3CR_1 has also been linked to microglial-mediated phagocytosis (Lampron et al., 2015; Reichert and Rotshenker, 2019). Finally, the expression of TREM2 promotes microglial survival and is upregulated in myelin-loaded microglia cells (Cignarella et al., 2020) (**Fig. 8, panel 23**).

Influence on OL lineage and remyelination. As defined during developmental myelination, a subset of $CD11c^+$ microglia cells exhibit pro-myelinating capacities and has been implicated in remyelination after myelin injury. These microglia cells are induced via CSF1 and IL- 34 signals and transduced through the CSF1 receptor (CSF1R) and lead to the enhanced expression of CCL2 expression and subsequent expansion of $CD11c^+$ microglia (Wlodarczyk et al., 2018). Microglia-promoted remyelination implicates the expression of genes such as Msh-like homeobox-3 (MSX3) and the purinergic receptor P2X4R which also negatively regulate pro-I genes (Yu et al., 2015; Zabala

et al., 2018). Pro-regenerative M2 microglia have a direct effect on OL lineage during remyelination. The neurotrophic factor IGF-1 regulates the OL population while the expression of TNFR2 enhances OPC proliferation. Also, Gal-3, activin-A, and HGF are known to induce their differentiation which collectively regulates the remyelination process (Arnett et al., 2001; Lalive et al., 2005; Pasquini et al., 2011; Dillenburg et al., 2018) (**Fig. 8, panel 20**). On the other hand, microglia secret IGF-2 protect OLs from TNF-α-induced apoptosis (Nicholas et al., 2002) (**Fig. 8, panel 21**). Interestingly, pro-I factors such as IL-1β and IL-6 are involved in OPC maturation at the initiation of the repair (Shigemoto-Mogami et al., 2014). Moreover, knock-out of TNF-α during remyelination reduced the proliferation of OPCs and delayed myelin repair. This emphasize the dual role of pro-I cytokines especially at the onset of remyelination (Arnett et al., 2001). Finally, a recent study emphasizes the importance of microglia in facilitating remyelination through sterol synthesis (Berghoff et al., 2021). Collectively, these data underline the importance of alternatively activated microglia to achieve efficient remyelination.

Microglia crosstalk with neighboring cells. Resolution of inflammation and tissue repair involves many cellular partners. Microglia act as an orchestrator of pro-resolving cells. Their expression of cytokines IL-4 and TGF-β as well as the chemokines CCL1, CCL17, CCL22, and CCL24 induce the differentiation of Th2 and Treg cells which exert neuroprotective effects and decrease CNS inflammation (Mantovani et al., 2004; Orihuela et al., 2016) (**Fig. 8, panel 24**). M2 microglia can induce astrocytes toward an A2 phenotype through the release of IL-10 and TGF-β (Liu et al., 2020) (**Fig. 8, panel 19**). Interestingly, the knockout of the microglial Hv1proton channel increase A2 astrocytes via ROS/STAT3 pathway, pointing out at their intricate relationship (Li et al., 2023b). Moreover, microglia -derived IL-1β during remyelination leads to the expression of LIF by astrocytes which promotes OLs survival (Butzkueven et al., 2002).

4.3.4.3. Intrinsic capacities of oligodendrocytes

In addition to all the signals from surrounding cells, OLs are capable of self-regulation by secreting growth factors in an autocrine manner and by upregulating intrinsic genetic programs to promote remyelination. OPCs express pro-myelinating factors such as FGF, IGF-1, and PDGF known to promote their migration and differentiation. Interestingly, they also produce VEGF-A, which usually triggers angiogenesis and promotes BBB repair after inflammatory damage. It can here promote OPC migration by inducing actin reorganization through a ROS-dependent mechanism (Hayakawa et al., 2011; Peferoen et al., 2014). RNA sequencing analysis of OPC gene expression revealed an upregulation of the cholesterol synthesis pathway modulated by estrogen signaling for myelin sheath synthesis (Voskuhl et al., 2019). Interestingly, pre-myelinating OLs upregulate the microRNA miR-27a during remyelination, inhibiting their final maturation into mature OLs by suppressing

myelinogenic signals (Tripathi et al., 2019). Overall, OLs also play a role in regulating remyelination following myelin disruption.

4.4. Technological modalities of the project

4.4.1. Intravital microscopy

4.4.1.1. Two-photon laser scanning microscopy

Intravital microscopy is a powerful technique allowing visualization of living cells in their native environment. Compared to the optical properties of conventional light microscopy, two-photon laser scanning microscopy (2P-LSM) enables the assessment of cellular responses in deep tissues of living animals. Combined with surgical implantation of cranial or dorsal windows on fluorescent transgenic mice for longitudinal chronic imaging, 2P-LSM has provided impressive advances in understanding the dynamic of cellular events *in vivo* (Fenrich et al., 2013a; Goldey et al., 2014; Buttigieg et al., 2023) (**Fig. 9A**).

Principle and benefits of 2P-LSM. Compared to conventional confocal microscopy, 2P-LSM allows the acquisition of deeper tissues and displays an improved signal-to-noise ratio with reduced phototoxicity. It relies on the simultaneous excitation of two photons by near-infrared lasers absorbed in a single event. Therefore, the excitation wavelength required is approximately twice as the one used in conventional light microscopy. Thus, the probability of photon/fluorophore interaction is increased and the quality of fluorescence detection, especially at the center of the focus, is increased (Benninger and Piston, 2013). This is further enhanced by the use of a pulsed laser source through a high numerical aperture which concentrates the photons at the focal plane, thereby increasing the likelihood that two or more photons will interact simultaneously with a single fluorophore. The significant reduction of the background noise compared to confocal microscopy is explained by its ability to solely excite the focal plane. Moreover, the reduced scattering of infrared photons enables to penetrate deeper in tissues and induces minimal perturbation in living animals with reduced v of phototoxicity and photobleaching, and increased the imaging depth capacity. Indeed, CNS parenchyma can be imaged approximatively to 1.2 mm depth (Theer et al., 2003).

Biological applications. 2P-LSM has been used to study a variety of glial cells in the spinal cord, including oligodendrocytes, microglia, and astrocytes. In a non-exhaustive way, cell dynamics during inflammatory demyelination could have been unraveled such as innate immune cells or glial cells involvement and highlighting their key contribution during disease progression (Caravagna et al., 2018; El Waly et al., 2020) but also cell interaction or cellular events during remyelination (Greenberg et al., 2014; Ronzano et al., 2021). 2P-LSM can be employed to achieve photoactivation

as well. The well-defined volume of excitation allows optically based stimulation experiments. Thus, neurotransmitter trafficking has been studied in living tissues such as in the case of the optical activation of GABAergic currents in neurons to map the $GABA_AR$ distribution at the cell surface (Matsuzaki et al., 2010).

4.4.1.2. Coherent Anti Stoke Raman Scattering (CARS) microscopy.

Conventionally, *in vivo* studies of the myelin sheath dynamic were achieved through the injection of myelin-specific dyes or the employment of transgenic mouse lines where myelin-specific promoters such as PLP drives the expression of a fluorescent protein (GFP, YFP, CFP) (Sobottka et al., 2011; Monsma and Brown, 2012). The development of Coherent Anti Stoke Raman Scattering (CARS) microscopy has revolutionized the field of neurodegenerative diseases by enabling myelin-free labeling imaging.

CARS methodology and advantages. CARS microscopy is a nonlinear optical imaging technique that relies on the coherent Raman scattering of two photons to generate an image (**Fig. 9C**). It is a non-destructive free-labeling imaging technique that prevents photodamage and toxicity to tissues, is spectrally easy to distinguish from the background, and is capable of 3D-sectioning (Li et al., 2020a). The CARS signal arises from the vibrational coherence of endogenous molecules. This type of microscopy requires two laser beams (pump and Stokes beam), which are spatially and temporally synchronized to excite the sample. When these two beams interact with the sample, they create a new beam called anti-stokes with a specific wavelength and a frequency equal to the difference between the frequencies of the pump and Stokes beams (Li et al., 2020a). In this way, CARS induces a symmetrical vibrational signature of CH_2 bonds contained in lipids. As a lipid-rich membrane, CARS microscopy enables the collection of a specific and quantifiable label-free signal of the myelin sheath (Poulen et al., 2021). Therefore, CARS microscopy is a valuable technique for deciphering myelin dynamics during neurodegeneration and CNS repair.

CARS microscopy and neurodegenerative Biology. As described above, the implementation of CARS microscopy to study the myelin sheath provided new insights into neurodegenerative mechanisms. This technique permits deep live imaging within a few hundred of microns with fast recording and is therefore valuable for capturing the dynamic of myelin lipid composition as well as myelin sheath thickness (Wang et al., 2005). Moreover, myelin undergoes gradual degeneration during demyelination that can be classified into different steps regarding the *in vivo* state of the sheath (El Waly et al., 2020). CARS imaging in active demyelinating lesions can monitor the stage of myelin degeneration, providing insight of myelinated axon density and the quantity of myelin debris within the lesion environment (**Fig. 9B**). CARS microscopy is also a powerful tool to determine effectiveness of therapy on remyelination (Turcotte et al., 2016). Moreover, multimodal imaging

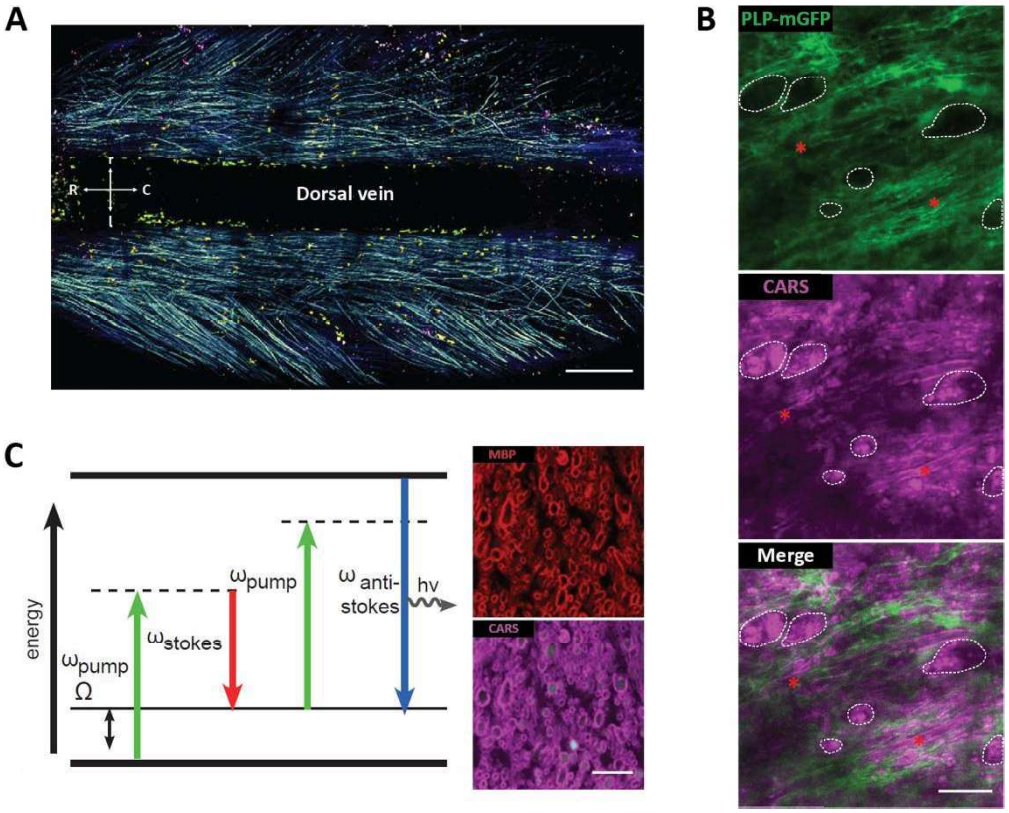

Figure 9. Non-linear two-photon and Coherent Anti Stoke Raman Scattering (CARS) microscopies to monitor cell dynamic and myelin content *in vivo*

A. Longitudinal view section of implanted window on the dorsal spinal cord of fluorescent transgenic mouse offering a large view of parenchyma to monitor deep-tissue cell dynamics in healthy and demyelinating conditions (Thy1-CFP axons (blue); LysM-EGFP innate immune cells (green); CD11c-YFP activated microglia (yellow)). **B.** Compared to transgenic mice (PLP-mGFP mice express GFP in the myelinating oligodendrocyte membranes), which allow for the visualization of the intact myelin sheath, CARS not only provides insight into the density of myelinated axons but also reveals myelin and lipid debris within the environment following a myelin insult (red stars show myelinated axons imaged with both modalities while white dashed lines refer to myelin debris only acquired by CARS microscopy). **C.** Physical principal of CARS microscopy. CARS provides accurate information on the state of myelination as depicted by the near perfect match between MBP immunostaining and CARS contrast (*unpublished data*).

using CARS microscopy combined with 2P-LSM can be even more valuable to address neurodegenerative questions. When choosing the appropriate wavelength, the living tissues or the samples can be acquired simultaneously by CARS and 2P-LSM to provide twice as much information at once. Thus, CARS can be overlaid onto the specific transgenic fluorescent signal of the myelin sheath to distinguish between the intact sheath and the accumulation of degenerated myelin debris (**Fig. 9B**). In the same way, myelinated axons and their interaction or dynamic with other cell types along the disease progression can be described (Shi et al., 2011; El Waly et al., 2020).

4.4.2. Transcriptomic approach – Next-generation sequencing

In the past, analysis of gene expression was based on "low-throughput" methods such as northern blots or quantitative PCR. These approaches limit the assessment to a specific gene of interest. Nowadays, the emergence of transcriptomics enables to investigate the whole-genome or specific genes through sequence-based approaches which provide the transcript sequences. The development of next-generation sequencing (NGS) represents a transformative leap in the realm of genomics. NGS platforms can sequence millions of fragments simultaneously, enabling a more efficient and comprehensive understanding of genomes and their functionalities, supported by the parallel development of powerful computing facilities and advanced statistical analysis methods. This approach is useful for the comprehension of neurodegenerative disease and provides insight into gene expression variability in MS to understand de- and remyelination mechanisms and further develop new therapeutic strategies.

4.4.2.1. RNA sequencing methodology.

NGS enables transcriptomic analysis sequencing of complementary DNA (cDNA) (Wang et al. 2009). This method called "RNA sequencing" allows to determine and quantify gene expression or the identification of novel transcripts, and allele-specific expression. This method can investigate several RNA populations such as total RNA, pre-mRNA, and noncoding RNA (microRNA and long ncRNA) depending on the depth of the sequencing method used. RNA sequencing is achieved through the cautious isolation of RNA from the tissue of interest to prevent contamination or degradation as well as stress-related gene expression, its conversion into cDNA followed by the preparation of the sequencing library, and finally, the sequencing on an NGS platform.

NGS platforms. Several NGS platforms have emerged: *Illumina sequencing* uses a sequencing-by-synthesis approach. It is a second generation of sequencing technologies using short read method (600 bp), where each fragment is attached to a unique molecular identifier and read in parallel; Ion semiconductor sequencing relies on the detection hydrogen ions released during DNA polymerization or synthesis; *PacBio* and *Oxford Nanopore* sequencing are third-generation sequencing methods and provide longer read lengths (10 kb), essential for specific applications like genome assembly. PacBio Sequencing combines fluorescent labelling of nucleotides and single-molecule real-time (SMRT) approach while Oxford Nanopore sequencing relies on the measurement of electrical currents changes induced by the passing on a single-stranded DNA through a nanopore to determine the DNA sequence (Satam et al., 2023).

Methodology and data analysis workflow. The efficiency of RNA sequencing depends on the quality of the RNA extracted from the sample to guarantee library preparation and it is determined by the RNA Integrity Number (RIN), which assesses the degree of degradation. To remove undesired

ribosomal RNA, mRNAs are further selected upon the total RNA sample population via Poly-A selection, subsequently converted to cDNA followed by library preparation and PCR amplification to finally be sequenced (Kukurba and Montgomery, 2015). The generated sequences are aligned to an annotated reference genome and assembled into transcripts to quantify gene expression. The biological relevance relies on the analysis of the differential gene expression (DEG), which informs on how cells or tissue phenotypes evolve depending of the given pathophysiologic context (**Fig. 10**).

RNA sequencing and MS pathology. Recently, the investigation of de- and remyelination in SC as well as the cells involved from a gene expression aspect provided useful insights into the regulation of these processes. Glial cells are known to be largely involved in neurodegeneration and repair. RNA sequencing of microglia during demyelination helped to define a new critical microglial state associated with an enrichment of genes involved in cytokine regulation, oxidative phenotype and phagocytosis (Zia et al., 2022). Microglia cells display heterogeneous responses to myelin injury and demonstrate their ability to orchestrate cellular interactions during repair (Plemel et al., 2020; Brennan et al., 2022). Analysis of astrocytic gene expression in EAE mice enabled deciphering gene programs promoting neuroinflammation (Jin et al., 2024). Moreover, comparison of glial cell transcriptomes permits to identify novel genes relevant for inflammatory and myelination during MS disease (Drake et al., 2023).

4.4.2.2. Cell-specific transcriptomic analysis: the RiboTag Method

RiboTag Principle. RNA sequencing allows transcriptomic analysis of cells or tissues. The Ribosomal Tagging strategy termed “RiboTag” enables the investigation of mRNA expression of a specific cell type *in vivo* (Sanz et al., 2019; Bravo-Ferrer et al., 2022). RiboTag mice harbor a modified allele (*Rpl22-HA*) inducing the expression of a hemagglutinin tag on the ribosomal subunit 60S. Crossbred with a Cre driver mouse line, the total RNA of a defined subset of cells is extracted through polysome immunoprecipitation. Therefore, this method is an advantageous tool for deciphering the transcriptomic signatures of the cells known to be involved in neurodegeneration and repair (**Fig. 10**).

RiboTag Sequencing Applications. Many studies with RNA sequencing analysis employed RiboTag strategy to decipher mRNA expression of a specific cell type, therefore making it a valuable tool to understand gene expression of glial cells in MS. This approach has been beneficial to evaluate microglia gene expression in an EAE model as well as the astrocytic pathway dysfunctions in demyelinating condition, and OLs gene expression during remyelination (Haimon et al., 2018b; Itoh et al., 2018; Voskuhl et al., 2019; Acharjee et al., 2021).

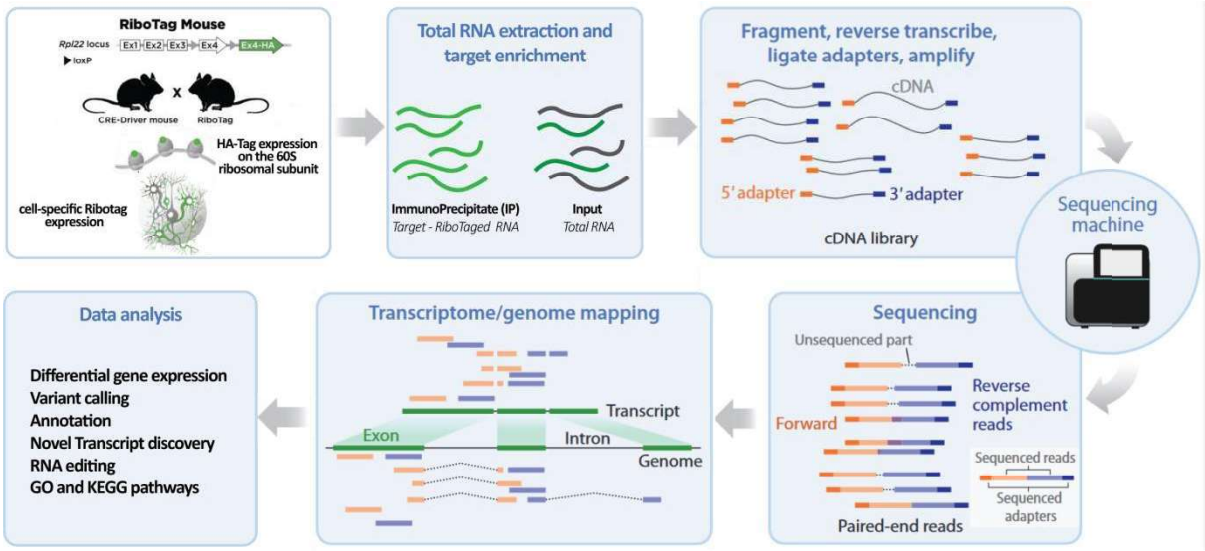

Figure 10. Workflow of RiboTag strategy for RNA sequencing

The use of RiboTag mouse line allows to perform RNA sequencing of a specific cell type. By crossbreeding it with a Cre driver line, cells of interest are isolated via immunoprecipitation, allowing specific RNA extraction (target or IP sample). These RNA molecules are pre-processed with poly-A enrichment followed by cDNA synthesis. Prior to sequencing, adapters are ligated to both ends of RNA fragments, enabling the reading by the sequencer and subsequent translation into gene sequences. These sequences are then aligned to a reference genome to determine their origin. Finally, bioinformatic analysis provides relevant information on differentially expressed genes in pathological conditions as well as dysregulated pathways (Kyoto Encyclopedia of Genes and Genomes KEGG and gene ontology GO), or enables the identification of novel genes (*modified from Sanz et al., 2019; Van den Berge et al., 2019)*.

5. AIMS OF THE STUDY

Several studies highlighted the essential role of glial cells, such as microglia and astrocytes, as well as the innate immune system in myelin injury. Collectively, these cells have the capacity to demyelination and remyelination processes, in particular by driving the fate of oligodendrocytes. However, the kinetics of recruitment of these cells to the lesion site, their inflammatory dynamics, interactions and signaling, as well as their intercellular communications along with the lesion progression until complete remyelination, are not fully understood

Therefore, the aim of this study is to decipher the time-dependent contribution of microglia, astrocytes and innate immune cells in the pathological context of de- and remyelination *in vivo*.

To this end, we organized the following work packages:

- **Uncover the dynamic effect of focal and reversible demyelination on the spinal myelin compartment**

We developed an innovative LPC-induced demyelination model based on dorsal incubation of mouse spinal tissue. Combined with window surgery implantation, we monitored the loss of myelin sheaths as well as the repair using intravital two-photon laser scanning microscopy (2P-LSM) on PLP-mGFP transgenic mice in parallel of the label-free myelin CARS microscopy, as well as its impact to neurons with the transgenic Thy1-CFP mouse line.

- **Assess the kinetics of microglia, astrocytes and innate immune cell recruitment to the demyelinated lesion site**

We investigated *in vivo* the accumulation of microglia, astrocytes and innate immune cells, respectively using the transgenic fluorescent mouse line CD11c-YFP, hGFAP-ECFP and LysM-EGFP for 2P-LSM recording, from the initial LPC myelin insult to complete remyelination.

- **Characterization of the inflammatory polarization of peripheral and CNS resident immune cells during de- and remyelination**

We examined the inflammatory phenotype in LPC treated mice using immunolabeling of spinal cross sections and quantitative real time PCR (qRT-PCR) of chosen pro- and anti-inflammatory genes on CD11c-YFP and LysM-EGFP FACS sorted cells

- **Investigation of the cell-specific translatome of OPCs, microglia and astrocytes according to lesion progression stage**

Finally, we used Cre-specific mouse lines combined with the expression of the RiboTag (60S subunit ribosomal hemagglutinin-tag) in microglia, astrocytes, and OPCs. We subsequently used the cell-specific mRNA immunoprecipitated fraction from LPC-treated mice to perform RNA sequencing. The translatome of each cell type was further evaluated through detailed bioinformatics analysis.

6. MATERIALS AND METHODS

6.1. Materials

6.1.1. Reagents

Standard chemicals were purchased from companies such as Sigma Aldrich, BD Biosciences, Eppendorf, Merck, BioRad, Invitrogen, Roche, Carl Roth, Amersham Biosciences, Serva, Thermo Fisher Scientific and BD Falcon.

6.1.2. Consumables

Pipette tips, Sarstedt; glass pipettes, VWR International; Falcon tubes, Greiner Bio-One; Eppendorf reaction tubes, Eppendorf; 96-well PCR reaction-tubes, 4titude; syringes, BD Biosciences; 48-well-culture plates, Sarstedt; object slides and cover slips, Menzel-Gläser.

6.1.3. Kits

ViewRNA™ ISH Cell Assay Kit, Invitrogen; NucleoSpin™ RNA Plus XS, Macherey-Nagel; MACs Adult Brain Dissociation Kit, mouse and rat, Miltenyi; LightCycler® 480 SYBR Green I Master, Roche;

6.1.4. Devices

Devices	Manufacturer
AxioScan Z1	Zeiss
Confocal LSM 780, 880	Zeiss
Mini star centrifuge	neoLab
Centrifuges 5418, 5804, 5430R	Eppendorf
Pipettes	Brand, Eppendorf
peqSTAR Thermo Cycler	peqlab Biotechnologie GMBH
Vortex Mixer	VWR International
Scales CPA 8201, 2245	Sartorius
Surgery, preparations and perfusion instruments	F.S.T
Magnetic stirrer C-MAG HS 7	IKA Gmbh
Consort EV231 Power Supply	Merk
Agarose and electrophoresis gel chambers	Workshop (CIPMM)
Gel documentation system	Bertin Technologie

Bead sterilisator	F.S.T
Vibratome VT1000S	Leica
Peristaltic pump LKB P-1	Pharmacia LKB
Thermomixer comfort	Eppendorf
Precellys® 24 (Homogenizer)	Peqlab Biotechnologie Gmbh
Water facility Milli-Q	Merk
Shaker DRS-12	neoLab
Mouse Transverse Clamps	Stoelting Europe
In vivo mouse microscopy support	S-PrIME platform (INT)
Surgical supports	S-PrIME platform (INT)

Table 1. List of devices

6.1.5. Buffers

All buffers were prepared with ultrapure water (ddH_20) from the MilliQ water purification system (Merk) and Ambion™ nuclease-free water (Invitrogen). All stated concentrations are final concentration.

Phosphate-buffered saline (PBS, pH 7.4)

NaCl	137	mM
KCl	2.7	mM
Na_2HPO_4	10	mM
KH_2PO_4	1.8	mM

Formaldehyde (FA, pH 7.4)

Paraformaldehyde (PFA)	4	%(w/v)
$Na_2H_2PO_4$	0.2	M
Na_2HPO_4	0.2	M

DNA extraction solution (pH 9.5)

KCl	0.25	M
Tris-HCl	0.1	M
Ethylendiamintetraacetic acid (EDTA, 0.5 M, pH 8.0)	0.01	M

Neutralization solution

Bovine Serum Albumin (BSA)	3	%(w/v)

Tris-Acetate-EDTA buffer (TAE, 50X)

Tris(hydroxylmethyl)aminomethane	1	M
Acetic acid (100%)	1	mM
EDTA	1	mM

Agarose gel in TAE buffer (1X)

Agarose powder	2	%(w/v)
Ethidium bromide	0.5	ug/ml

Immunohistochemistry

Blocking- and primary antibody buffer in PBS (1X)

Horse Serum (HS)	5	%(v/v)
Triton-X-100	0.3	%(v/v)

Secondary antibody buffer in PBS (1X)

Horse Serum (HS)	2	%(v/v)

Low salt buffer in nuclease-free water

Tris-HCl	50	mM
KCl	100	mM
$MgCl_2$	12	mM
DL-Dithiothreitol (DTT)	1	mM
Cycloheximide	0.1	mg/ml
Heparin	0.2	mg/ml
Ribonuclease inhibitor	200	units/ml
Protease inhibitor	1	X

High salt buffer in nuclease-free water

Tris-HCl	50	mM
KCl	300	mM
$MgCl_2$	12	mM
DL-Dithiothreitol (DTT)	1	mM
Cycloheximide	0.1	mg/ml
Heparin	0.2	mg/ml
Ribonuclease inhibitor	200	units/ml
Protease inhibitor	1	X

6.1.6. Drugs

Tamoxifen (Sigma-Aldrich)	10 mg/ml
Ketamine hydrochloride (Serumwerk Bernburg AG)	100mg/ml
Xylazine hydrochloride (WDT)	20 mg/ml

6.1.7. Biochemical compound

L-α- Lysophosphatidylcholine (LPC) (cat. no. L1381, Sigma-Aldrich) 12.5 mg/ml. LPC powder was dissolved in 0.9% NaCl using a manual vortex mixer (VWR International) until complete dissolution (~ 15 min). Then, the solution was aliquoted in Eppendorf tubes and kept at -20°C, no longer than a year.

6.1.8. Enzymes

RedTaq™DNA Polymerase (Sigma-Aldrich Co.)
DreamTaqTM Hot Start Green DNA Polymerase (ThermoFischer)

6.1.9. Primers

6.1.9.1. Genotyping primers

	Type	Serial Number	Sequence (5' → 3')	Product size (bp)
• **Cre inducible mouse lines**				
NGCE	WT fw	19398	GGCAAACCCAGAGCCCTGCC	WT 557 KI 829
	WT rev	19399	GCTGGAGCTGACAGCGGGTG	
	KI rev	19400	GCCCGGACCGACGATGAAGC	
CXCT	WT fw	5927	TCAGTGTTTTCTCCCGCTTGC	WT 410 KI 380
	WT rev	5929	CAGTGATGCTCTTGGGCTTCC	
	KI fw	CXCT R2 neu	ATCAACGTTTTGTTTTCGGA	
GCTF	TG fw	4750	CAGGTTGGAGAGGAGACGCATCA	WT 700 TG 517
	TG rev	7963	CGTTGCATCGACCGGTAATGCAGGC	
	WT fw	11984	GAGGCACTTGGCTAGGCTCTGAGGA	
	WT rev	11985	GAGGAGATCCTGACCGATCAGTTGG	
Nex-Cre	KI rev	2409	CCGCATAACCAGTGAAACAG	WT 770 KI 520
	WT fw	3131	GAGTCCTGGAATCAGTCTTTTTC	
	WT rev	3132	AGAATGTGGAGTAGGGTGAC	

• **Floxed mouse lines**				
RiboTag	fw	ST03799480	GGGAGGCTTGCTGGATATG	WT 243 KI 290
	rev	ST03799481	TTTCCAGACACAGGCTAAGTACAC	
RATO	KI fw	27491	CTGTTCCTGTACGGCATGG	WT 297 KI 197
	KI rev	27490	GGCATTAAAGCAGCGTATCC	
	WT fw	27488	AAGGGAGCTGCAGTGGAGTA	
	WT rev	27489	CCGAAAATCTGTGGGAAGTC	
• **Reporter mouse lines**				
CXCR	WT fw	5927	TCAGTGTTTTCTCCCGCTTGC	WT 400 KI 800
	WT rev	5929	CAGTGATGCTCTTGGGCTTCC	
	KI rev	5928	GTAGTGGTTGTCGGGCAGCAG	
GCFD	WT fw	4750	CAGGTTGGAGAGGAGACGCATCA	WT 700 TG 517
	TG rev	4749	CCAGCTTGTGCCCCAGGATGT	
PLPG	TG fw	11111	ATGCGTACCTGACTTTCTCCTTCT	WT 400 TG 750
	TG rev	11112	ACTGGGTGCTCAGGTACTGGTTGT	
	WT fw	5927	TCAGTGTTTTCTCCCGCTTGC	
	WT reV	5929	CAGTGATGCTCTTGGGCTTCC	
LysM	WT fw		AAGCTGTTGGGAAAGGAGGG	WT 220 KI 617
	KI rev		GACTGGGTGCTCAGGTAGTG	
	WT rev		TCGGCCAGGCTGACTCCATA	

Table 2. Genotyping primers list

6.1.9.2. Real Time PCR primers

Name	Type	Sequence (5' → 3')
EYFP (CD11c-)	fw	CTCTGAGTCACGCTGACAACTT
	rev	AATCAAGGGTCCCCAAACTC
Thy1(-CFP)	fw	CTGACCTGTAGCTTTCCCCA
	rev	GCTGAACTTGTGGCCGTTTA

Table 3. Real Time PCR primers

6.1.10. Antibodies

6.1.10.1. Primary antibodies

Target	Clonality	Host	Dilution	Manufacturer
Ki-67	Monoclonal	Rat	1:500	Invitrogen

PDGFRα	Polyclonal	Goat	1:500	R&D Systems
CC1	Monoclonal	Mouse	1:200	Calbiochem
iNOS	Polyclonal	Rabbit	1:100	Abcam
IL6r	Monoclonal	Rat	1:500	Abcam
HA.1	Monoclonal	Mouse	1:500	BioLegend
CD68	Monoclonal	Rat	1:500	Bio Rad
Iba1	Polyclonal	Goat	1:500	Abcam
GFAP	Polyclonal	Rabbit	1:1000	Dako

Table 4. Primary antibodies for immunochemistry

6.1.10.2. Secondary antibodies

Host α-target	Conjugated fluorophore	Dilution	Manufacturer
Donkey α-mouse	Alexa Fluor® 488	1:1000	Invitrogen
	Alexa Fluor® 555	1:1000	Invitrogen
	Alexa Fluor® 647	1:1000	Invitrogen
Donkey α-rabbit	Alexa Fluor® 555	1:1000	Invitrogen
	Alexa Fluor® 750	1:1000	Invitrogen
Donkey α-rat	Cy3	1:1000	Jackson ImmunoResearch
	Alexa Fluor® 750	1:1000	Invitrogen
Donkey α-rat	Alexa Fluor® 647	1:1000	Invitrogen

Table 5. Secondary antibodies for immunochemistry

6.1.11. Dyes

4′,6-diamidino-2-phenylindole (DAPI) (Sigma-Aldrich)	0.025	µg/ml
Ethidium Bromide (Carl Roth)	10	mg/ml
Easy Ladder (500 lines) (BioLine)	50	ng/ml

6.1.12. Genetically modified mouse lines

6.1.12.1. Tamoxifen-inducible DNA recombination

To induce reporter protein expression we employed the Cre^{ERT2}–loxP system (Feil et al., 2009). Unlike the constitutive Cre recombinase, Cre^{ERT2} is fused with a mutated estrogen ligand binding domain and restricted in the cytosol by the heat shock proteins 90 (HSP90) (Brocard et al., 1997; Metzger and Chambon, 2001). Since Cre^{ERT2} is highly sensitive to synthetic steroids such as to 4-

hydoxytamoxifen, tamoxifen administration disrupts Cre^{ERT2}/HSP90 complex leading to nuclear translocation of Cre^{ERT2} (Feil et al., 1997). Consequently, Cre^{ERT2} catalyzes DNA recombination in accordance with target sequences flanked by loxP sites (Sternberg and Hamilton, 1981; Hamilton and Abremski, 1984). Therefore, Cre^{ERT2}-loxP system enables time-controlled of DNA recombination determined by the tamoxifen administration but also cell-type specificity relying on the promoter driving the Cre^{ERT2} expression.

Mouse line	Short name	Description	MGI ID	Reference
TgH(NG2-CreERT2)	NGCE	Specific expression of inducible CreERT2 in NG2 glia (OPCs).	5566862	(Huang et al., 2014)
TgH(CX_3CR_1-CreERT2)	CXCT	Specific expression of inducible CreERT2 in microglia	6724385	(Yona et al., 2013)
TgN(hGFAP-CreERT2)	GCTF	Specific expression of inducible CreERT2 in astrocytes	4418665	(Hirrlinger et al., 2006)
TgH(Rpl22-fl-exon4-fl-exon4Ribotag)	RiboTag	Cre-mediated expression of hemagglutinin (HA) tag on ribosomes	4355967	(Sanz et al., 2009)
TgH(Rosa26-CAG-fl-stop-fl-tdTomato-WPRE)	RATO	Cre-medicated expression of tdTomato		(Madisen et al., 2010)
TgH(CX_3CR_1-EGFP)	CXCR	Expression of EGFP in microglia	2670351	(Jung et al., 2000)
TgN(hGFAP-ECFP)	GCFD	Expression of ECFP in astrocytes		(Hirrlinger et al., 2005)
TgN(PLP-EGFP)	PLPG	Expression of EGFP in cell body and processes of OLs		(Sobottka et al., 2011)
TgH(LysM-EGFP)	LysM	Expression of EGFP in myeloid cells	2654931	(Faust et al., 2000)
TgH(CD11c-EYFP)	Cd11c-EYFP	Expression of EYFP in primed microglia and dendritic cells	3835666	(Lindquist et al., 2004)
TgN(Thy1-CFP)	Thy1-CFP	Expression of CFP in neuronal compartment	3505582	(Feng et al., 2000)

Table 6. Single transgenic mouse lines

CAG, cytomegalovirus-immediate early enhancer/chicken β-actin/rabbit β-globin hybrid promoter; CreERT2, inducible Cre DNA recombinase fused to the mutant ligand binding domain of the human estrogen receptor; fl, loxP floxed site; NG2, nerve/glia antigen-2; CX_3CR_1, fractalkine receptor; hGFAP, human glial fibrillary acidic protein; Nex, neuronal helix-loop-helix protein-1; PLP, proteolipid protein; LysM, LysM domain containing 1; Cd11c, cluster of differentiation 11c; Thy1, Thymus cell surface antigen 1; lsl, floxed STOP cassette; MGI, Mouse Genome Informatics database; TgH: genetically modified mouse line via homologous targeted recombination; TgN: genetically modified mouse line via non-homologous targeted recombination.

6.1.12.2. Astrocytes-, microglia-, and OPCs-specific RiboTag expression

To assess cell-specific gene expression we took advantage of the RiboTag mouse line TgH(Rpl22-fl-exon4-fl-exon4Ribotag), in which the flowed wild-type exon 4 is replaced by hemagglutinin (HA)-

tagged exon in presence of active Cre recombinase (Sanz et al., 2009). These mice were subsequently crossbred with the following Cre^{ERT2} driver lines to obtain OPC-, microglia- and astrocyte-specific $RPL22^{HA/+}$-tagged ribosomes. In the single transgenic TgH(NG2-Cre^{ERT2}) driver line, the open reading frame of the Cre^{ERT2} protein is knocked into exon 1 of the *Cspg4* gene locus (Huang et al., 2014). The TgH(CX_3CR_1-Cre^{ERT2}) driver line contains the Cre^{ERT2} cassette inserted into the gene locus and replacing the first 390 bp of the Cx_3Cr_1 gene. The TgN(hGFAP-Cre^{ERT2}) driver line is made up of the insertion of the open reading frame for Cre^{ERT2} placed under the control of the human GFAP promoter (Hirrlinger et al., 2006). All Cre^{ERT2} mice were heterozygous (ct2/+) and treated with tamoxifen at about 12 weeks old with a daily dose for five consecutive days.

6.1.12.3. Cell-specific fluorescent reporter protein expression

Part of this study focused on *in vivo* cell dynamics followed by 2P-LSM imaging. For this purpose, we used two transgenic mouse lines. Firstly, we employed the LysM-EGFP x Cd11c-EYFP x Thy1-CFP line to monitor innate immune cells (LysM), microglia and dendritic cells (Cd11c-EYFP) and axons (Thy1-CFP). The TgH(LysM-EGFP) line contains an Enhanced Green Fluorescent Protein (EGFP) cassette knocked-in exon 1 of the *Lyz2* gene (Faust et al., 2000) while the TgH(CD11c-EYFP) line is made up of EYFP-Venus cloned into the CD11c promoter (Lindquist et al., 2004). The TgN(Thy1-CFP) has a modified Thy1.2 promoter lacking exon 3 and its flanking intron is replaced by the CFP sequence to avoid reporter protein expression in nonneural cells (Caroni, 1997; Feng et al., 2000). Secondly, we used the double transgenic hGFAP-ECFP x PLP-EGFP mouse line to label astrocytes and OLs (cell bodies and processes). The single transgenic TgN(hGFAP-ECFP) line places the fluorescent enhanced-CFP under the control of the human GFAP promoter while in the TgN(PLP-EGFP) line the EGFP expression is driven by the promoter and regulatory sequences of the *Plp1*gene (Hirrlinger et al., 2005; Sobottka et al., 2011). All the mice were heterozygous (xfp/+) for each individual transgene.

To assess the cell density and the inflammatory phenotype of the microglia cells we took advantage of the single transgenic TgH(CX_3CR_1-EGFP) mouse line. The inserted sequence of the EGFP replaces part of exon1 impairing the interaction with the endogenous ligand CX_3CL_1 (Jung et al., 2000).

The triple heterozygote CX_3CR_1-$Cre^{ERT2/+}$ x Rosa26-$TdTom^{fl/fl}$ x hGFAP-$ECFP^{xfp/+}$ was used to study glial cell proliferation. The TgH(Rosa26-CAG-fl-stop-fl-tdTomato-WPRE) reporter line carries the expression of the fluorescent protein tdTomato under the control of the cytomegalovirus-immediate early enhancer/chicken β-actin/rabbit β-globin hybrid promoter (pCAGGs) (Niwa et al., 1991) and inserted into the ubiquitous *Rosa26 locus* (Friedrich and Soriano, 1991). The woodchuck hepatitis virus posttranscriptional regulatory element (WPRE) enhances the mRNA stability (Madisen et al., 2010).

6.1.13. Software

ZEN blue imaging software was used for 2P-laser scanning microscopy (Zeiss); *in vivo* data and immunohistological data were blindly and manually quantified with ImageJ collection Fiji and analyzed with GraphPad Prism 8 and Microsoft Office Excel 2016. The Adobe Creative Suite 2021 (Adobe InDesign®, Adobe Illustrator®, Adobe Photoshop®) was used for figure layout. Bibliography research was done on PubMed of the National Center for Biotechnology Information (NCBI) website. Mice administration was operated with Maya Kind® from FLPG Software society at the Institut de Neurosciences de la Timone (INT, France) and PyRAT Animal Facility Software from Scionics Computer Innovation at the Center of Integrative Physiology and Molecular Medicine (CIPMM, Germany).

6.1.14. Graphical elements

The figures 1, 2, 3, 5, 7, 8, 10, 11, 12, 16 (panel E), and 18 (panel E) in this manuscript included graphical elements generated with Biorender (https://biorender.com/).

6.2. Methods

6.2.1. Genotyping

Tail biopsy or ear punch samples were collected from weaned pups at about 3 weeks of age and incubated with 62.5 µl DNA extraction solution for 10 min at room temperature (RT). Then, the samples were immersed in a water bath at 95°C for 20 min and 50 µl of neutralization solution was added. For genotyping, the extracted DNA samples were diluted 1:10 in ddH2O with DreamTaqTM Hot Start Green DNA Polymerase (ThermoFisher) and oligonucleotides primers (**Table 2**). The PCR reactions were run in 96-well PCR plates in peqSTAR ThermoCyclers (PeqLab Biotechnologie). Gel electrophoresis was run on 1-3% agarose gel with ethidium bromide (0.015%) and, subsequently exposed and documented with the Quantum Gel documentation system (peQlab Biotechnologie).

6.2.2. Tamoxifen treatment

Tamoxifen administration was performed by the animal caretakers at the animal facility of the Center for Integrative Physiology and Molecular Medicine (CIPMM, Homburg). At about 12 weeks of age, mice were daily i.p. injected with tamoxifen (100 mg/kg body weight) for five consecutive days to

induce maximal DNA recombination (Jahn et al., 2018). Experiments were conducted on the animals three to four weeks after TAM injection and analyzed at corresponding time points of the experimental design.

6.2.3. Whole body fixation

Animals were lethally anesthetized with ketamine (250 mg/kg body weight) and xylazine (50 mg/kg) diluted in 0.9% NaCl. After heart exposition done by bilateral axillary thoracotomy, the animals were transcardially perfused using a butterfly needle inserted into the left ventricle with a pre-incision in the superior vena cava to drain off the blood. Then, 10 ml of 1x PBS followed by 15 ml of 4% FA (5 ml/min) were injected. Spinal cord was subsequently dissected and post-fixed in 4% FA overnight at 4°C. The tissues were stored until use at 4°C in 1x PBS.

6.2.4. Immunohistochemistry

The fixed spinal cords were sliced with a vibratome VT1000S (Leica) into sagittal (50 µm), longitudinal (35 µm), and coronal (35 µm) sections and collected in 48-well culture plates with 1X PBS. Free floating-slices were first incubated for 1h with the blocking buffer (5% HS, 0.3% Triton X in 1x PBS) at RT. Slices were then incubated with the primary antibody diluted in a blocking buffer solution at 4°C overnight. The next day, sections were washed in 1x PBS (three times, 10 min) and incubated in the dark for 2h with the secondary antibody and DAPI diluted in secondary-antibody buffer (2% HS in 1x PBS) (**Table 4, 5**). Finally, the SC slices were washed in 1x PBS (three times, 10 min) and mounted on glass slides in Shandon ImmuMount (ThermoScientific).

6.2.5. Quantitative real time PCR

Animals were lethally anesthetized with ketamine (250 mg/kg body weight) and xylazine (50 mg/kg) diluted in 0.9% NaCl. They were subsequently perfused as described with 1x PBS until complete blood draining and cold sterile Hank´s balanced sodium solution without Ca^{2+} and Mg^{2+} (HBSS, GibcoTM, Thermo Fisher Scientific). Spinal cords were extracted 4, 7, or 14 days after LPC treatment, dissected manually, and spinal tissues were subsequently dissociated using the MACs Adult Brain Dissociation Kit, mouse and rat (Miltenyi Biotec, Paris, France). $EGFP^{+}$ cells were sorted using FACS (fluorescence-activated cell sorting) into lysis buffer 10:1 mix of Resuspension Buffer and Lysis Enhancer from CellsDirect™ One-Step qRT-PCR Kit (Thermo Fisher Scientific, United States). The RNA was extracted following the above kit's protocol and the reverse transcription reactions were performed using 5 µg total RNA. Polymerase chain reaction reactions were completed

in 20 µL of SuperScript™ II reaction buffer (Invitrogen, United States) (0.01 M dithiothreitol, 7.5 ng/µL of dN6, 20 U of RNase inhibitor (Invitrogen, United States), 10 mM dNTP and 200 U of SuperScript™ reverse transcriptase (Invitrogen)) for 1 h at 42°C. Then, Real-time PCR reactions were achieved with the LightCycler® 480 SYBR Green I Master kit (Roche, United States), by mixing 2 µL of cDNA with 200 nM of each PCR primer. Each reaction was performed in triplicate.

6.2.6. RNA extraction and purification

Animals were lethally anesthetized and perfused with 1x PBS until complete blood draining and cold sterile Hank´s balanced sodium solution without Ca^{2+} and Mg^{2+} (HBSS, GibcoTM, Thermo Fisher Scientific). The dorsal part of the spinal cord segment under the window was dissected, subsequently frozen in liquid nitrogen (LN_2), and stored at -80°C (maximum two months). The RNA extraction procedure was performed on two consecutive days. On the first day, tissues were thawed on ice, and low salt buffer (10% w/v) and beads are added to each sample to homogenize the tissues with the homogenizer Precellys® 24 (Bertin Technologies). After centrifugation (10.000 g, 10 min at 4°C) to remove cell debris, the supernatants were incubated 4h with an anti-HA.1 antibody (cat. no. 901513, BioLegend) at 4°C under slow rotation. Then, samples were incubated with Dynabeads protein G (cat. no. 10003D, Thermo Fischer Scientific) overnight at 4°C under slow rotation (maximum 12h). On the second day, samples were washed (three times, 10 min) with high salt buffer and the buffer was removed using a magnetic support. The following RNA purification was performed using the NucleoSpin™ RNA Plus XS kit (Macherey-Nagel) according to the manufacturer's instruction. The extracted RNA quantity was measured with a Spectrophotometer / Fluorometer (Ds-11 fx, Denovix) and stored at -80°C until the shipment to the company for sequencing (Novogene (UK) Company Limited) (**Fig. 11, steps 3 and 4**).

6.2.7. RNA sequencing

The RNA library preparation as well as the sequencing was performed by Novogene Company (Cambridge, UK). First, the samples underwent initial quality control where the RNA Integrity Index (RIN) was assessed. RIN values, which reflect RNA quality on a scale of 1 to 10 (10 indicating the highest quality), were used as criteria for sample processing. Only samples with a RIN value ≥ 6.8 were included in further steps (**Fig. 11, step 5**). Then, the pre-processing "Poly-A enrichment" step isolated mRNA from the total RNA pool. This enrichment relies on the affinity of the poly-A tails, located at the 3' end of mRNA molecules, to short thymine sequences attached to magnetic beads. Subsequently, mRNAs were fragmented, and cDNA synthesis was performed. This was achieved by converting the mRNA template into a cDNA strand using a reverse transcriptase enzyme and a short oligo-dT primer. After end repair and A-Tailing, fragmented cDNA strands were used to create a

sequencing library by ligation of sequencing adapters to both ends of cDNA fragments providing specific binding sites for the sequencer (NovaSep 6000, Illumina). The ligated cDNA fragments were then amplified using polymerase chain reaction (PCR) and, quality control of the library was done before proceeding with the sequencing. The first read of the NovaSeq sequencer began with one end of the cDNA fragment (150 bp) and consisted of fluorescently labeled nucleotide incorporation, emitting a unique fluorescent signal for each nucleotide. After the second read (reverse strand, 150 bp), the files containing the fluorescent signals recorded during sequencing were converted into sequences of bases (A, T, C, G) for both reads to reconstruct the full sequence of the RNA molecule (**Fig. 11, step 6**). Finally, these sequences were aligned to a reference genome to determine their origin (**Fig. 11, step 7**).

6.2.8.Surgery

Animals were implanted with a spinal cord window based on the protocol published by (Fenrich et al., 2013b). Mice were anesthetized with Ketamine (120 mg/kg body weight) and Xylazine (12 mg/kg), monitored by no pedal reflex in response to a firm toe pinch. Animals were kept on a heating pad and eyes hydration preserved by application of Bepanthen or ocrygel ophthalmic ointment (Bayer and TVM Lab). Instruments were sterilized in a hot-bead sterilizer (FST) and the skin disinfected with a povidone-iodine solution (Betaisodona, Mundipharma or Vetedine® Solution, Vetoquinol). Shortly, dorsal skin was longitudinally open over vertebrates T11 to L1, and the mouse was placed into transverse clamps support (Stoelting Europe, S-PrIME platform (INT)) to lift up the spine flatly. Once the muscles on either side of the spine were removed, the spine was fixed with modified staples and a paperclip sealed with dental cement. Vertebras (T12/13) were bilaterally removed by laminectomy while preserving the integrity of the spinal cord (SC) and meninges. To induce focal demyelination, 1% lysophosphatidylcholine (LPC) (dissolved in NaCl 0.9%) was incubated at the SC surface through a calibrated aperture of the dura mater (El Waly et al., 2020). After an hour of incubation, LPC was washed away with 1x PBS. Control animals were incubated with 1x PBS (3x, 2 min). Finally, Kwik Sil™ Low toxicity and bio-compatible silicone adhesive (World Precision Instruments) was applied on exposed parenchyma and covered with a custom cut cover slip sealed with dental cement (**Fig. 12B**). Mice received anti-inflammatory drugs administration (dexamethasone (0.2 mg/kg, i.p.) and

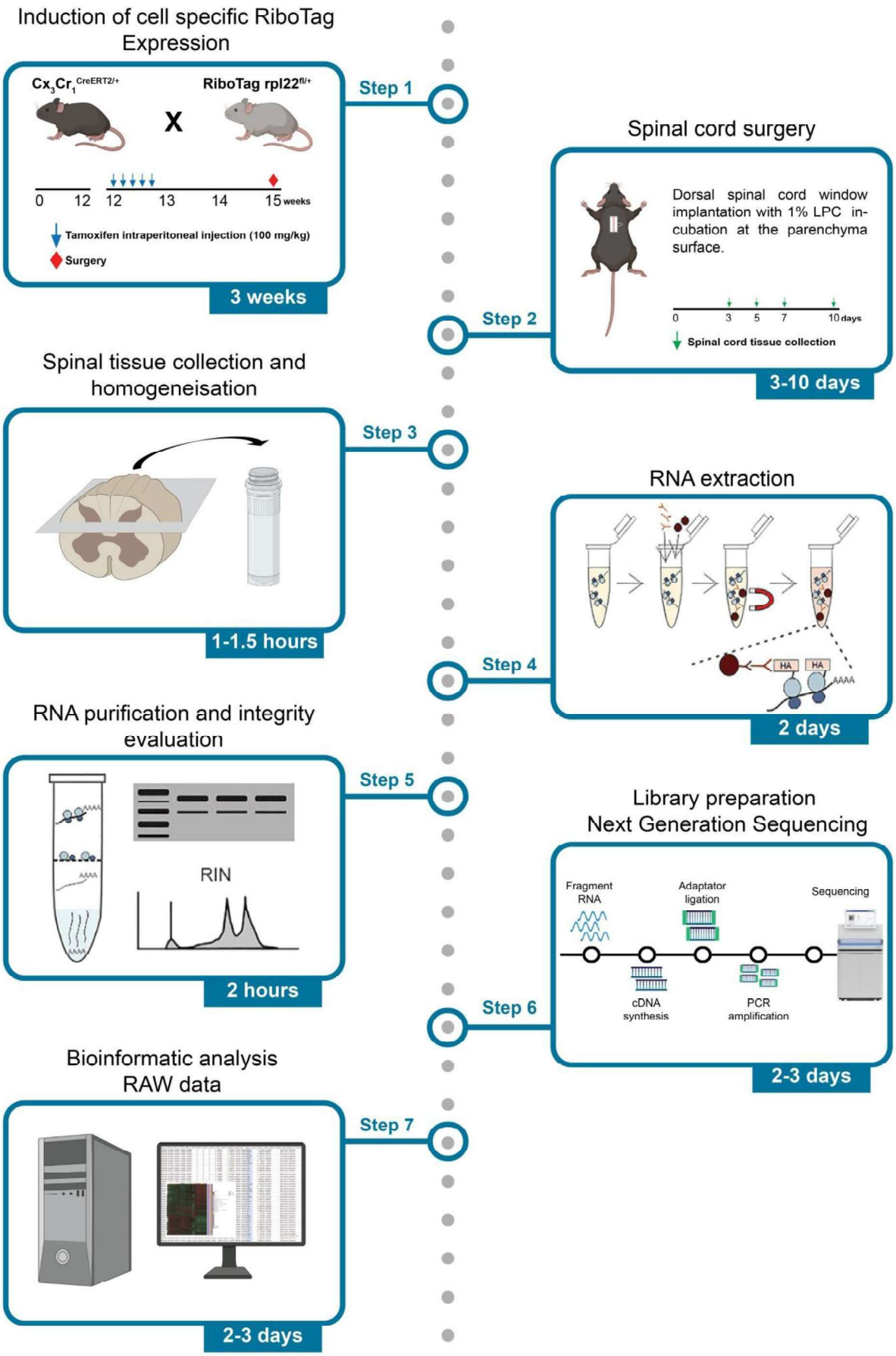
Induction of cell specific RiboTag Expression
Cx3Cr1 CreERT2/+
RiboTag rpl22 fl/+
X
0 12 12 13 14 15 weeks
Tamoxifen intraperitoneal injection (100 mg/kg)
Surgery
3 weeks
Step 1
Spinal cord surgery
Dorsal spinal cord window implantation with 1% LPC incubation at the parenchyma surface.
0 3 5 7 10 days
Spinal cord tissue collection
3-10 days
Step 2
Spinal tissue collection and homogeneisation
1-1.5 hours
Step 3
RNA extraction
HA
HA
AAAA
2 days
Step 4
RNA purification and integrity evaluation
RIN
2 hours
Step 5
Library preparation
Next Generation Sequencing
Fragment RNA
Adaptator ligation
Sequencing
cDNA synthesis
PCR amplification
2-3 days
Step 6
Bioinformatic analysis
RAW data
2-3 days
Step 7

Figure 11. RiboTag RNA sequencing strategy

After crossbreeding of the RiboTag mouse line to cell specific CreERT2 driver line (step 1), animals were implanted with a spinal cord window and treated with LPC to induce focal demyelination (step 2). Tissues were collected at various time points (3, 5, 7 and 10 days post-surgery) (step 2 – 3) and total RNA extraction was performed (step 4). The samples were then sent to Novogene Company which validated the RNA quality and integrity before proceeding with the sequencing (steps 5 – 7). *Modified from Bravo-Ferrer et al., 2022)*.

carprofen (5 mg/kg, i.p.) and, an analgesic treatment (Buprenorphin (0.1 mg/kg, i.p.) in accordance with veterinary recommendations.

6.2.9. Microscopy

6.2.9.1. In vivo two-photon laser scanning microscopy

In vivo recording was achieved using a laser scanning microscope (LSM) 780 on a static Axio Examiner Z1 (Carl Zeiss), equipped with Ti:Sapphir femtosecond pulsed laser, Ultra II (Coherent) with a tuning range of 680 to 1080 nm and a compact optical parametric oscillator (OPO, Coherent A.P.E) for automated wavelength extension of Ti:Sapphir laser to 1300 nm. The microscope is supplied with a thermoregulated opaque chamber at 30°C to maintain the mice's body temperature with a tubing system to keep the animal under anesthesia (isoflurane, 1.5%) if needed. The custom-made motorized plate (S-PrIME platform, INT) placed inside the chamber allows to accommodate the mouse imaging support and automated tiling mode acquisition controlled with ZEN imaging Software (Zeiss). The mouse imaging support (S-PrIME platform, INT) was designed to enable fine tunes positioning of the dorsal spinal cord window. The window can be adjusted laterally and, in a rostro-caudal position to get the window and field of view as flat as possible (**Fig. 12B**). The same volume of interest in the spinal parenchyma was repeatedly imaged over time through the window to follow the dynamics of cellular events in a reproducible way (**Fig. 12C**). The laser excitation wavelength was set at 940 nm, with power adjustment according to the depth of tissue acquired and using a W Plan-Apochromat 20x/1.0 DIC M27 75 mm objective (421452-9600, Zeiss). The complete spinal cord window area, from the surface to the depth, was recorded with the tiling mode (10% overlap) with a Z-scaling of 3 µm and, a resolution of 512 x 512 pixels per image with a pixel dwell time of 3.15 µs. The fluorescent signals were collected to the objective using an LP775 dichroic mirror (Semrock) and detected by specific photomultiplier tube depending on their spectral band. Thus, Thy1-CFP mice were acquired using a Band Pass filter (BP) of 390/485 nm, PLP-EGFP with a BP 498/512 nm and, CD11c-YFP with a BP 520/549 nm (**Fig. 12A)**.

6.2.9.2. *Automated epifluorescence microscopy on fixed spinal cord sections*

Immunostained spinal cord sections mounted on glass slides were scanned with the AxioScan.Z1 automatic scanner (Zeiss). This is an epifluorescence microscope equipped with a LED light source (Colibri 7, Zeiss) with 10x / 0.45 and 20x / 0.8 Plan-Apochromat objectives and operated using ZEN blue 2.3 software (Zeiss). Z-Stack images were acquired (5 µm stacks, variance projection) with appropriate filter sets (**Table 6**).

Dye	Excitation (nm)	Beam splitter (nm)	Emission (nm)
DAPI	353	405	410 - 440
Alexa Fluor 488	475	495	503 - 537
Alexa Fluor 546/ 555	567	573	580- 611
Alexa Fluor 633/ 647/ Cy5	630	652	661 - 703
Alexa Fluor 750	735	762	770 - 800

Table 6. List of filter sets for the Axioscan Z1

6.2.10. Data analysis

6.2.10.1. *Immunohistochemistry data*

Cells of interest were individually quantified in the region of interest (ROI), determined by the accumulation of cells on the lesion site. IHC and ISH slices were analyzed in stack acquisitions respectively in 5 µm and 10~14 µm depth. Mice used to assess the cell specify of RiboTag expression were quantified in the entire dorsal half part of the slice consistent with the segment of the spinal cord tissue used for the RNA sequencing. All data analysis of cell density were done blindly and manually quantified with ImageJ collection Fiji using the cell counter plugin at least three slices for each mouse and a minimum of three mice per group were analyzed.

6.2.10.2. *In vivo 2P-LSM acquisition*

$CD11c^+$ microglia cells, $LysM^+$ innate cells, and $GFAP^+$ astrocytes were manually quantified on 2P-LSM *in vivo* acquisitions. Two ROIs were drawn on the acquired parenchyma on each side of the dorsal vein with one of them containing the LPC-induced demyelinating lesion. Cells were counted with the cell counter plugin from ImageJ collection Fiji software, from the first one discernible at the surface of the tissue to the most ventral one, between 30 and 105 µm of depth due to macroscopy variability. The analyzed volume was normalized for all animals to 0.01 mm^3.

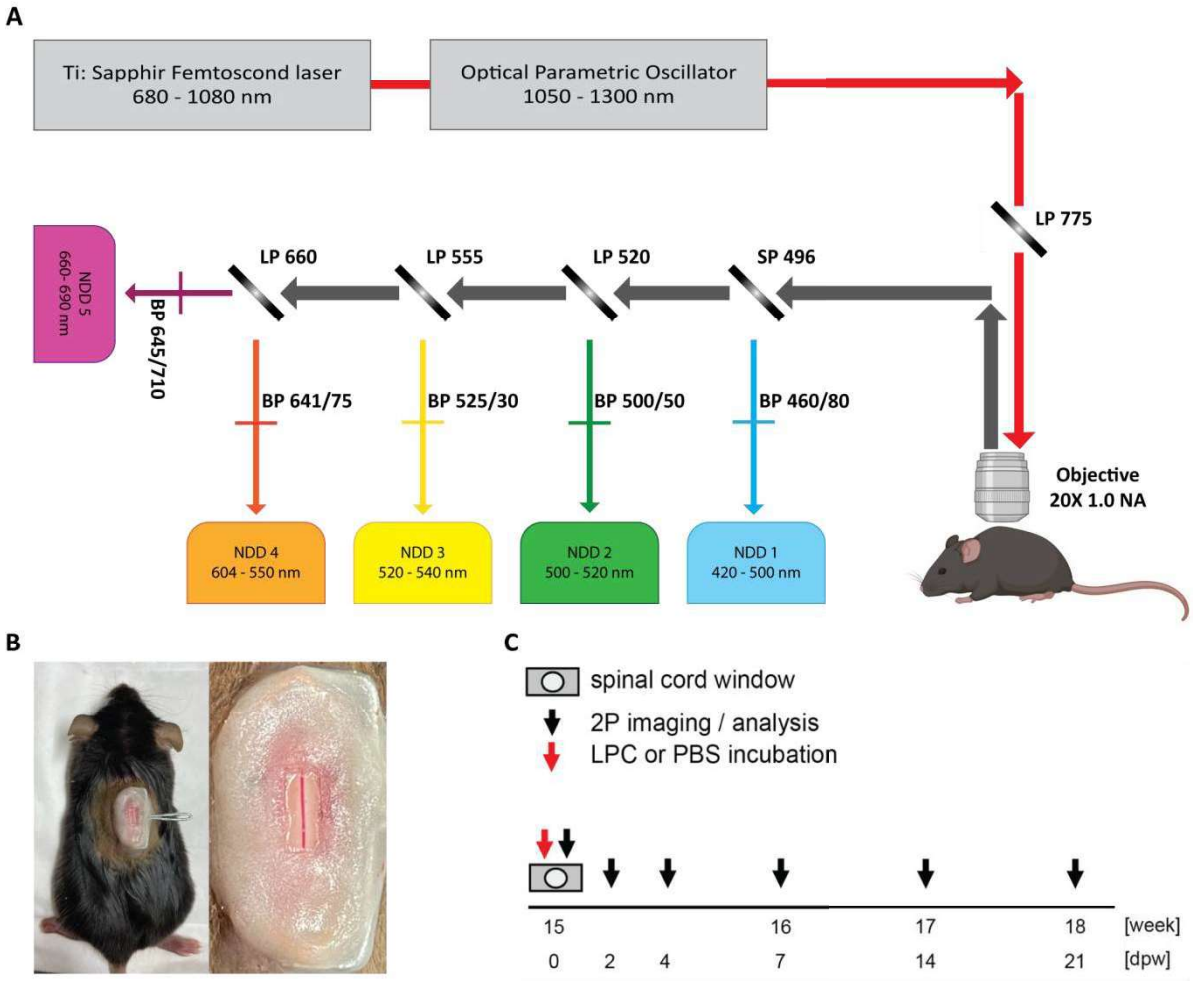

Figure 12. *In vivo* two-photon laser scanning microscopy

A. Schematic view of the 2P-LSM 780 optic path. The visible signal, separated from the infrared light by the dichroic mirror (LP 775), is sent to the detection chain, which consists of three PMTs (NDD 1 - 3) and two GaAsP detectors (NDD 4 - 5). GaAsP detectors have improved sensitivity and signal-to-noise ratio compared to traditional PMTs. LP: Long Pass dichroic mirror / Beamsplitter; SP: Short Pass dichroic mirror / Beamsplitter; BP: Band Pass filter; NDD: Non-Descaned Detection. **B.** Superior view of a spinal cord window after surgery and ready for *in vivo* imaging. **C.** Protocol of chronic *in vivo* imaging of LPC-induced demyelinated mice and control mice up to 21 days post-surgery. Dpw: days post window.

The *in vivo* myelination rate was assessed by measuring the area of interest overlapping with the fluorescent signal of the PLP-EGFP mouse line. A specific threshold was defined for each acquisition to avoid background noise and non-specific signals. The percentage of area covered by the EGFP signal was calculated by averaging the individual values of the two ROIs (as previously defined).

6.2.10.3. RNA sequencing

Raw sequencing data in fastq format were processed with the nf-core/rnaseq [XYZ] pipeline v3.12.0 using Star-Salmon against the GRCm39 mouse genome and v110 of the Ensembl gene annotations. Expression values were then imported into R and processed with DESeq2 v1.44.0 [XYZ]. Low

expressed genes (< 20 median normalized reads across samples per cell type) were removed, leaving 14.654, 14.459, 13.923 genes for astrocyte, oligendendrocyte, and microglia samples, respectively. Genes were deemed differential when they had Benjamini-Hochberg-adjusted p-value < 0.05. No effect size threasholding was applied. Enrichments of gene sets for Gene Ontology terms, KEGG pathways, etc were determined with gprofiler2 v0.2.3 against all default databases. Only terms with FDR-adjusted p < 0.05 were considered.

6.2.11. Statistical analysis

Statistical analysis was conducted using GraphPad Prism 8. Datasets were initially assessed for normality using the Shapiro-Wilk normality test. Based on the results, appropriate parametric or non-parametric statistical procedures were applied. Outlier detection was performed using GraphPad Prism's Rout method (Q = 1%). Data are presented as mean ± SEM, and detailed test information is provided in the corresponding figure legends. The following p-values were employed for statistical comparisons: * p < 0.05; ** p < 0.01; *** p < 0.001; **** p < 0.0001.

6.2.12. Mouse administration and veterinary licenses

Mice administration was performed with Maya Kind® software (FLPG Software Society) in France and the PyRAT Animal Facility software (Python-based Relational Animal Tracking, Scionics Computer Innovation) in Germany. The animals were housed and bred at either the Center for Integrative Physiology and Molecular Medicine (CIPMM, Homburg) or the Institut de Neuroscience de la Timone (INT, Marseille), in strict accordance with the European, German, and French guidelines for the welfare of experimental animals. Animal experiments received ethical approval from the Saarland state's 'Landesamt für Gesundheit und Verbraucherschutz' in Saarbrücken, Germany (license numbers: Perfusion 2020, 36/2016, 07/2021, 08/2021), as well as from the “Direction Départementale des Services Vétérinaires” and the ethics committee in France (ID numbers #18555-2019011618384934 and A1305532) for the animal facility and research project, respectively.

7. RESULTS

7.1. Spinal incubation of lysophosphatidylcholine (LPC) induced focal and reversible demyelination associated with transient axonal loss

7.1.1. LPC triggered death of myelinating oligodendrocytes *in vivo* leading to neurodegeneration

Demyelination is a process that profoundly affects the CNS cellular homeostasis. To study the cellular processes occurring in spinal cord (SC) demyelination, we used a murine model of focal and reversible demyelinating lesion by incubating the surface of the spinal parenchyma with lysophosphatidylcholine (LPC), thereby preserving the axons from the mechanical degeneration induced by its injection (Fenrich et al., 2013b; El Waly et al., 2020). To this aim, we used *in vivo* chronic two-photon laser scanning microscopy (2P-LSM) through an implanted spinal cord glass window on Thy1-CFP^{+} transgenic mice, in which neuronal axons are fluorescently labelled and we were able to follow axonal density in the same volume of interest (VOI) over weeks after LPC treatment. In addition, we employed Coherent anti-Stokes Raman spectroscopy (CARS) as a reliable tool to visualize myelin content - irrespective of its structure organization (Gasecka et al., 2017) - since Thy1^{+} axons are myelinated in the dorsal SC (**Fig. 13A**). While CARS myelin signal remained stable over time in PBS-incubated CTL mice (*data not shown*) LPC incubation reliably triggered fast demyelination within two days upon application that extended massively to reach a loss of ~58 % of its initial value between D4 and D7 (**Fig. 13B**). Myelin loss was concomitant to axonal degeneration. We quantified axonal density following the initial LPC insult within the same VOI equivalent to a 400 µm square with a depth of 100 µm (0.016 mm^3) and we found that ~56% of Thy1^{+} axons were already lost at D2. This Wallerian degeneration of axons further extended until D4 to ~72% of loss (**Fig. 13B**). In comparison, the axonal degeneration process was faster than myelin degradation, probably enhanced by the absence of myelin insulation or the myelin debris in the environment. Conversely, axonal density started to recover earlier than myelin by the end of the first week, but only ~57% of its initial value was regenerated compared to ~80% for the CARS signal, ultimately both being fully restored by D28 (**Fig. 13A, B**). This time difference between axons and the myelin sheath recoveries could be attributed to independent regulation of neuronal and oligodendroglial processes during remyelination and repair. In addition to the myelin-dependent CARS signal we used PLP-mGFP mice expressing membrane-bound GFP selectively in OLs to further confirm the impact of LPC on the myelinating oligodendrocytes (mOLs) (**Fig. 13C**). These observations supported our previous results and shown a significant reduction of the *in vivo* myelin coverage. Myelinated surface shrunk by ~35% to ~31% of the surface covered by the sheath between D4 and D7 and reached full

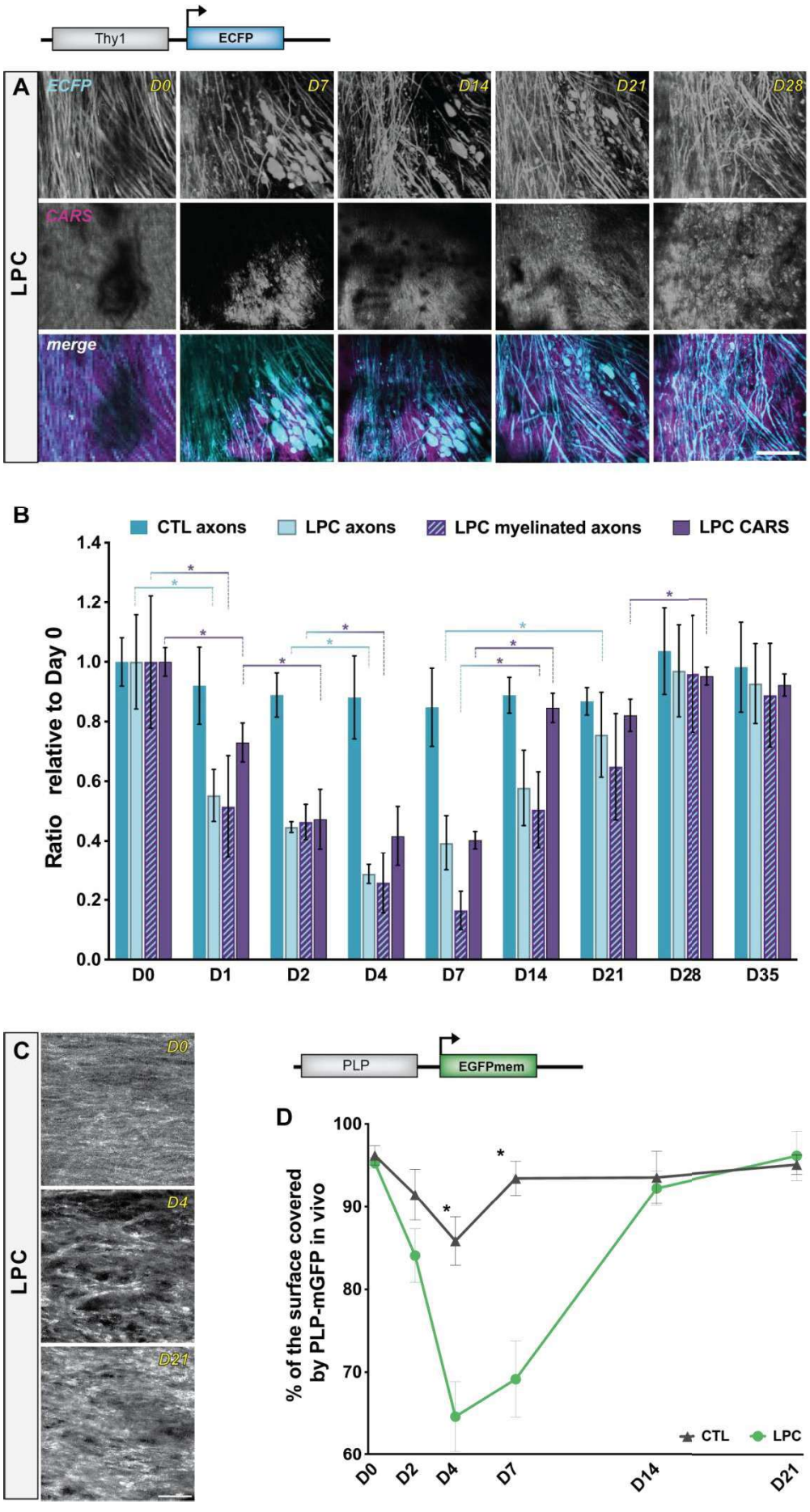
Thy1
ECFP
A
ECFP
D0
D7
D14
D21
D28
CARS
merge
LPC
B
CTL axons
LPC axons
LPC myelinated axons
LPC CARS
Ratio relative to Day 0
1.4
1.2
1.0
0.8
0.6
0.4
0.2
0.0
D0
D1
D2
D4
D7
D14
D21
D28
D35
C
LPC
D0
D4
D21
PLP
EGFPmem
D
% of the surface covered by PLP-mGFP in vivo
100
90
80
70
60
CTL
LPC
D0
D2
D4
D7
D14
D21

Figure 13. Spinal incubation of lysophosphatidylcholine (LPC) triggered efficient demyelination *in vivo* followed by spontaneous remyelination

A. 2P-LSM *in vivo* monitoring of the myelin content (CARS signal) and Thy1$^+$ axons within the same volume of interest after LPC treatment at days (D) 0, 7, 14, 21 and, 28. Scale bar, 200 µm. **B.** Quantitative analysis of axon density and myelin-dependent CARS signal inside LPC lesion. **C.** 2P-imaging of membrane-tagged GFP (PLP-mGFP transgenic mice) reflecting myelin density within the same VOI of LPC-incubated spinal cord at D0, 4 and, 21. Scale bar, 500 µm. **D.** Quantification of *in vivo* myelin loss (up to ~35 % at 4 and 7 days post-LPC) after LPC or PBS incubation and recovery (14 and 21 days post-LPC). Panels A and B *modified from El Waly et al., 2020*.

recovery by D28, emphasizing an efficient remyelination of axons (**Fig. 13D**). Analysis on cross-section of fixed SC of the impact of LPC on the oligodendrocyte lineage revealed a transient decrease of CC1$^+$ mature OLs at D2 compared to the baseline and CTL group. Conversely, PDGFRα$^+$ cells density was unchanged indicating that number of OPs was not affected, consistent with the reported effect of LPC selectively on mature OLs (**Fig. 14**).

Altogether, these data highlight the efficient ability of the LPC mouse model to induce myelin degeneration and repair in a defined sequence of time and follow molecular and cellular events during demyelination and remyelination.

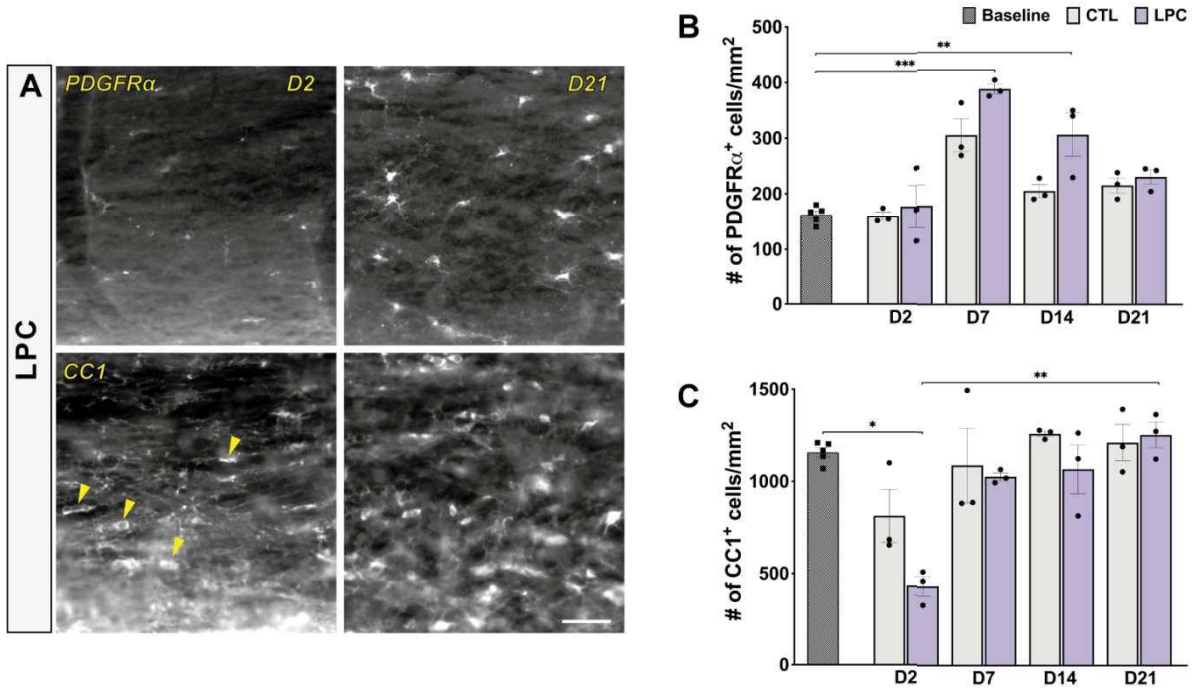

Figure 14. Lysophosphatidylcholine (LPC) induced specific transitory cell death of myelination OLs

A. Immunofluorescence labelling of OL precursor cells (PDGFRα) and mature OLs (CC1) on spinal cross-sections of LPC treated mice. Scale bar, 50 µm. **B-C.** Quantitative analysis of PDGFRα and CC1 marker densities in the dorsal white mater describing initial loss of mature OLs followed by the proliferation of OPCs with return to baseline levels (healthy spinal parenchyma) three weeks post-LPC.

7.1.2. Myelin disruption led to morphological and cellular modifications

Our previous data showed the intricate relationship of myelin sheath and axons. Therefore, we decided to investigate fine modification of myelinated axon morphologies following LPC incubation and potentially reflecting its disrupting action on OLs and axons. Based on *in vivo* 2P-LSM acquisitions, we could identify eight typical morphology features of demyelination. These patterns can be classified into two categories: early events (events 1 to 4) and advanced events (events 5 to 8) (**Fig. 15A**). They can be described as follow: (1) healthy axons and myelin sheath with smooth and linear shape; (2) axons and surrounding sheath present curvy distortions; (3) axons and myelin show bubble-like swelling deformation; (4) axons are fragmented into bubbles with gaps inside a straight myelin sheath; (5) axon bubbles are encircled by the swelling sheath; (6) axons and myelin formed disconnected bubbles structures; (7) mixture of solely myelin bubbles or including degenerated axon fragments; (8) circular myelin debris. Quantifying the occurrence of these events revealed that on the day of LPC incubation (D0), 28% of the axons already displayed pathological mechanical stress with swelling structures, highlighting the rapid detergent effect of LPC on myelin and axonal compartments. After one week, all axons presented a diseased-like condition and only displayed advanced events. Indeed, myelinated axon bubbles and myelin debris each represented ~47%. However, the ratio of these events decreased in parallel as the lesion resolved until D35. Pattern 7 appeared to be transient as observed only at D7 and D14, while the events 6 to 8 seemed to be characteristic of the early demyelination stage. Finally, the proportion of healthy axons gradually increased by 59% between D14 and D35, consistent with the axonal repair process observed in our previous data (**Fig. 15B**). The time-lapse analysis on *in vivo* recordings accurately demonstrated the dynamic of transitioning from one event to another (**Fig. 15C**). While first distortions of axons appeared in few minutes post LPC incubation (**Fig. 15C, top panel**), a shift from early to advanced events can occur within the same range of time (**Fig. 15C, lower panel**), pointing out the rapidity of the degeneration process once initiated in SC. Furthermore, the time-codded images for both CARS and CFP enabled to decipher that the disturbance of the myelin sheath preceded axonal deformation.

Collectively, our results enabled to identify numerous morphological modifications of the myelin sheath and associated axons appearing after the induction of the demyelination. Thus, their precise classification and arising time could inform, just by looking at the aspect of these cellular compartments, on the evolutionary stage of the demyelinating lesion.

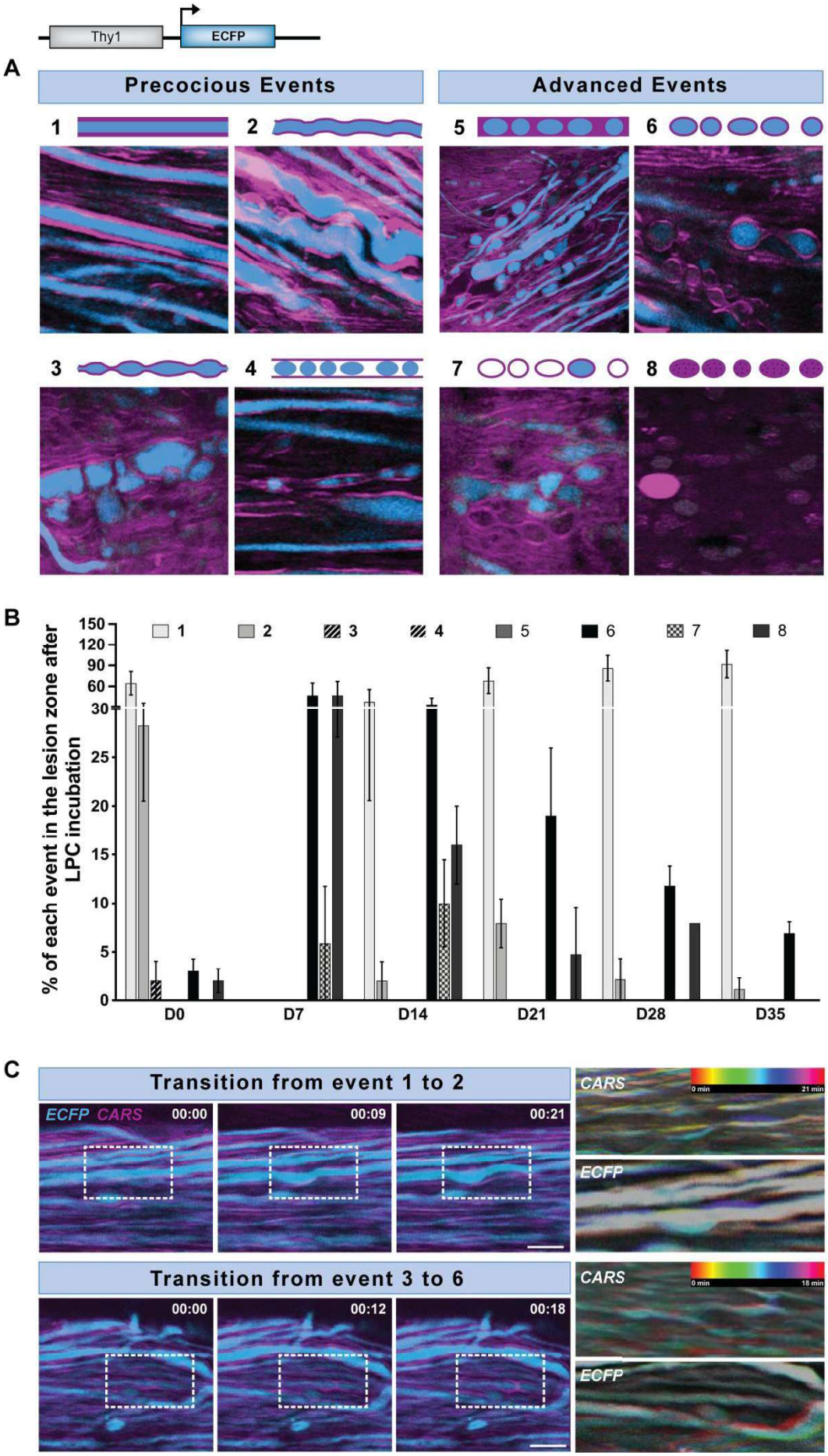
Thy1
ECFP
A
Precocious Events
Advanced Events
1
2
3
4
5
6
7
8
B
% of each event in the lesion zone after LPC incubation
150
120
90
60
30
25
20
15
10
5
0
D0
D7
D14
D21
D28
D35
C
Transition from event 1 to 2
ECFP CARS
00:00
00:09
00:21
CARS
0 min
21 min
ECFP
Transition from event 3 to 6
00:00
00:12
00:18
CARS
0 min
18 min
ECFP

Figure 15. The LPC treatment induces specific patterns of myelin sheath disruption and axonal degeneration classified into eight categories

A. Schematic representation of the molecular events identified in LPC lesions juxtaposed with corresponding 2P-LSM *in vivo* acquisitions showing the myelin sheath (CARS signal, magenta) and Thy1$^+$ axons (cyan). Scale bar, 100 µm. **B.** Quantification of the occurrence of each individual event within the lesioned parenchyma during 35 days following the initial LPC insult. **C.** Time-lapse of event transitions (from 1 to 2, top – from 3 to 6, bottom) highlighting myelin (CARS signal) and Thy1$^+$ axon (ECFP) fine morphological modifications. Scale bar, 100 µm. Figure *modified from El Waly et al., 2020.*

7.2. Innate immune cells and glial cells were recruited at the onset of demyelination and orchestrated lesion resolution

7.2.1. LysM$^+$ immune cells invaded spinal demyelinated parenchyma in two waves

Demyelination is known to involve peripheral infiltrating immune cells with functional inflammatory capacities (Chu et al., 2019; McMurran et al., 2019). To further evaluate the dynamic of these innate immune cells within the LPC demyelinating lesion, we used the double transgenic mouse line Thy1-CFP x LysM-EGFP. In these mice, the EGFP is constitutively expressed in myelomonocytic cells as monocytes, neutrophils granulocytes, as well as macrophages throughout their lifetime. Using 2P-LSM, we monitored these EGFP$^+$ cells within LPC-induced demyelination lesions over a period of five weeks (**Fig 16A**). In comparison to PBS incubated CTL mice, where the EGFP$^+$ cell density was stable over time, in LPC treated mice EGFP$^+$ cells significantly accumulated in the lesion at D4 resulting in a six-fold increase of their density compared to D0 (**Fig 16B**). Their involvement is transiently decreased at D7, preceding a second massive wave of cells accruing within the lesioned parenchyma at D14. Finally, EGFP$^+$ cells gradually dwindle until D28, coinciding with the end of axonal repair. In this line, we further investigated the impact of the inflammatory cells on the axonal compartment. We found that EGFP$^+$ cells and axons densities were both linearly correlated across the different time points (**Fig 16C**). During the first week, animals exhibiting lower EGFP$^+$ cell densities were found to have a greater number of axons. However, axonal regeneration was more efficient in animals with high EGFP$^+$ densities at D14 and D21. Therefore, these data emphasized that the two waves identified *in vivo* after LPC treatment may be composed of cells with distinct inflammatory properties. To further extend our comprehension of the inflammatory phenotypes of EGFP$^+$ cells, we performed a qRT-PCR on FACS sorted LysM-EGFP$^+$ cells (**Fig. 16D**). We accessed six pro-inflammatory (pro-I) genes (TNF-α, CD86, CD32, CD16, Nos2 and, IL-6) and six anti-inflammatory (anti-I) genes (TGF-α, IGF1, Arg1, CD206, IL-10) together with the neutrophil marker Ly6G (**Fig. 16E**). Interestingly, most of the pro-I genes were actively expressed at D7 such as TNF-α, CD32, CD16, Nos2 and, IL6 in contrast to anti-I gene expression which were up regulated at D14. Noteworthy, Ly6G expression dropped after D4 indicating that the first wave seems to be enriched in inflammatory neutrophils.

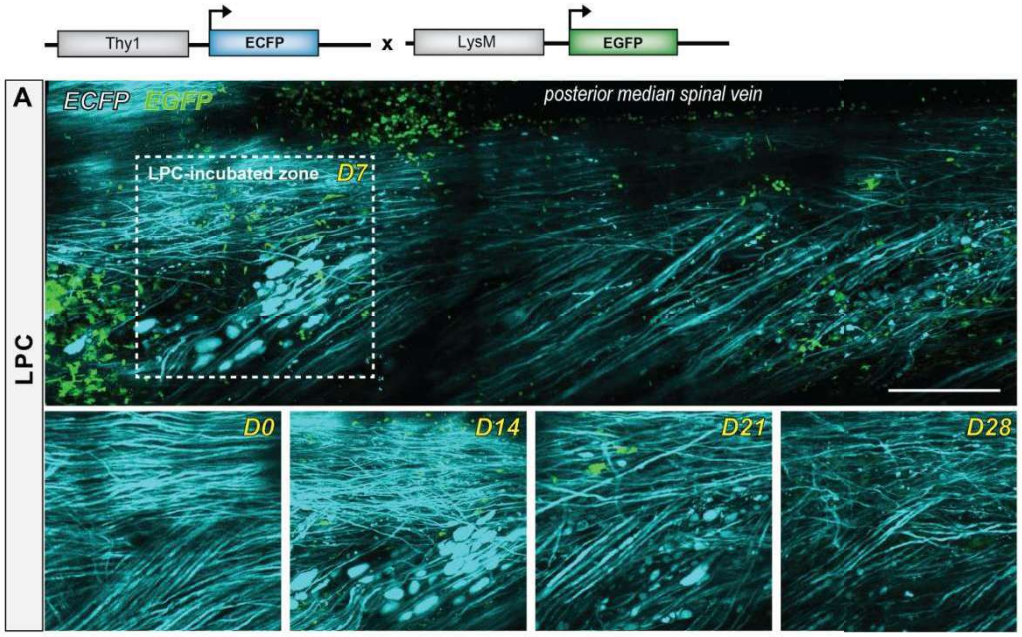
Thy1
ECFP
x
LysM
EGFP
A
LPC
ECFP EGFP
posterior median spinal vein
LPC-incubated zone D7
D0
D14
D21
D28

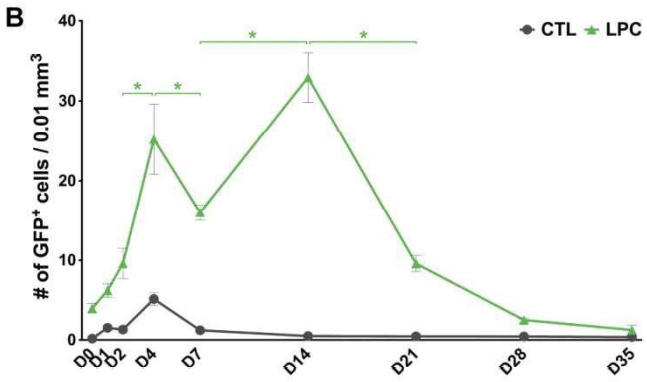
B
CTL
LPC
# of GFP+ cells / 0.01 mm3
D0
D1
D2
D4
D7
D14
D21
D28
D35

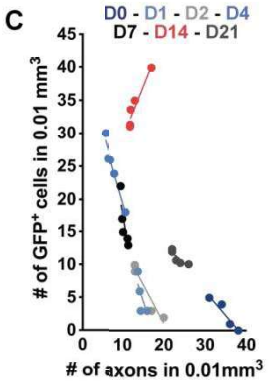
C
D0 - D1 - D2 - D4
D7 - D14 - D21
# of GFP+ cells in 0.01 mm3
# of axons in 0.01mm3

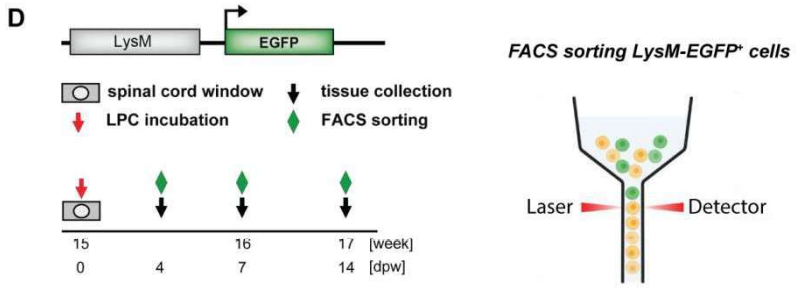
D
LysM
EGFP
spinal cord window
tissue collection
LPC incubation
FACS sorting
15
16
17
[week]
0
4
7
14
[dpw]
FACS sorting LysM-EGFP+ cells
Laser
Detector

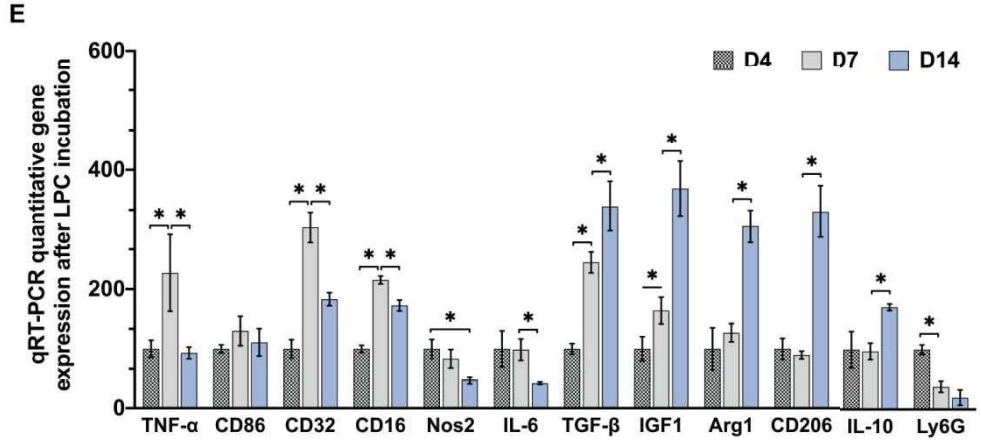
E
D4
D7
D14
qRT-PCR quantitative gene expression after LPC incubation
TNF-α
CD86
CD32
CD16
Nos2
IL-6
TGF-β
IGF1
Arg1
CD206
IL-10
Ly6G

Figure 16. Myelin sheath disruption induces two waves of infiltrating EGFP$^+$ immune cells with different inflammatory phenotypes

A. *In vivo* 2P-LSM acquisitions of the same VOI over time reveal Thy1-ECFP$^+$ axons and the infiltration of LysM-EGFP$^+$ immune cells to the lesion. Scale bar, 200 µm. **B.** Quantification of EGFP$^+$ cells infiltrating the dorsal spinal cord in LPC and PBS incubated mice between day (D) 0 and D35. **C.** Correlative analysis of GFP$^+$ cells and axonal density within the LPC lesion. **D.** Schematic protocol of EGFP+ innate immune cells isolation. Mice were implanted with a spinal window following LPC incubation and the SC were collected at D4, D7, and D14 and FACS sorted based on their EGFP fluorescence. dpw: day post-window. **E.** Quantitative reverse transcription-PCR on LysM-EGFP FACS sorted cells of pro- (TNF-α, CD86, CD32, CD16, Nos2 and, IL-6) and anti-inflammatory (TGF-β, IGF1, Arg1, CD206, IL-10) gene expression and the neutrophil marker (Ly6G) gene expression post-LPC and normalized to D4. Figure *modified from El Waly et al., 2020.*

Our data described the involvement of innate immune cells occurring in two waves during demyelination and remyelination, respectively. The cells composing the first wave displayed a pro-I phenotype deleterious for axonal survival, while the second wave of infiltration supports repair through an anti-I phenotype.

7.2.2. Astroglia and microglia were involved with different time-scales at the lesion site

Microglia and astrocytes are the main glial cells involved following a myelin insult and act inflammatory mediators capable of driving demyelination and remyelination processes (Coutinho Costa et al., 2023). To decipher how their recruitment is modulated *in vivo* subsequently to LPC-induced demyelination, we used two mouse lines, CD11c-YFP and hGFAP-CFP, labelling a subset of activated microglia and astrocytes respectively to monitor the cell dynamics using 2P-LSM (**Fig. 17A, C**). Since previous data showed spontaneous remyelination and repair within three weeks, we focus our analysis from D0 to D21. The investigation of CFP$^+$ and YFP$^+$ cell densities within the same VOI revealed distinct time-dependent patterns of glial cell recruitment. At the onset of demyelination, YFP$^+$ microglia were recruited faster to the myelin insulted site, with an increased number of cells already observed at D2. On the other hand, the recruitment of the CFP$^+$ astrocytes, was delayed until D4 within the lesion site. Both cell types exhibited the highest cell density at D7. However, while CFP$^+$ cell involvement remained relatively high and stable until D21, the density of YFP$^+$ cells drastically decreased after D7, eventually showing no difference compared to the PBS-incubated CTL group at D21 **(Fig. 17B, D)**. Interestingly, the comparison of both glial cell densities over time sowed that the recruitment of microglia cells was much more important. Between D4 and D14, when the recruitment of both cell types was significant, the density of microglia was almost twice as high as that of astrocytes within the active LPC lesion. (**Fig. 17E**). We further extended our analysis of microglial dynamics throughout the spontaneous resolution of the lesion using the CX_3CR_1-EGFP$^+$ mouse line, which labels microglia with EGFP independently of their activation state (**Fig. 17F**). Quantification of EGFP$^+$ cells on fixed spinal cross-sections demonstrated a cell density four times

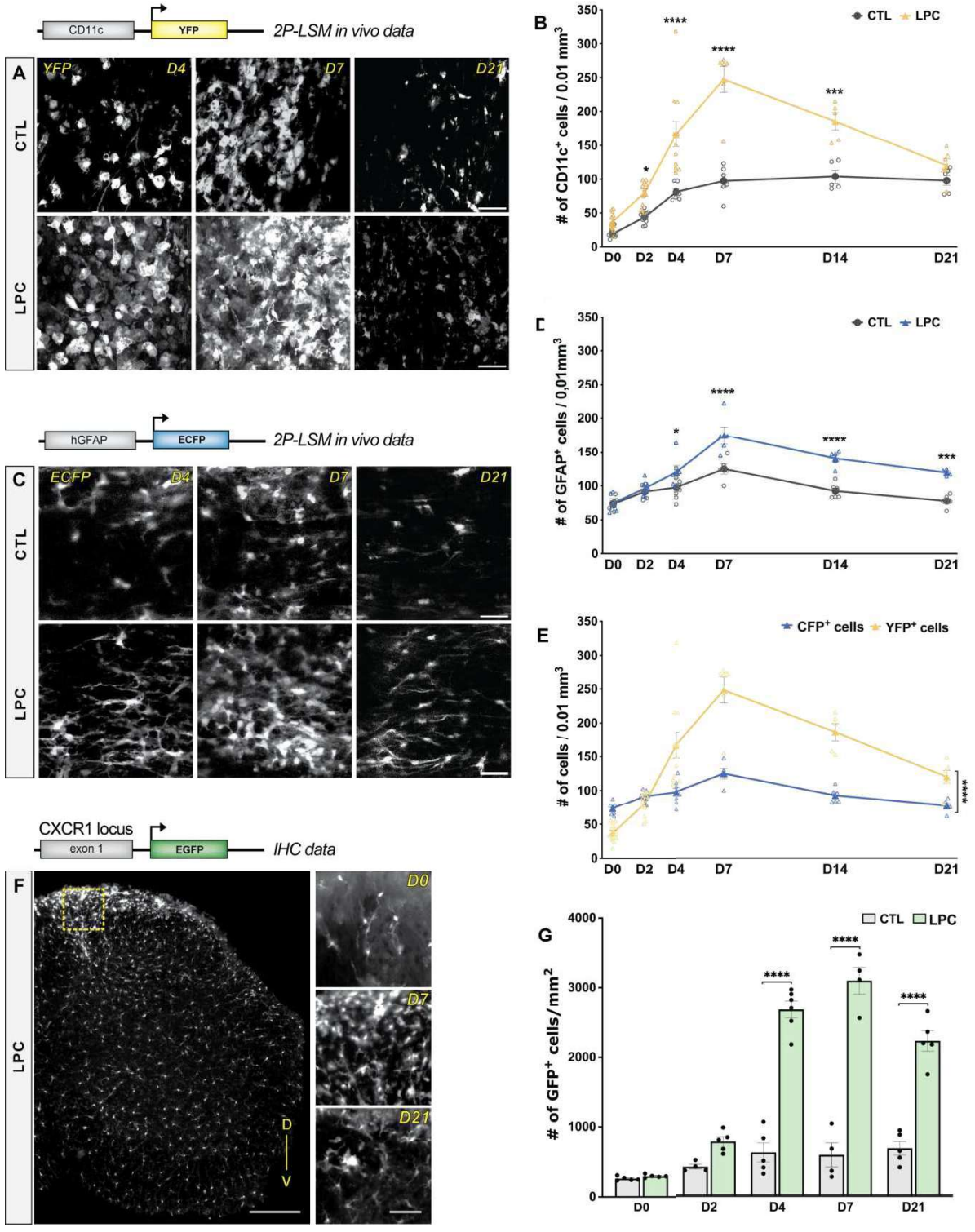

Figure 17. Microglia and astrocytes exhibit distinct time scales of involvement during the evolution of LPC-induced demyelinating lesion

A-C. Chronic *in vivo* 2P-LSM acquisitions of dorsal white matter Cd11c-YFP^{+} cells (panel A.) and hGFAP-CFP^{+} cells (panel C.) within the same region of interest reveals massive recruitment of activated microglia and astrocytic cells inside LPC-induced lesion compared to CTL PBS incubated mice. Scale bar, 100 µm. **B-D.** Quantifications of YFP^{+} cells (panel B.) and CFP^{+} cells (panel D.) densities in the same lesioned volume of interest describe time-dependent involvement of glial cells (full and empty symbols respectively represent total mean of animals and each individual) **E.** Comparison of Cd11c-YFP^{+} cells and hGFAP-CFP^{+} cells densities

within the LPC-induced demyelinating lesion *in vivo* (respectively from panel B and D). **F.** Epifluorescence acquisitions on cross-sections of CX_3CR_1-EGFP transgenic mice showing the evolution of GFP^+ cell density at 4, 7, and 21 days post-LPC treatment. Scale bar, (left panel) 200 µm and, (right panels) 50 µm. **G.** Quantification of GFP^+ cells reveals their significant accumulation four days after the initial LPC insult and, persistence until full recovery at D21.

higher compared to the CTL group at D4 (**Fig. 17G**). In contrast to $CD11c^+$ microglia, the involvement of $CX_3CR_1^+$ microglia was sustained until D21, emphasizing an intense but transient involvement of the activated microglial subset within demyelinating context.

Therefore, microglia cells and astrocytes are both recruited during demyelination until complete remyelination and repair. However, the specific subset of activated microglia expressing CD11c, although exhibiting transient activity over time, appears to exert its action earlier during the initial demyelinating events. Additionally, it would be interesting to understand whether the increase in glial cell number within the lesion is due to the recruitment of distant cells in the spinal parenchyma or from an extensive proliferation of cells that were initially involved within the lesioned area

7.2.3. Microglia cells modulated their inflammatory phenotype according to myelin status

After a myelin insult, microglia are known to release various inflammatory cyto- and chemokines. Thus, the fate of the lesion depends on their inflammatory phenotype, with a pro-inflammatory phenotype worsening demyelination and axon loss, while an anti-inflammatory phenotype promoting remyelination and repair. Therefore, to better understand the microglial phenotype following LPC lesion, we performed immunolabeling of fixed spinal cord tissue of CX_3CR_1-EGFP mice with two pro-inflammatory markers, IL6R and iNOS (**Fig. 18A**). We quantified the number of $EGFP^+$ cells expressing either IL6R or iNOS or both within the lesion area (on average 0.05 mm^2) between D0 and D21 (**Fig. 18B-D**). In comparison to PBS-incubated CTL mice, LPC treatment rapidly induced the appearance of $EGFP^+$ $iNOS^+$ $IL6R^+$ microglia cells at D2, whereas $EGFP^+$ $IL6R^+$ $iNOS^-$ and $EGFP^+$ $iNOS^+IL6R^-$ were delayed at D4. Interestingly, among these three different microglial subtypes, only the subtype $EGFP^+$ $iNOS^+IL6R^-$ was still significantly expressed at D21. Moreover, its cell density was two to three times higher than the other two subtypes, possibly indicating a greater importance, especially during remyelination and repair. To further elucidate the microglial inflammatory phenotype, we analyzed their gene expression by qRT-PCR on FACS CD11c-YFP^+ sorted cells (**Fig. 18E**). We examined the expression of six pro-I genes (TNF-α, CD86, CD32, CD16, Nos2 and, IL-6) and six anti-I genes (TGF-β, IGF1, Arg1, CD206, IL-10) at 4, 7 and, 14 days after LPC incubation (**Fig. 18F**). We observed that TNF-α, CD32 and CD16 gene expression

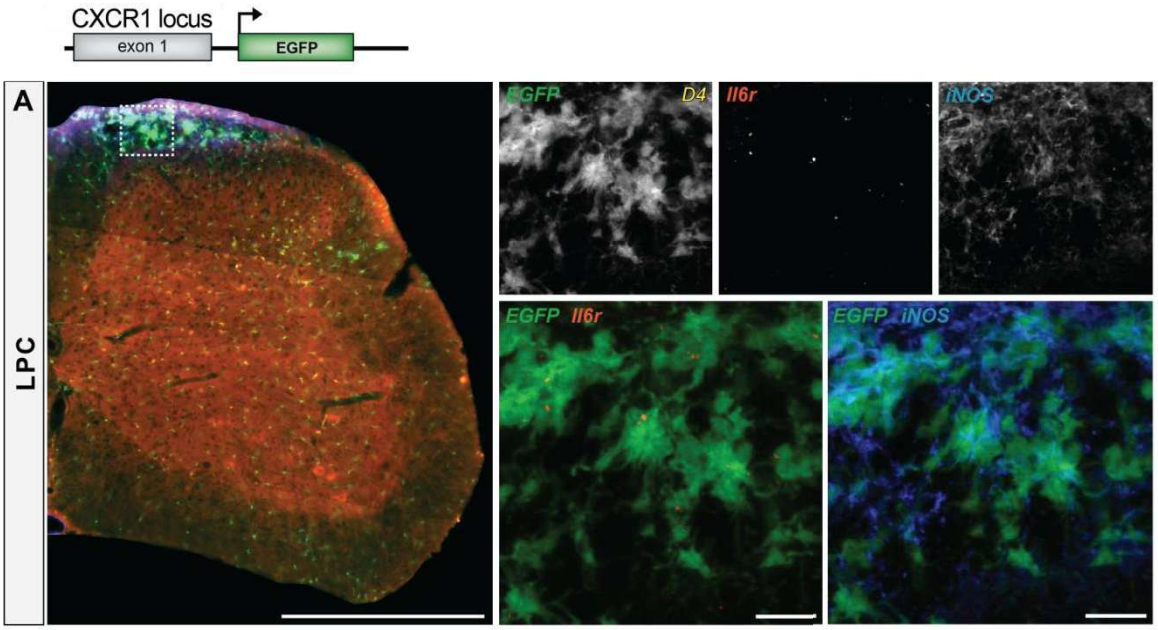
CXCR1 locus
exon 1
EGFP
A
LPC
EGFP
D4
Il6r
iNOS
EGFP Il6r
EGFP iNOS

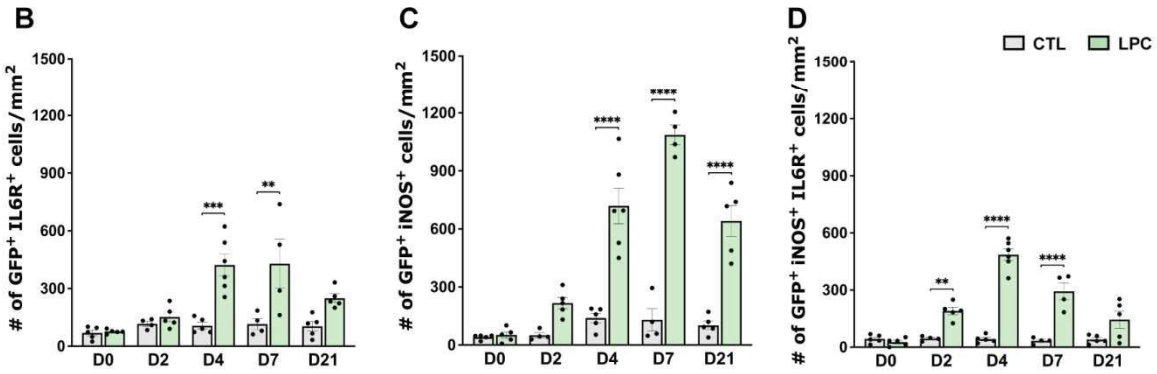
B
# of GFP+ IL6R+ cells/mm2
C
# of GFP+ iNOS+ cells/mm2
D
# of GFP+ iNOS+ IL6R+ cells/mm2
CTL
LPC
D0
D2
D4
D7
D21

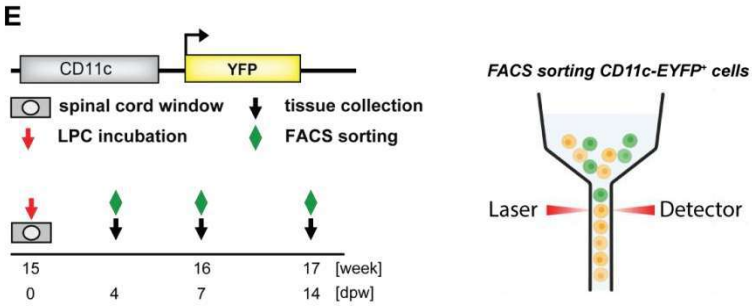
E
CD11c
YFP
spinal cord window
tissue collection
LPC incubation
FACS sorting
15
16
17
[week]
0
4
7
14
[dpw]
FACS sorting CD11c-EYFP+ cells
Laser
Detector

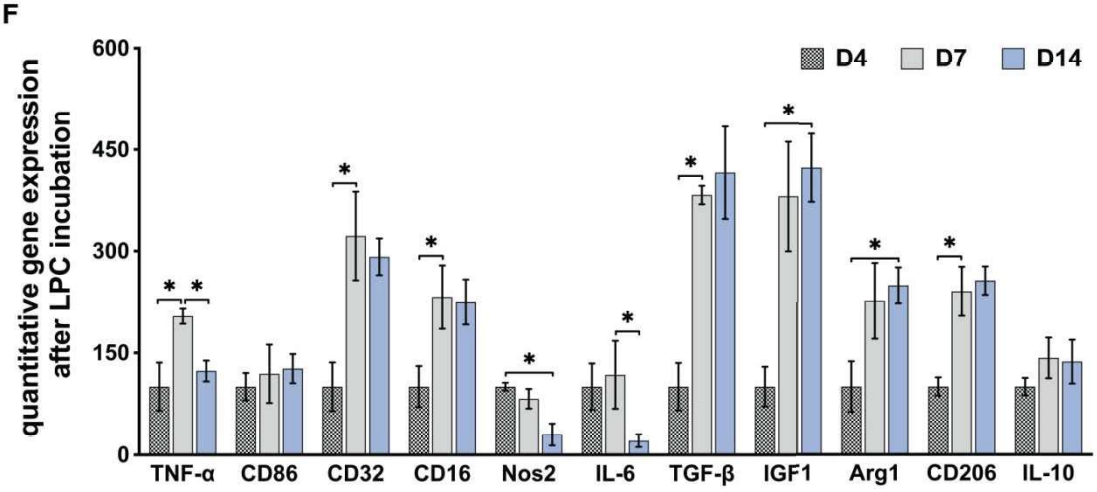
F
quantitative gene expression after LPC incubation
D4
D7
D14
TNF-α
CD86
CD32
CD16
Nos2
IL-6
TGF-β
IGF1
Arg1
CD206
IL-10

Figure 18. Activated microglia cells exhibit various inflammatory phenotypes concurrent with demyelination and, subsequent repair and remyelination

A. Immunofluorescence staining against two pro-inflammatory markers, iNOS and IL6R, of CX_3CR_1-EGFP expressing microglia cells four days after LPC. Scale bar, 500 µm (left panel) and 50 µm (right panels). **B-D.** Quantification of GFP^+ cells expression either IL6R (panel B) or iNOS (panel C) or both markers (panel D) from the initial LPC insult on day (D) 0 to complete spontaneous remyelination at D21. **E.** Schematic protocol of Cd11c-EYFP expressing cells isolation. Mice were implanted with a spinal window immediately after LPC treatment. Spinal cords were collected at D4, D14 and, D21 and FACS sorted based on their EYFP fluorescence. **F.** Quantitative reverse transcription-PCR on Cd11c-EYFP FACS sorted cells of pro-inflammatory (TNF-α, CD86, CD32, CD16, Nos2 and, IL-6) and anti-inflammatory (TGF-β, IGF1, Arg1, CD206, IL-10) gene expression post-LPC and normalized to D4. dpw: day post window; FACS: Fluorescence-Activated Cell Sorting.

were largely upregulated at D7, underlying pro-I phenotype of $CD11c^+$ cells during demyelination. However, while the expression of TNF-α, Nos2 and IL-6 significantly decreased at D14 when remyelination occurred, both CD32 and CD16 genes remained sustained, perhaps emphasizing the persistence of an M1-like pro-I microglial population contributing to lesion recovery. On the other hand, all the anti-I genes were strongly upregulated by D7 after LPC treatment and maintained until D14. Furthermore, the expression level of these genes was at least equal to or 1.5 times higher than that of pro-I genes highlighting the strong induction of an anti-I profile in microglial cells as the remyelination process takes place.

The comparison of qRT-PCR data from both $LysM^+$ cells and $CD11c^+$ cells demonstrated differential regulation of inflammatory gene expression (**Fig. 19**). Indeed, $LysM^+$ immune cells exhibited down-regulation of pro-I genes by D14, whereas $CD11c^+$ cells sustained the expression of CD16 and CD32 genes, both associated with the induction of a pro-I phenotype in microglia cells (Kigerl et al., 2009) (**Fig. 19A**). Conversely, while all anti-I-associated genes were already upregulated by D7 in $CD11c^+$ cells, their expression was mostly delayed until D14 in innate immune cells, as evidenced by Arg1, CD206, and IL-10 genes (**Fig. 19B**). However, the expression levels of anti-I genes were generally higher in $LysM^+$ cells compared to $CD11c^+$ cells. Overall, innate immune cells and microglia exhibited a pro-I phenotype consistent with demyelination, although it is likely sustained by a microglial subpopulation during remyelination. However, $CD11c^+$ cells express anti-I genes earlier, which could underlie a delayed phenotypic shift for immune cells during remyelination.

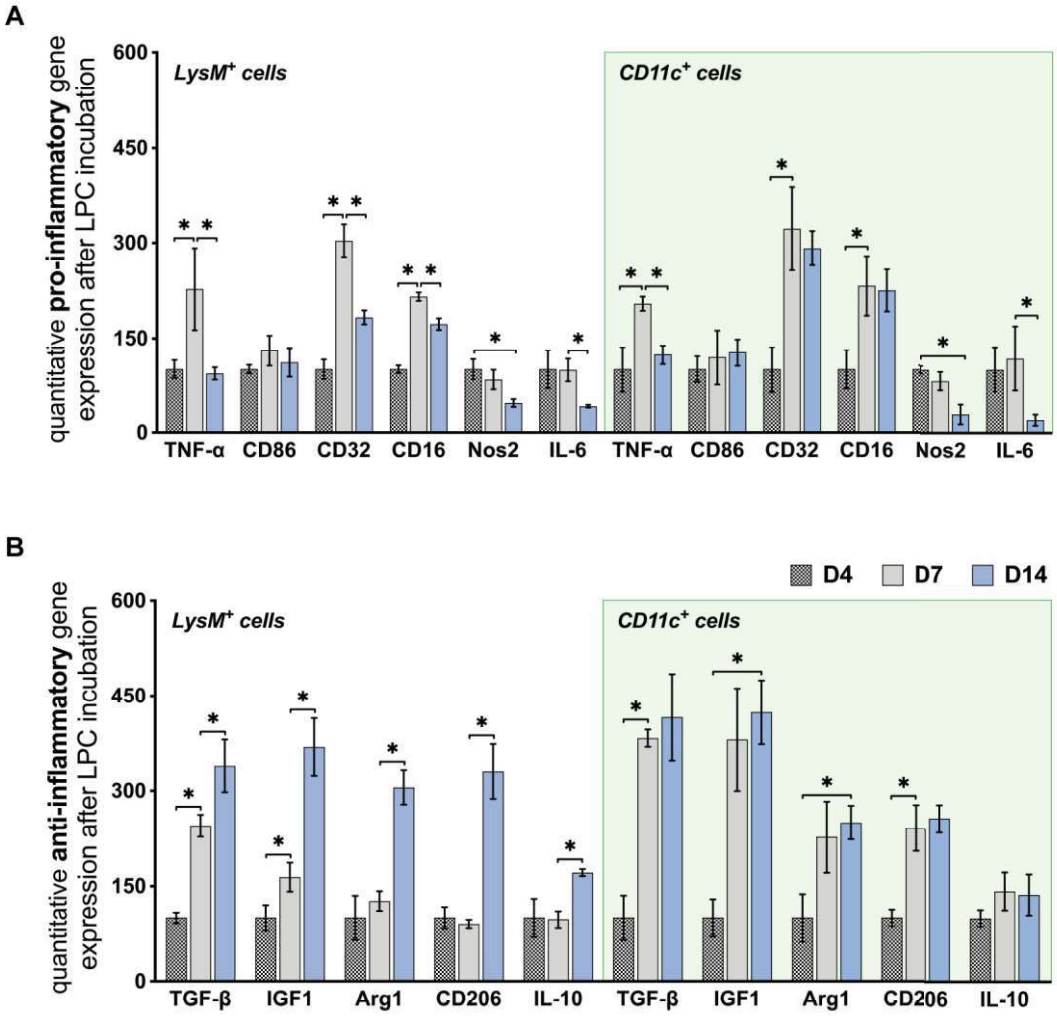

Figure 19. Microglia and innate immune cells displayed differential time-dependent expression pro- and anti-inflammatory gene expression

A-B. Comparison of pro- (A) and anti-inflammatory (B) gene expression of LysM-EGFP and Cd11c-YFP FACS sorted cells at D4, 7, and D14 following LPC incubation and normalized to D4.

7.3. 0Transcriptomic analysis of microglia, astrocytes, and OPCs following LPC-induced demyelination using RiboTag methodology

7.3.1. Cell-specific RiboTagged-mRNA isolation and sequencing approach

The intricate relationship between glial cells and neurons after a white matter lesion in the SC complicates our understanding of the precise cellular events occurring during demyelination and remyelination. To decipher the role of glial cells during the progression of the injury, as well as their interactions and crosstalk between them and with the other cell types of the CNS, we performed a cell-specific mRNA sequencing (RNAseq) using the RiboTag methodology. The RPL22fl/fl mouse

line was crossbred with a Cre driver line to obtain specific expression of the epitope-tagged ribosomal protein RPL22HA in microglia (CX_3CR_1-CreERT2), astrocytes (hGFAP-CreERT2) and, OPCs (NG2-CreERT2) (**Fig. 20A**). We first assessed the proper cellular localization of hemagglutinin (HA)-Tag expression on the 60S ribosomal subunit for each line. Three weeks after receiving the initial tamoxifen injection (**Fig. 20B**), the SC were collected, cross-sectioned and labeled via immunostaining. Microglial expression was evaluated based on Iba1, while the astrocytes were identified with GFAP and OPCs with PDGFRα (Fig. 20C). The quantifications revealed that within the CX_3CR_1-CreERT2 and hGFAP-CreERT2 lines, 98 % of the HA-Tag expressing cells were Iba1+ whereas 95 % were GFAP+, respectively (**Fig. 20D, E**). The analysis of the NG2-CreERT2 line unveiled that 72 % of HA-Tag^+ cells were indeed OPCs cells as referred to the double labeled PDGFRα$^+$ Olig2$^+$ cells while 27% were PDGFRα Olig2$^+$, indicating that part of mature OL cell population express the ribosomal HA-Tag, which is consistent with the interval after tamoxifen induction allowing the maturation of a portion of the tagged OPCs (**Fig. 20F**).

We further performed RNAseq of microglia, astrocytes, and OPCs. Mice were treated with LPC followed by the implantation of the spinal glass window. The dorsal fractions of the spinal parenchyma under the window were collected at days 3, 5, 7, and 10 after LPC treatment (see materiel and methods, 4.2.6), ensuring comprehensive coverage of gene expression associated with demyelination, as well as the onset of remyelination and repair. To corroborate our previous IHC data, we analyzed the enrichment of the gene driving CreERT2 expression as well as cell type-specific gene markers within the cell-specific mRNA immunoprecipitated (IP) fractions. The normalized Reads Per Kilobase per Million mapped reads (nRPKMs) values for each gene have been averaged for the time points and normalized to input samples (total mRNA) considering nRPKMs equal 1. As expected, the microglial IP fractions are, on average, 53-fold more enriched of CX_3CR_1 and Siglec-H - a microglial-specific marker (Konishi et al., 2017) - compared to nonspecific GFAP and MBP genes (CX_3CR_1, 12.8; Siglec-H, 19; GFAP, 0.6; MBP nRPKMs) (**Fig. 20G**). Similarly, astrocytic IP fractions exhibited an enrichment of GFAP and Aldh1l1 about 56 times higher than MBP and Siglec-H (GFAP, 7; Aldh1l1, 10.6; MBP, 0.2; Siglec-H, 0.13 nRPKMs) (**Fig. 20H**), while OPCs showed an expression of NG2 and PDGFRα around 36 times higher in comparison with the expression levels of GFAP and Siglec-H (NG2, 10.5; PDGFRα, 13; GFAP, 0.9; Siglec-H, 0.2 nRPKMs) (**Fig. 20I**).

The Principal Component Analysis (PCA) plot demonstrated that replicates of IP samples from each cell-type – microglia, astrocytes and, OPCs – clustered together as well as the input sample, indicating a distinct gene expression signature characterizing each cell type and conditions, with high degree of consistency and reproducibility within these RNAseq data (**Fig. 21A**). These observations were further supported by the heatmap color-coding transcriptomic similarity between samples, providing a detailed representation of gene expression patterns across cell-type specific samples and conditions. As before, both IP and input samples exhibited distinct cohesive clustering patterns. Furthermore, the IP samples from each cell type formed discrete clusters characterized by minimal inter-sample

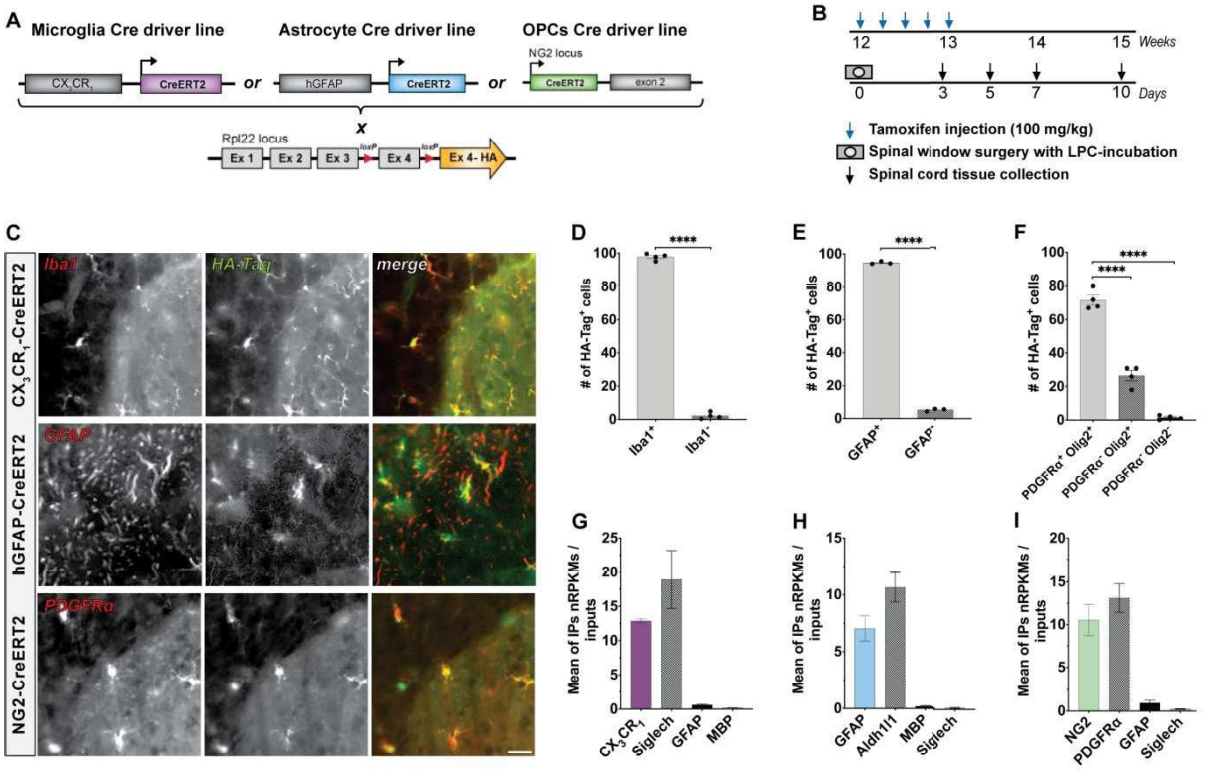

Figure 20. Specific microglia, astrocytes, and OPCs mRNA sequencing using the RiboTag methodology

A. Cell specific HA-tagged mRNA line were obtained by crossbreeding a single Cre-ERT2 driver line to the RiboTag ($Rpl22^{fl/+}$) line. **B.** Mice were injected five consecutive days with Tamoxifen to produce effective DNA recombination. The spinal window as well as LPC treatment were performed three weeks later and, spinal tissues (dorsal segment of the SC under the window) collected at D3, D5, D7 and, D10 after initial insult with LPC. **C.** Immunostaining on cross-sections of each Cre driver line with HA-Tag antibody and the corresponding glial cell marker (Iba1 for microglia, GFAP for astrocytes and, PDGFRα for OPCs) in naïve spinal tissues. **D-F.** Quantification of $HA\text{-}Tag^{+}$ cells colocalizing with microglia (Iba1, panel D), astrocytes (GFAP, panel E) and OPCs (PDGFRα) markers showing cell specific of RiboTag expression. **G-H.** nRPKMs means of IP samples (n=4) for each gene at D3, 5, 7 and, 10 and normalized to inputs (n=2) RPKMs = 1, showing the enrichment for each cell type of specific gene marker expression - CX_3CR_1 and Siglec-H for microglia (panel G), GFAP and Aldh1l1 for astrocytes (panel H) and, NG2 and PDGFRα for OPCs (panel I).

distance within their respective clusters, suggesting cell type-specific transcriptional signatures (**Fig. 21B**). PCA plots of single replicates within the different time points groups of microglia, astrocytes and, OPCs samples described comparable time gradient partitioning of replicates. This reflects time-dependent transcriptomic similarities as well as dynamic changes in gene expression over time (**Fig. 21C-E**).

Collectively these data demonstrated the robustness of the RiboTag approach in capturing cell type-specific RNA transcripts. The clustering of samples based on their cell type but also the time points highlighted their specific transcriptomic activity thereby enabling the elucidation of unique transcriptomic profiles associated with astrocytes, microglia, and OPCs during demyelination and remyelination

7.3.2. Transcriptomic analysis of OPC cells following LPC treatment

7.3.2.1. Differentially expressed genes during demyelination and remyelination

To understand how OLs lineage, and specifically OPCs, is impacted by LPC treatment, we focused our analysis on the specific mRNA IP samples isolated from NG2 expressing cells. The comparison of differentially expressed (DE) genes throughout the different time points enabled us to appreciate their dynamics of gene expression. The volcano plots provided visual representation of the magnitude of gene expression changes (log_2 fold-change) as well as the statistical significance (-log_10(p_adj)) (**Fig. 22A**). The comparison between D3 and D5 revealed 100 differentially expressed (DE) genes, with 54 genes showing a positive fold-change (FC) and 46 with a negative FC (**Fig. 22A, left panel**). Similarly, we identified 123 DE genes between D5 and D7, encompassing 36 genes upregulated and 87 genes downregulated (**Fig. 22A, middle panel**). Finally, OPCs exhibited the lowest modulation of their gene expression during the transition from D7 to D10, where only 47 genes were DE including six with a positive FC and 41 with a negative FC (**Fig. 22A, right panel**).

According to these DE genes, we subsequently conducted an enrichment analysis (Fig. 22B). By annotating genes based on Gene Onthology (GO) database, it provides insight into potentially affected and involved pathways associated with our set of genes. This analysis annotates genes according to three categories: Molecular Functions (MF) gives hints on molecular-level activities, Biological Process (BP) denotes biological program or cellular function accomplished by multiple molecular activities and, Cellular Component (CC) indicates subcellular location or structure associated with macromolecular machinery. The statistical significance tests are used to identify GO terms that are significantly over-represented (enriched) in your gene set compared to what would be expected by chance. Interestingly, all the terms generated between D3 and D5 displayed similar significance. The term “CC: cell population proliferation” reflected the expansion of the OPCs population following LPC-induced demyelination. Their close relationship with the neuronal compartment under injury condition, supporting its regeneration, is depicted by the terms “BP: neuronal development”, “BP: neuron projection development” and ``BP: neurogenesis”. Moreover, these cells are actively implicated in cell communication, signaling, and interactions with neighboring cells and the environment through “MF: protein binding”. However, they undergo also intracellular reorganization and structural modifications in line with their myelinating functions within the CNS, as illustrated by the terms “BP: plasma membrane bounded cell projection organization”, “anatomical structure morphogenesis” and, “cell projection organization” (**Fig. 22B, a**). Interestingly, between D5 and D7, we found the previous terms “MF: protein binding” and “MF: binding” demonstrated their sustain receptiveness to the environment as well as “BP: cellular component organization” and “BP: component organization or biogenesis” corresponding to self-organization of the cell structure. The multiple appearance of “TF: factor E2F” has been linked to cell proliferation. The upregulated

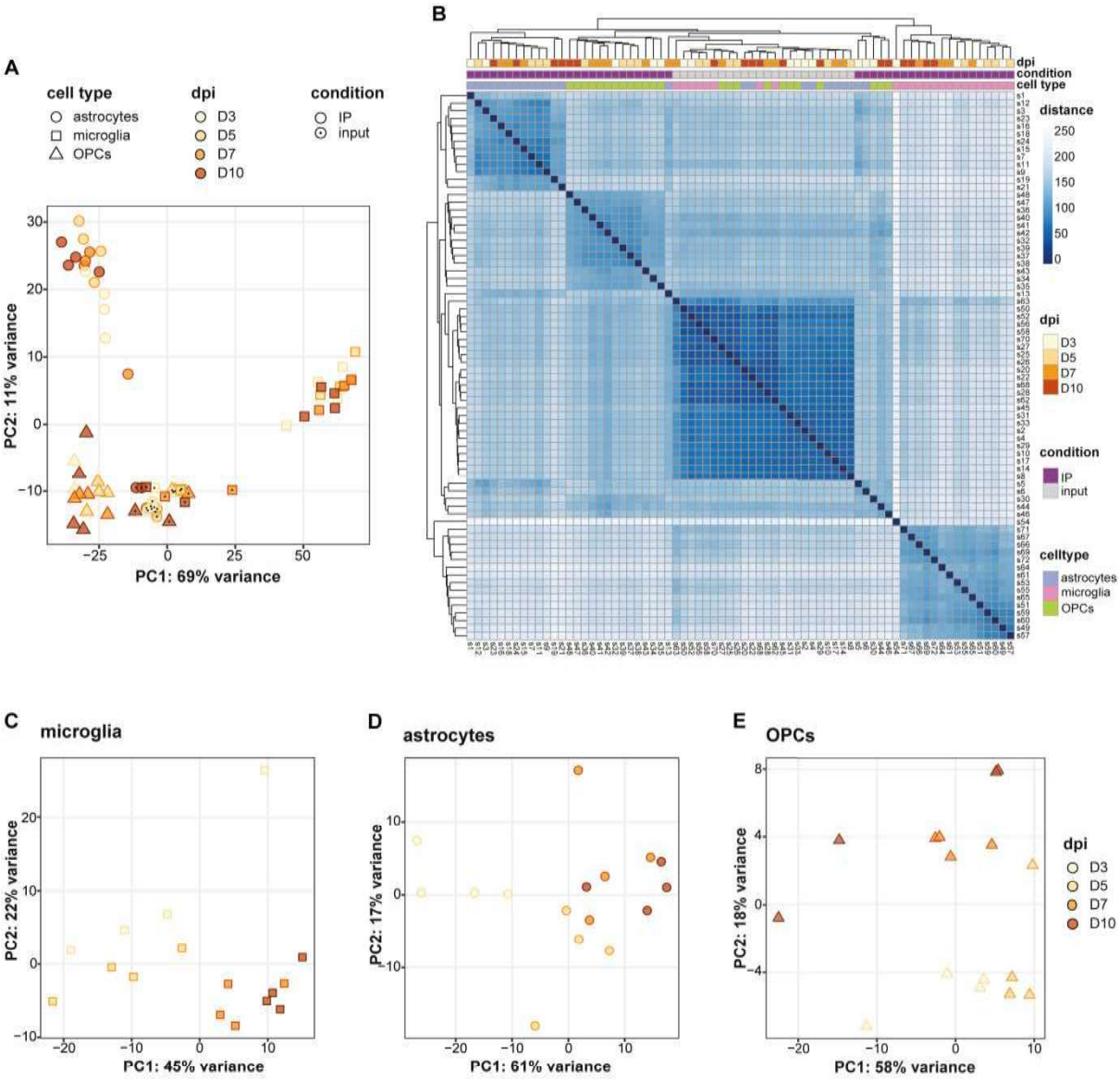

Figure 21. RNA sequencing revealed distinct cell type- and time-specific gene expression

A. Principal Component analysis (PCA) plot based on the top 500 most variable genes, showing cell specific clustering according to the cell type and conditions. IP: immunoprecipitated; dpi: days post-incubation. **B.** Heatmap color-coding pair-wise distance of gene expression profile between samples. The darker the blue shade indicates transcriptomic similarity, indicating the closer expression between any two samples. s: sample number replicate. **C-E.** PCA graphs of microglia (C), astrocytes (D), and OPCs (E) showing time gradient partitioning of individual sample replicates.

expression of E2F upon injury condition led to enhanced expression of cell cycle-related genes and aberrant proliferation (**Fig. 22B, b**). However, the concomitant occurrence of "TF: factor E2F-1" implies the entry into the apoptosis pathway of these OPCs (Wu et al., 2015). Finally, the terms associated with the time transition from D7 to D10 are all related to cell proliferation meaning that OPCs are actively increasing their cell population at the onset of remyelination (**Fig. 22B, c**).

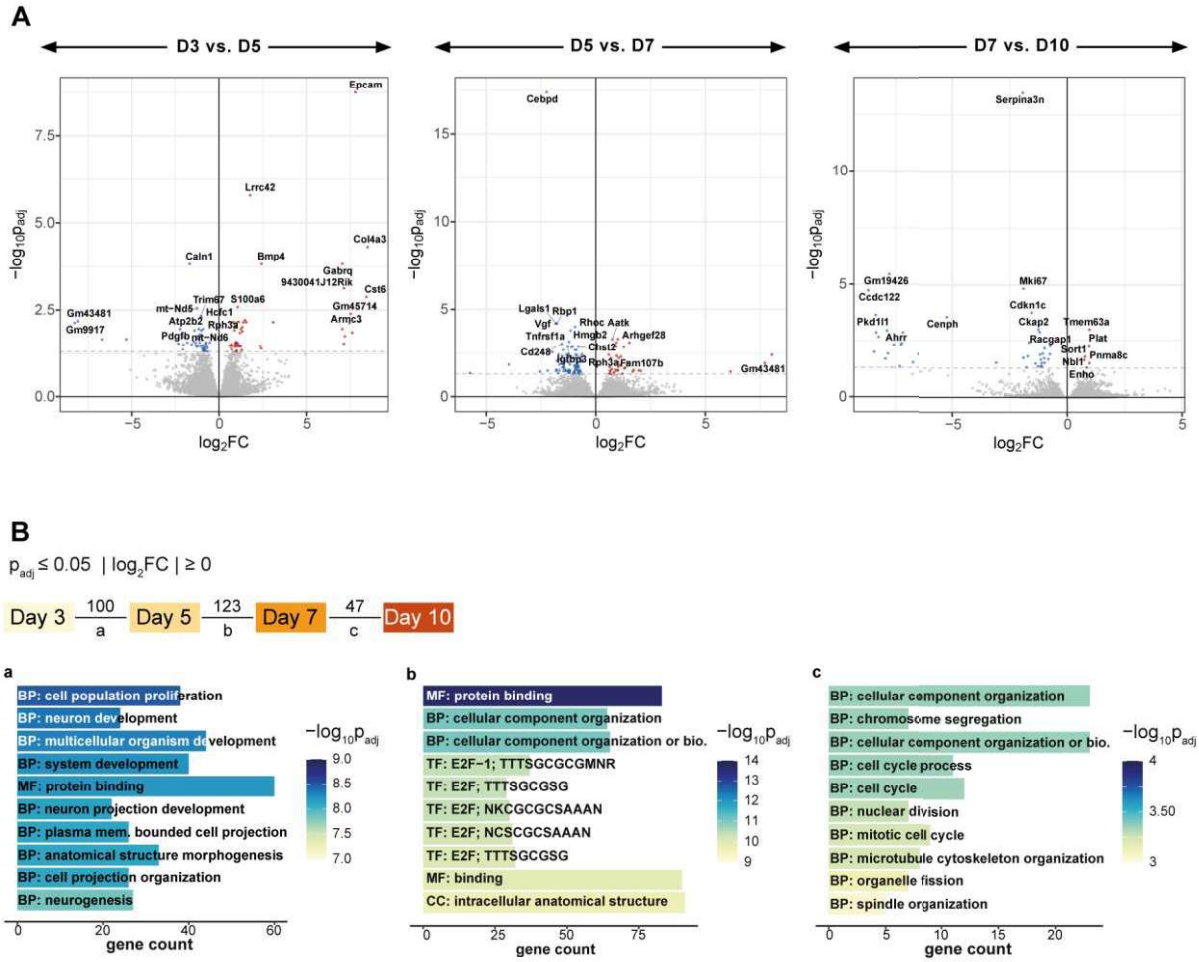

Figure 22. Comparison of differentially expressed genes in OPCs across demyelination and remyelination

A. Visual representation of Differential Gene Expression (DEG) from immunoprecipitated (IP) samples between D3 and D5 (left panel), D5 and D7 (middle panel) and, D7 and D10 (right panel). Genes with a positive FoldChange (FC) are presented in red and those with a negative FC in blue. **B.** Gene Ontology (GO) functional enrichment analysis of the DEGs identified between time points. Comparison of D3 to D5 revealed 100 DEGs included in the as well as 123 DEGs between D5 and D7 and, 47 DEGs comparing D7 to D10 with respective corresponding ten top most significant GO terms (a, b and c).

To delve further into the transcriptomic analysis of OPCs cells after LPC treatment, we generated a heatmap based on the previously identified DE (**Fig. 23C**). We could identify five clusters made of genes displaying a distinct expression pattern according to the time evolution of the lesion. The first cluster includes four genes upregulated at D3, while the second cluster counts 69 genes enhanced initially at D3 and further from D7 and D10. The third cluster contains 49 genes specifically involved between D5 and D10. Finally, the fourth cluster exhibits 34 genes important from D3 to D7, whereas the last and biggest cluster displays 88 genes whose expression is enhances between D3 and D5.

We performed a functional enrichment analysis for each cluster, using Gene Ontology (GO) resources, the Kyoto Encyclopedia of Genes and Genomes (KEGG) - a molecular-level information database -, Reactome (REAC) - a database of molecular and cellular pathways -, and TRANSFAC® -

a database of eukaryotic transcription factors (TF) - to ensure the most comprehensive and detailed analysis. Thereafter, we identified the top 10 most significant pathways based on the -log10Padj value to focus our investigation (**Fig. 23D-H**).

7.3.2.2. Detailed investigation of gene clusters

- **Cluster 1**

With only four genes, the terms and pathways generated from this cluster included two genes, *Trim67* and *Il-33*. *Trim67* has been identified as a negative regulator of TNFα-induced NF-κB pathway, which is critical for promoting OPCs-mediated CNS inflammation as well as white matter loss (Fan et al., 2022; Schlett et al., 2023). Therefore, the upregulation of Trim67 might aggress with a decrease of pro-inflammatory behavior and promoted self-protection within the OPCs population. *Il-33* expression also protects OLs against morphological impairment and subsequent myelin damage but act on OPCs maturation for remyelination (Huang and Tzeng, 2024) (**Fig. 23D**).

- **Cluster 2**

The most significant terms in the enrichment analysis were Biological Process (BP) GO terms. As indicated by the terms “neuron projection development”, “neuron development”, “neuron projection morphogenesis”, “nervous system development”, and “generation of neurons”, OPCs seemed to enhance their signaling to neurons immediately after myelin insult and subsequently at the onset of remyelination, between D7 and D10 (**Fig. 23E**). We found genes associated with neuronal projection and elongation such as *Arghef28*, *Kif5a* and *Fat4*. However, *Fat4*, as a protocadherin involved in adhesive complexes, indirectly influences neurodevelopment (Butler et al., 2015). The upregulation of *Nurr1* and *Sad2* could promote neuronal differentiation. Conversely, OPCs may partially impede regeneration, as evidenced by the enhancement of *Rph3a*, known to restrict axonal repair (Sekine et al., 2022).

Although many genes are shared across terms, the gene composition analysis of the terms “cellular component organization” and “cellular component organization and biogenesis” revealed an upregulation of genes linked endocytosis such as *Esp15*, voltage-gated K^+ channels like *Kv3.3* and, mitochondrial-associated genes, specifically the within the complex I, as *MT-ND5*, *MT-ND6*.

We found *Hcfc1* gene expression related to NPCs cell proliferation suggesting the involvement of newly generated OPCs independently from self-proliferation of OPCs found with the LPC lesion. Finally, we specifically identified genes associated with oligodendrocyte lineage maturation within the last GO terms, “cellular anatomical entity morphogenesis”, “plasma membrane bounded cell projection organization” and “cell projection morphogenesis”. We found genes regulating OPCs differentiation such as *Map18*, *Tppp*, *Ryr3*, as well as *Ank3*, *Fnbp1*, *Eml1* acting as “late differentiation genes” (Dugas et al., 2006). Interestingly, while *Fnbp1* is involved in mediating

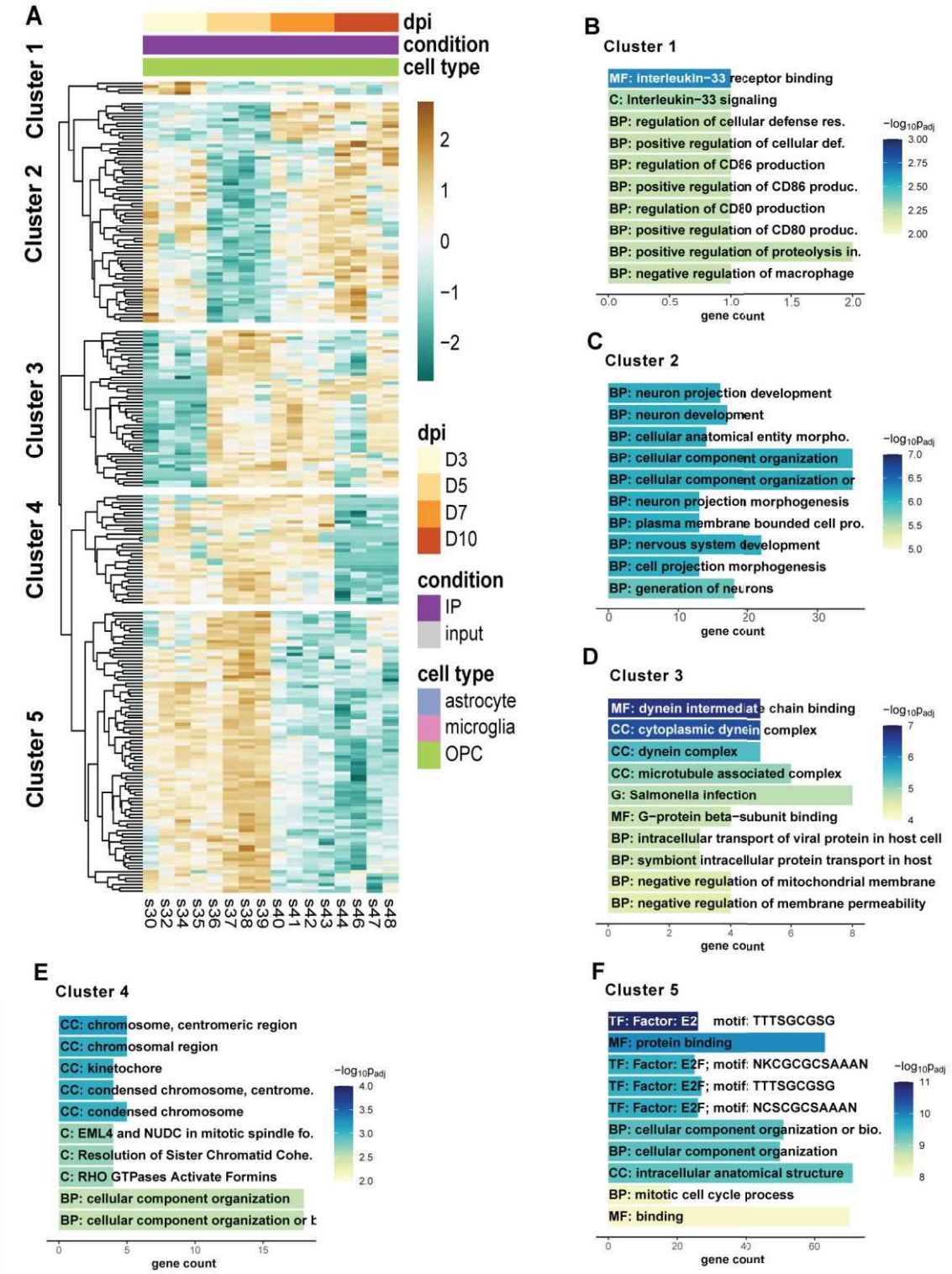

Figure 23. Functional analysis of transcriptomic diversity and gene expression dynamic in OPC cells during demyelination and remyelination

A. Heatmap based on the all DEGs identified in OPCs between time points analysis. Their gene expression can be divided in five different clusters according to transcriptomic activity. dpi: days post-incubation; s: sample number replicate. **B-F.** Enrichment analysis of each cluster based on GO (referred to MF: molecular functions, BP: biological process, and CC: cellular component, terms) , KEGG (referred to G terms) , Reactome (referred to C terms), and TRANSFAC® (referred to TF terms) databases. In each panel are presented the top 10 most significant terms and pathways.

membrane remodeling via actin polymerization, we identified the upregulation of *Sptbn4* (β4 spectrin) which, together with *Ank3*, regulate nodal architecture of voltage-gated Na^+ channels (Zhou et al., 1998). Additionally, the transferrin receptor gene *Tfrc* was as well enhanced, assuming the role of iron uptake in OPCs maturation (Cheli et al., 2023). In line with this, we found genes involved in myelination. Indeed, the upregulation of *Ptprd1* may reflect the initiation of axonal myelination (Zhu et al., 2015). *Cpeb1* enhancement may have a role in the molecular cascade regulating MBP RNA translation, while *Pmca2* has been identified as myelin proteome component (Carson et al., 2008; Jahn et al., 2009). Finally, we found as well the expression of *Dusp3* and *Nbl1* that could be both indirectly linked to the remyelination process. *Dusp3* induce ERK dephosphorylation mediating OPCs proliferation as well as process extension, while *Nbl1* is an antagonist of BMP signaling known to suppress myelination (Chew et al., 2010; Nolan and Thompson, 2014).

- **Cluster 3**

The third cluster displayed genes enhanced from D5 to D10, during acute demyelination to the initiation of remyelination. The highest significance was attributed to terms related to motor protein and intracellular transport named "MF: dynein intermediate chain binding", "CC: cytoplasmic dynein complex", "CC: dynein complex" and "CC: microtubule associated complex" (**Fig. 23F**). The expression of genes related to dynein light chain were upregulated such as *Dynll1*, *Dynll2*, *Dynlt1b*, *Dynlt1c* and *Dynlt1f*. They are implicated in cargo transportation along microtubules within OPCs and OLs processes. However, *Dynll1* facilitate dimerization of L-MAG and subsequent partners binding to form the paranodal myelin, while both *Dynll1* and *Dynll2* are involved in subcellular localization of gephyrin which is needed for myelination (Fuhrmann et al., 2002; Li et al., 2024a).
Interestingly, although the above-mentioned genes were also found in the other terms, we identified under "G: Salmonella infection" the upregulation of *Arp5c*, which is a partner in the Arp2/3 complex which induces actin cytoskeleton remodeling needed for initial extension of OLs processes and myelin wrapping around axons. However, we identified the concomitant enhancement of *Bak1* and *Casp3* highlighting potential OPCs death through the activation of intrinsic apoptosis pathway mediated by mitochondrial dysfunction.

- **Cluster 4**

The GO terms "CC: chromosome, centromeric region", "CC: chromosomal region", "CC: kinetochore", "CC: condensed chromosome, centromeric region", and "CC: condensed chromosome" and Reactome pathways "C: EML4 and NUDC in mitotic spindle formation", C: Resolution of sister chromatid cohesion", and "C: RHO GTPases activate formin" are collectively linked to cell population proliferation (**Fig. 23G**). Indeed, we identified as upregulated centromeric proteins (*Cenph*, *Cenpu*), microtubules-associated proteins (*Knstrn*, *Tubb6*), gene regulating the cell-cycl (*Mki67*) and spindle formation (*Ska2*).

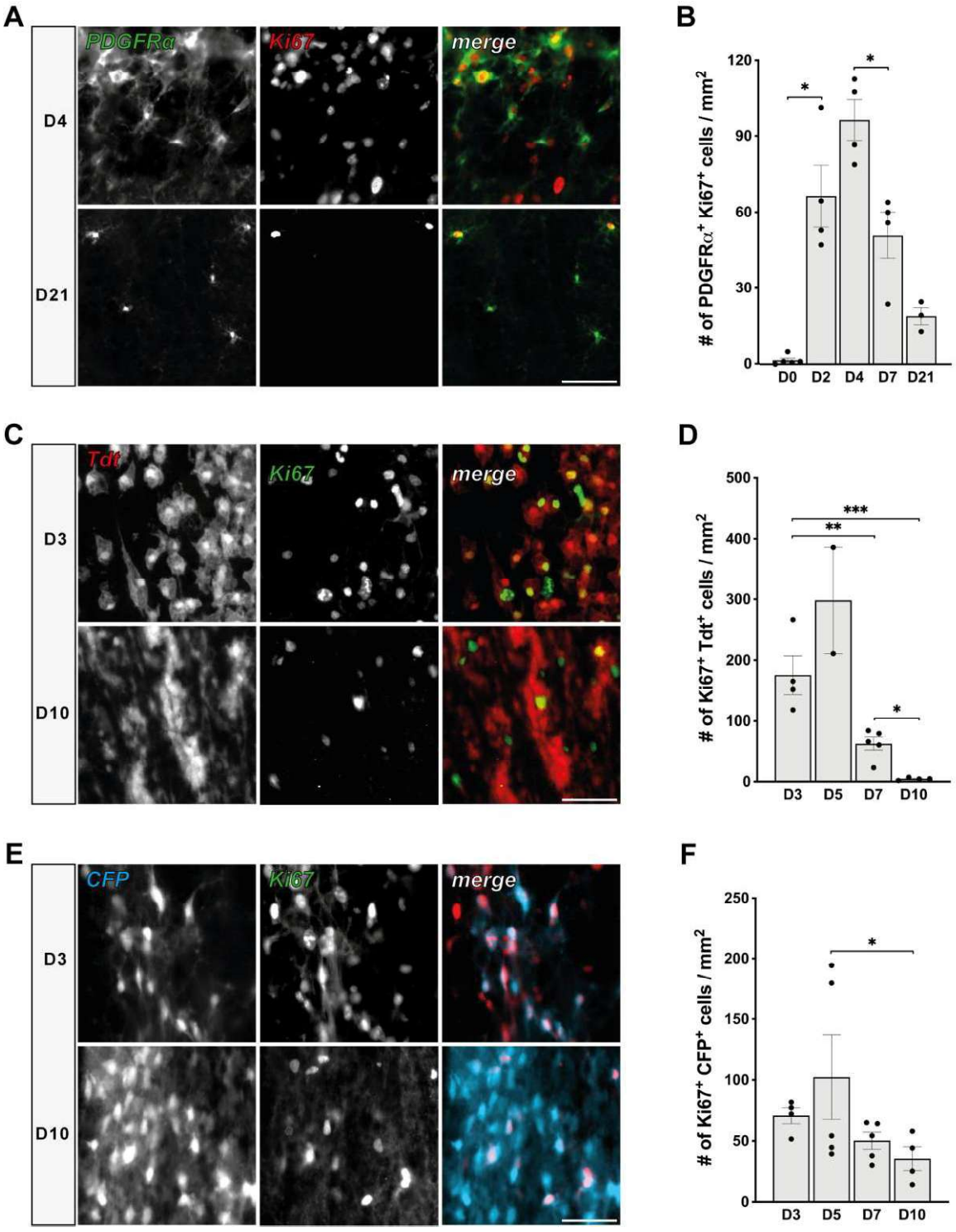

Figure 24. Glial cells transitory proliferated after LPC-induced demyelination

A, C, E. Immunofluorescence of the proliferative marker Ki-67 combined with the OPC marker PDGFRα (panel A) or the intrinsic expression of the fluorescent protein tdT in CX_3CR_1 microglia cells (panel C), or the CFP in GFAP astrocytes (panel E) after LPC treatment. Scale bars, 50 µm. **B, D, F.** Quantification of proliferative OPCs (panel B), microglia (panel D), and astrocytes (panel F) within the LPC lesion showing rapid proliferation of glial cells during early demyelination

The two last GO terms contained the exact same list of genes. OPCs enhanced the expression of the protocadherin *Pcdhgc4*, the EMC-related proteins coding for collagen subtype *Col16A1*, *Col18A1.* Surprisingly we found also in this cluster genes related to NPC cells as depicted by the upregulation of *Mmp16, Cdkn1c,* and *Il-15*, inducing their proliferation, specification into OPC lineage and their neuronal cell fate, respectively (Park et al., 2005; Pan et al., 2013; Gorter and Baron, 2020).

- **Cluster 5**

In this last cluster, we found gene annotating into the "TF: factor E2F" (**Fig. 23H**). As explained before, the upregulation of the transcription factor E2F upon disease injury led to pathologic entry into the cell-cycle leading to excessive proliferation. Accordingly, we found the GO term "BP: mitotic cell cycle process" containing genes involved in promoting cell proliferation with *Hmga1b*; DNA replication such as *Rrm1*, *Rrm2*, *Cdt1*, *Pcna, mcm5*; Cyclin-Dependent Kinases (CDKs) like *Ccna2*, *Ccnb1*, *Cdk1, Ccn1* or the CDKs inhibitor *Cdkn1a* collectively participating to checkpoints control of the cell-cycle ensuring the correct mitosis achievement; the mitotic spindle formation is ensured by the spindle pole body components *Nek2* and *Tpx2*, and the kinesin *Kif22; Chap2* and *Ndc80* contribute to centrosome and kinetochore assembly. Finally, *Rhoa* controls the cytokinesis. However, we also identified genes linked to cell cycle arrest and DNA damages such as *Gadd45b*, *H2ax*, *Lig1* and *Cdkn1a/p21* as well as DNA repair with up regulation of *H2az1* and *Fanci*. Of note, the p21 protein is required for the differentiation of non-proliferative cells, particularly here for OPCs, where it enables the remyelinating process to continue despite cell cycle arrest (Zezula et al., 2001). The OPC proliferation was also observed *in vivo*, on spinal cross-section double labeled with PDGFRα and Ki-67 (**Fig. 24A**). As expected, the number of proliferative OPCs PDGFRα^{+} Ki67^{+} increased until D4 before gradually decrease until D21. However, the upregulation of the neural stem cell marker (NSCs) S100a6 suggested the involvement of NSCs independently of OPC proliferation.

The analysis of gene composition of the remaining GO terms asserted to this cluster, revealed genes taking part in the cell cycle such as *Top2a*, the transmembrane proteins *Tmem176a* and *Tmem176b*, and *Vgf* that promotes oligodendrogenesis. OPCs also enhanced intracellular machineries such as Ca^{2+} signaling (*S100a11*), self-protection against oxidative stress (*Prdx1*, *Prdx4*), Glycolysis (*Ldha*) and protein (*Ube3d*, *Uhrf1*) and proteoglycan (*Chst2*) degradation pathways.

Finally, we found genes related to OPCs differentiation such as *Arl6p1*, *Hmgn*, *Lgals1* and *Lig1*. The particular expression of *Hmgn* might regulate OLs lineage specification by controlling the expression of Olig1/2 through the remodeling of the chromatin structure (Deng et al., 2017). Some genes may specifically support myelination like *Tpx2* and *Aldh1a2*, both implicated in MBP expression while *Tagln2* and *Stmn1* via supported the wrapping process the regulation of actin cytoskeleton. *Lgals1* emerged here as a multifaceted gene, at times involved in OPC differentiation as mentioned, but also known to control myelin compaction, and inducing M2 microglial phenotype with enhanced phagocytosis activity. However, OPCs also described opposite regenerative behaviors. While the

upregulation of *Htra1* probably promoted remyelination through preventing BMP-signaling, *Tnfr1* self-promoted proliferation for remyelination (Arnett et al., 2001; Fuller et al., 2007)

Collectively, these data demonstrated that plausibly OPCs played an active role in resolving LPC-induced white matter lesions. Although the clusters did not have the same activation time windows, the majority (clusters 1, 2, 4, and 5) showed strong gene activation during demyelination, between D3 and D5. During this period, OPCs underwent significant population proliferation. This behavior, crucial to ensure subsequent efficient remyelination, appeared partly reactive to the insult suffered by their lineage, as indicated by terms involving the transcription factors E2F and E2F-1. However, we also found cues of NPC involvement through the expression of *Mmp16*, *Il-15*, *S100a6*, and *Hcfc1* indicating an additional pathway generating OPCs. They also demonstrated intrinsic property of to self-decrease pro-I phenotype induced by TNF-α by *Trim67*. As expected, OPCs have a transcriptional profile consistent with their myelinating functions. Between D5 and D10, numerous genes involved in their differentiation are upregulated, such as *Arl6p1*, *Ank3*, *Eml1*, and *Lig1*. They also significantly increased genes related to cytoskeletal remodeling (*Arp5c*, *Tagln2*, *Stmn1*, *Fnbp1*), needed to extend their processes around axons. They initiated the transcription of MBP via *Tpx2* and *Aldh1a2*, as well as MAG through *Dynll1*, which are both major proteins found in myelin sheath. Surprisingly, OPCs participated in CNS degeneration by limiting axonal repair (*Rph3a*) or remyelination (*HtrA1*, *Tnfr1*). Finally, OPCs seemed to establish few connections by themselves with microglia and astrocytes during demyelination and remyelination. However, they sustained a close relationship with the neuronal compartment to promote differentiation (*Nurr1*, *Sad2*) and growth (*Arghef28*, *Kif5a*, *Fat4*) of neurons.

7.3.3. Transcriptomic analysis of microglia cells following LPC treatment

7.3.3.1. Differentially expressed genes during demyelination and remyelination

To decipher the role of microglial population following the LPC-induced white mater insult and their implication during remyelination, we focused our analysis on the specific mRNA IP samples from microglia cells. Initially, we compared DE genes across different time points to assess the transcriptomic dynamics of microglia over time. On the volcano plots, we observed between D3 and D5 differential expression in 41 genes, comprising 38 genes with a positive FC and three with a negative FC (**Fig. 25A, left panel**), while between D5 and D7 we identified 223 DE genes with 43 gene up-regulated but the preponderance of DEGs down-regulated (**Fig. 25A, middle panel**). Finally, during the transition from D7 to D10, corresponding to the onset of remyelination, only six genes

exhibit a differential expression including two upregulated genes and five down regulated genes (**Fig. 25A, right panel**).

As we did for OPCs, we performed a Gene Ontology (GO) term enrichment analysis based on these DE genes (**Fig. 25B**). The two most significant terms identified between D3 and D5 are "CC: extracellular region" and "CC: extracellular space". This reflects an upregulation of genes involved in secretion of molecules participating in cell signaling, communication or interactions with the surrounding microenvironment. Microglia, as expected, are involved in immunomodulatory functions, acting as antigen-presenting cells (i.e. *MHC class I peptide loading complex* term) as well as controlling the expansion of immune system (i.e. *regulating of immune system process* term). Finally, microglia cells are already involved during early demyelination process in the phagocytosis and degradation of cellular debris in the extracellular environment as reflected by the CC terms "lytic vacuole", "lysosomes" and, "vacuole". This is reinforced by the occurrence of the CC terms "plasma lipoprotein particle", "lipoprotein particle" and, "high-density lipoprotein particle" suggest that microglia are involved in lipid metabolism (**Fig. 25B, a**). Indeed, myelin degeneration not only led to an accumulation of lipids such as cholesterol, sphingolipids and phospholipids, which cleared by microglia through the activation of specific receptors on the cell surface, but also an increase in cholesterol metabolism, which contributes to the oxidative and inflammatory functions of microglia (Loving and Bruce, 2020). In contrast, the analysis of DE genes between D5 and D7 demonstrated that all BP GO terms were related to cell population proliferation such as "mitotic cell cycle", "cell cycle process" or "cell cycle" (**Fig. 25B, b**). This implies a significant upregulation of genes related to cell proliferation, thereby increasing the number of cells within the microglial cell population to a sufficient level to fulfill their function inside the demyelinating lesion.

To further decipher the microglial transcriptomic activity, we took the union of all DEGs identified in Fig. 25A to generate a heatmap (**Fig. 26A**). We could identify three different clusters based on their transcriptional dynamic from D3 to D10. The first cluster contains 182 genes specifically upregulated between D3 and D5, while the second cluster encounters 27 genes whose expression was enhanced from D5 to D10. The third cluster includes counts 51 genes involved at later stages from D7 to D10. As previously done with OPCs cells, we conducted functional enrichment analysis for each cluster, incorporating various databases such as GO, KEGG, REAC and, TRANSFAC®. We further selected the top most significant terms and pathways and, conducted a detailed analysis of their associated genes (**Fig. 26B-D**).

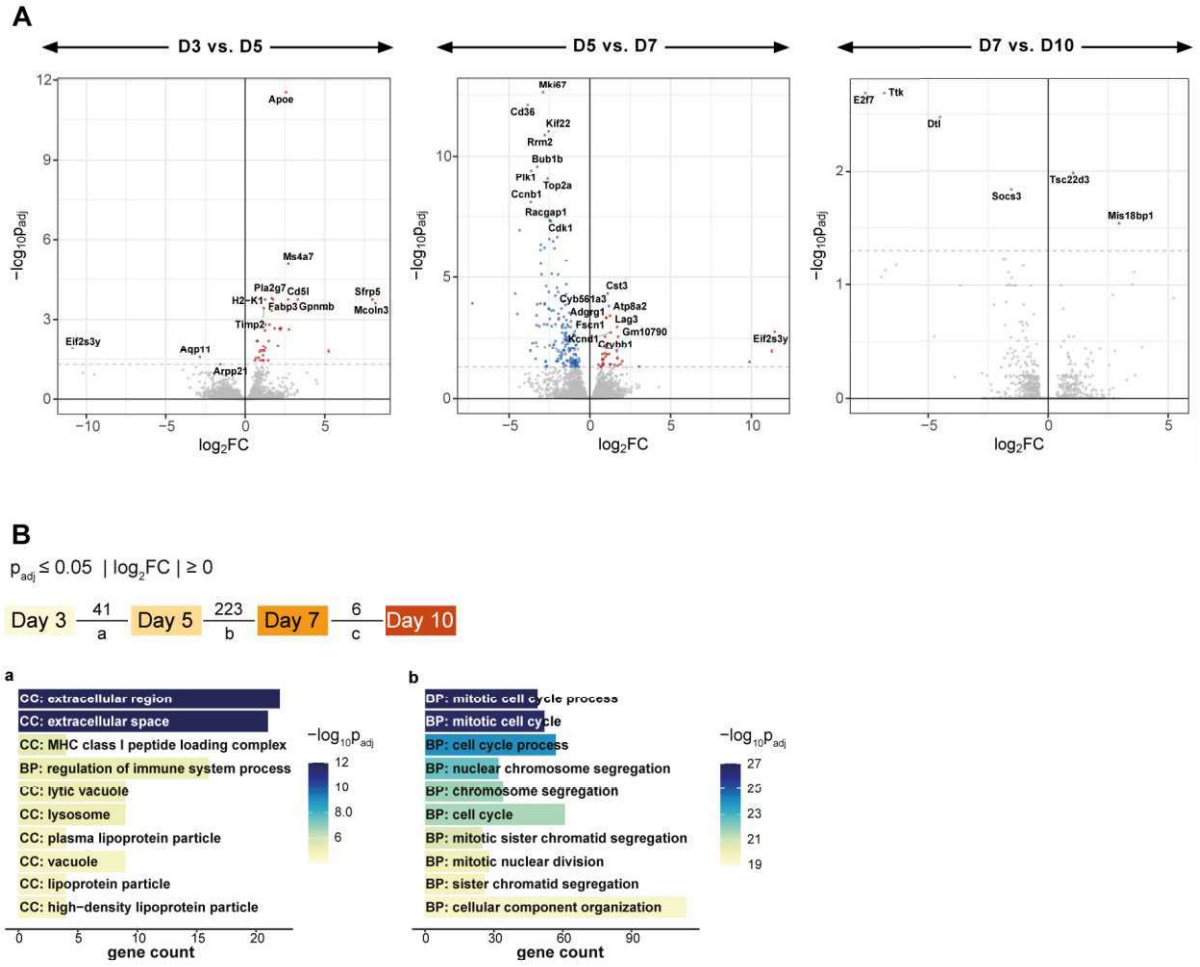

Figure 25. Comparison of differentially expressed genes in microglia cells across demyelination and remyelination

A. Visual representation of Differential Gene Expression (DEG) from immunoprecipitated (IP) samples between D3 and D5 (left panel), D5 and D7 (middle panel) and, D7 and D10 (right panel). Genes upregulated are presented in red and those downregulated in blue. **B.** Gene Ontology (GO) functional enrichment analysis of the DEGs identified between time points. Comparison of D3 to D5 revealed 41 DEGs as well as 223 DEGs between D5 and D7 and, 6 DEGs comparing D7 to D10 with respective corresponding 10 top most significant GO terms (a, b).

7.3.3.2. Detailed investigation of gene clusters

- **Cluster 1**

The first cluster consists exclusively of Biological Process (BP) GO terms, all referring to cell proliferation (**Fig. 26B**). The global analysis of their gene composition confirmed the upregulation of genes implicated in cell proliferative process, specifically between D3 and D5. Notably, we could identity some key genes participating in cell division such as *Plk1* and *Ran* regulating mitosis process; *Pclaf*, *Rrm1*, *Rrm2*, *Tk1* or Mini Chromosome Maintenance (MCM) complex subfamily (*Mcm2*, *Mcm4*, *Mcm5*, *Mcm6*, *Mcm7*) involved in DNA replication; *Ncaph*, *Top2a*, required for chromosomes

condensation; *Bub1b*, *Clspn* and, Cyclin-Dependent Kinases (CDKs) and associated proteins (*Ccna2*, *Ccnb1*, *Ccnb2*, *Cdk1*, *Cdkn2c*, *Cdkn2d*) ensuring functions in cell-cycle checkpoints and the proper course of mitosis; *Cep55*, *Nusap1*, *Tubb5*, the spindle pole body components (*Spc24*, *Spc25*), kinesins (*Kif22*, *Kif2c*, *Kif3a*, *Kif4*, *Kifc1*) as well as aurora kinases (*Aurka*, *Aurkb*) involved in mitotic spindle formation or centrosome for sister chromatids alignment and segregation; *Cenpa*, *Cenpf*, *Incenp*, *Knstrn*, *Ndc1* contributing to centromere and kinetochore functions; *Pcr1* controlling the final mitosis step or cytokinesis. These transcriptomic data were further corroborated by immunolabelling of the proliferative marker Ki-67 on spinal cord cross-sections from CX_3CR_1-TdTomato expressing mice after LPC treatment (**Fig. 24B**). Microglia displayed high Ki-67 expression on D3 and D5, which then decreased on D7 and was ultimately abolished by D10.

- **Cluster 2**

The second cluster displayed genes whose expression is enhanced from D5 to D10, in correspondence of remyelination and repair. Looking at the REAC, KEGG and, GO terms generated from those 51 genes, we found that they were all linked to lipid metabolism (Fig. 26D). The upregulation of *Fabp3* and *Pla2* are associated with fatty acids (FAs) binding and hydrolysis, as well as lipids transporters (*Apoc1*, *Apoc4*). Moreover, the concomitant enhanced expression of *Abca1* and *ApoE* is triggered by myelin degeneration and responsible of microglial-derived lipoprotein synthesis to eliminate cytotoxic accumulation of cholesterol and oxysterol within the cell (Loving and Bruce, 2020). However, microglial cells are highly involved in myelin clearance as reflected by the upregulation of lysosomal-related genes. Indeed, *Nceh1* is related to cholesterol trafficking to lysosome, while *Creg1* and *Lipa* are crucial for acidification of lysosomal compartment and Fas protein degradation. Interestingly, this cluster exhibits simultaneous upregulation of *Lyz2* and *Fcgrt*, together associated with early or immature microglia cells, while the expression of *Igf1* and *Gpx3* are critical for neurite outgrowth and (re)myelination (Wlodarczyk et al., 2017; Pettas et al., 2022).

- **Cluster 3**

Cluster 3 analysis demonstrated that microglial cells exerted immunomodulatory functions between D7 and D10 (**Fig. 26C**). Indeed, terms related to "antigen processing" shared the same genes, partially regulating microglial immune functions. Among them, we found genes encoding the MHC complex class I (*B2m*, *H2-D1*, *H2-T24*, *H2-Q6*), as well as the *Cd74* gene encoding the invariant chain of the MHC complex class II. Noteworthy, the expression of the MHC-I complex by microglial cells enables the recruitment and activation of pro-inflammatory $CD8^+$ T cells, while the MHC-II complex is associated with the involvement and modulation of $CD4^+$ T cells (Schetters et al., 2017; Malo et al., 2018).

The “cell surface” GO term refers to molecules found at the cells surface such as cell markers or receptors and ligands. Although it also contains genes found within the “antigen processing” terms as they include gene expressed at the cell surface, we found that microglia cells expressed specific signature makers genes such as *Siglec-H* and *Cst3*. Interestingly, the upregulation of homeostatic genes has been reported as an indicator of a cell transition from a pro-I phenotype to a resting or anti-I state (Böttcher et al., 2020). On the same way, we found that microglia enhanced the expression of *SPARC* known for its anti-proliferative properties reducing microgliosis (Lloyd-Burton et al., 2013). Moreover, upregulation of *Cd83*, exerts pro-resolving functions, decreasing M1 behavior and enhancing myelin clearance, while *Lag3* gene, immune checkpoint receptor induced by IFNγ signaling, can dampen excessive inflammatory response and promote neuronal survival (Rimmerman et al., 2022; Sinner et al., 2023). The activation of *Grin2A* encoding GluN2A receptor subunit emphasizes microglia-neurons interactions. Finally, we found up regulation of genes involved in phagocytosis, *ATP8A2* and *Axl*, required for neurons and myelin debris clearance, respectively.
The terms “endosome”, “lysosome” and, “lytic vacuole” highlight the degrading function of microglia cells consistent with their phagocytic activation during remyelination. The genes *Rnf167* and *Neurl3* enable ubiquitination of proteins, marking them for degradation by the proteasome. The lysosomal functions are also upregulated as reflected by the expression of *Ctss*, *Cyb561a3* and, *Slc29a3/Ent3*. Furthermore, we performed immunostaining spinal cross-section of CX_3CR_1-tdt expressing mice with the lysosomal protein CD68 (**Fig. 26E-F**). We observed an increase of the $CD68^+$ tdT^+ microglia cells density between D0 and D7. Although CD68 is constitutively expressed by microglia cells, its upregulation reflected cell activation associated with enhanced phagocytosis and microglial lysosomes formation (Wu et al., 2021)

Collectively, the detailed analysis of transcriptomic microglial clusters enabled us to decipher their behavior during demyelination, remyelination, and repair. Following LPC-induced white matter injury, microglial cells underwent intense cell proliferation to increase their population. As the lesion progressed, they acquired antigen-presenting capacities through the expression of the MHC complex. Therefore, they were able to recruit and modulate the activation of peripheral adaptive immune cells into the lesioned parenchyma. In parallel, microglial cells undertook phagocytosis and myelin clearance, as evidenced by the enhancement of lipid metabolism and lysosomal-mediated debris degradation. This pro-regenerative behavior was further sustained by the expression of genes mediating anti-I responses, such as *Cd83* and *Lag3*. Finally, microglia supported neuronal repair (*Grin2A*, *Gpx3*) and remyelination (*Igf1*).

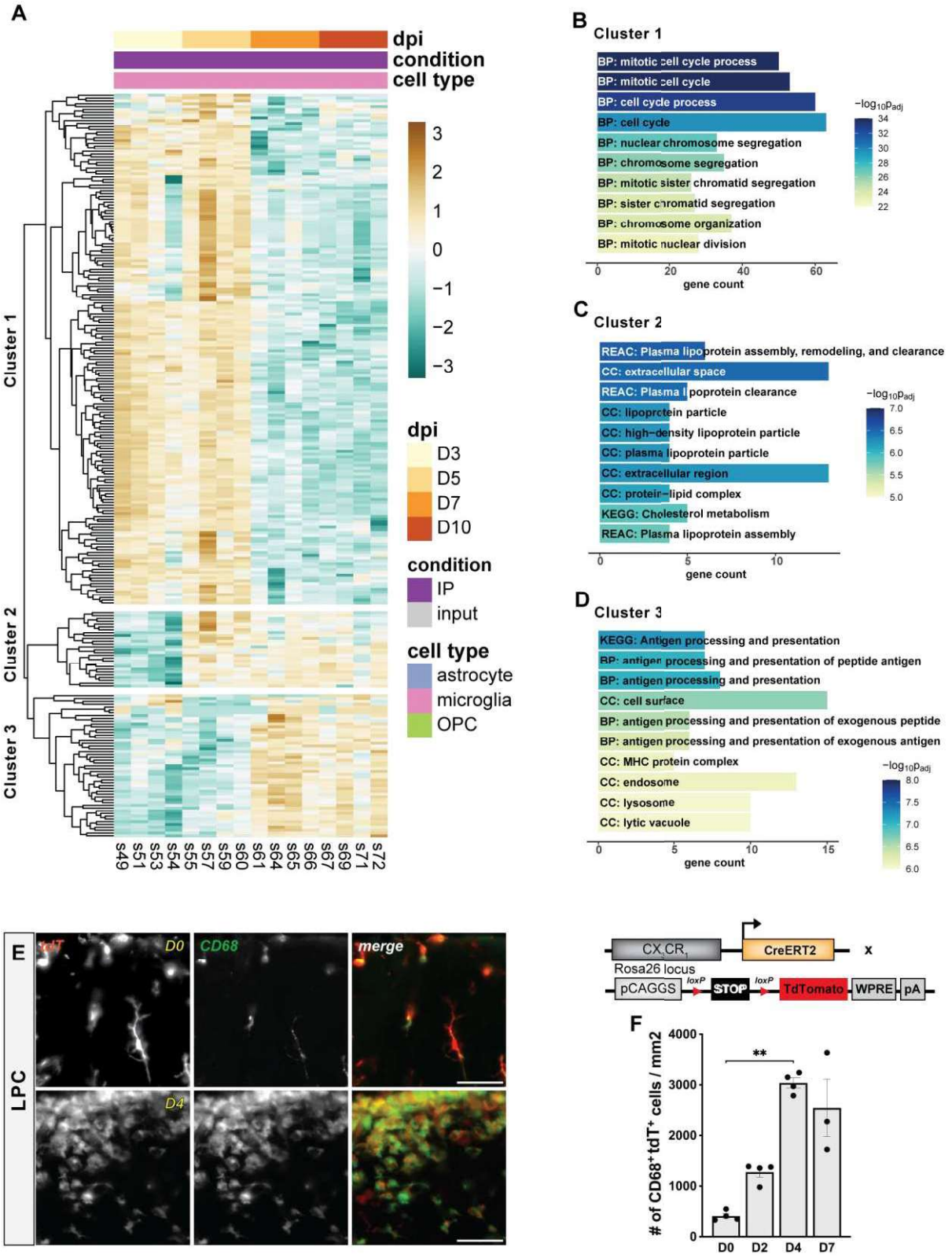

Figure 26. Functional analysis of transcriptomic diversity and gene expression dynamic in microglia cells during demyelination and remyelination

A. Heatmap based on the union of DE genes identified in microglia between all-time points analysis. Their gene expression can be divided in three different clusters according to transcriptomic activity. dpi: days post-incubation; s: sample number replicate. **B-D**. Enrichment analysis of each cluster based on GO, KEGG, Reactome, and TRANSFAC® databases. In each panel are presented the top 10 most significant terms and

pathways. **E.** Immunolabeling of the lysosomal marker CD68 in tdTomato-expressing microglia cells, depicting their strong activation and enhanced phagocytic activity, at D0 and D4 following LPC-incubation. Scale bar, 50 µm. **F.** Quantification of double positive TdT^{+} $CD68^{+}$ microglia cells within the lesion site from D0 to D7.

7.3.4. Transcriptomic analysis of astrocytes cells following LPC treatment

7.3.4.1. Differentially expressed genes during demyelination and remyelination

Although the role of astrocytes in demyelination conditions have been extensively studied, the precise underlying gene regulatory program associated with demyelination and remyelination are not yet fully understood. To gain a detailed view of astrocytic gene expression, we focused our analysis on the specific mRNA IP samples isolated from GFAP expressing cells.

Astrocytes were the most challenging cell type to analyze. Compared to OPCs and microglia, which respectively differentially expressed 270 and 271 genes in total between D3 and D10, astrocytes exhibited 2029 DE genes. This means that astrocytes displayed seven times more DE gene pointing out that the gene expression of glial cells differed profoundly between experimental conditions. This intense transcriptomic activity was reflected in the volcano plots, illustrating DE genes between time point comparisons (**Fig. 27A**). Between D3 and D5, astrocytes totaled 1736 DE gene, corresponding to 712 genes with a positive FC and 1024 gene with a negative FC (**Fig. 27A, left panel**), while between D5 and D7, astrocytes shown transcriptomic modulation of 286 gene, with 158 upregulated genes and 109 downregulated genes (**Fig. 27A, middle panel**). Finally, it appeared that astrocytes did not exhibit as high a level of difference in their gene transcription at the onset of remyelination, as only seven genes were differentially expressed between D7 and D10, comprising two genes with a positive FC and five with a negative FC (**Fig. 27A, right panel**).

Between D3 and D5, the transcription factor “TF: ZF-5” was significantly enriched. It is a Kruppel-Type Transcriptional Repressor. Although, its precise function in astrocytes has not yet been being unraveled, it depicted intense difference in genes transcription. Another enriched transcription factor in GO terms was "TF: E2F-1". While in OPCs it has been linked with apoptosis, in astrocytes its expression was associated with neuroinflammatory cell activation and may have implications in glial scar formation (Wu et al., 2015). The terms “intracellular anatomical structure”, and “CC: cytoplasm” reflected the reorganization or formation of cytoplasmic organelles, while the term “CC: cellular anatomical entity” is linked to cell shape modification according to their activity (i.e. BBB and support, phagocytosis). Finally, the last term “MF: protein binding” highlighted enhanced cell signalizing and communication mediated through ligand-receptor interaction with other cells or with soluble mediators inducing intracellular cascade signaling (**Fig. 27B, a**). Although the terms within the cluster generated between D5 and D7 still included “MF: protein binding”, the majority of them

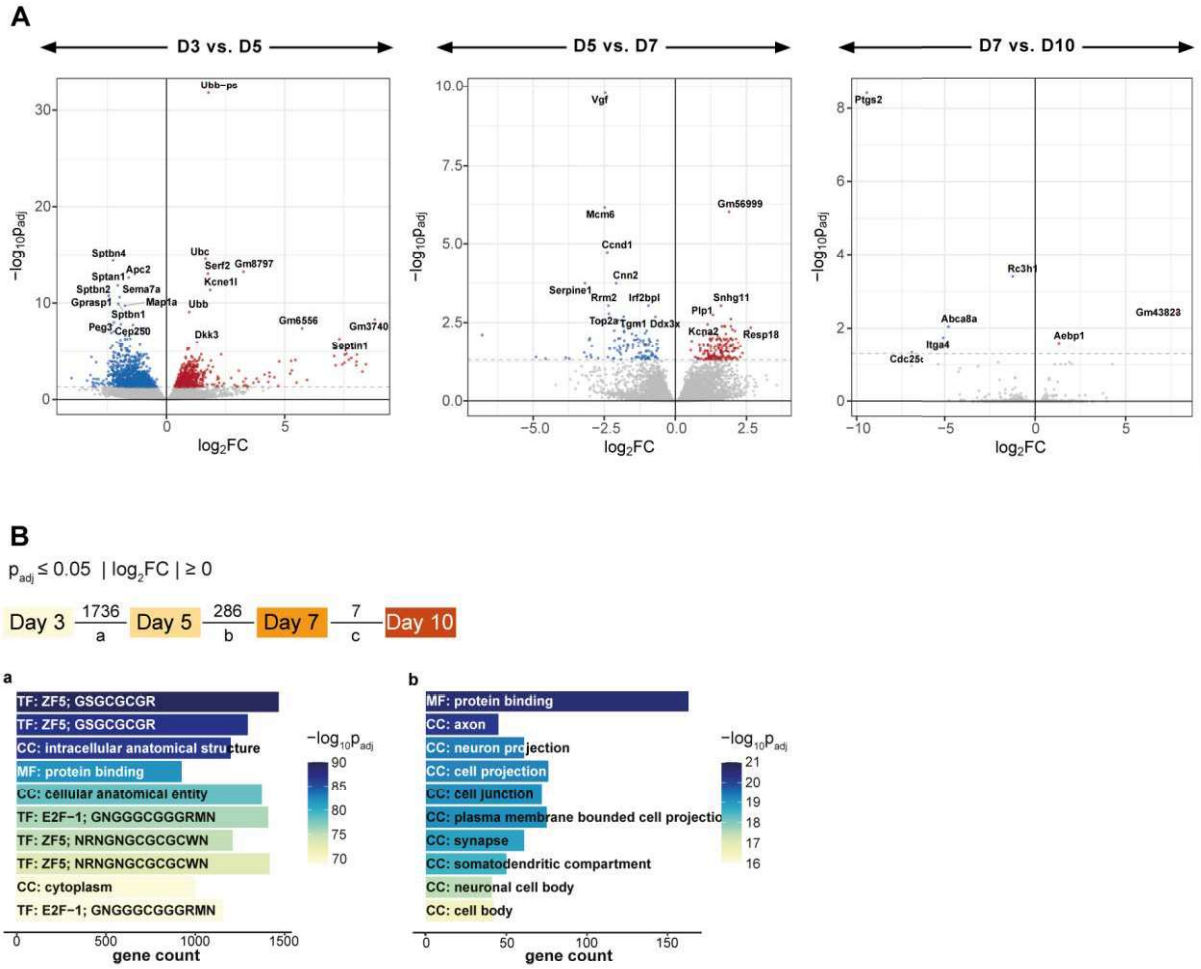

Figure 27. Comparison of differentially expressed genes in astrocytes across demyelination and remyelination

A. Visual representation of Differential Gene Expression (DEG) from immunoprecipitated (IP) samples from GFAP expressing cells between D3 and D5 (left panel), D5 and D7 (middle panel) and, D7 and D10 (right panel). Genes with a positive FoldChange (FC) are presented in red and those with a negative FC in blue. **B.** Gene Ontology (GO) functional enrichment analysis of the DEGs identified between time points. Comparison of D3 to D5 revealed 1736 DEGs included in the as well as 286 DEGs between D5 and D7 and, 7 DEGs comparing D7 to D10 with respective corresponding 10 top most significant GO terms (a, b).

were related to neurons (i.e., "CC: axon", "CC: neuron projection", "CC: synapse", "CC: somatodendritic compartment", and "CC: neuronal cell body") (**Fig. 27B, b**). This underlined the intense activation of astrocytic protection of neurons or restauration of synaptic transmission under pathological conditions, or conversely, astrocytic-mediated neuronal death. Finally, astrocytes were establishing cell-cell contacts as indicated by the term "CC: cell junction", involving cell shape remodeling and deployment their processes to reach their partners, as seen by "CC: cell projection", "CC: plasma membrane bounded cell projection" and "CC: cell body".

To continue our investigation of the transcriptomic activity of astrocytes following LPC treatment, we proceeded as we did before for OPCs and microglia. We generated a heatmap based on the DE genes

identified with the time point comparisons (Fig. 28A). We further identified three clusters based on the dynamic gene activation over time. The first cluster contained 1068 genes upregulated at D3, whereas the second cluster displayed 706 genes whose expression were enhanced from D5 to D10. Finally the last cluster was the smallest, with 109 genes required between D3 and D5. Subsequently, we carried out a functional enrichment analysis for those three clusters, accounting four different databases: GO, KEGG, REAC and, TRANSFAC®. Then, we chosen on the ten most significant terms and pathways and focused our analysis on their gene composition (**Fig. 28B-D**).

7.3.4.2. Detailed investigation of gene clusters

- **Cluster 1**

Within this first cluster, we found again the terms related to the transcription factors E2F, E2F-1, and ZF-5 (**Fig. 28B**). As explained, E2F and E2F-1 were associated with enhanced cell proliferation under injury conditions as well as pro-I activation of astrocytes. However, the grouped analysis of the genes found within the terms "MF: protein binding", "BP: cellular component organization", and "CC: cell junction" gave a detailed view of astrocytic behaviors following demyelination at D3.

We found that astrocytes significantly upregulated intrinsic cellular activities. They increased various genes related to cell surface protein - mediating cell-cell communication, signal transduction, adhesion, and recognition - such as glycoproteins (*Adam1a*, *Adam22*, *Adam23*), transmembrane adenyl-cyclases (*Adcy4*, *Adcy5*), kinases anchor proteins (*Akap6*, *Akap8*, *Akap11*), and subtypes of the Ankyrin family (*Ank1*, *Ank3*, *Ank13a*, *Ank24*). Additionally, we observed enhanced translation of genes controlling cytoskeletal remodeling - implicated in intercellular communication, migration or phagocytosis - like coronins (*Coro1a*, *Coro2a*, *Coro6*, *Coro7*), filamin (*Flna*, *Flnb*), centrosomal proteins (*Cep131*, *Cep250*, *Cep290*, *Cep295*, *Cep350*), dynein protein needed for centrosome reorientation during migration (*Dync1h1*, *Dync1i1*, *Dync2h1*), but also Nestin (*Nes*), Distonin (*Dst*), *Net1*, and *App*. Astrocytes intensified cholesterol efflux processes to maintain lipid balance, as seen by the expression of *Ldlr*, *Ldrap1*, *Lsr*, and *Pltp*. As buffering cells involved in maintaining CNS homeostasis, astrocytes expressed a myriad of transporters following demyelination to prevent excitotoxicity. Among them, we found transporters for glutamate (*Slc1a1/EAAT3*), glucose (*Slc2a1/Glut1*), anions (*Slc22a8/Oct3*), copper (*Slc31a1/Ctr1*), zinc (*Slc39a10*), iron (*Slc40a1/Fpn1*), cationic amino acids (*Slc7a1/Cat*), L-amino acids (*Slc7a5, Lat1*), and carbon dioxide/hydrogen ions ($Co2/H^+$, *Slc9a5*). They enhanced as well intracellular transport through kinesins (*Kif13b, Kif5c, Klc2*) and myosins (*Myo10, Myo18a, Myo1b, Myo1c, Myo1d, Myo5a, Myo9a*). Furthermore, astrocytes elevated their rate of vesicle trafficking (*Rab27a*, *Rab3a*, *Rab3c*, *Tg2*, *Rph3a*, *Pclo*, *Cavin1*, *Cavin2*) and exocytosis to secrete their molecules into the extracellular space (*Fcho1*, *Mical3*, *Prkcb*, *Rims3*).

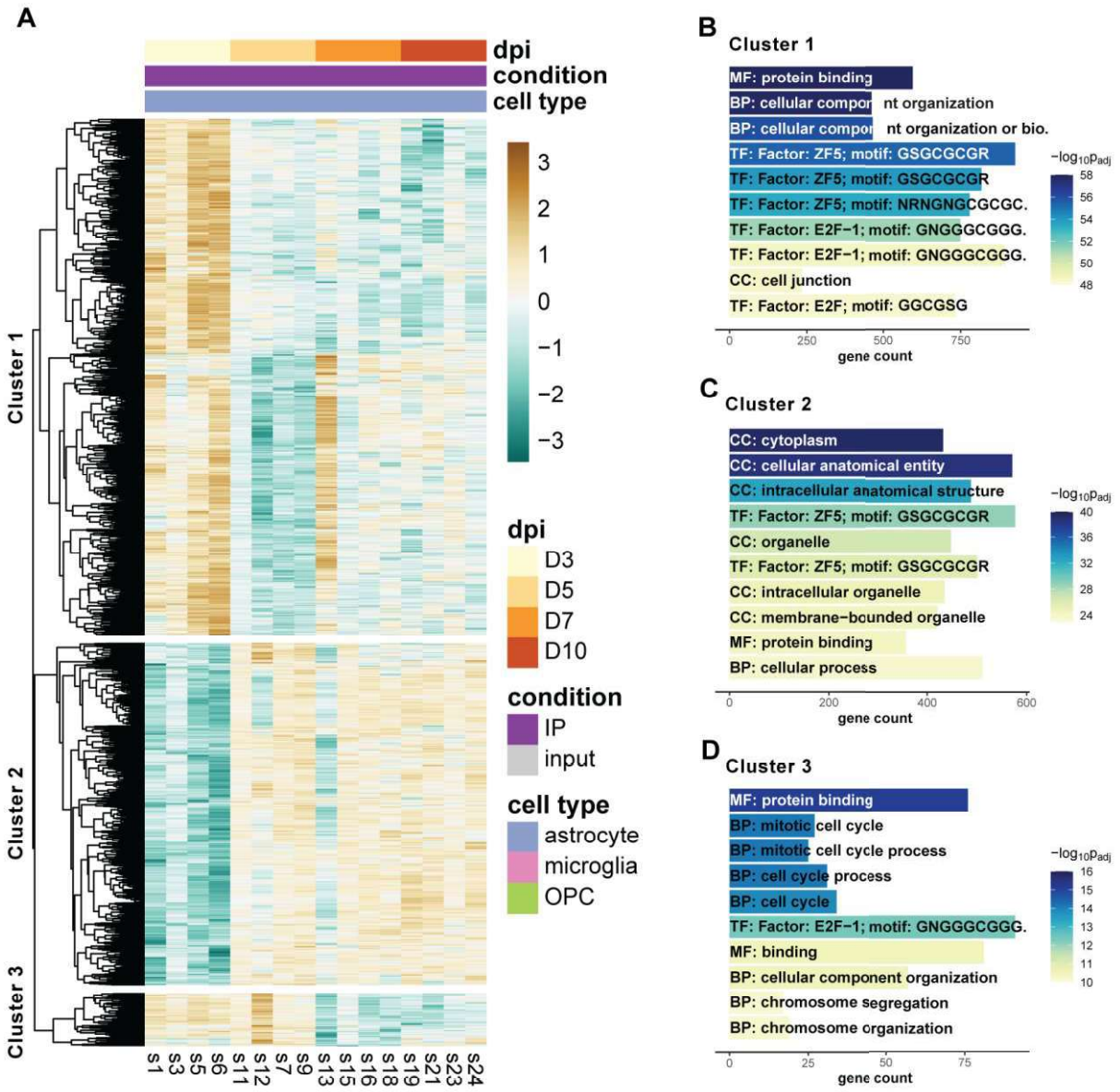

Figure 28. Functional analysis of transcriptomic differences and gene expression dynamic in astroglia cells during demyelination and remyelination

A. Heatmap based on the union of the DE genes identified in astrocytes between time points analysis. Their gene expression can be divided in three different clusters according to transcriptomic activity. dpi: days post-incubation; s: sample number replicate. **B-D.** Enrichment analysis of each cluster based on GO, KEGG, Reactome, and TRANSFAC® databases. In each panel are presented the top 10 most significant terms and pathways.

During early demyelination, a portion of the astrocytic population was actively proliferating within the lesion. This was evidenced by the upregulation of genes such as *Dixdc1*, *Rgmb*, and *Ets*, as well as signaling pathways like Ras signaling (*Rasgrf1*, *Rasgrp3*, *Rasip1*, *Rassf3*) and *Braf*, an intermediate of the pathway, along with Rap1 signaling (*Rap1gap*, *Rapgef4*, *Rapgef6*). However, we also observed genes indicating that some newly generated astrocytes were derived from NPC cells (*Plp1*, *Epac2*) (Seo and Lee, 2016; Guo et al., 2020). Conversely, mature astrocytes within the lesion were self-

protecting from apoptosis-mediated death via the enhanced expression of anti-apoptotic genes like *Bmp2* and *Xiap*.

Surprisingly, we found that astrocytes expressed myelin-related genes such as *Mag*, *Mbp*, *Plp* and *Mylt1* but also gap junctions usually found in OLs or neurons like *Gjb1/Cx32* and *Gjb3/Cx31*. We could also identify the expression of axons guidance molecules, including *Map1b*, *Plxna2*, *Plxnb3*. However, astrocytes also amplified synaptic transmission as depicted by gene coding for proteins involved in the membrane of synaptic vesicle (*Sv2*a, *Sv2c*) as well as the excitatory neurotransmission through NMDA (*Grin1*) and AMPA receptors (*Pacsin1*) with a scaffold protein involved the excitatory synapse architecture (*Nsf*).

The transcriptome of astrocytes reflected their inflammatory polarization. Indeed, at D3, they expressed genes associated with the A1 phenotype, including *Bin1*, *Synm*, and *Dbn* involved in scar formation, and *Ano1* mediating NF-κB activation. Additionally, *Mafg* was found to promote the A1 phenotype (Dulin, 2020; Wheeler et al., 2020; Schiweck et al., 2021). This behavior was associated with astrocyte-mediated CNS inflammation through *Cd74*, *Il2rg*, and *Il34*, as well as neurodegeneration via *Cox2*, impeding OPC differentiation (Shiow et al., 2017), and BBB breakdown via *Vegfr2* and *Nkd1*, involved in the VEGF-A and Wnt pathways, respectively (Argaw et al., 2012; Guérit et al., 2021). Reactive astrocytes enhance Ca^{2+} signaling, which potentiates cellular excitability. Accordingly, we found an enhancement in the expression of genes such as *Cacna1a*, *Cacna1b*, *Cacna1c*, *Cacna1d*, *Cacna1g*, *Cacna1h*, and *Cacnb4*. Astrocytes expressed *Sema7a*, whose expression has been associated with inhibition of axonal recovery and pro-I polarization of monocytes and macrophages (Holmes et al., 2002). Finally, astrocytes were able to induce pro-I polarization and proliferation of microglia cells through the expression of *Csf1* (Hagan et al., 2020) .

Conversely, during demyelination, astrocytes exhibited enhanced expression of anti-inflammatory and neuroprotective-associated genes. The upregulation of *Tgfbr2*, *Tnc*, and *Socs5* correlated with the A2 phenotype, conferring neuroprotective effects through *Ndrg1*, *Ndrg4*, and *Rph3a* gene expression (Schonkeren et al., 2019; Zhu et al., 2022). Additionally, increased expression of *Rictor* and *Reck* facilitated functional recovery as well as *Ncs1* providing neurotropic support to neurons via BDNF secretion (Wang et al., 2010; Nakamura et al., 2017; Chen et al., 2020). However, *Reck* has also been implicated in vascular development via the Wnt-signaling pathway (Ulrich et al., 2016). Accordingly, we identified genes linked to BBB integrity and repair such as *Agrn*, *Lama5*, *Ly6a* and *Radil*, as well as those inducing angiogenesis like *Endoglin-1*, *Fmnl3*, *Nr2f2*. Moreover, the Wnt pathway was as well enhanced as depicted by the upregulation of *Blv1*, *Bvl2*, *Igf1r*, *EphrB4*, and *Fel1*. A2 astrocytes established interactions with synapses to promote their recovery via the expression of *Efna3*, *Pkd1*, *Pdgfrβ*, *Plekha1*, *Plekha2*, *Plekha3*, *Plk2*, *Slitrk3*, *Fgf13*. Astrocytes possibly supported OPCs migration via upregulation of semaphorins, *Sema3a* and *Sema6c*, both acting as a signal for migratory OPCs to detach from the vasculature and subsequently differentiate (Su et al., 2023). Finally,

astrocytes could have suppressed inflammatory T cells response via the cell surface enzyme *Entpd1*/*Cd39* (Ulivieri et al., 2019).

- **Cluster 2**

Among the 706 genes constituting the cluster 2, the functional annotation enabled to assign 639 to biological GO terms (**Fig. 28C**). Through the detailed analysis of the genes within these terms, we were able to identify specific astrocytic features between D5 and D10, following LPC treatment.

Although the function of the transcription factor ZF5 is not yet understood (i.e. "TF: factor ZF5), we found genes coding for proteins that belong to the Kruppel-like factor (KLF) as *Zfp385a*, *Zfp423*, and *Zfp661*.

However, astrocytes are involved in a myriad of different tasks. We identified upregulation of transmembrane channels and transporters supporting their buffering functions to maintain extracellular environment homeostasis. Thus, we found increased gene expression related to K^+ channels, including *Kcne1l*, *Kcng4*, *Kctd5*, and *Kctd1*, as well as *Nkain4*, which regulates Na^+/K^+ transport. They also enhanced the expression of neurotransmitter transporters such as *Slc1a2*/*Glt-1* and *Slc1a3*/*Glast* for glutamate reuptake; amino acid transporters including *Slc13a3*/*Nac3* (N-acetyl-L-aspartate) and *Slc38a1*/*Snat1* (neutral amino acids); cation and anion transporters such as *Slc22a4*/*Octn1* (organic cations), *Slc30a6*/*Znt6*, *Slc39a12*/*Zip12* (Zinc), *Slc41a1*/*Mgt2* (magnesium), and *Slc35b2* (3'phosphoadenosine 5'-phosphosulfate, PAPS); dipeptides (*Slc15a2*, glycylsarcosine), urea (*Slc14a1*), and long-chain fatty acid (*Slc27a1*/*Fat1*) transporters; the Na^+/H^+ exchanger *Slc9a9*; as well as mitochondrial transporters for nucleotides (*Slc24a4*), glutathione (*Slc25a39*), and Ca^{2+} (*Slc24a4*).

Similarly, astrocytes participated in clearing the ECM by engaging in the phagocytosis of cellular debris and neurons through the expression of genes such as *Abca1*, *Axl*, and *Elmo2* (Konishi et al., 2020). Additionally, they upregulated cellular pathways involved in degradation. Among them, we identified genes related to autophagy, including *Wipi1*, *Atg12*, *Map1lc3b*, *Rab1a*, and *Rab7*. Similarly, astrocytes enhanced genes involved in lysosomes such as *Lamp1*, *Lamp2*, *Tmem9*, *Laptm4a*, *Scarb2*, *Ttyh1*, *Rnf5*, *Rnf115*, as well as cathepsin genes like *Ctsb*, *Ctso*, and *Ctsl*. They actively participate in protein degradation, as reflected by the expression of ubiquitination-related genes such as *Ubb*, *Ubc*, *Ube2h*, *Ube213*, and *Ube2n*, along with genes corresponding to proteasome activity such as *Psmd3*, *Psmd7*, and *Psmd10*.

As observed within the first cluster, astrocytes displayed cytoskeletal remodeling through the expression of *Spire1*, *Cnn1*, *Colt1*, *Map4*, *Marcksl1*, *Rab13*. This was linked to cellular migration as seen by the enhanced regulation of related genes such as *Dennd2b*, *Mmp14*, whose expression are induced by Il-6, *Amer2* or cyclase associated actin cytoskeleton proteins, *Cap2*, *Cap2a2*, *Cap2b*. Interestingly, we observed an increased expression of *Aqp4* and *Aqp9*. Although both were implicated in water homeostasis, Aqp4 was also implicated in cell migration by facilitating water entry into

astrocytic protrusions (Saadoun et al., 2008). They increased the intracellular transport cargo mediated by dynein like *Dync2li1*, *Dynclt3*, or kinesin *Kifbp*, as well as vesicles trafficking via *Mpdu1*, *Scg3*, *Itsn1* but also the ESCRT proteins (*Chmp1a*, *Chmp4b*, *Chmp5*) required for endosomal transport and *Tspan15*, coding for a protein at the surface of extracellular vesicle mediating their docking to neuronal membranes (Upadhya et al., 2020; Stajano et al., 2023). Finally astrocytes internalized cell surface or extracellular molecules via clathrin-mediated endocytosis mediated by *Aagab* gene expression (Gulbranson et al., 2019).

Moreover, we found that astrocytes were actively taking part into lipid metabolism through the expression of numerous genes including those required for biosynthesis *Acot1*, *Acot11*, *Acsf2*, *Acsl6*, *Agpat3*, *Echdc2*, *Elov2*, *Elovl5*, *Hacd2*, *Hacd3*, *Srebf1*, as well as FA desaturation like *Fads1*, *Fads2*. Additionally, they exerted specific cholesterol metabolism via *Apoc1*, *Apoe*, and *Lcat*.

To meet the demand associated with their cellular activation, astrocytes increased metabolic pathways enabling them to fulfill energy needs. Thus, we observed an upregulation of glycolysis through the expression of genes such as *Eno1*, *Eno1b*, *Pfkp*, *Pgam1*, and *Pgk1*, which catalyze the breakdown of glucose to pyruvate, as well as *Ldhb* and *Pdha1*, respectively facilitating the conversion of pyruvate to lactate or acetyl-CoA. Finally, *Pfkfb3* and *Pfkm expression* enabled regulation of the cellular rate of glycolysis. In parallel, we identified enhanced expression of genes related to the respiratory chain complexes within the mitochondria. *Ndufa2*, *Ndufa4*, *Ndufab1, Tmem242* were controlling the assembly of complex I, while *Sdhaf2* and *Sdhc* were associated with complex II, and both *Uqcc5* and *Uqcr11* with complex III. Moreover, astrocytes were actively engaged in fatty acid beta-oxidation, which also provides energy. Typically, β-oxidation predominantly occurs in mitochondria, as indicated by the increased expression of *Acat1*, transporting FA into mitochondria. These FAs were subsequently activated by enzymes encoded by *Acsbg1* and *Acsl6* before undergoing β-oxidation, facilitated by *Acad11*, *Acadm*, *Acadsb*, *Acox1*, *Ech1*, and *Echs1*. However, *Ech1* and *Echs1* encode both mitochondrial and peroxisomal isoforms, so we cannot exclude that part of the β-oxidation was occurring within the peroxisomes as well. Interestingly, when acetyl-CoA entering the Tricarboxylic Acid Cycle (TCA) preferentially relies on fatty acid oxidation, various additional enzymes are activated to ensure the availability of intermediates required for the cycle. This was observed in astrocytes, where these intermediates were generated through the catabolism of glycogenic amino acids such as valine (*Hibadh*, *Hibch*, *Aldh6a1*) and alanine (*Gpt2*), as well as through the conversion of glutamate, initially transported into the mitochondria (S*lc25a18*) and subsequently converted into alpha-ketoglutarate (*Glud1*). Concurrently, astrocytes protected themselves from fatty acid oxidation-induced oxidative stress by expressing genes with antioxidant activity, including *Prdx6*, *Cryz*, *Gstm6*, *Higda1*, *Mgst1*, *Pon2/3* (Eraso-Pichot et al., 2018). Finally, pyruvate and acetyl-CoA were also produced based on the amino acids degradation as seen by the up regulation of *Bckdha* (leucine, isoleucine, and valine), *Bbox1* (lysine), and *Dao* (d-serine).

Astrocytes exerted various cell functions through the expression of cell-surface binding proteins. We found that they upregulated various transmembrane proteins such as *Tmem100*/ *185a*/ *47*/ *50a*/ *59*. Although their precise role in astrocytes has not be studied yet, *Tmem100* controls astrocytes activation, *Tmem47* regulates tight junctions formation, and *Tmem59* controls Golgi glycosylation reactions (Ullrich et al., 2010; Dong and Simske, 2016; Cui et al., 2023). However, through the expression of these binding proteins, astrocytes established as well contacts with surrounding cells. They contacted microglia through the expression of *Anax5* (Liu et al., 2024a). Astrocytes also contacted neurons, as seen by the enhanced expression of *Astn1*, *HtrA1* regulating neurite length, *Dner*, involved neuronal control of astrogenesis, *Ctnnd2*, controlling astrocyte morphogenesis, and *Syndecan-4*, which mediates interaction with neuronal Thy1 inducing astrocytes migration (Eiraku et al., 2005; Kong et al., 2013; Chen et al., 2018; Tan et al., 2023). They established as well contacts at the synaptic level via *Gpm6a*, enabling their adhesion, and *Mlc1*, expressed at astrocyte leaflets and interacting with excitatory synapses. Interestingly, we found that the expression of *Gja1*/*Cx43* could have mediated interactions among astrocytes, but also with neurons. Indeed, under diseased conditions, healthy astrocytes can establish contact with injured astrocytes (Cx43-Cx43) or injured neurons (Cx43-Cx46) to supply their vital needs of ions and metabolites. However, this connection can be harmful and lead to a wave of death of healthy astrocytes or neurons, contaminated by their dysfunctional counterparts (Liang et al., 2020). Additionally, *Cx43* may enable the interaction with OLs (Cx43-Cx47) which was found to impede OPCs differentiation (Li et al., 2020b). Finally, the upregulation of *Hepacam* emphasized astrocytic self-organization regulating competition for territory and morphological complexity (Baldwin et al., 2021).

Furthermore, astrocytes proliferated, as indicated by the upregulation of *Pcbp2* (Mao et al., 2016). Conversely, they were also controlling their own proliferative rate in a cell-autonomous manner via *Llgl1* gene expression (Beattie et al., 2017). However, we discovered that newly generated astrocytes could partially originated from NSCs. Indeed, they exhibited enhanced expression of *Tsku*, which regulates GFAP expression in NSCs, while *Ecrg4* and *Hopx* ensured the astrocytic NSCs cell fate, and *Ndgr2* (Ito et al., 2016; Zweifel et al., 2018; Istiaq et al., 2022). We also found evidence that some astrocytes might be generated through conversion from neurons, as reflected by the expression of *Neuronatin*/*Nnat* (Ma et al., 2019). Additionally, astrocytes upregulated the expression of *Cd81*, encoding a cell surface glycoprotein that interacts with neurons to control astrocytic proliferation rate (Kelić et al., 2001). Furthermore, we observed gene expression associated with astrocyte progenitor cells (*Pbxip1*), immature astrocytes (*Sh3pxd2b*), mature astrocytes (*Nfix*, *Dbx2*, *Plag2g7*), and those undergoing the maturation process (*Pax6*, *Ntrk2*, *Dlg5*). Finally, we identified specific astrocyte subpopulations through the expression of *Camk2g*, and the concurrent upregulation of *Olig2* and *Gat3* highlighted the existence of a $GFAP^-$ population involved in neuronal transmission (Erickson et al., 2018; Tatsumi et al., 2018).

Between D5 and D10, astrocytes increased their involvement in the regulation of neurotransmission. They enhanced the expression of the glutamate receptor subunit *Gria1*, as well as genes participating in the control of glutamatergic transmission such as *Lrp4*. Furthermore, they expressed *Gabrg1*, implicated in GABAergic transmission, while *Aldh1a1* enabled GABA synthesis and *Abat* participated in its degradation.

Numerous of genes within this second cluster have been linked to reactive A1 astrocytes. We found gene expression associated with A1 phenotype such as *Cntn1*, *Bcl6*, *Itm2b*/*2c*, *Msi1*, *Mdm2*, *Mif*, *Ntsr2*, and *Bmpr1b*, while the upregulation of *Id2*/*3* induced their pro-I polarization via TNF-α signaling (Abd-El-Basset et al., 2021). Reactive astrocytes increased their proliferation, participating in glial scar formation via *Cspg5* expression (Anderson et al., 2016). These astrocytes upregulated genes specifically inducing the activation of NF-κB signaling, thereby promoting pro-I release in astrocytes such as *Trim8* and *Parp12* (Welsby et al., 2014; Bai et al., 2020). In addition, these astrocytes upregulated *Lgals3* and co-activators *Lgals3bp* and *Lgalsl*, which control the proper activation of the Notch signaling. This was further supported by the expression of Hey genes (*Hey1*, *Hey2*) both induced by Notch pathway, collectively resulting in cell proliferation and glial scar formation (LeComte et al., 2015; Zhong et al., 2018; Ribeiro et al., 2021). Furthermore, we identified genes promoting pro-I cytokine release. The gene *Irak2*, by forming a complex with Myd88 and Irak1, induced the gene transcription of Il-1β, Il-6, and TNF-α, while *Mgl* generated arachidonic acid, a precursor of inflammatory prostaglandins (Grabner et al., 2016; Manu et al., 2023). As expected, those reactive astrocytes with such pro-I phenotype may have enhanced neurodegeneration. Through the upregulation of *Gm2a*, astrocytes mediated neurites loss, while the expression of *Prdx6* contributed to p romoting apoptosis-mediated neuronal death (Hsieh et al., 2022; Hou et al., 2023b). Moreover, astrocytes were able to induce synapses damage via enhancement of *Ranbp9* and *Vangl2* (Palavicini et al., 2013; Thakar et al., 2017). In addition, they might have worsened the demyelinating process via *Sema4a* expression, which facilitated the loss of mOLs, but also impeded remyelination via *Ednrb* and *Gdpd2* (Hammond et al., 2015; Chiou et al., 2019; Lin et al., 2023). Finally, reactive astrocytes seemed to actively signal to recruit and activate pro-I cells within the lesion. Through the expression of *Prkcsh* (enhancing the expression of Ccl2) and *Cxcl10*, astrocytes mediated the parenchymal infiltration of peripheral immune cells (Phares et al., 2013; Chen et al., 2022a). *Mdk* acted as chemoattractants for monocytes and macrophages (Neumaier et al., 2023). However, both were involved in recruiting M1 microglia cells while the astroglial expression of *Plxnb1* may allow interaction with microglial through their Sema4d receptor, inducing release of I-1β and Nos2 by astrocytes (Sanmarco et al., 2021).

Finally, we found transcriptomic evidence of alternatively activated A2 astrocytes. We identified the upregulation of *Nfia* which is governing the switch of astrocytes toward an A2 phenotype (Tchieu et al., 2019). Moreover, we found that *Loxl1* and *Prnp* expression were correlated with a decrease of A1 polarization, while the upregulation of the metallothionen-related genes *Mt1*/*3* and *Ndgr3* conferred

neuroprotection (Schonkeren et al., 2019; Tahir et al., 2022; Paryani et al., 2023; Hariani et al., 2024). The expression of *Ncam1*, *Trim9*, *Matn3*, and *Gas6* participated in decreasing the activation of the pro-I NF-κB pathway (Zeng et al., 2019; Gilchrist et al., 2021; Eve et al., 2022; Zhou et al., 2024). In addition, we observed enhanced expression of genes involved in reducing astroglial-mediated inflammation such as *Arl6ip1*, *Apelin*, and *Pebp1*, whereas *Ptgr2* inactivated the prostaglandins (Wu et al., 2008; Kim et al., 2019; Liu et al., 2022; Lim et al., 2024). Astrocytes potentially decreased the expression of MMPs, implicated in tissue inflammation and degeneration, via the expression of tissue inhibitor of metalloproteinases *Timp2* and *Timp4* (Kikuchi et al., 2021; Britton et al., 2023). Moreover, they increased the TGF-β signaling via the expression of *Tgfb3*, *Romo1*, and *Ltbp3* (Todorovic and Rifkin, 2012; Liu et al., 2017). These anti-I astrocytes perhaps supported neuronal survival through the demyelination process via the expression of *Cd63*, and *Cst3* (Pan et al., 2020; Sarkar et al., 2021). They were exhibited a close relationship with the neuronal compartment. They could have contributed to neuritogenesis through expression of *Prnp* and *Arsb* (Zhang et al., 2014; Amin et al., 2016) and axonal pathfinding via gene expression of *Adcy8*, *Robo1*, *Spon1*, and *Pcdh17* (Burstyn-Cohen et al., 1999; O'Sullivan et al., 2017; Mancini et al., 2020; Devasani and Yao, 2022). Additionally, they might have promoted synaptogenesis of excitatory neurons through the expression of *Cd38* and *Fabp7* (Ebrahimi et al., 2016; Hattori et al., 2023), as well as synapse assembly via upregulation of *Lgi1* and *Nrxn1* (Thomas et al., 2018; Trotter et al., 2021), and the synaptic connectivity with *Gpr179* (Condomitti et al., 2018). Astrocytes were highly committed to BBB integrity and repair. They plausibly conferred BBB protection through the expression of *Aggf1*, *Neo1*, and *Ntn1* (Zhu et al., 2018; Yao et al., 2020), while *Ndrg2* decreased the expression of MMPs (Takarada-Iemata et al., 2018). Astrocytes promoted collagen IX synthesis involved in the epithelial membrane via *Col9a3* expression as well as junctional adhesion molecules *Jam2*, and claudins involved in BBB tight junctions through *Cldn10* and *Cldnd1* gene expression (Vong et al., 2021). Finally, they seemed to promote microglia-mediated phagocytosis through the upregulation of *Il-33* (Vainchtein et al., 2018) as well as remyelination by enhancing OPCs recruitment through *Fgf1* expression, and differentiation via *Matn2* gene (Mohan et al., 2014; Sozmen et al., 2019).

- **Cluster 3**

The third cluster contained DE genes upregulated between D3 and D5, during demyelination (**Fig. 28D**). As observed in the comparison of DE genes between D3 and D5 (**Fig. 27B, a**), many genes were associated with the expression of the transcription factor E2F-1. This factor has been linked to reactive astrocytes, inducing their intense proliferation to form the glial scar, as well as neuroinflammation and degeneration (Wu et al., 2015). Accordingly, the majority of the terms generated within this cluster correlated with cell proliferation such as “BP: mitotic cell cycle”, “BP: mitotic cell cycle process”, “BP: cell cycle process”, “BP: cell cycle”, “BP: chromosome segregation”, and “BP: chromosome organization”. Within these terms, we found genes related to

DNA replication such as mini chromosome maintenance subfamily (*Mcm2*, *Mcm3*, *Mcm5*, *Mcm6*), spindle assembly (*Nusap1*, *Prc1*), centrosome (*Plk4*), kinetochore (*Nuf2*), microtubule assembly (*Tpx2*, *Tubb5*, *Tubb6*, *Racgap1*) chromatid segregation (*Aurka*, *Aurkb*), mitotic checkpoint (*Bub1b*), and regulation of cell cycle (*Cdc25c*, *Ccnd1*, *Cdkn2c*). These transcriptomic observations were further sustained on SC cross-section of hGFAP-CFP transgenic mice labeled the proliferative marker Ki-67. The density of CFP^+ $Ki67^+$ significantly increased between D3 and D5 during demyelination to further decline at the onset of demyelination at D10 (**Fig. 24C**).

We subsequently focused our analysis on the gene composition of the last terms "MF: protein binding", "MF: binding", and "BP: cellular component organization". We identified that astrocytes increased nucleocytoplasmic trafficking through the upregulation of importins (*Ipo5*, *Kpna2*), exportin (*Eef1a1*), nuclear membrane (*Lmna*), and nuclear architecture (*Tmpo*). Astrocytes also described possible enhanced migration via the upregulation of *Ugdh* and *Itgav*/*Cd51* (Tao and Zang, 2016; Cho, 2017). This was linked to cytoskeletal remodeling as reflected by the expression of *Actg1*, *Actn1* and *Tpm4*. These astrocytes seemed to increase protein degradation through ubiquitination-mediated gene expression such as *Uba1*, *Uhrf1*, and *Usp14*. Finally, they were probably self-protecting against apoptosis through the expression of *Birc5* and *Birc6*, and engaging cell contacts with neurons through expression of *Ncam2* and *Itgav*/*Cd51* (Lamers et al., 2011; Cho, 2017; Liu et al., 2024b).

Within this cluster, we identified genes related to A1 polarization of astrocytes, such as *Hspb6* and *Tspo* (Peferoen et al., 2015; Tournier et al., 2023). These astrocytes enhanced TNF-α signaling and *Tweak* expression respectively, both participating to pro-I polarization (Saas et al., 2000). Finally, they might have restricted OPCs differentiation and subsequent remyelination via *Ccn2* expression, as well as axonal growth via the enhancement of *Chl1*.

Conversely, we also observed gene expression related to anti-I A2 astrocytes. Indeed, they upregulated genes known to decrease neuroinflammation such as *Fgf2* and *Anax2* (Liu et al., 2019; Zou et al., 2019). We also found that these astrocytes upregulated Notch signaling pathway via *Notch1* gene expression, typically activated under anti-I conditions and promoting resting astrocytic morphology via MAPK signaling (Acaz-Fonseca et al., 2019). Moreover, the expression of *Lgals1* promoted microglial polarization upon M2 phenotype (Starossom et al., 2012). They were also maintaining BBB integrity via *Iqgap2* expression (Katdare et al., 2024). Finally, we identified a strong support to the neuronal compartment. Astrocytes were preventing neurodegeneration via *Hspb1* gene expression as well as neuron growth through *Vgf*, and synaptogenesis via *Thsb2*, *Flbn2* and *Nrcam* (Burnside et al., 2015; Takano et al., 2020; Patel and Weaver, 2021; Yang et al., 2024).

Altogether, these data demonstrate the extensive transcriptomic diversity of astrocytes following LPC-induced demyelination. They enhance the expression of transcription factors, particularly E2F and E2F-1, characteristic of proliferative reactive astrocytes that mediated the formation of the glial

scar after SC injury. This proliferation was observed within the astroglial gene regulatory program between D3 and D5, with enhanced expression of cell-cycle-associated genes, as well as *in vivo* on the SC of treated mice. However, it appeared that some of the newly generated astrocytes were arising from NSC differentiation (*Plp1*, *Epac2*, *Tsku*, *Ndgr2*) or neuronal reprogramming (*Nnat*) rather than intrinsic gene pathways. From D3 to D10, astrocytes demonstrated high motility within the lesion site, associated with cytoskeletal remodeling, as evidenced by the expression of actin, myosin, or kinesin subfamilies. They were significantly involved in buffering the extracellular environment to prevent excitotoxicity through the expression of a myriad of channels and transporters, including those related to ions, water, amino acids, FAs, and the reuptake of neurotransmitters like glutamate or GABA to ensure correct neurotransmission. To meet the increasing energy demand due to cell activation, we found that astrocytes upregulated different key pathways such as glycolysis, FA β-oxidation, the mitochondrial respiratory chain, and the TCA cycle. Finally, we found genes related to pro- and anti-I behavior at all time points, emphasizing a duality between A1 and A2 phenotypes during demyelination and remyelination. A1-related astrocytes were found to secrete pro-inflammatory cytokines through the expression of *Cd74*, *Il34*, *Irak2*, or *Tweak* and the activation of NF-κB signaling (*Ano1*, *Trim8*, *Parp12*). They induced BBB breakdown (*Vegfr2*, *Nkd1*), promoted neurodegeneration (*Prdx6*, *Gm2a*, *Vangl2*), impeded repair and remyelination (*Ccn2*, *Chl1*, *Sema4a*, *Ednrb*), recruited pro-inflammatory peripheral immune cells (*Cxcl10*, *Prkcsh*, *Sema7a*), and induced M1 microglial activation (*Csf1*, *Plxnb1*). Conversely, those exhibiting an A2 phenotype decreased neuroinflammation (*Loxl1*, *Prnp*, *Fgf2*, *Anax2*, *Apelin*), enhanced BBB integrity (*Aggf1*, *Neo1*, *Ntn*, *Cldn10*, *Cldnd11*), promoted OPCs differentiation and remyelination (*Matn2*, *Sema3a*, *Sema6c*), as well as neuroprotection (*Hspb1*, *Cd63*, *Cst3*) or neuronal growth (*Vgf*, *Flbn2*). Finally, we found regulation of genes mediating the M2 microglia phenotype (*Il-33*) and suppressing T cell activation (*Cd39*).

8. DISCUSSION

In this project, we investigated the involvement and roles of microglial, astroglial, oligodendrocyte cells, and innate immune cells in a mouse model of demyelination induced by spinal incubation of lysophosphatidylcholine (LPC). By using multifluorescent transgenic mice in combination with two-photon intravital imaging and CARS microscopy, immunohistochemical (IHC) analysis on fixed spinal slices, quantification of inflammatory-related gene expression via reverse transcription, and cell-specific RNA sequencing of microglia, astrocytes, and oligodendrocyte-precursor cells (OPCs) using the RiboTag method, we demonstrated that:

- LPC incubation on dorsal spinal parenchyma efficiently produced focal and reversible demyelination

- Myelin disruption displayed remarkable cellular patterns concomitant to a transitory axonal loss, while both cellular compartments were regenerated by 28 days.

- Two waves of $LysM^{+}$ innate immune cells with contrasted functional phenotypes invaded the spinal cord *in vivo* regarding axonal cell density and along the lesion resolution.

- Microglia and astrocytes were actively recruited at the lesion site *in vivo* following LPC incubation with different time-scales and participated in both demyelination and remyelination processes.

- Microglia and innate immune cells adapted their inflammatory phenotypes according to myelin state, upregulated pro-inflammatory expression during demyelination and anti-inflammatory expression during remyelination.

- OPCs, microglia and astrocytes presented clear distinct gene expression after LPC treatment and modulated their transcriptomic gene activity separately along the lesion evolution.

8.1. Lysophosphatidylcholine-induced demyelination mouse model as a reliable tool to study cellular events following spinal myelin loss and remyelination.

8.1.1. LPC-incubation targeted myelinating oligodendrocytes to induce demyelination

To study the cellular events inherent to the demyelination process itself, we developed an innovative murine model of spinal incubation with lysophosphatidylcholine (Lysolecithin, LPC). The LPC toxin-induced demyelination model is one of the most commonly used and is typically performed by injection into the brain or spinal parenchyma, at the ventral or dorsal horns (Kuroda et al., 2017; Wang and Kotter, 2018). However, this method induces mechanical axonal degeneration due to needle insertion, mistakenly considered as a consequence of myelin and oligodendrocytes (OLs) loss (Hall, 1972; Keough et al., 2015). Thus, in our model, the LPC is incubated for one hour on the spinal cord's dorsal surface (SC), thereby preventing any mechanically-induced phenomena (El Waly et al., 2020). Although LPC incubation has been successfully used *in vitro*, this is the first time to our knowledge that it has been applied *in vivo* (Jarjour et al., 2012).

Compared to other MS mouse models such as cuprizone-fed mice (CPZ) or EAE, both producing random lesion sites in CNS, LPC instead induces focal lesions with a well-known defined time-sequence of resolution (Chu et al., 2019). We demonstrated that LPC incubation triggered fast demyelination of the SC within two days, reaching a maximum four to seven days after treatment and followed by spontaneous remyelination by 28 days, comparable to the known progression of such a lesion. LPC acts as a membrane-dissolving detergent of myelinating oligodendrocytes (mOLs), whose lack the enzymatic ability to metabolize and decrease its concentration to prevent cell impairment like the other cells in CNS (McMurran et al., 2019). Moreover, LPC mediates myelin loss through massive Ca^{2+} influx leading to degradation of myelin-containing lipids and proteins (Fu et al., 2007). We analyzed the impact of LPC on OLs lineage in SC two days after the incubation and demonstrated a significant decrease of $CC1^{+}$ mOLs while the PDGFRα^{+} OPCs seemed not to be impacted by LPC treatment at that time. In line with our data, previous *in vivo* studies demonstrated an early drop in mOLs density within 24h following LPC injection, mediating demyelination. However, this was accompanied by a decrease in PDGFRα^{+} OPCs. Although these two populations are restored within three to four days without affecting remyelination capacity, this underscores the potential global impact of LPC on the OL lineage (Plemel et al., 2018; Chu et al., 2019).

LPC is thought to induce non-immune mediated demyelination, enabling study of de- and remyelination processes themselves (Buttigieg et al., 2023). However, LPC was found to act on resident and infiltrated immune cells in the CNS. LPC application led to an immediate perturbation microglia homeostasis *in vitro*, causing a hyperpolarization of their membrane through modulation of ion channel activity leading to their de-ramification which adopted amoeboid shape (Schilling et al.,

2004). Despite this, we did not observe such microglial reaction *in vivo*. Microglia from LPC-incubated mice were displaying similar ramified shape than those of CTL PBS-incubated mice on the day of treatment (data not shown). Finally, a study demonstrated that within 12h following a spinal microinjection of LPC, a brief infiltration of T cells occurs, possibly linked to the activation of microglia and macrophages and subsequent demyelination via the expression of IL-12 (Ghasemlou et al., 2007).

8.1.2. Myelin disruption induced unique cellular pattern followed by spontaneous remyelination

To monitor the loss of the myelin sheath following LPC treatment, we took advantage of the dorsal window and performed chronic *in vivo* CARS microscopy from the initial day incubation until full recovery on day 35. Thus, we demonstrated that LPC triggered fast demyelination within two days, reaching a maximal loss of myelin coverage by one week with subsequent engagement of remyelination which was fully achieved by 28 days. Additionally, we employed the PLP-mGFP mice expressing membrane-bound GFP selectively in OLs and confirmed the same time-sequence of myelin disruption and remyelination. For years, it was widely believed that remyelination solely relied on the migration, proliferation, and differentiation of OPCs within the demyelinating lesion. However, new advances questioned this belief, considering OPCs not as the unique source of new myelin by demonstrating the ability of the surviving OLs to contribute to remyelination. Unfortunately, studies have emphasized their poor capacity to form accurate new myelin sheath. Indeed, under inflammatory conditions, although surviving OLs were able to extend their processes, they failed to form internodes in contrast to newly generated OPCs that demonstrated an efficient capacity of remyelination (Mezydlo et al., 2023). Similarly, in comparison to OPCs, surviving OLs undertook the formation of fewer new sheaths which were often mistargeted to the neuronal cell body instead of the axons (Neely et al., 2022). To corroborate these data, our results demonstrated the proliferation of PDGFRα^{+} OPCs, already labeled with Ki-67 during demyelination, and sustained until the onset of remyelination. Moreover, the RNA sequencing of NG2 expressing OPCs further demonstrated the up regulation of genes known to be involved in cell proliferation and cell cycle regulation specifically between D3 and D5 after the induction of demyelination with the LPC incubation. Interestingly, in MS patients, researchers found that most of the demyelinating plaques that underwent remyelination were repaired by preexisting OLs, raising questions about the differences in myelin regeneration mechanisms between rodents and humans (Yeung et al., 2019). Additionally, quiescent OPCs may not be the only source of newly generated mOLs. Neural progenitor cells can as well migrate into the lesion and differentiate into mOLs for remyelination (Nait-Oumesmar et al., 1999). In this sense, we observed in OPCs transcriptome the upregulation of specific genes involved in NPCs cell fate and differentiation

into OLs such as Hcfc1 or Cdkn1c. Finally, it has often been mistakenly thought that the CNS and PNS are two distinct entities with little interactions. However, we cannot exclude the possibility that remyelination may be partially accomplished by Schwann cells (SchCs). Indeed, a study demonstrated through fate-mapping that PDGFRα and NG2-expressing progenitor cells were able to generate both myelinating OLs and SchCs (Zawadzka et al., 2010). Moreover, SchCs possess the ability to migrate to demyelinated lesions in the CNS and remyelinate the axons (Ma and Svaren, 2018). Furthermore, these data were confirmed in SC of post mortem MS patients, where SchCs were found in remyelinated lesions with lower density than activated astrocytes (Ghezzi et al., 2023). To conclude, compared to developmental myelination, the remyelination appeared to form thinner sheaths around axons with short internodes. Despite these characteristics, these newly formed myelin sheaths enable the same electrical parameters for neurotransmission as well as metabolic support for long-term health and function of the CNS (Duncan et al., 2017).

Using the CARS microscopy, which enabled the labeling-free visualization of the myelin sheath *in vivo*, we described for the first time the precise modifications at the cellular level following LPC-induced demyelination. Surprisingly, myelin loss appeared to be sequential and could be classified based on its degeneration-acquired morphology. We identified eight canonical demyelinating patterns, classified in early (events 1 to 4) or advanced events (events 5 to 8), regarding the degenerating stage. One hour after LPC incubation, the myelin sheath already displayed curvy shape or bubble-like swelling deformation, progressing within a week to advanced events and forming isolated bubbles and myelin debris. However, we observed the strong reoccurrence of healthy sheath with linear shape from D21 until D35, testifying of the efficient remyelinating process. A previous study monitored how myelin sheath reacted within the first few hours after LPC treatment and described similar formation of bubble-like structure (Plemel et al., 2018). Our fine analysis brought a new light on our capacity to determine how far demyelination has progressed. Just by looking at the myelin aspect, we could attempt to determine the evolutionary stage of demyelination in MS disease.

8.1.3. Myelin loss impaired axonal compartment and led to transient neurodegeneration

We previously demonstrated that LPC effectively induced demyelination followed by spontaneous remyelination. However, our data also showed that this OLs loss was accompanied by massive axonal degeneration. Despite studies in genetic chronic model of demyelination emphasizing that axon could survive unmyelinated upon myelin injury without altering their health (Edgar et al., 2010; Smith et al., 2013), we demonstrated, using transgenic mice expressing CFP under the control of the Thy1 promoter, that axonal loss began as early as the first day after incubation with LPC. This loss continuously increased until reaching a maximum between four and seven days, which coincided with the period when demyelination was also at its peak. Such axonal pathology was also reported in other

models of MS such as CPZ and EAE, as well as in MS patients where demyelinated axons were fastly degenerating in active lesions (Klistorner et al., 2022; Schäffner et al., 2023). Moreover, myelin insulation was recently identified as an increased risk factor of degeneration to axons within an inflammatory environment, making them targets for autoimmune attacks (Schäffner et al., 2023).

Furthermore, our data demonstrated a transiently faster axonal repair compared to myelinated axons and the CARS signal. Specifically, we identified that the axonal compartment slowly initiated its repair starting from D7, whereas myelinated axons and the CARS signal only showed increases indicative of the ongoing repair process starting from D14. Additionally, we noted a discrepancy between the values of myelinated axons and the CARS signal, with the CARS signal remaining higher until D21, when remyelination was completed. Several hypotheses could explain our observations. Firstly, CARS microscopy captures a myelin signal regardless of its state or organization (Gasecka et al., 2017). Therefore, a CARS signal is recorded not only for the healthy myelin sheath but also for myelin debris or myelosomes due to demyelinating conditions, spreading lipids in the lesion environment. Thus, this discrepancy likely indicates the progress of environmental cleanup of myelin debris by activated phagocytic cells such as microglia or macrophages. Second, myelin cannot regenerate without physical interaction with axons, which act as a substrate essential for remyelination, thereby underwriting the physical necessity of axonal regeneration to occur first. Moreover, axonal regeneration and remyelination both rely on distinct intrinsic and extrinsic mechanisms (Uyeda and Muramatsu, 2020). However, it has been recently shown that OPCs can proliferate and migrate to the lesion to support axon growth (Zawadzka et al., 2022). But the glial scar, as well as myelin debris in the environment, are both known to impede their differentiation which delays remyelination (Kotter et al., 2006). Yet, unmyelinated axons are capable of generating signals to request their remyelination by mature OLs. Indeed, unmyelinated axons have been shown to be electrically active. This electrical activity is then perceived by the OPCs via their AMPA receptors, thanks to the newly formed synapses they established with axons. Thus, the release of glutamate induces the differentiation of OPCs into myelinating OLs able to remyelinate these axons (Gautier et al., 2015). Additionally, axons can use neuregulin signals to modulate the myelination of circuits. Neuregulin type II acts through neuronal ErbB2 receptors leading to myelination of spinal sensory neurons (Lysko and Talbot, 2022).

Finally, the notion of axonal regeneration is still in debate within the scientific community. We demonstrated through *in vivo* monitoring of Thy1-CFP axons, that the axonal compartment was back to its initial density by 28 days following LPC injury. Moreover, in our publication El Waly et al., 2020, the individual axon imaging supported that axonal reparation started between D4 and D7. However, there is a common consensus in the field that, unlike the PNS, the CNS is incapable of axonal regeneration. Indeed, we observe very little regeneration *per se*, but some damaged axons might have generated branches and extend neurites toward the lesion, while preserved axons can

undergo collateral sprouting. Moreover, we observed *in vivo* the formation of Thy1$^+$ retraction bulbs, typical of microtubules disorganization and intracellular transport impairment leading to regeneration failures (Hilton and Bradke, 2017). In addition, it has been demonstrated that there are intrinsic barriers to their regeneration, the first being the physical barrier formed by the glial scar that contains the lesion. Astrocytes secrete chondroitin sulfate proteoglycans (CSPGs), forming part of the extracellular matrix of the glial scar, while OLs express membrane-bound regeneration inhibitors (Sema4D, MAG, oMgp, and NogoA), both inducing growth cone collapse and subsequent axonal regeneration failure (Cooke et al., 2022). Therefore, rather than providing irrefutable proof that axons are regenerating, we emphasized here that the quick reparation of impaired Thy1$^+$ axons following LPC incubation suggests that neuronal death was minimal and axons were probably regenerating through sprouting once inflammatory conditions were favorable.

8.2. Innate immune cells and glial cells are dynamically involved at the lesion site

8.2.1. LysM$^+$ innate immune cells invade the spinal parenchyma in two distinct waves

Innate immune cells are known to take part in demyelinating events and remyelination (Mayo et al., 2012; McMurran et al., 2016). To determine the sequence of their recruitment, we used the transgenic LysM-EGFP mouse to label innate immune cells with GFP throughout their lifetime. Combined with two-photon microscopy, we performed chronic *in vivo* imaging from the day of LPC incubation (D0) to complete remyelination at D28. Surprisingly, we found that, in contrast to CTL PBS-incubated mice, LPC treated mice exhibited two distinct waves of LysM$^+$ cells infiltration at D4 and D14. The first wave occurred during the peak of myelin loss and was correlated with axon loss, while the second wave arose during remyelination and axonal repair. Therefore, we concluded that these innate immune surges may have different functional phenotypes.

The LysM-GFP$^+$ cells acquired within the lesion could be blood-circulating monocytes which, once penetrating into the spinal parenchyma, differentiated into monocyte-derived macrophages (MDMs) or neutrophils. To further investigate the cell composition of these innate immune cells, we analyzed by qRT-PCR the expression of the Ly6G gene, a known neutrophil marker. It appeared that Ly6G was specifically upregulated at D4, compared to D14, hence supporting the notion that the first wave may be mainly composed of neutrophil cells. Neutrophils have been described as contributing in mediating demyelination in CPZ and EAE mouse models (Carlson et al., 2008; Liu et al., 2010). Indeed, CXCR2$^+$ neutrophils have been demonstrated as essential for inducing OLs death and subsequent demyelination *in vivo*, which cannot be induced solely by toxin-mediated treatment. These cells probably infiltrated the SC within the first events of the demyelination process (Liu et al., 2010). In addition, in EAE model, the increased neutrophil cell density within the spinal parenchyma was

correlated with a circulating surge of these cells, driven by dynamic production and supply bythe bone marrow (Shi et al., 2022). However, even if neutrophils are massively recruited in the first days following LPC, we cannot exclude the effect of MDMs on demyelination. Indeed, MDMs are known to trigger demyelination *via* direct interaction with the node of Ranvier (Yamasaki et al., 2014). Finally, although circulating monocytes are not directly acting in spinal parenchyma since they are in the blood circulation, their depletion prevented demyelination suggesting their importance in this process through the production of ROS (Baaklini et al., 2019).

The second wave occurred at D14 during remyelination. At that time, we did not identify neutrophils recruitment but $LysM^+$ cells upregulated the expression of the mannose receptor CD206. This marker has been identified as expressed by M2 macrophages, indirectly involved in remyelination and repair through their phagocytic activity (Radandish et al., 2021). Hence, they participate to myelin clearance *in vivo* at least within the same extent as microglia cells through the expression of specific receptors mediating myelin debris uptake such as TREM2, CD36 or CR3 (Hammel et al., 2022; Baaklini et al., 2023). Moreover, their depletion resulted in impaired mOL density and, *in fine*, remyelination (Ruckh et al., 2012). Interestingly, a study reported the same observation after SC wound injury with immediate activation and recruitment of neutrophils and monocytes. As the injury progressed, the innate immune cells organized the repair phase and tissue remodeling (Franklin and Simons, 2022).

Finally, the origin of these innate immune cells infiltrating the LPC-injured parenchyma is various. The sources of $LysM^+$ cells within the CNS are those coming from the choroid plexus, the leptomeninges, and the parenchymal BBB (Marchetti and Engelhardt, 2020). During the surgery, the LPC incubation requires the opening of the leptomeninges to expose spinal tissue which induces partial release of the CSF. Monocytes contained in CSF may have been directly in contact with the spinal parenchyma and already on the lesion site for subsequent differentiation. Therefore, we have to consider this as a potential additional source of $LysM^+$ cells.

8.2.2. Microglia and astrocytes contributed to both de- and remyelination *in vivo*

The involvement of both microglia and astrocytes has been demonstrated during demyelination and remyelination (Traiffort et al., 2020). To investigate their dynamic of involvement within the LPC-demyelinating lesion, we employed the transgenic mice line CD11c-EYFP and hGFAP-ECFP, to respectively label microglia and astrocytes. The integrin CD11c is expressed by a specific subset of activated microglia cells as well as dendritic cells. However, the analysis of the occurrence of CD11c microglia cells compared to infiltrating DC cells in inflammatory demyelinating conditions revealed a drastic increase of this microglial sub-population (Wlodarczyk et al., 2014; Wlodarczyk et al., 2015).

Following LPC incubation, $CD11c^+$ cells rapidly migrated into the lesion within two days while astrocytes recruitment was delayed by D4. Both cell populations increased until reaching a maximum

of cell density at D7. Interestingly, $CD11c^+$ microglia ceased their implication at D14 whereas astrocytes sustained their support until remyelination and repair. Similar observations were done in the EAE model, where $CD11c^+$ microglia cells are recruited in the early onset, gradually increasing until the peak of the disease and encountering $CD11c^-$ microglia cells (Benmamar-Badel et al., 2020). However, the density of microglia cells within the lesion site is higher than astrocytes between D4 and D14, time-window where both cells are significantly enriched. As $CD11c^+$ cells being a subset of microglia, we were here not looking at the whole microglial population. The quantification of CX_3CR_1-$EGFP^+$ microglia on spinal fixed slices, where CX_3CR_1 is considered as a general marker of the cell population (Jurga et al., 2020), demonstrated that GFP^+ microglia cells were involved in the exact same time-scale of astrocytes. Thus, $CD11c^+$ microglial subset cells may be the first responder *in vivo* following white matter demyelination with transient activity. In this sense, these microglia are known to mediate immunomodulatory functions required during demyelination. Indeed, they express the MHC-I and MHC-II as well as costimulatory molecules CD80/CD86 implicated in the reactivation of T cells during the demyelination (Lewis et al., 2014; Wlodarczyk et al., 2014). Moreover, they can behave as APC cells and induce $CD4^+$ T cells proliferation, known to worsen myelin and OL loss as well as neurodegeneration (Remington et al., 2007; Wlodarczyk et al., 2014). However, these microglia cells exhibit a high pro-remyelinating potential emphasizing their importance during this phase as we observed. $CD11c^+$ cells are implicated in myelin clearance through the expression of TREM2 and are the major source of IGF1 to promote OPC differentiation and myelination (Wlodarczyk et al., 2015; Wlodarczyk et al., 2017; Sato-Hashimoto et al., 2019; Jia et al., 2023). On the other hand, the recruitment of $CX_3CR_1^+$ microglia cells during demyelination is consistent with previous observations following LPC injection in ventral SC (Plemel et al., 2020). They are known to trigger demyelination but also astrogliosis and OLs loss (Marzan et al., 2021). The enhanced expression of the fractalkine receptor has been associated with the phagocytic activity of microglia, whose impairment led to defective remyelination (Lampron et al., 2015). Moreover, their implication throughout remyelination certainly relied on their capacity to promote *in vivo* remyelination via supporting OPCs differentiation (Baaklini et al., 2023). Indeed, CX_3CR_1 microglia synthetize sterols derived from phagocytosed myelin debris, leading to a decrease of environment inflammation and promoting OPCs differentiation (Berghoff et al., 2021). Finally, they have been implicated in the control of myelination by regulating the pool of viable OPCs and subsequently myelin thickness (Nemes-Baran et al., 2020).

As observed in our data, $GFAP^+$ astrocytes accumulated within the tissue especially when myelin loss was maximal prior to decrease during repair in CPZ model (Schröder et al., 2023). However, a recent study revealed that following intra-cortical LPC injection, astrocytes significantly accumulated from D10 to D14 at of the onset of remyelination, but they were not involved in late remyelination between D14 to D21 (Molina-Gonzalez et al., 2023). These contrasting data may suggest a distinct glial activation within the CNS, depending on the location of the lesion in the brain or SC. The

detrimental role of astrocytes associated with demyelination has been extensively shown (see 2.3.3.1. section). However, their engagement that we observed until complete remyelination may rely on their pro-remyelinating capacities. Indeed, although this is not their primary attribute, astrocytes have been described as phagocytic cells, actively taking part in myelin debris clearance as well as enhance microglial phagocytic capacities (Skripuletz et al., 2013; Xu et al., 2023). They participate to remyelination by recruiting OPCs on the lesion site, promoting their maturation through the expression of growth factors such as TIMP-1, IGF1, or FGF2, as well as conducting a favorable remyelinating environment (Rawji et al., 2020).

At last, the higher microglial density has been observed after spinal LPC injection as well (Plemel et al., 2020). Compared to astrocytes, microglial cells are fast responders to injury while astrocytes often display delayed activation. This may suggest that the activation of these cells relies on temporally distinct events. Indeed, microglia can induce a reactive phenotype of astrocytes through secretion of IL-1β and TNF-α (Liu et al., 2020). Moreover, local microglial cells are known to rapidly proliferate in reaction to injury, as they transition from resting to activated state to reach a sufficient cell number to ensure their functions (Kettenmann et al., 2011; Almolda et al., 2015). This proliferation has been reported as much more pronounced in microglia than astroglia (Remington et al., 2007; Plemel et al., 2020). Our data pointed to similar observations since the number of proliferative Ki-67$^+$ microglia was on average three times higher between D3 and D5 following LPC incubation, emphasizing here that the difference of glial cell density at the lesion site depends on their local proliferative capacities more that their distal recruitment and migration at the lesion site.

8.3. Infiltrated and resident CNS immune cells modulated their inflammatory phenotype *in vivo* depending on myelin state

The inflammatory phenotype of microglial cells during demyelination has been extensively studied, demonstrating how their polarization is important in shaping the lesion environment. Pro-inflammatory microglia are linked to demyelination, while anti-inflammatory activation corresponds to the induction of a pro-regenerative phenotype (Guo et al., 2022). Moreover, many studies have emphasized the need for a phenotypic shift to anti-I microglia to promote remyelination and repair (Jurga et al., 2020; Guo et al., 2022). To further identify how microglial cells modulate their inflammatory phenotype after LPC-induced demyelination, we performed a quantitative analysis of pro-inflammatory markers, iNOS and IL6R, expressed by CX_3CR_1-EGFP$^+$ microglia. It appeared that myelin injury rapidly induced the occurrence of EGFP$^+$ iNOS$^+$ IL6R$^+$ microglia at D2, while EGFP$^+$ iNOS$^+$ IL6R$^-$ and EGFP$^+$ IL6R$^+$ iNOS$^-$ cells were delayed until D4. Although the expression of IL6R and iNOS/IL6R was consistent with the time of demyelination, the microglial subpopulation expressing iNOS showed the highest cell density and was sustained until remyelination at D21.

Although a study reported its protective effect during acute inflammatory demyelination by decreasing apoptosis of mOLs (Arnett et al., 2002), the scientific community largely agrees that iNOS is identified as a pro-I marker, only expressed by classically activated M1 microglia. Indeed, its expression is correlated with inflammation, BBB disruption, myelin impairment, glutamate-mediated neuronal excitotoxicity and damage, and axonal loss (Brown and Sawchenko, 2007; Ono et al., 2010; Kabba et al., 2018; Zarini et al., 2024). The explanation may rely on the fact that even during the remyelination, there may be a residual inflammatory response, especially if there are persistent factors in the microenvironment that maintain this state, such as remnants of myelin debris or ongoing oxidative stress. Thus, the persistence of iNOS in microglia cells at D21 may be attributed to the persistence of an activated state, where some microglia retained M1 phenotype and continued to express iNOS as part of a chronic, low-level inflammatory environment. This late expression of iNOS was also observed in the brain 21 days following LPC injection (Miron et al., 2013a).

Innate immune cells are also known to modulate their inflammatory phenotype under myelin injury. We performed quantitative analysis on $LysM^+$ FACS sorted cells and compared it with the $CD11c^+$ microglia cells. We found that both cell types modulated their phenotype according to demyelination and remyelination. Indeed, $LysM^+$ and $CD11c^+$ upregulated pro-I-associated genes from D4 to D7. However, microglia sustained until D14 the expression of Cd32 and Cd16 attributed to M1 phenotype, emphasizing the persistence of such activation within the microglial population during remyelination (Kigerl et al., 2009). $Cd11c^+$ microglia started to shift to an anti-I phenotype at D7 while $LysM^+$ innate immune cells were delayed to D14. The polarization of innate immune cells toward an anti-I phenotype relies on several extrinsic factors, such as cytokines and chemokines released by microglia cells or astrocytes. As the lesion progresses, microglia adopt an anti-I phenotype needed for proper remyelination. Notably, they release IL-4, IL-13, IL-10, Arg1, IGF1 and TGF-β known to trigger M2 phenotypes of macrophages (Sica and Mantovani, 2012; Zhou et al., 2012). We found that these factors are upregulated by microglia one week after the initial myelin insult and later on inducing a shift of innate immune cells toward a regenerative phenotype as observed two weeks post LPC.

8.4. RiboTag methodology enabled identification of transcriptomic variability of glial cells following LPC treatment

As far as we know, this study is the first to conduct a cell-specific transcriptomic analysis of glial cells as a whole using the RiboTag method in an LPC-induced demyelination model in the SC to understand which genes are involved in glial modulation of demyelination and remyelination, we collected spinal cords from mice treated at days 3, 5, 7, and 10 after LPC incubation and isolated

hemagglutinin-tagged RNAs via immunoprecipitation. Following unbiased bioinformatics analysis, we identified the DEGs in each cell type during lesion progression. This allows us to gain further insights into the precise roles of these cells as well as their communication to resolve inflammation and promote remyelination and CNS repair.

8.4.1. Cell-specific HA-Tag expression and technical limitations

The efficiency of the RiboTag methodology relies on the specificity of the used transgenic CreERT2 recombinase mouse line. To induce HA-Tag expression in microglial cells, astrocytes, and OPCs, we drove CreERT2 expression under the CX_3CR_1, hGFAP, and NG2 promoters, respectively. Subsequently, we established a three-week delay after tamoxifen injections before proceeding with RNA isolation to solely target the cells of interest. Indeed, it has been shown that the adult microglial population undergoes very little turnover compared to peripheral macrophages expressing CX_3CR_1, which disappear during this period (Parkhurst et al., 2013; Acharjee et al., 2021). Similarly, astrocytes are post-mitotic in the homeostatic CNS with little turnover or proliferation, ensuring the vast majority to be targeted (Sofroniew and Vinters, 2010). We demonstrated this cellular specificity *via* IHC staining, where the HA-Tag was expressed by 98% of Cre expressing microglia, 95% of astrocytes, and 72% of OPCs. However, it should also be considered that this time lapse allowed a portion of them to mature into mOLs, accounting to 27%. Our sequencing data confirmed these observations since we identified the enrichment of cell type-specific genes in the immunoprecipitated (IP) fractions for glial cells, further validating the robustness of our approach.

Unlike scRNAseq, the RiboTag method did not require tissue dissociation known to produce artifacts, cargo contamination, and transcripts sequestered from ribosomes (Haimon et al., 2018a). Moreover, it induces gene expression changes that may bias transcriptome analysis while it causes mechanical impairment of cell fine structures, ripping of microglia processes or astrocyte end-feet (van den Brink et al., 2017; Haimon et al., 2018a; Bravo-Ferrer et al., 2022). Therefore, using RiboTag significantly improved our RNA isolation quality, decreased background noise and unspecific transcript but also enabled us to capture gene with low expression through high sequencing depth as well as gene translated in subcellular compartments. While the Principal Component analysis (PCA) demonstrated clustering of each single replicate sample according to the cell type and separately from input samples, the general heatmap of the experiment depicted distinct transcriptomic cores with clear cuts between cell types. This demonstrates the clarity of our samples and the purity of RNA extraction, free from contaminations that could subsequently induce artifacts during transcriptomic analysis.

However, as with any sequencing methods, the RiboTag technology has some limitations. The protocol allows accessing the cell-translatome of a unique cell type per mouse. If we consider that the robustness of the data requires at least three replicates, the whole experiment implies extensive time

and costs including mice lines, regents, and devices (Sanz et al., 2019). Moreover, this technique captures only the RNA in translation. It informs only of the translatome of the cell, like a snapshot with a precise timing. It does not inform on the overall transcriptome dynamics or the total RNA content, including non-coding RNAs or transcripts that are not currently being translated (Huang et al., 2023).

8.4.2. LPC-induced demyelination triggered time-dependent modulation of gene expression in glial cells

8.4.2.1. OPCs actively proliferate in response myelin loss and completed remyelination

To get insight into the transcriptomic dynamic of OPCs following LPC-induced demyelination, we proceeded with the analysis of their translatome isolated from NG2 expressing cells. We firstly compared the Differentially Expressed (DE) genes between the different time points. In contrast to microglia and astrocytes, OPCs only moderately modulated their gene expression in response to LPC. Comparisons during demyelination showed a similar number of regulated genes, with 100 DEGs between D3-D5 and 123 DEGs between D5-D7. However, the initiation of remyelination significantly slowed their transcriptional activity, since 41 genes were downregulated out of the 47 identified DE genes. We subsequently confronted these DE genes to an enrichment analysis using Gene Ontology (GO) database to annotate them regarding their putative biological function. Based on the terms generated through this unbiased bioinformatics analysis, we found that OPCs were actively proliferating during both demyelination and remyelination as depicted by the terms “BP: cell population proliferation” between D3-D5, those related to E2F transcription factor between D5-D7, and all the terms established at the onset or remyelination from D7 to D10. Moreover, it seemed that OPCs engaged close contacts with the suffering neuronal compartment during early demyelination through terms as “BP: neurogenesis” or “BP: neuron development”. Simultaneously, we got hints of their maturation into OLs lineage to produce mOLs for remyelination as depicted by “BP: cell projection organization” and “BP: cellular component organization”. However, since this analysis might have been too simplistic to fully assess the biological relevance of their translatome, we generated a heatmap based on all the previously identified DE genes. This allowed us to isolate five distinct clusters of gene expression based on their specific upregulation regarding stages of lesion evolution. The analysis of the genes contained within the top ten most significant terms generated based on transcriptomic databases allowed us to precisely decipher the biological activity of OPCs after myelin injury.

Following LPC-induced demyelination, we identified gene expression as specific to early demyelination at D3, such as the upregulation of Il-33 (**Fig. 29a**). Remarkably, a single-nucleus RNA

sequencing study on the CPZ model demonstrated that the expression of IL-33 was enhanced during remyelination by mature OLs. They hypothesized that IL-33 was released by dying OLs into the extracellular space leading to microglia and astrocytes activation to promote repair, and subsequently re-expressed in the nuclei of newly generated OLs (Hou et al., 2023a). Moreover, the IL-33 was found to be highly expressed in OPCs due to its essential role in driving OPC differentiation and maturation into mOLs (Sung et al., 2019). Interestingly, our immunochemistry data indicated ongoing proliferation of $Ki67^+$ OPCs already from D2, emphasizing the rapid establishment of OPC differentiation and maturation through IL-33 expression, while demyelination progresses.

In general, we were able to demonstrate that the main response of OPCs to white matter insult is the active proliferation of the cell population (**Fig. 29a, b**). We found that the OPCs were extensively proliferating in response to LPC treatment, as suggested by the upregulation of key proliferative genes such as Mki67 or Hmgb1 as well as group of genes collectively involved in DNA replication, mitotic spindle formation, centrosome and kinetochore assembly or cytokinesis. After myelin loss, OPCs rapidly get activated through the induction of transcription factors maintaining them into the cell cycle thereby accounting for their fast ability to proliferate (Fancy et al., 2004). They subsequently exit the cell cycle to differentiate and mature into mOLs. Their proliferation was particularly significant as it was correlated with the expression of the transcription factor E2F, especially between D3 and D5, which enables the transcription of genes essential for entry into the S phase (Caillava and Baron-Van Evercooren, 2012). These transcriptomic data were validated i*n vivo*, where we actually observed an upsurge of $Ki67^+$ $PDGFR\alpha^+$ cells increasing from D2 to a maximum cell density reached at D4 to slowly decreasing until full remyelination at D21. Although OPCs are the major source of new myelin, we found hints of NPC's involvement as an additional source of OPCs and mOLs to remyelination (Hesp et al., 2015). The OPC translatome demonstrated an upregulation of genes related to Neural Precursor Cells (NPCs), both during demyelination and remyelination such as Cdkn1, Mmp16, Il-15, Hcfc1 and S100a6 (**Fig. 29b**). After myelin injury, OPCs and NPCs can compete to remyelinate axons, although OPCs remain the main origin of the vast majority of the remyelinating OLs (Moyon et al., 2023). As OPCs, NPCs are proliferating, migrating and subsequently differentiating into OPCs (Li et al., 2023a). The expression of the cyclin-dependent kinase inhibitor 1c (Cdkn1c) is required during development for OPC specification upon neuronal fate. As the Notch signaling decreases, Cdkn1c expression prevents precursor proliferation leading to OPC generation (Park et al., 2005). Similarly, expression of Hcfc1 correlates with control of NPC proliferation which over-expression induced a decrease of NPC density (Castro et al., 2020). Moreover, the expression of Mmp16 by OPCs may enhance NPCs proliferation into the demyelinating lesion (Gorter and Baron, 2020). The importance of NPCs in remyelination is growing, and increasing studies highlight their potential therapeutic interest. The transplantation of NPCs into

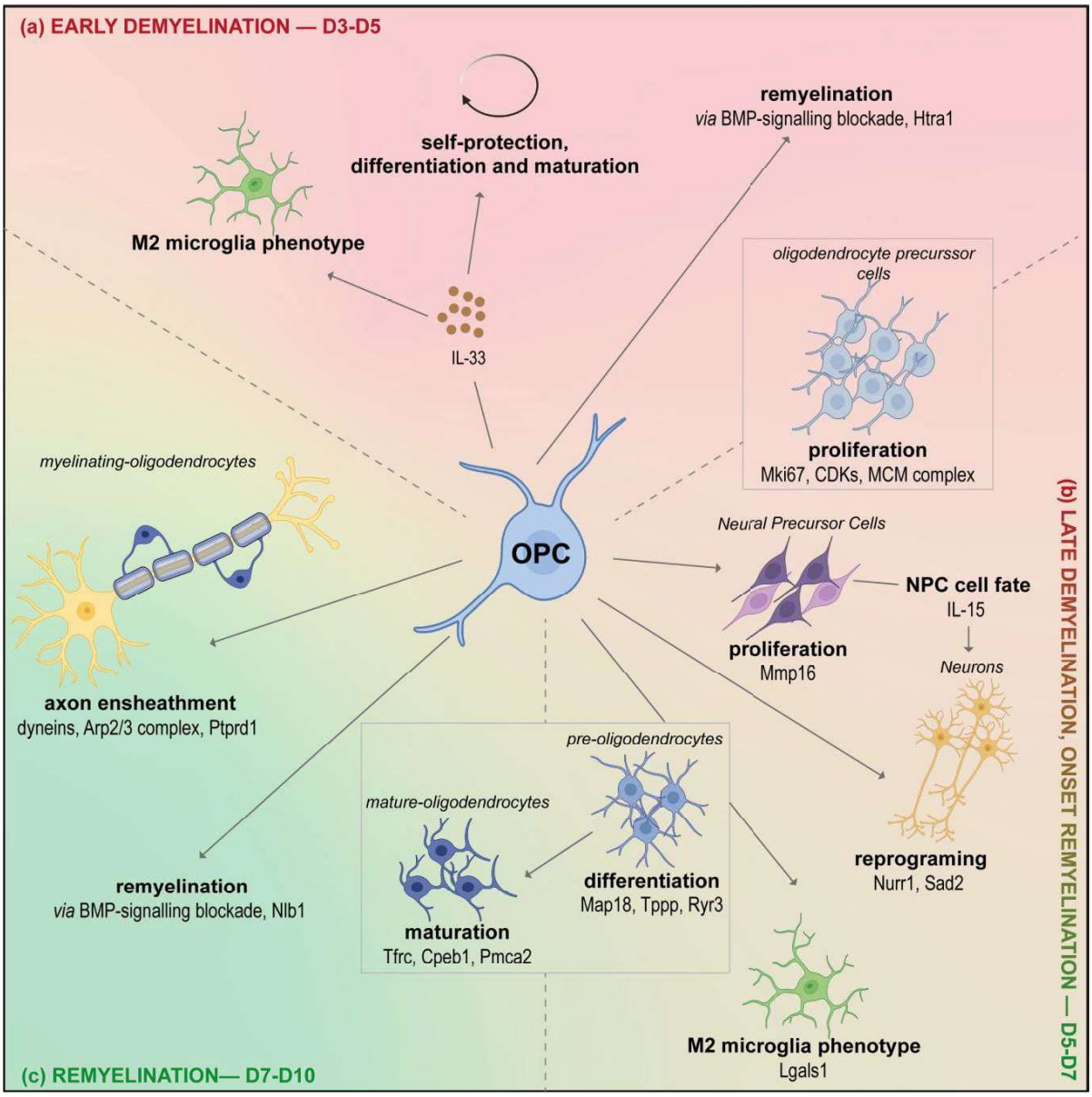

Figure 29. Transcriptomic analysis of OPCs revealed the dynamic of their functions following LPC-induced demyelination

Following demyelination, OPCs enhanced the expression of IL-33 to promote self-protection against damages and microglia-mediated phagocytosis. Moreover, they likely supported remyelination through the blockade of BMP-signaling (**a**). In addition, and until the onset of remyelination, OPCs significantly expanded their population density through the activation of related gene programs (**a-b**). As the lesion progressed, they sustained their signaling to support pro-regenerative phenotype of microglia. Simultaneously, OPCs upregulated genes related to neural precursor cells, potentially promoting their proliferation and neuronal cell fate as well as their direct differentiation into neurons (**b**). From late demyelination to remyelination, OPCs began their differentiation and maturation, giving rise to myelinating oligodendrocytes (**b-c**). Subsequently, these oligodendrocytes engaged remyelination marked by the enhancement of cytoskeletal reorganization-related genes, emphasizing the physical ensheathment of axons (**c**).

demyelinating lesions significantly improves remyelination. Although their contribution remains minor, it has been demonstrated through *in vivo* two-photon imaging that engrafted NPCs preferentially accumulated around damaged axons and were able to form new myelin sheaths (Greenberg et al., 2014). Moreover, NPCs have been shown to have a mitogenic effect on OPCs. Through the expression of PDGF-AA, they promote the proliferation and differentiation of OPCs (Einstein et al., 2009). Thus, the transplantation of NPCs would have a pro-regenerative effect and potentiate remyelination efficiency by OPCs. Finally, we identified the upregulation of IL-15 expression, usually associated with neural cell fate of NPCs (Huang et al., 2009). In addition, we identified the upregulation of Nurr1 and Sad2, both involved in neuronal differentiation of OPCs (**Fig. 29b**). Interestingly, scRNAseq identified neuronal-like gene expression in OPCs, attributed to a "transitioning state" of progenitors that would give rise to neurons (Li et al., 2023a). This finding may reflect the implication of OPCs in neuronal regeneration following LPC-induced demyelination. Indeed, OPCs reprogrammed into NPCs can generate neurons *in vitro*, while an *in vivo* study demonstrated the pro regenerative capacities of OPCs on motor and sensory functions recovery after spinal cord injury (Kondo and Raff, 2000; Li et al., 2024b).

Regarding the myelination function of OLs, we found a myriad of genes involved in OL lineage maturation and remyelination process (**Fig. 29b, c**). All along the lesion progression, from D3 to D10, OPCs enhanced the expression of genes inducing their differentiation such as Map1β, Tppp, Ryr3, Arl6p1, Hmgn, Lgals1 and Lig1. Moreover, we could identify genes involved in late differentiation of OPCs, and usually attributed to mOLs like Ank3, Fnbp1, and Eml1 within cluster 2. Although these genes are upregulated during remyelination, they were also enhanced during early demyelination at D3, correlating with the expression of Il-33 and precocious maturation of OPCs following LPC insult. Consistently, the genes promoting myelination were mainly induced during remyelination although some of them were expressed during demyelination. At last, the OPCs translatome reflected the physical modification of cell membranes and illustrated the precise time of axon wrapping during remyelination through genes involved in cytoskeletal remodeling like Arp5c, Tagln2, Stmn1, and Fnbp1 (**Fig. 29c**). Collectively, it appears that the differentiation, maturation, and myelination of OPCs are not confined to the time window of remyelination or segregated from demyelination, but rather constitutes a continuous process where the progression of OLs into the lineage is ensured from the earliest events of demyelination and throughout remyelination.

In the same line, we observed the intrinsic capacity of OPCs to promote remyelination. We noted the upregulation Htra1 consistent with myelin loss (**Fig. 29a**). Although the precise role of Htra1 in the CNS is not fully understood, RNA sequencing study reported its expression in OPCs in disease conditions as well (Jäkel et al., 2019). Moreover, MS patients displayed increased Htra1 levels in their CSF correlating with disease progression but this finding was not associated with axonal damages and identified astrocytes as the main source of Htra1 during MS (Hjæresen et al., 2021). However, the

increased expression of Htra1 in OPCs may have a link to the remyelination. Htra1 has been identified as a BMP-responsive protease able to decrease BMP-signaling known to inhibit remyelination in OPCs (Fuller et al., 2007). Moreover, Htra1 can degrade ECM components such fibronectin or aggrecan thereby overpassing the ECM-mediated restrictive effect on remyelination (Stoffels et al., 2013; Pan et al., 2023). However, it has also been shown to digest growth factors such as FGF 8 and 18, which are likely involved in OPC proliferation and migration, potentially further supporting their subsequent differentiation for remyelination (Cruz-Martinez et al., 2014; Fex Svenningsen et al., 2017). Similarly, OPCs translatome revealed the upregulation of Nbl1, which is known as an antagonist of the BMP signaling thereby promoting remyelination (Nolan and Thompson, 2014).

Finally, we did not find evidence of an inflammatory profile of OPCs correlated with demyelination as seen in other neurodegenerative diseases such as Alzheimer's (Buchanan et al., 2023). As the opposite, we found the upregulation of Trim67 in OPCs within the first demyelinating events, a gene identified as anti-inflammatory. Indeed, it has been recently established that it is able to block TNF-α-induced NF-κB signaling. By impeding IκBα degradation, a key partner in nuclear translocation of NF-κB, Trim67 prevents activation of pro-I gene programs such as cytokine or chemokines (Fan et al., 2022). In the same line, OPCs expressed Lgals1, a gene known to shut down the pro-inflammatory and deleterious activation of microglia and promote CNS protection against inflammatory-mediated neurodegeneration (Starossom et al., 2012) (**Fig. 29b**). Therefore, it appeared that OPCs adopted in our LPC model an anti-I and pro-resolving phenotype.

8.4.2.2. Microglia performed immunoregulatory and phagocytic functions promoting remyelination

Similarly to our analysis on OPCs, we investigated the translatome of $CX_3CR_1^+$ microglia cells captured through RiboTag mRNA immunoprecipitation. Regarding the DE genes, microglia cells appeared to have higher transcriptomic versatility between D5 and D7. Indeed, we identified 41 DE genes in early demyelination before D5 compared to 223 DE genes from D5 to D7. Conversely, microglia drastically reduced their transcriptomic activity after D7 where we detected only 7 DE genes, mostly downregulated, emphasizing a stabilization of gene expression at the onset of remyelination. Thus, microglial cells thus appeared to have a predominant and essential role specifically during demyelination. Although microglia have been shown to exhibit a pro-inflammatory M1 phenotype deleterious for OPC and axon survival, the depletion of microglial cells during demyelination led to an exacerbation of myelin sheath loss, increased inflammation, and impaired remyelination highlighting their key role in this phase (Wies Mancini et al., 2023). The subsequent functional enrichment analysis via GO database of these DE genes revealed their high commitment to cell signaling and communication in early demyelination through the terms "CC:

extracellular space - region", as well as a close relationship to the immune system as it was depicted by "CC: MHC class I peptide loading complex" or "BP: regulation of immune system process". As expected, we found evidence of their phagocytic activity and myelin clearance through their engagement in lysosomal and lytic pathways as well as intracellular vacuole formation. Finally, we noticed an extensive proliferation of microglial cell population during demyelination. To gain further insight into the detailed biological functions achieved by microglial cells during demyelination and remyelination, we generated a heatmap integrating all the DE genes, providing a comprehensive overview of microglial transcriptomic activity. Based on it, we were able to identify three distinct clusters according to time-dependent gene expression. The first cluster contained genes upregulated between D3 and D5 while the second displayed enriched gene expression from D5 to D10. Finally, the last cluster included enhanced translation of genes at the onset of remyelination at D7 and D10.

As we noticed in OPCs, the primary response induced in microglia cells following LPC-mediated demyelination is their fast proliferation as seen by a drastic increase of proliferation-related gene expression (**Fig. 30a**). Indeed, the genes identified as upregulated within the cluster 1 between D3 and D5 were all associated with cell cycle and proliferation. During this time period, we found that microglia significantly enhanced the expression of key genes involved in DNA replication such as mini chromosome subfamily, mitosis check-points like Cyclin-Dependent Kinases (CDKs) and associated proteins, as well as mitotic spindle formation, centrosome, kinetochore functions, until the cytokinesis which is giving birth to the daughter cell. Thus, this thorough analysis offers a comprehensive view of the molecular machinery orchestrating the intense cell proliferation observed in microglia. These transcriptomic data were confirmed *in vivo* where we observed a recrudescence of the Ki-67^{+} microglia cells restricted to demyelination. As mentioned in paragraph 6.2.2., microglia are known to proliferate locally following their activation in reaction to CNS injury. This reactive behavior allows them to rapidly increase their cell density in order to fulfill their assigned functions. The intense proliferation that we observed following demyelination could be induced by complex genetic regulation, possibly involving several genes controlling the proliferation mechanism upstream. The activation and proliferation of microglia in response of demyelination have recently been shown to be regulated by the lysosomal transmembrane TMEM106B. Moreover, this protein participates to regulate TREM2 levels in microglia thereby indirectly controlling their survival, but also their phagocytic activity and, *in fine*, the efficiency of the remyelination process (Zhang et al., 2023). Additionally, using scRNA-Seq and microglia-specific RiboTag method, researchers demonstrated the importance of the expression of Myc conjointly with cyclin dependent kinase 1 (Cdk1) during the early phase of microglial proliferation while the downregulation of Tnfaip3 mediated the late proliferative phase (Tan et al., 2022). Finally, the pathway involving CSF1R and the transcription factors PU.1 and C/EBPα have been, as well, described as regulating microglial proliferation rate in chronic neurodegeneration (Gómez-Nicola et al., 2013). Moreover, a study

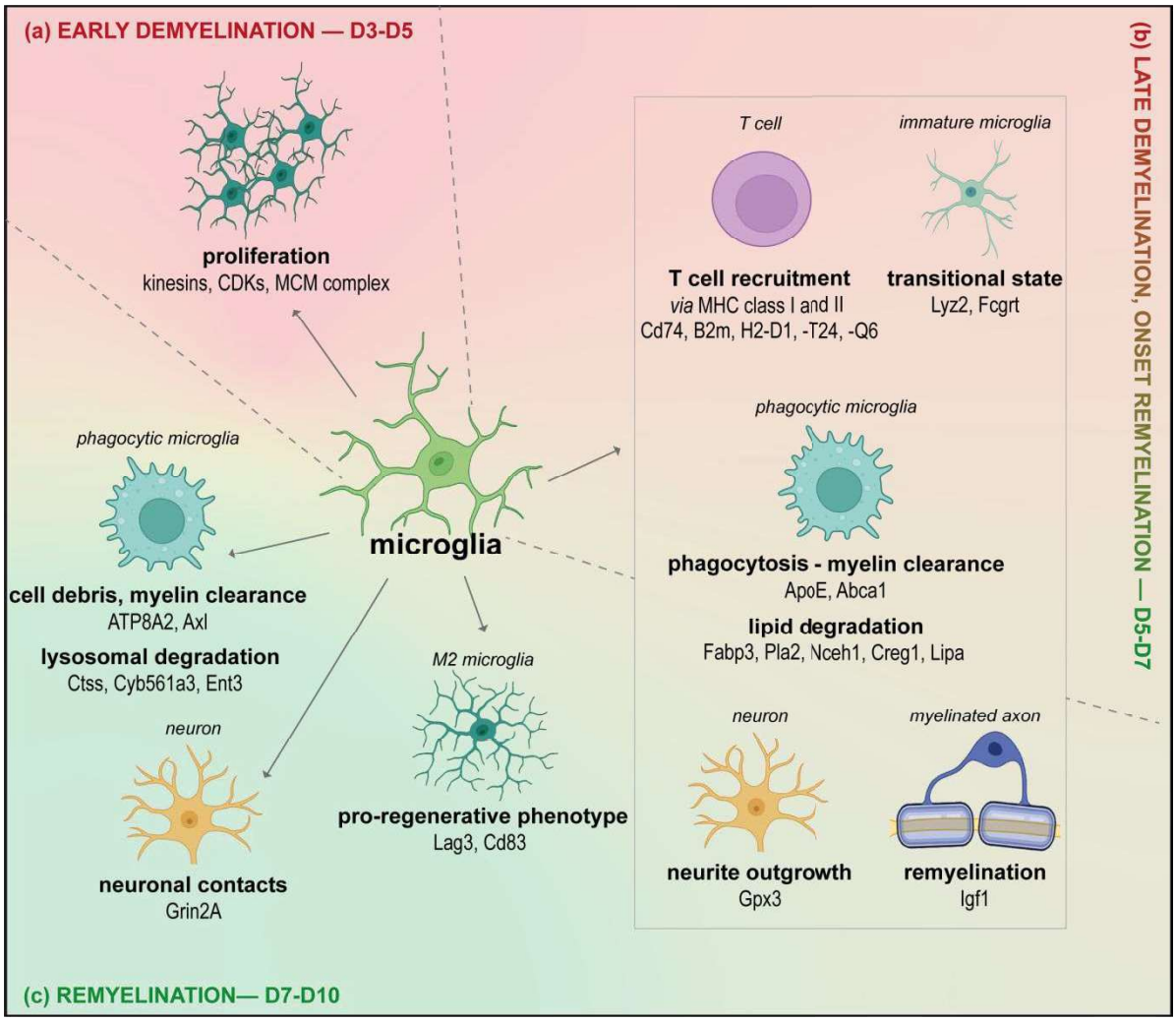

Figure 30. The translatome of microglia following demyelination underscored the modulation of key cell functions

LPC-induced demyelination triggered fast upregulation of gene programs related to cell proliferation, leading to an increase in microglial cell density (**a**). As the lesion progressed from late demyelination to the onset of remyelination, microglia cells seemed to be engaged various tasks. They likely recruited T helper cells *via* MHC-I and II, while signaling to neurons to promote neurites outgrowth and remyelination. In addition, microglia elevated the translation of genes involved in myelin clearance and subsequent lipid hydrolysis to create favorable remyelinating environment. The enhancement in immature genes signatures may indicate a transitional state of microglia towards the pro-regenerative phenotype observed during remyelination (**b-c**). Finally, microglia sustained their involvement in environment clearing consistent with the ongoing remyelination, while they probably established communication with neurons to facilitate repair (**c**).

indicated that, in addition to the proliferation of CNS-resident microglia cells, microglial expansion during demyelination could be attributed to the recruitment of microglial progenitors from the blood, accounting for 30% of the total microglia density in the lesion (Remington et al., 2007). Interestingly, we found the upregulation between D7 and D10 of the expression of SPARC gene known to inhibit cell proliferation emphasizing an intrinsic program decreasing microgliosis when remyelination takes place. Interestingly, it has been shown that this surge in microglia density during demyelination could

restrict macrophages infiltration and dispersion within the lesion through physical limitation (Plemel et al., 2018).

Along with the progression of the lesion, we identified different key functions of microglia from late demyelination to the onset of remyelination. Microglia displayed immunomodulatory functions, especially in signaling to the adaptive immune system (**Fig. 30b, c**). The upregulation of genes involved in the expression of MHC class I (B2m, H2-D1, H2-T24, H2-Q6) and II (Cd74) demonstrated their ability to act as APCs). The expression of MHC-I by microglia has been associated to $CD8^+$ T cell infiltration and activation, while MHC-II signaling modulates the density of $CD4^+$ T cells into the injured CNS (Schetters et al., 2017; Malo et al., 2018; Goddery et al., 2021). Classically, both these cells are associated to enhanced neuroinflammation, axonal damages and myelin loss. Indeed, during demyelination, $CD8^+$ and $CD4^+$ T cells are known to secrete pro-I cytokines such as IFN-γ, IL-17, or TNF-α, collectively mediating neuroinflammation, BBB permeability, OL loss, and defective remyelination (Fletcher et al., 2010; Lin and Lin, 2010). However, depletion of T cells after LPC challenge impaired spontaneous remyelination, emphasizing their essential role in repair (Bieber et al., 2003). Indeed, under the influence of the local environment, particularly TGF-β and IL-2, both $CD8^+$ cytotoxic and $CD4^+$ helper T cells can eventually differentiate into regulatory T cells, known for their pro-regenerative properties (Mishra et al., 2021; Wang et al., 2023). These regulatory cells, in turn, secrete the neurotrophic factor CNTF protecting neuronal compartment, but also TGF-β which decrease neurotoxic astrogliosis and pro-I microglial responses, as well as CCN3, a secreted protein promoting OLs maturation and myelination (Reynolds et al., 2007; Dombrowski et al., 2017; Ciurkiewicz et al., 2020). Consequently, although the recruitment of T cells during remyelination by microglial cells might suggest a persistent M1 inflammatory phenotype, it could actually be a mechanism to promote remyelination through the involvement of adaptive immune cells.

Using immunochemistry and qRT-PCR, we previously identified a shift of microglial inflammatory phenotype, from pro-I phenotype coinciding with demyelination to an anti-I polarization at the onset of remyelination. Through our analysis of the microglial translatome, it also appears that these cells modulate their inflammatory state to favor remyelination and repair. Indeed, we found an upregulation of specific microglia homeostatic genes such as Siglec-H and Cst3 from D5 to D10. The loss of such genes is linked to disease-associated microglia (DAM) emergence and neurodegeneration (Deczkowska et al., 2018; Sobue et al., 2021). Interestingly, to counterbalance the deleterious effects that microglial activation could have on tissues, microglia cells intrinsically possess “restraining mechanisms”. The interaction of CX_3CR_1 and CD200 – which were both upregulated at the same time- with their ligands promote homeostatic phenotype which negatively competing with DAM transition (Deczkowska et al., 2018). Moreover, such homeostatic gene expression under inflammatory challenge has been associated to resting or anti-I transition of activated microglia (Böttcher et al., 2020). To further decrease M1-assotiated behaviors, microglia were found to enhance

Cd83 and Lag3, both reducing pro-I cytokine release and promoting myelin clearance, key features of M2 microglia (Rimmerman et al., 2022; Sinner et al., 2023) (**Fig. 30c**). However, a recent study investigated the inflammatory phenotype of microglia regarding the remyelination process. They demonstrated that LPC-induced demyelination led to necroptosis-mediated cell death of pro-I microglia, followed by the lesion repopulation with anti-I microglia needed for remyelination (Lloyd et al., 2019). Therefore, we can hypothesize that this process might be specific of the CNS region where demyelination occurs, highlighting a potential different regulation between the brain and the SC to modulate microglial phenotypes during remyelination. On the other hand, although robust, the RiboTag method does not capture the RNAs of all microglial cells involved in the lesion. Indeed, some microglia might originate from circulating progenitor cells as discussed above, while others could arise from the proliferation of non-RiboTag expressing resident microglia cells, thereby escaping our transcriptomic analysis.

As expected, microglia cells were highly committed to phagocytosis to clean the lesion environment during late demyelination events at the onset of remyelination (**Fig. 30b, c**). This process is vital since impaired microglial clearance functions have been linked to defective remyelination and compromised axon integrity (Lampron et al., 2015). Microglia cells upregulated phagocytosis-associated genes such as ATP8A2 and Axl involved in neurons and myelin debris removal. Moreover, we found several genes involved in lytic or lysosomal pathways, depicting their high commitment into degrading functions (**Fig. 30c**). The lysosomal engagement was reflected through the expression of various genes such as Ctss, Cyb561a3, Ent3, Creg1, and Lipa. Creg1 and Lipa are crucial for acidification of lysosomal compartment. Their expression is here particularly important since dysfunctions of lysosomal acidification is linked to neuroinflammation and neurodegeneration due to amplified pro-I cytokines release, neuronal death and activation of peripheral immune cells (Quick et al., 2023). Additionally, we confirmed the lysosome formation via IHC in vivo, where microglia expressing the lysosomal protein CD68 were drastically increased during demyelination. Moreover, myelin debris triggered cholesterol and lipid metabolism in microglia. Although we found the upregulation of lipid transporters like Apoc1 and Apoc4, as well as genes mediating FAs binding and hydrolysis such Fabp3 and PLA2, it seemed that the concomitant expression of Abca1 and ApoE was essential for remyelination. Indeed, Abac1 is responsible of cholesterol efflux. Subsequently incorporated into Apoe, microglia cells use this pathway as an attempt to eliminate the cholesterol contained in myelin debris to prevent massive cholesterol accumulation leading to defect in their phagocytosis capacities (Loving and Bruce, 2020). Moreover, cholesterol efflux has been associated to enhance homeostatic glial phenotype, indirectly decreasing neuroinflammation (Cantuti-Castelvetri et al., 2018). On the other hand, Abca1 and ApoE are linked to liver X receptor (LXR)-signaling. Recently, microglia has been demonstrated to be involved in sterol synthesis under an inflammatory environment via the activation of LXR-signaling and promote remyelination (Berghoff et al., 2021).

Finally, microglia enhanced genes associated with ubiquitin-proteasome degradation system such as E3 ubiquitin ligases, Rnf167 and Neurl3. The activity of the Rnf167 was linked to TNF-α. Indeed, the ubiquitination of Toll-interacting protein (Tollip) by Rnf167 inhibits both NF-κB and MAPK signaling promoted by TNF-α, pointing out a potential self-mechanism of microglia cells to decrease their inflammatory activation (Yan et al., 2023). Although the expression Neurl3 may be modulated by NF-κB signaling, it has recently been found as ubiquitinating K63-linked poly-ubiquitination on Interferon Regulatory Factor 7 (IRF7) lysine 375 which induces the expression of type I Interferon (IFN-I), including IFN-α and INF-β (Qi et al., 2022). While IFN-I signaling has been implicated in demyelination, some studies emphasized its putative role in remyelination (Berg et al., 2017). The abolition of IFN-I signaling was found to impair microglia phagocytic properties whereas short-term IFN-α/β treatment improved remyelination (Njenga et al., 2000; Moore et al., 2020). Therefore, these data provide an unexpected way of microglia to regulate their inflammatory phenotype and balance the remyelination process.

8.4.2.3. Astrocytes are multitaskers following white matter injury

To understand how LPC-induced demyelination modulated gene expression in astrocytes, we analyzed the RiboTag-translatome of GFAP expressing cells. Similarly to our previous analysis of OPCs and microglia, we first deciphered the influence of the lesion on gene expression levels. Among the three cell types, astrocytes are the most transcriptionally active, with no less than 2029 DE genes between D3 and D10. They exhibited the highest transcriptional engagement between D3 and D5, with 1736 DE genes, highlighting their significant transcriptomic reorganization as they transitioned from an homeostatic state to an activated state during the early events of demyelination. However, despite remaining highly active during late demyelination between D5 and D7 with 286 DE genes, we observed a decrease in genetic modulation after D5. Indeed, astrocytes adopted at D10 a transcriptional state similar to that observed at D7, with only 7 DE genes identified between these two time points, with the majority downregulated. The terms generated based on the enrichment analysis with the GO database revealed the involvement of two transcription factors, ZF-5 and E2F-1, between D3 and D5 emphasizing a complex transcriptomic regulation. Although ZF-5 functions in astrocytes are not yet understood, the expression of E2F-1 has been correlated with astrocytic activation following demyelination (Wu et al., 2015). In line with this, their activation is known to trigger morphological modifications such as reduced number of synapses, cell hypertrophy with increased body size and the thickening of their processes (Liddelow and Barres, 2017; Cheng et al., 2019). This was depicted through the terms “CC: intracellular anatomical structure” and “CC: cellular anatomical identity”. Through all demyelination, astrocytes were actively establishing cell contacts as well as intracellular communication as seen by the high significance of the term “MF: protein binding”, while

in the later phase of demyelination, astrocytes seemed dedicated to neuronal compartment. The heatmap generated based on all DE genes revealed three clusters according to the time-dependent of containing genes. The cluster 1 was specific to early demyelination at D3, while cluster 3 covered the whole demyelination time from D3 to D5. On the other hand, cluster 2 was mainly activated in late demyelination and at the onset of remyelination between D5 to D10. The precise gene composition of the terms generated based on different databases, indicated heterogenous behavior of astrocytes alongside the lesion progression and resolution.

Similarly to what we previously described for OPCs and microglia, LPC-induced demyelination triggered the fast proliferation of local astrocytes already at D3 (**Fig. 31a**). We first identified in $GFAP^+$ cells translatome the upregulation of the transcription factor (TF) E2F-1. Its expression is upregulated in activated astrocytes following spinal injury (Wu et al., 2015). This TF regulates the astrogliosis process by controlling the cell cycle-related genes inducing their proliferation. Moreover, E2F-1 expression was linked to neuroinflammation associated with tissue damage. We here demonstrate a similar mechanism following demyelination. In addition, we found a myriad of genes associated with cell cycle and cell proliferation. Indeed, astrocytes upregulated genes related to Rap1 and Ras signaling as well as mini chromosome maintenance subfamily, genes involved in centrosome, mitotic spindle formation, kinetochore, chromatid segregation, mitotic checkpoint, and cell cycle regulation. We further transposed these transcriptomic data into *in vivo* observations where $Ki\text{-}67^+$ proliferative astrocytes mostly accumulated within the lesion during demyelination, before decreasing at the onset of remyelination. However, the upregulation of Plp1, Tsku, Hopx, Ndgr2, and Epac2 may indicate that part of the astrocyte population was derived from NPCs as an additional source of the newly generated astrocytes within the lesion. Indeed, following demyelination, it has been shown that NPCs could migrate to the lesion and give rise to OLs or astrocytes. The astrocytic cell fate is determined by the local environment such as Notch signaling, JAK/STAT or Bone Morphogenetic Protein (BMP) pathways (David-Bercholz et al., 2021). However, it remains unclear if NPC-derived astrocytes are functionally different from those generated from local proliferation. The NPC transplantation after spinal injury demonstrated the ability of differentiated astrocytes to enhance vasculogenesis and repair through secretion of growth factors, supporting the beneficial impact of NPC involvement after LPC treatment (Suzuki et al., 2021). Conversely, we found intrinsic anti-apoptotic mechanisms in activated astrocytes, since they upregulated the apoptosis-inhibitors Xiap, Bmp2, Birc5/6 to protect themself from cell death (**Fig. 31a**).

Following demyelination, astrocytes immediately adopted a “buffering phenotype” (**Fig. 31a**). They increased genes involved in glutamate, glucose, anions, copper, zinc, iron, amino-acids channels and transporters. This recapture activity prevents excitotoxicity-mediated cell death within the lesion, especially for neurons. Indeed, during demyelination zinc, copper and iron can be released by injured or inflammatory cells. When dysregulated, the excessive accumulation of these metals acts as a potent

neurotoxin, eventually leading to mitochondrial dysfunctions and neuronal death (Núñez and Hidalgo, 2019; Granzotto et al., 2020). Moreover, the reuptake of copper by astrocytes may serve to supply neurons to support their function and survival, participating with cytochrome c oxidase in the mitochondria for energy production and superoxide dismutase (SOD) for protection against oxidative stress.(Dringen et al., 2013; An et al., 2022). Similarly, astrocytic uptake of iron has been already described in MS, where defects in astrocytes-OLs iron supplementation impaired OPCs differentiation and remyelination demonstrating the importance of astrocytic-mediated iron balance after myelin loss (Schulz et al., 2012b). Although glutamate can be released from suffering neurons during neurodegeneration, microglia and macrophages are the major source of glutamate, intensively produced through their glutaminase activity, converting more glutamine to glutamate. However, since they lack glutamine synthetase, the release of their excess intracellular glutamate is toxic for neurons (Kostic et al., 2013). In addition, the glutamate buffering from astrocytes probably protected the white matter from increased damages. Indeed, alterations of glutamate homeostasis led to overactivation of AMPA and kainate receptor leading to excitotoxic death of OLs (Matute et al., 2001). Finally, the glucose buffering protected glutamate transmission because long-term exposure has been described as increasing the sensitivity of AMPA- or NMDA-induced neurotoxicity in neurons but also an impairment of their capacity to recapture the glutamate (Sasaki-Hamada et al., 2022).

As microglia cells, the inflammatory phenotype of astrocytes has been demonstrated as modulating demyelination and remyelination (Rawji et al., 2020). Throughout these both processes, we found gene expression associated with both A1 and A2 inflammatory phenotypes (**Fig. 31a, b**). This may indicate either the presence of two distinct populations with different inflammatory polarizations coexisting within the lesion, or a single astroglial population with different balanced phenotypes or subtypes, adjusting their polarization according to the immediate need to resolve the lesion. This second hypothesis is in line with many studies identifying simultaneous expression of A1 and A2 markers in neurodegenerative diseases (Lo et al., 2021). Interestingly, in EAE model, seven astrocytic subtypes have been identified within the lesions through scRNA-sequencing. The predominant subpopulation was associated with pro-I and neurotoxic pathways, including unfolded protein response (UPR) and activation of NF-κB and iNOS pathways and driven by Mafg expression (Wheeler et al., 2020). Our transcriptomic data demonstrated upregulation of various genes associated with A1 phenotype. In addition, astrocytes enhanced Notch signaling, known to promote glial scar through the simultaneous activation of Lgals3 and co-activators, leading to subsequent expression of Hey genes Hey1/2 which promoted cell proliferation and glial scar formation. As Wheeler et al, we found upregulated genes involved in activation of NF-κB signaling like Ano1, Trim8 and Parp12 as well as a significant expression of Mafg, emphasizing the emergence of those pathogenic astrocytes following LPC treatment (Wheeler et al., 2020). Interestingly, we did not find direct evidence of UPR system but we noted several genes related to ubiquitin-proteasome system (UPS). Astrocytes

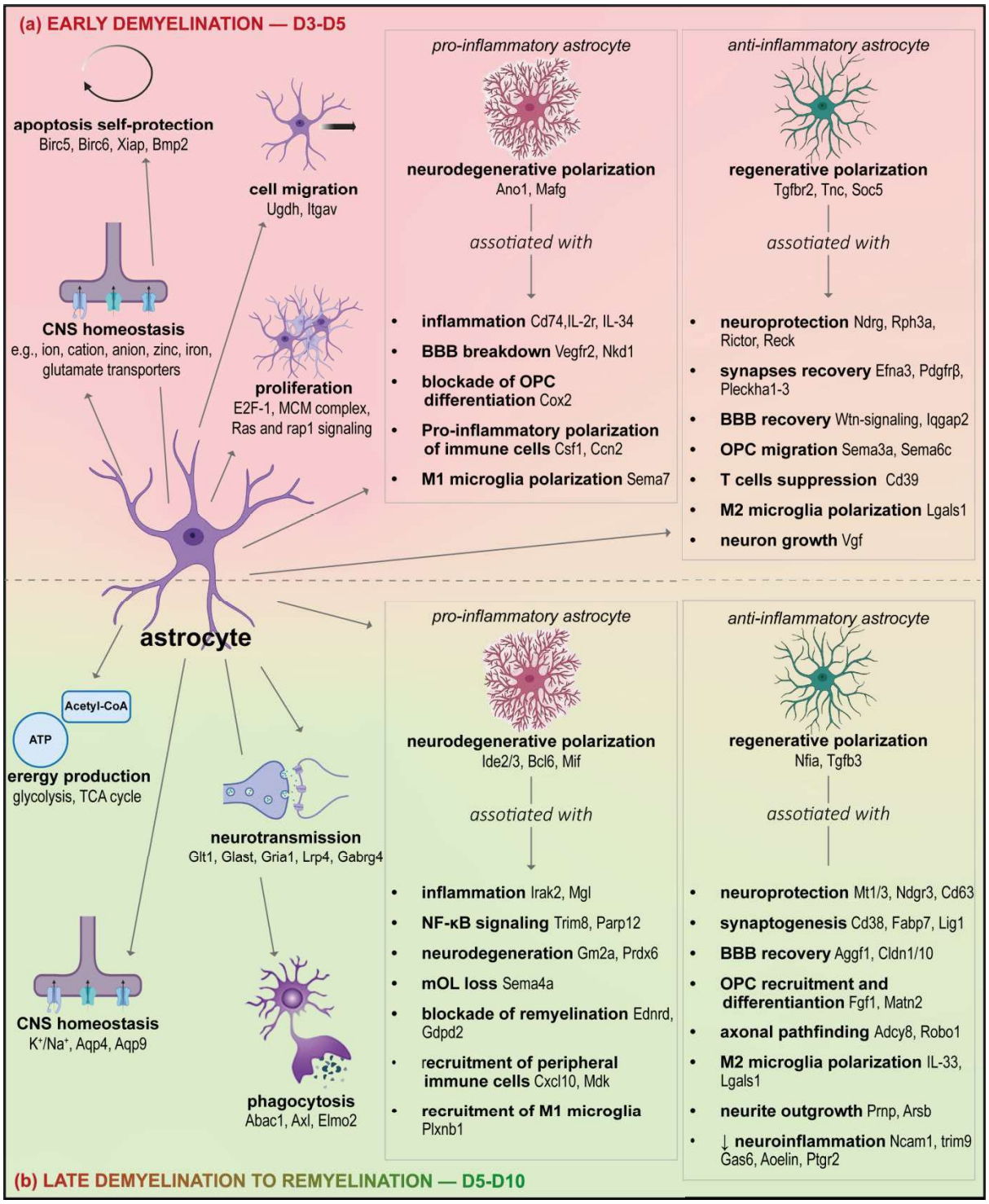

Figure 31. Astrocytes activated a broad range of time-dependent gene programs regulating their cell activity following LPC-induced myelin loss

The loss of myelin sheath induced rapid activation and migration of astrocytes to the lesion site. Their transcriptome revealed a rapid induction of genes related to proliferation while protecting themselves from apoptotic cell death, which participated to guaranteed sufficient cell density. In parallel, they enhanced the expression of various transporters/channels to ensure buffering functions and CNS homeostasis (**a**). As the lesion progressed, astrocytes seemed to meet their increasing energy demands through glycolysis and the TCA cycle. Additionally, they maintained their role in preventing excitotoxicity and upregulated genes associated with neurotransmission. Interestingly, astrocytes may have been involved in the phagocytosis of myelin and

cellular debris (**b**). However, rather than adopting a single phenotype associated with the state of myelin, the astrocyte transcriptome revealed the simultaneous involvement of both pro- and anti-inflammatory phenotypes throughout demyelination and remyelination. Indeed, astrocytes upregulated genes related to both polarizations with their associated behaviors. Thus, they likely contributed to inflammation/neurodegeneration and the recruitment of inflammatory cells while simultaneously providing support to limit extensive tissue damage, promote BBB repair, and facilitate the regeneration of the neuronal compartment (**a-b**).

upregulated the expression of Ubb and Ubc both encoding the ubiquitin as well as Ube2h, Ube2j3, and Ube2n all encoding for E2 ubiquitin-conjugating enzymes and required with E3 ligases to transfer ubiquitin to target proteins for subsequent degradation. Indeed, as the unfolded proteins exceed the endoplasmic reticulum (ER) capacity, it induces ER stress which in turn activates UPS to degrade those proteins (Qu et al., 2021). So, it may be plausible that the activation of the UPS actually reflected the UPR system activation. In line with A1 phenotype, we identified genes related to astrocyte-mediated CNS inflammation. The interaction of the Macrophage migration inhibitory factor (MIF) expressed by immune cells during demyelination interact with Cd74 receptor, whose expression is enhanced by D3 in astrocytes, to produce TNF-α and IL-1β (Su et al., 2017). Similarly, the upregulation of the gene Irak2 may have, by forming a complex with Myd88 and Irak1/4, induced the gene transcription of IL-1β, IL-6, and TNF-α (Manu et al., 2023). Finally, the induction of Tweak has been linked to release of IL-8 and IL-6 pro-I cytokines in astrocytes as well (Saas et al., 2000).
Consistent with A1 polarization, we uncovered deleterious effects of astrocytes lasting through demyelination until the onset of remyelination, although these effects were much more pronounced between D3 and D5. They were involved in neurite loss and apoptosis of neurons as well as synapse damages. In addition, they were worsening the demyelinating process by inducing mOL loss, impeding axonal repair and remyelination while impeding OPC differentiation. Interestingly, the ability of astrocytes to cause neuronal loss or damages has already been demonstrated (Guttenplan et al., 2020). However, this may reflect another biological meaning. A hypothesis would be that these cytotoxic A1 astrocytes target neurons too severely impacted by demyelination and therefore incapable of regenerating. These impaired neurons contribute to the pro-I activation of microglia through the release of death/suffering signals, thus creating an inflammatory loop. Therefore, by inducing their death, A1 astrocytes actually protect the rest of the neuronal network (Liddelow and Barres, 2017). In addition, our transcriptomic data demonstrated that astrocytes delayed remyelination either by blocking it or by transiently preventing OPC differentiation. Indeed, when optimal conditions are not met and remyelination occurs too early in the lesion process, it fails (Heß et al., 2020). Among these conditions, the clearance of myelin debris in the environment is a prerequisite for efficient remyelination. The transcriptomic and *in vivo* data on microglia demonstrated their phagocytic engagement from D5 to, at least, D14. Moreover, astrocytes themselves were found to promote microglial phagocytic capacity by expressing Il-33 between D5 and D10. Since microglia are not the only cells dedicated to myelin phagocytosis, our quantitative gene expression data have shown

the involvement of macrophages in this function from D14. Therefore, it would be plausible that astrocytes delayed OPC differentiation during demyelination to give them a chance to successfully carry out their remyelinating function when optimal conditions were met. This seems even more likely given that, at the same time, we found that astrocytes promoted OPCs migration via semaphorins Sema3a and Sema6c, the step preceding their differentiation in their lineage progression.

In parallel to their A1 polarization, we found that astrocytes enhanced A2-related gene expression (**Fig. 31a, b**). However, most DE genes identified as participating in this transition were induced during late demyelination and remyelination, indicating their engagement to promote CNS repair. Notably, astrocytes enhanced the expression of Nfia, a key gene inducing the switch toward an A2 phenotype, thus reinforcing the idea of a local phenotypic modulation of existing astroglia within the lesion (Tchieu et al., 2019). In line, we found genes involved in the decrease of the pro-I NF-κB pathway or A1 polarization. We observed enhanced expression of genes reducing astroglial-mediated inflammation as well as increasing the anti-I TGF-β signaling while participating to decrease overall neuroinflammation through the expression of Fgf2 and Anax2 (Liu et al., 2019; Zou et al., 2019). Consequently, it appeared that A2 astrocytes from D3 to D5 were already involved in neuroprotection. They were facilitating functional recovery, and providing neurotrophic support to neuron growth via BDNF releasing and synaptogenesis. These astrocytes increased their support to maintain BBB integrity or repair as well as the vascular development through the activation of the Wnt-signaling pathway and the angiogenesis. From D5 to D10 or late demyelination to the onset of remyelination, astrocytes were involved in a broad range of pro-regenerative functions. They sustained neuroprotection, promoted synaptogenesis of excitatory neurons, neuritogenesis, as well as synapse assembly and connectivity. Moreover, they guided axonal regrowth, providing axonal pathfinding. They kept their involvement to the BBB, preserving its integrity and decreasing the attack from neighboring cells, such those induced by MMP. Indeed, as microglia and immune cells promoting BBB disruption, astrocytes provided tight junction proteins such as claudins and occludins to protect BBB permeability. Finally, A2 astrocytes supported remyelination through enhancing both OPC recruitment and differentiation.

Their inflammatory polarization also influenced the nature of communications between astrocytes and surrounding cells within the lesion. Their translatome revealed heterogeneous signaling during both demyelination and remyelination, either worsening the tissue lesion or mediating repair. Indeed, during demyelination from D3 to D5 after LPC treatment, astrocytes promoted microglial proliferation as well as their pro-I polarization through the expression of Csf1 (Hagan et al., 2020). Surprisingly, they enhanced at the same time the expression of Lgals1 encoding for galectin-1, an immunosuppressive protein known to promote microglial transition toward M2-phenotype and amplified their phagocytic activity (Starossom et al., 2012; Rinaldi et al., 2016). Additionally, astrocytes modulated the immune responses by suppressing inflammatory T cell response via the cell

surface enzyme Cd39 (Ulivieri et al., 2019). As the lesion progressed to late demyelination/initiation of remyelination from D5 to D10, astrocytes described pro-injury signaling. Indeed, they enhanced the expression of Ccl2 and Cxcl10 to recruit peripheral immune cells. The chemokine CCL2 led to pro-I macrophages and cytotoxic T cell infiltration associated with white matter loss, while astrocytic CXCL10 has been described as enhancing the recruitment of antibody-secreting cells or plasma cells derived from B cells, which have been shown to release autoantibodies leading to myelin and axonal loss (Engelhardt and Ransohoff, 2005; Phares et al., 2013; Kim et al., 2014; Blauth et al., 2015). Moreover, astrocyte-derived CXCL0 can interact with CXCR3 on neurons to induced their death via ferroptosis through STAT3/SLC7A11 pathway (Liang et al., 2023). In the same way, astrocytes elevated Mdk translation. Its expression in reactive astrocytes was shown to act as chemoattractants for such as neutrophils, macrophages, and lymphocytes. (Neumaier et al., 2023). However, through the IL-2-dependent SHP2/STAT3-5/FOXP pathway, Mdk promotes the induction of both regulatory dendritic cells and Treg kwown to alleviate inflammation, promoting myelin debris clearance and remyelination (Hu et al., 2018). Finally, the upregulation of Plxnb1 in astrocytes inducted interaction with Sema4d receptor on activated microglia inducing release of IL-1β and Nos2 by astrocytes (Sanmarco et al., 2021). Conversely, they promoted microglia-mediated phagocytosis through the upregulation of Il-33 (Vainchtein et al., 2018). These motley responses of astrocyte communications reinforce the coexistence of multiple astrocyte subtypes with different inflammatory phenotypes.

Finally, to meet the energy demand required for such vast cellular activation, our analysis of the astroglial translatome revealed three different pathways providing cell energy during remyelination (**Fig. 31b**): the glycolysis, the mitochondrial respiratory chain, and the Tricarboxylic Acid Cycle (TCA). We found that, through glycolysis, astrocytes produced lactate and acetyl-CoA via Ldhb and Pdha1. Lactate is an end product that cannot be directly used but rather serves as a carbon source for the TCA (Barros et al., 2020). Interestingly, glycolysis in astrocytes is enhanced according to neuronal activity and may have a role in neuroprotection (Takahashi, 2021). Recently, astrocyte-derived lactate has been described as critical for synaptic plasticity and neurogenesis. In addition, lactate prevents glutamate-induced neuronal death under glutamate excitotoxicity conditions by decreasing NMDA receptor-mediated signaling, as well as hypoxia-induced neurodegeneration (Jourdain et al., 2018; Yamagata, 2022). In the same way, astrocytes upregulated genes involved in TCA cycle, which is used in astrocytes to synthesize and deliver the vast majority of nutrients to neighboring cells. Although part of the acetyl-CoA from glycolysis was incorporated in TCA cycle, we found that astrocytes mostly incorporated into TCA the acetyl-CoA produced from FA oxidation. This implied synthesis of TCA intermediates, produced by astrocytes by the catabolism of valine and alanine but also the alpha-ketoglutarate converted from glutamate. In addition, we found that astrocytes produced pyruvate through amino acids degradation such as leucine, isoleucine, valine, lysine, d-serine. Finally, TCA produced NADH and FADH2 that can be further used by the respiratory chain to produce ATP. Indeed, astrocytes upregulated genes associated with complex I, II,

and III in the mitochondrial respiratory chain. This was correlated with an increased FA oxidation, critical in order to degrade FAs to maintain lipid homeostasis and ultimately relies on a process called "OxPhos" to prevent neuroinflammation and neurodegeneration (Mi et al., 2023). Indeed, OxPhos deficit in astrocytes decreased their metabolic support to neurons and neuronal oxidative stress leading to synaptic dysfunction. Moreover, OxPhos-deficient astrocytes induce microglial activation through Il-33 signaling. Collectively, these intracellular energy pathways in astrocytes were useful to support neuronal metabolism but also to prevent additional sources of inflammation and neurodegeneration.

8.4.3. De- and remyelination are tightly cell-coordinated processes – Summary of transcriptomic findings

The implementation of the RiboTag RNA sequencing method following LPC-induced demyelination provided significant added value in understanding the cellular and molecular events after myelin loss based on glial transcriptomic analysis. De- and remyelination processes unfold in a coordinated, step-by-step manner involving the cell-specific functions of microglia, astrocytes, and OPCs, as well as their intricate interactions.

During the **early phase of demyelination**, the LPC-induced death of mOLs rapidly triggered the loss of the myelin sheath. The suffering signals combined with environment modifications induced micro- and astroglial both activation. With OPCs, these cells upregulated genes involved in cell proliferation programs (e.g., Cyclin-Dependent Kinases (CDKs), MCM complex, Mki67), which significantly increased cell density within the lesion site. At that time, astrocytes adopted a "buffering phenotype" to prevent excitotoxicity, which consisted to the upregulation of genes related to various channels or neurotransmitter receptors and protecting neurons from further damages. Moreover, astrocytes might have enhanced microglial proliferation (Csf1) and promoted - conjointly with OPCs (Il-33) - their pro-resolving phenotype (Lgals1). Although debated, it appeared that the pro- vs. anti-inflammatory classification of glial cells following myelin injury is far too simplistic. Rather than a strict adherence to polarization 1 or 2, it is more likely a balance of concomitant expression of genes associated with both statuses, with the majority defining the cell's predominant phenotype during the evolution of the lesion. Thus, the astrocytes enhanced Notch and NF-κB signaling, which is typical of pathogenic astrocytes and released of pro-I cytokines (e.g., IL-1β, IL-6, IL-8). This likely produced neurons apoptosis and mOLs loss as well as impeding OPC differentiation. Conversely, anti-I-associated genes simultaneously promoted BBB repair through Wnt-signaling pathway or synapses recovery.

Simultaneously, OPCs may have self-decreased their inflammatory release via of TNF-α-induced NF-κB pathway (e.g., Trim67).

As the lesion evolves **to late demyelination and the onset of remyelination**, microglia already enhanced the translation of genes related to myelin phagocytosis and debris clearing (e.g., Axl, ApoE, ATP8A2), which promotes efficient remyelination, and usually attributed as a function of anti-I microglia restricted to repair phase. Microglia phagocytosis was as well supported by astrocytes (e.g., Il-33), which themselves might have engaged clearing of cells debris (e.g., Axl, Elmo2, Abca1). In parallel, OPCs began their differentiation and maturation into mOLs. Although astrocytes promoted OPC migration via semaphorins expression and their differentiation, they were paradoxically probably concomitantly impeding remyelination and worsening mOL loss. However, astroglial might have promoted at the same time neuronal survival, synaptogenesis and BBB restoration. With microglia, astrocytes promoted infiltration of peripheral immune cells.

Finally, as the **remyelination** progresses, microglia cells sustained their involvement in clearing the environment (e.g., Cd83) and degrading fatty acids (e.g., Fabp3, ApoE) to ensure continuous efficient remyelination. In addition, might have promoted neuronal repair (e.g., Lag3). Surprisingly, microglia seemed to recruit peripheral immune T helper cells through the upregulation of genes involved in MHC-I and II complexes, which is usually described as happening during demyelination. Concurrently, astrocytes seemed to sustained neuroprotection (e.g., Cd63, Cst3), guidance for axonal regrowth by providing axonal pathfinding (e.g., Robo1, Spon1). They kept their involvement to the BBB, preserving its integrity and decreasing the attack from neighboring cells (e.g., Cldn10, Cldnd1), such those induced by MMP (e.g., Ndrg2). However, the favorable environment shaped by microglia and astrocytes likely ensured well differentiation and maturation of OPCs (e.g., Fgf1, Matn2). As OPCs mature, they begin wrapping myelin around the axons (e.g., MBP, PLP), restoring the lost insulation and facilitating the recovery of nerve function. Throughout this process, the interactions between microglia, astrocytes, and OPCs are dynamic and continuous, with each cell type influencing the others to ensure a coordinated and efficient repair of the CNS.

9. CONCLUSION AND OUTLOOK

Through this analysis, we demonstrated the concomitant and synergistic involvement of glial cells, as well as the critical contribution of innate immune cells in de- and remyelination. Although their individual contributions to these pathological processes were already known, this study provides, for the first time, the real-time *in vivo* recruitment dynamics of these cells at the lesion site, from the initial insult to myelinating oligodendrocytes (mOLs) to complete remyelination and repair. Moreover, the use of our innovative mouse model of LPC incubation-mediated demyelination added significant value to this work, by focusing solely on the cellular events resulting from demyelination. Our data demonstrated for the first time the precise events of myelin disruption, from the gradual loss to first events of regeneration until complete remyelination. Taking advantage of CARS microscopy, we described time-dependent fine cellular patterns evoked during myelin degeneration. LPC-induced demyelination as expected triggered cell invasion within the lesion site. Microglia cell were the first cells activated and recruited, later followed by astrocytes and innate immune cells. Of note, while glial cells were invading the spinal parenchyma into a unique wave culminating on the seventh day post-LPC, the innate peripheral cells infiltrated the tissue in two distinct waves. Moreover, we showed that conjointly with microglia cells, they exhibited pro-I phenotype during demyelination. Although both cell types shifted their polarization towards an anti-I phenotype consistent with remyelination and axonal repair, the early shift in microglia suggests that microglia might act as the initial orchestrator to recruit and activate partners cells in this pathological context. However, the current research focused on a specific time window. Extending the analysis to a longer period could reveal potential issues with long-term remyelination stability or the development of chronic neurodegeneration. Also, studying the behavioral consequences over time would provide a more comprehensive understanding of functional recovery.

Furthermore, our results illustrated an intense and concomitant cell population proliferation in early demyelination of microglia, astrocytes and microglia. Although some studies have emphasized the need for glial cell proliferation to fulfill remyelination and repair processes, the exact function of this behavior in these cells is not well characterized. Therefore, it would be interesting to selectively block the proliferation of microglia and astrocytes *in vivo* using cell-specific Cre-mediated conditional knockout of key genes in the cellular proliferative cascade, such as *Mki67* or cyclins like Cyclin-Dependent Kinase 1 (*Cdk1*), both of which are found to be upregulated in these cells. This approach would enable us to decipher the biological and functional relevance of such reactional behavior, such as its implication in cellular inflammatory phenotype.

Finally, we presented an ambitious study based on transcriptomic analysis specific to microglia, astrocytes, and OPCs following a myelin injury using the RiboTag method. This analysis provides an excellent starting point to understand all the putative mechanisms and cellular pathways involved in

myelin sheath loss and the initiation of remyelination. Although previous studies have demonstrated some of the important key functions of these cells in de- and remyelination, such as their inflammatory status or phagocytosis, it appears that the situation is far more complex than it seems. Indeed, through this unprecedented chronological work, we highlighted the extensive capabilities of each cell type, as well as how they are orchestrated during the evolution of the lesion. However, the evaluation of differentially expressed genes over the lesion evolution is not sufficient. The bioinformatic analysis must be continued to obtain a more detailed transcriptomic view, including the analysis of gene-target expression across time points, the study of transcript isoforms of selected genes as it can impact related biological functions, gene co-expression networks to identify co-regulated gene modules, and protein-RNA interaction analysis. While we plausibly described what microglia, astrocytes, and OPCs were doing, plausibility is not necessarily causality. To infer causation and validate our observations *in vivo*, it will be necessary to manipulate the system with genetic knock-in or knock-out of a gene of interest in our LPC mouse model and investigate the gene protein product since being translated does not necessarily mean it is an active gene product.

10. REFERENCES

Abd-El-Basset EM, Rao MS, Alshawaf SM, Ashkanani HK, Kabli AH (2021) Tumor necrosis factor (TNF) induces astrogliosis, microgliosis and promotes survival of cortical neurons. AIMS Neurosci 8:558-584.

Acaz-Fonseca E, Ortiz-Rodriguez A, Azcoitia I, Garcia-Segura LM, Arevalo MA (2019) Notch signaling in astrocytes mediates their morphological response to an inflammatory challenge. Cell Death Discov 5:85.

Acharjee S, Gordon PMK, Lee BH, Read J, Workentine ML, Sharkey KA, Pittman QJ (2021) Characterization of microglial transcriptomes in the brain and spinal cord of mice in early and late experimental autoimmune encephalomyelitis using a RiboTag strategy. Sci Rep 11:14319.

Acs P, Selak MA, Komoly S, Kalman B (2013) Distribution of oligodendrocyte loss and mitochondrial toxicity in the cuprizone-induced experimental demyelination model. J Neuroimmunol 262:128-131.

Alcina A, Abad-Grau MeM, Fedetz M, Izquierdo G, Lucas M, Fernández O, Ndagire D, Catalá-Rabasa A, Ruiz A, Gayán J, Delgado C, Arnal C, Matesanz F (2012) Multiple sclerosis risk variant HLA-DRB1*1501 associates with high expression of DRB1 gene in different human populations. PLoS One 7:e29819.

Almad A, Sahinkaya FR, McTigue DM (2011) Oligodendrocyte fate after spinal cord injury. Neurotherapeutics 8:262-273.

Almeida RG, Williamson JM, Madden ME, Early JJ, Voas MG, Talbot WS, Bianco IH, Lyons DA (2021) Myelination induces axonal hotspots of synaptic vesicle fusion that promote sheath growth. Curr Biol 31:3743-3754.e3745.

Almolda B, González B, Castellano B (2015) Are Microglial Cells the Regulators of Lymphocyte Responses in the CNS? Front Cell Neurosci 9:440.

Amin L, Nguyen XT, Rolle IG, D'Este E, Giachin G, Tran TH, Šerbec V, Cojoc D, Legname G (2016) Characterization of prion protein function by focal neurite stimulation. J Cell Sci 129:3878-3891.

An Y, Li S, Huang X, Chen X, Shan H, Zhang M (2022) The Role of Copper Homeostasis in Brain Disease. Int J Mol Sci 23.

Anderson MA, Burda JE, Ren Y, Ao Y, O'Shea TM, Kawaguchi R, Coppola G, Khakh BS, Deming TJ, Sofroniew MV (2016) Astrocyte scar formation aids central nervous system axon regeneration. Nature 532:195-200.

Arbour N, Prat A (2015) Roles of CD4 and CD8 Lymphocytes in Multiple Sclerosis and Experimental Autoimmune Encephalomyelitis. In: Neuroinflammation: New Insights into Benficial and Detrimental Functions, First Edition (David S, ed), pp 39-52. Wiley Online Library: John Wiley & Sons.

Argaw AT, Gurfein BT, Zhang Y, Zameer A, John GR (2009) VEGF-mediated disruption of endothelial CLN-5 promotes blood-brain barrier breakdown. Proc Natl Acad Sci U S A 106:1977-1982.

Argaw AT, Zhang Y, Snyder BJ, Zhao ML, Kopp N, Lee SC, Raine CS, Brosnan CF, John GR (2006) IL-1beta regulates blood-brain barrier permeability via reactivation of the hypoxia-angiogenesis program. J Immunol 177:5574-5584.

Argaw AT, Asp L, Zhang J, Navrazhina K, Pham T, Mariani JN, Mahase S, Dutta DJ, Seto J, Kramer EG, Ferrara N, Sofroniew MV, John GR (2012) Astrocyte-derived VEGF-A drives blood-brain barrier disruption in CNS inflammatory disease. J Clin Invest 122:2454-2468.

Arnett HA, Mason J, Marino M, Suzuki K, Matsushima GK, Ting JP (2001) TNF alpha promotes proliferation of oligodendrocyte progenitors and remyelination. Nat Neurosci 4:1116-1122.

Arnett HA, Hellendall RP, Matsushima GK, Suzuki K, Laubach VE, Sherman P, Ting JP (2002) The protective role of nitric oxide in a neurotoxicant-induced demyelinating model. J Immunol 168:427-433.

Arnett HA, Fancy SP, Alberta JA, Zhao C, Plant SR, Kaing S, Raine CS, Rowitch DH, Franklin RJ, Stiles CD (2004) bHLH transcription factor Olig1 is required to repair demyelinated lesions in the CNS. Science 306:2111-2115.

Arroyo EJ, Xu T, Grinspan J, Lambert S, Levinson SR, Brophy PJ, Peles E, Scherer SS (2002) Genetic dysmyelination alters the molecular architecture of the nodal region. J Neurosci 22:1726-1737.

Baaklini CS, Rawji KS, Duncan GJ, Ho MFS, Plemel JR (2019) Central Nervous System Remyelination: Roles of Glia and Innate Immune Cells. Front Mol Neurosci 12:225.

Baaklini CS, Ho MFS, Lange T, Hammond BP, Panda SP, Zirngibl M, Zia S, Himmelsbach K, Rana H, Phillips B, Antoszko D, Ibanga J, Lopez M, Lee KV, Keough MB, Caprariello AV, Kerr BJ, Plemel JR (2023) Microglia promote remyelination independent of their role in clearing myelin debris. Cell Rep 42:113574.

Bai X, Zhang YL, Liu LN (2020) Inhibition of TRIM8 restrains ischaemia-reperfusion-mediated cerebral injury by regulation of NF-κB activation associated inflammation and apoptosis. Exp Cell Res 388:111818.

Balabanov R, Strand K, Goswami R, McMahon E, Begolka W, Miller SD, Popko B (2007) Interferon-gamma-oligodendrocyte interactions in the regulation of experimental autoimmune encephalomyelitis. J Neurosci 27:2013-2024.

Baldwin KT, Tan CX, Strader ST, Jiang C, Savage JT, Elorza-Vidal X, Contreras X, Rülicke T, Hippenmeyer S, Estévez R, Ji RR, Eroglu C (2021) HepaCAM controls astrocyte self-organization and coupling. Neuron 109:2427-2442.e2410.

Ball JB, Green-Fulgham SM, Watkins LR (2022) Mechanisms of microglia-mediated synapse turnover and synaptogenesis. Prog Neurobiol 218:102336.

Barros LF, San Martín A, Ruminot I, Sandoval PY, Baeza-Lehnert F, Arce-Molina R, Rauseo D, Contreras-Baeza Y, Galaz A, Valdivia S (2020) Fluid Brain Glycolysis: Limits, Speed, Location, Moonlighting, and the Fates of Glycogen and Lactate. Neurochem Res 45:1328-1334.

Barry DS, Pakan JM, McDermott KW (2014) Radial glial cells: key organisers in CNS development. Int J Biochem Cell Biol 46:76-79.

Baxi EG, DeBruin J, Jin J, Strasburger HJ, Smith MD, Orthmann-Murphy JL, Schott JT, Fairchild AN, Bergles DE, Calabresi PA (2017) Lineage tracing reveals dynamic changes in oligodendrocyte precursor cells following cuprizone-induced demyelination. Glia 65:2087-2098.

Beattie EC, Stellwagen D, Morishita W, Bresnahan JC, Ha BK, Von Zastrow M, Beattie MS, Malenka RC (2002) Control of synaptic strength by glial TNFalpha. Science 295:2282-2285.

Beattie R, Postiglione MP, Burnett LE, Laukoter S, Streicher C, Pauler FM, Xiao G, Klezovitch O, Vasioukhin V, Ghashghaei TH, Hippenmeyer S (2017) Mosaic Analysis with Double Markers Reveals Distinct Sequential Functions of Lgl1 in Neural Stem Cells. Neuron 94:517-533.e513.

Bechler ME, Byrne L, Ffrench-Constant C (2015) CNS Myelin Sheath Lengths Are an Intrinsic Property of Oligodendrocytes. Curr Biol 25:2411-2416.

Beers DR, Henkel JS, Xiao Q, Zhao W, Wang J, Yen AA, Siklos L, McKercher SR, Appel SH (2006) Wild-type microglia extend survival in PU.1 knockout mice with familial amyotrophic lateral sclerosis. Proc Natl Acad Sci U S A 103:16021-16026.

Beiter RM, Rivet-Noor C, Merchak AR, Bai R, Johanson DM, Slogar E, Sol-Church K, Overall CC, Gaultier A (2022) Evidence for oligodendrocyte progenitor cell heterogeneity in the adult mouse brain. Sci Rep 12:12921.

Ben-Nun A, Lando Z (1983) Detection of autoimmune cells proliferating to myelin basic protein and selection of T cell lines that mediate experimental autoimmune encephalomyelitis (EAE) in mice. J Immunol 130:1205-1209.

Benmamar-Badel A, Owens T, Wlodarczyk A (2020) Protective Microglial Subset in Development, Aging, and Disease: Lessons From Transcriptomic Studies. Front Immunol 11:430.

Bennett ML, Bennett FC, Liddelow SA, Ajami B, Zamanian JL, Fernhoff NB, Mulinyawe SB, Bohlen CJ, Adil A, Tucker A, Weissman IL, Chang EF, Li G, Grant GA, Hayden Gephart MG,

Barres BA (2016) New tools for studying microglia in the mouse and human CNS. Proc Natl Acad Sci U S A 113:E1738-1746.
Benninger RKP, Piston DW (2013) Two-photon excitation microscopy for the study of living cells and tissues. Curr Protoc Cell Biol Chapter 4:4.11.11-14.11.24.
Benveniste EN (1997) Role of macrophages/microglia in multiple sclerosis and experimental allergic encephalomyelitis. J Mol Med (Berl) 75:165-173.
Berg CT, Khorooshi R, Asgari N, Owens T (2017) Influence of type I IFN signaling on anti-MOG antibody-mediated demyelination. J Neuroinflammation 14:127.
Berghoff SA et al. (2021) Microglia facilitate repair of demyelinated lesions via post-squalene sterol synthesis. Nat Neurosci 24:47-60.
Bezzi P, Domercq M, Brambilla L, Galli R, Schols D, De Clercq E, Vescovi A, Bagetta G, Kollias G, Meldolesi J, Volterra A (2001) CXCR4-activated astrocyte glutamate release via TNFalpha: amplification by microglia triggers neurotoxicity. Nat Neurosci 4:702-710.
Bieber AJ, Kerr S, Rodriguez M (2003) Efficient central nervous system remyelination requires T cells. Ann Neurol 53:680-684.
Billiau A, Matthys P (2001) Modes of action of Freund's adjuvants in experimental models of autoimmune diseases. J Leukoc Biol 70:849-860.
Birey F, Kloc M, Chavali M, Hussein I, Wilson M, Christoffel DJ, Chen T, Frohman MA, Robinson JK, Russo SJ, Maffei A, Aguirre A (2015) Genetic and Stress-Induced Loss of NG2 Glia Triggers Emergence of Depressive-like Behaviors through Reduced Secretion of FGF2. Neuron 88:941-956.
Bitsch A, Schuchardt J, Bunkowski S, Kuhlmann T, Brück W (2000) Acute axonal injury in multiple sclerosis. Correlation with demyelination and inflammation. Brain 123 (Pt 6):1174-1183.
Bjornevik K, Cortese M, Healy BC, Kuhle J, Mina MJ, Leng Y, Elledge SJ, Niebuhr DW, Scher AI, Munger KL, Ascherio A (2022) Longitudinal analysis reveals high prevalence of Epstein-Barr virus associated with multiple sclerosis. Science 375:296-301.
Blakemore WF (1976) Invasion od Schwann Cells into the Spinal cors of the Rat following Local injection of Lysolecithin. In, pp 21-39: Neuropathology and Applied Neurobiology.
Blauth K, Soltys J, Matschulat A, Reiter CR, Ritchie A, Baird NL, Bennett JL, Owens GP (2015) Antibodies produced by clonally expanded plasma cells in multiple sclerosis cerebrospinal fluid cause demyelination of spinal cord explants. Acta Neuropathol 130:765-781.
Boiko T, Rasband MN, Levinson SR, Caldwell JH, Mandel G, Trimmer JS, Matthews G (2001) Compact myelin dictates the differential targeting of two sodium channel isoforms in the same axon. Neuron 30:91-104.
Borggrewe M, Kooistra SM, Noelle RJ, Eggen BJL, Laman JD (2020) Exploring the VISTA of microglia: immune checkpoints in CNS inflammation. J Mol Med (Berl) 98:1415-1430.
Boyle ME, Berglund EO, Murai KK, Weber L, Peles E, Ranscht B (2001) Contactin orchestrates assembly of the septate-like junctions at the paranode in myelinated peripheral nerve. Neuron 30:385-397.
Bradl M, Lassmann H (2010) Oligodendrocytes: biology and pathology. Acta Neuropathol 119:37-53.
Brambilla R, Morton PD, Ashbaugh JJ, Karmally S, Lambertsen KL, Bethea JR (2014) Astrocytes play a key role in EAE pathophysiology by orchestrating in the CNS the inflammatory response of resident and peripheral immune cells and by suppressing remyelination. Glia 62:452-467.
Bravo-Ferrer I, Khakh BS, Díaz-Castro B (2022) Cell-specific RNA purification to study translatomes of mouse central nervous system. STAR Protoc 3:101397.
Brennan FH, Li Y, Wang C, Ma A, Guo Q, Pukos N, Campbell WA, Witcher KG, Guan Z, Kigerl KA, Hall JCE, Godbout JP, Fischer AJ, McTigue DM, He Z, Ma Q, Popovich PG (2022) Microglia coordinate cellular interactions during spinal cord repair in mice. Nat Commun 13:4096.
Britton R, Wasley T, Harish R, Holz C, Hall J, Yee DC, Melton Witt J, Booth EA, Braithwaite S, Czirr E, Kerrisk Campbell M (2023) Noncanonical Activity of Tissue Inhibitor of Metalloproteinases 2 (TIMP2) Improves Cognition and Synapse Density in Aging. eNeuro 10.

Brocard J, Warot X, Wendling O, Messaddeq N, Vonesch JL, Chambon P, Metzger D (1997) Spatio-temporally controlled site-specific somatic mutagenesis in the mouse. Proc Natl Acad Sci U S A 94:14559-14563.

Brown DA, Sawchenko PE (2007) Time course and distribution of inflammatory and neurodegenerative events suggest structural bases for the pathogenesis of experimental autoimmune encephalomyelitis. J Comp Neurol 502:236-260.

Buchanan J, da Costa NM, Cheadle L (2023) Emerging roles of oligodendrocyte precursor cells in neural circuit development and remodeling. Trends Neurosci 46:628-639.

Burnside MN, Pyatt RE, Hughes A, Baker PB, Pierson CR (2015) Complex brain malformations associated with chromosome 6q27 gain that includes THBS2, which encodes thrombospondin 2, an astrocyte-derived protein of the extracellular matrix. Pediatr Dev Pathol 18:59-65.

Burstyn-Cohen T, Tzarfaty V, Frumkin A, Feinstein Y, Stoeckli E, Klar A (1999) F-Spondin is required for accurate pathfinding of commissural axons at the floor plate. Neuron 23:233-246.

Bushong EA, Martone ME, Ellisman MH (2004) Maturation of astrocyte morphology and the establishment of astrocyte domains during postnatal hippocampal development. Int J Dev Neurosci 22:73-86.

Butler MG, Rafi SK, Hossain W, Stephan DA, Manzardo AM (2015) Whole exome sequencing in females with autism implicates novel and candidate genes. Int J Mol Sci 16:1312-1335.

Butovsky O, Ziv Y, Schwartz A, Landa G, Talpalar AE, Pluchino S, Martino G, Schwartz M (2006) Microglia activated by IL-4 or IFN-gamma differentially induce neurogenesis and oligodendrogenesis from adult stem/progenitor cells. Mol Cell Neurosci 31:149-160.

Buttigieg E, Scheller A, El Waly B, Kirchhoff F, Debarbieux F (2023) Contribution of Intravital Neuroimaging to Study Animal Models of Multiple Sclerosis. Neurotherapeutics.

Butzkueven H, Zhang JG, Soilu-Hanninen M, Hochrein H, Chionh F, Shipham KA, Emery B, Turnley AM, Petratos S, Ernst M, Bartlett PF, Kilpatrick TJ (2002) LIF receptor signaling limits immune-mediated demyelination by enhancing oligodendrocyte survival. Nat Med 8:613-619.

Böttcher C, Fernández-Zapata C, Snijders GJL, Schlickeiser S, Sneeboer MAM, Kunkel D, De Witte LD, Priller J (2020) Single-cell mass cytometry of microglia in major depressive disorder reveals a non-inflammatory phenotype with increased homeostatic marker expression. Transl Psychiatry 10:310.

Cahoy JD, Emery B, Kaushal A, Foo LC, Zamanian JL, Christopherson KS, Xing Y, Lubischer JL, Krieg PA, Krupenko SA, Thompson WJ, Barres BA (2008) A transcriptome database for astrocytes, neurons, and oligodendrocytes: a new resource for understanding brain development and function. J Neurosci 28:264-278.

Cai J, Qi Y, Hu X, Tan M, Liu Z, Zhang J, Li Q, Sander M, Qiu M (2005) Generation of oligodendrocyte precursor cells from mouse dorsal spinal cord independent of Nkx6 regulation and Shh signaling. Neuron 45:41-53.

Caillava C, Baron-Van Evercooren A (2012) Differential requirement of cyclin-dependent kinase 2 for oligodendrocyte progenitor cell proliferation and differentiation. Cell Div 7:14.

Calabrese V, Mancuso C, Calvani M, Rizzarelli E, Butterfield DA, Stella AM (2007) Nitric oxide in the central nervous system: neuroprotection versus neurotoxicity. Nat Rev Neurosci 8:766-775.

Cantuti-Castelvetri L, Fitzner D, Bosch-Queralt M, Weil MT, Su M, Sen P, Ruhwedel T, Mitkovski M, Trendelenburg G, Lütjohann D, Möbius W, Simons M (2018) Defective cholesterol clearance limits remyelination in the aged central nervous system. Science 359:684-688.

Caravagna C, Jaouën A, Desplat-Jégo S, Fenrich KK, Bergot E, Luche H, Grenot P, Rougon G, Malissen M, Debarbieux F (2018) Diversity of innate immune cell subsets across spatial and temporal scales in an EAE mouse model. Sci Rep 8:5146.

Carlson T, Kroenke M, Rao P, Lane TE, Segal B (2008) The Th17-ELR+ CXC chemokine pathway is essential for the development of central nervous system autoimmune disease. J Exp Med 205:811-823.

Caroni P (1997) Overexpression of growth-associated proteins in the neurons of adult transgenic mice. J Neurosci Methods 71:3-9.

Carson JH, Gao Y, Tatavarty V, Levin MK, Korza G, Francone VP, Kosturko LD, Maggipinto MJ, Barbarese E (2008) Multiplexed RNA trafficking in oligodendrocytes and neurons. Biochim Biophys Acta 1779:453-458.
Carson MJ, Behringer RR, Brinster RL, McMorris FA (1993) Insulin-like growth factor I increases brain growth and central nervous system myelination in transgenic mice. Neuron 10:729-740.
Castro VL, Reyes JF, Reyes-Nava NG, Paz D, Quintana AM (2020) Hcfc1a regulates neural precursor proliferation and asxl1 expression in the developing brain. BMC Neurosci 21:27.
Cellerino A, Carroll P, Thoenen H, Barde YA (1997) Reduced size of retinal ganglion cell axons and hypomyelination in mice lacking brain-derived neurotrophic factor. Mol Cell Neurosci 9:397-408.
Cencioni MT, Mattoscio M, Magliozzi R, Bar-Or A, Muraro PA (2021) B cells in multiple sclerosis - from targeted depletion to immune reconstitution therapies. Nat Rev Neurol 17:399-414.
Ceruti S, Villa G, Genovese T, Mazzon E, Longhi R, Rosa P, Bramanti P, Cuzzocrea S, Abbracchio MP (2009) The P2Y-like receptor GPR17 as a sensor of damage and a new potential target in spinal cord injury. Brain 132:2206-2218.
Chamberlain KA, Huang N, Xie Y, LiCausi F, Li S, Li Y, Sheng ZH (2021) Oligodendrocytes enhance axonal energy metabolism by deacetylation of mitochondrial proteins through transcellular delivery of SIRT2. Neuron 109:3456-3472.e3458.
Chandel NS, Trzyna WC, McClintock DS, Schumacker PT (2000) Role of oxidants in NF-kappa B activation and TNF-alpha gene transcription induced by hypoxia and endotoxin. J Immunol 165:1013-1021.
Chang KJ, Redmond SA, Chan JR (2016) Remodeling myelination: implications for mechanisms of neural plasticity. Nat Neurosci 19:190-197.
Chari DM (2007) Remyelination in multiple sclerosis. Int Rev Neurobiol 79:589-620.
Charles P, Hernandez MP, Stankoff B, Aigrot MS, Colin C, Rougon G, Zalc B, Lubetzki C (2000) Negative regulation of central nervous system myelination by polysialylated-neural cell adhesion molecule. Proc Natl Acad Sci U S A 97:7585-7590.
Cheli VT, Santiago González DA, Wan R, Rosenblum SL, Denaroso GE, Angeliu CG, Smith Z, Wang C, Paez PM (2023) Transferrin Receptor Is Necessary for Proper Oligodendrocyte Iron Homeostasis and Development. J Neurosci 43:3614-3629.
Chen J, Van Gulden S, McGuire TL, Fleming AC, Oka C, Kessler JA, Peng CY (2018) BMP-Responsive Protease HtrA1 Is Differentially Expressed in Astrocytes and Regulates Astrocytic Development and Injury Response. J Neurosci 38:3840-3857.
Chen JN, Zhang YN, Tian LG, Zhang Y, Li XY, Ning B (2022a) Down-regulating Circular RNA Prkcsh suppresses the inflammatory response after spinal cord injury. Neural Regen Res 17:144-151.
Chen M, Ingle L, Plautz EJ, Kong X, Tang R, Ghosh N, Romprey MK, Fenske WK, Goldberg MP (2022b) LZK-dependent stimulation of astrocyte reactivity promotes corticospinal axon sprouting. Front Cell Neurosci 16:969261.
Chen N, Zhou P, Liu X, Li J, Wan Y, Liu S, Wei F (2020) Overexpression of Rictor in the injured spinal cord promotes functional recovery in a rat model of spinal cord injury. FASEB J 34:6984-6998.
Cheng X, Wang J, Sun X, Shao L, Guo Z, Li Y (2019) Morphological and functional alterations of astrocytes responding to traumatic brain injury. J Integr Neurosci 18:203-215.
Chesnut M, Paschoud H, Repond C, Smirnova L, Hartung T, Zurich MG, Hogberg HT, Pamies D (2021) Human IPSC-Derived Model to Study Myelin Disruption. Int J Mol Sci 22.
Chew LJ, Coley W, Cheng Y, Gallo V (2010) Mechanisms of regulation of oligodendrocyte development by p38 mitogen-activated protein kinase. J Neurosci 30:11011-11027.
Chiou B, Neely E, Kallianpur A, Connor JR (2019) Semaphorin4A causes loss of mature oligodendrocytes and demyelination in vivo. J Neuroinflammation 16:28.
Cho CH (2017) Commentary: Identification of diverse astrocyte populations and their malignant analogs. Front Mol Neurosci 10:193.
Chong SY, Rosenberg SS, Fancy SP, Zhao C, Shen YA, Hahn AT, McGee AW, Xu X, Zheng B, Zhang LI, Rowitch DH, Franklin RJ, Lu QR, Chan JR (2012) Neurite outgrowth inhibitor

Nogo-A establishes spatial segregation and extent of oligodendrocyte myelination. Proc Natl Acad Sci U S A 109:1299-1304.
Christopherson KS, Ullian EM, Stokes CC, Mullowney CE, Hell JW, Agah A, Lawler J, Mosher DF, Bornstein P, Barres BA (2005) Thrombospondins are astrocyte-secreted proteins that promote CNS synaptogenesis. Cell 120:421-433.
Chu T, Zhang YP, Tian Z, Ye C, Zhu M, Shields LBE, Kong M, Barnes GN, Shields CB, Cai J (2019) Dynamic response of microglia/macrophage polarization following demyelination in mice. J Neuroinflammation 16:188.
Cignarella F, Filipello F, Bollman B, Cantoni C, Locca A, Mikesell R, Manis M, Ibrahim A, Deng L, Benitez BA, Cruchaga C, Licastro D, Mihindukulasuriya K, Harari O, Buckland M, Holtzman DM, Rosenthal A, Schwabe T, Tassi I, Piccio L (2020) TREM2 activation on microglia promotes myelin debris clearance and remyelination in a model of multiple sclerosis. Acta Neuropathol 140:513-534.
Ciurkiewicz M, Herder V, Beineke A (2020) Beneficial and Detrimental Effects of Regulatory T Cells in Neurotropic Virus Infections. Int J Mol Sci 21.
Clarke LE, Liddelow SA, Chakraborty C, Münch AE, Heiman M, Barres BA (2018) Normal aging induces A1-like astrocyte reactivity. Proc Natl Acad Sci U S A 115:E1896-E1905.
Clemente D, Ortega MC, Melero-Jerez C, de Castro F (2013) The effect of glia-glia interactions on oligodendrocyte precursor cell biology during development and in demyelinating diseases. Front Cell Neurosci 7:268.
Codarri L, Greter M, Becher B (2013) Communication between pathogenic T cells and myeloid cells in neuroinflammatory disease. Trends Immunol 34:114-119.
Colombo E, Farina C (2016) Astrocytes: Key Regulators of Neuroinflammation. Trends Immunol 37:608-620.
Colombo E, Cordiglieri C, Melli G, Newcombe J, Krumbholz M, Parada LF, Medico E, Hohlfeld R, Meinl E, Farina C (2012) Stimulation of the neurotrophin receptor TrkB on astrocytes drives nitric oxide production and neurodegeneration. J Exp Med 209:521-535.
Colonna M, Butovsky O (2017) Microglia Function in the Central Nervous System During Health and Neurodegeneration. Annu Rev Immunol 35:441-468.
Condomitti G, Wierda KD, Schroeder A, Rubio SE, Vennekens KM, Orlandi C, Martemyanov KA, Gounko NV, Savas JN, de Wit J (2018) An Input-Specific Orphan Receptor GPR158-HSPG Interaction Organizes Hippocampal Mossy Fiber-CA3 Synapses. Neuron 100:201-215.e209.
Cooke P, Janowitz H, Dougherty SE (2022) Neuronal Redevelopment and the Regeneration of Neuromodulatory Axons in the Adult Mammalian Central Nervous System. Front Cell Neurosci 16:872501.
Correale J, Farez MF (2015) The Role of Astrocytes in Multiple Sclerosis Progression. Front Neurol 6:180.
Coutinho Costa VG, Araújo SE, Alves-Leon SV, Gomes FCA (2023) Central nervous system demyelinating diseases: glial cells at the hub of pathology. Front Immunol 14:1135540.
Croxford JL, Yamamura T (2009) Back to the future for multiple sclerosis therapy: focus on current and emerging disease-modifying therapeutic strategies. Immunotherapy 1:403-423.
Cruz-Martinez P, Martinez-Ferre A, Jaramillo-Merchán J, Estirado A, Martinez S, Jones J (2014) FGF8 activates proliferation and migration in mouse post-natal oligodendrocyte progenitor cells. PLoS One 9:e108241.
Cui H, Guo Z, Fan Z, Shen N, Qi X, Ma Y, Zhu Y, Wu X, Chen B, Xiang H (2023) TMEM100 Regulates Neuropathic Pain by Reducing the Expression of Inflammatory Factors. Mediators Inflamm 2023:9151967.
Czopka T, Ffrench-Constant C, Lyons DA (2013) Individual oligodendrocytes have only a few hours in which to generate new myelin sheaths in vivo. Dev Cell 25:599-609.
Câmara J, Wang Z, Nunes-Fonseca C, Friedman HC, Grove M, Sherman DL, Komiyama NH, Grant SG, Brophy PJ, Peterson A, ffrench-Constant C (2009) Integrin-mediated axoglial interactions initiate myelination in the central nervous system. J Cell Biol 185:699-712.
Dalmau I, Finsen B, Zimmer J, González B, Castellano B (1998) Development of microglia in the postnatal rat hippocampus. Hippocampus 8:458-474.

Das Sarma J, Kenyon LC, Hingley ST, Shindler KS (2009) Mechanisms of primary axonal damage in a viral model of multiple sclerosis. J Neurosci 29:10272-10280.
David-Bercholz J, Kuo CT, Deneen B (2021) Astrocyte and Oligodendrocyte Responses From the Subventricular Zone After Injury. Front Cell Neurosci 15:797553.
Dawson MR, Levine JM, Reynolds R (2000) NG2-expressing cells in the central nervous system: are they oligodendroglial progenitors? J Neurosci Res 61:471-479.
De Bondt M, Hellings N, Opdenakker G, Struyf S (2020) Neutrophils: Underestimated Players in the Pathogenesis of Multiple Sclerosis (MS). Int J Mol Sci 21.
de Sèze J, Maillart E, Gueguen A, Laplaud DA, Michel L, Thouvenot E, Zephir H, Zimmer L, Biotti D, Liblau R (2023) Anti-CD20 therapies in multiple sclerosis: From pathology to the clinic. Front Immunol 14:1004795.
Deczkowska A, Keren-Shaul H, Weiner A, Colonna M, Schwartz M, Amit I (2018) Disease-Associated Microglia: A Universal Immune Sensor of Neurodegeneration. Cell 173:1073-1081.
Dekkers MP, Barde YA (2013) Developmental biology. Programmed cell death in neuronal development. Science 340:39-41.
Deneen B, Ho R, Lukaszewicz A, Hochstim CJ, Gronostajski RM, Anderson DJ (2006) The transcription factor NFIA controls the onset of gliogenesis in the developing spinal cord. Neuron 52:953-968.
Deng T, Postnikov Y, Zhang S, Garrett L, Becker L, Rácz I, Hölter SM, Wurst W, Fuchs H, Gailus-Durner V, de Angelis MH, Bustin M (2017) Interplay between H1 and HMGN epigenetically regulates OLIG1&2 expression and oligodendrocyte differentiation. Nucleic Acids Res 45:3031-3045.
DePaula-Silva AB, Hanak TJ, Libbey JE, Fujinami RS (2017) Theiler's murine encephalomyelitis virus infection of SJL/J and C57BL/6J mice: Models for multiple sclerosis and epilepsy. J Neuroimmunol 308:30-42.
Dessaud E, Ribes V, Balaskas N, Yang LL, Pierani A, Kicheva A, Novitch BG, Briscoe J, Sasai N (2010) Dynamic assignment and maintenance of positional identity in the ventral neural tube by the morphogen sonic hedgehog. PLoS Biol 8:e1000382.
Devasani K, Yao Y (2022) Expression and functions of adenylyl cyclases in the CNS. Fluids Barriers CNS 19:23.
Dillenburg A, Ireland G, Holloway RK, Davies CL, Evans FL, Swire M, Bechler ME, Soong D, Yuen TJ, Su GH, Becher JC, Smith C, Williams A, Miron VE (2018) Activin receptors regulate the oligodendrocyte lineage in health and disease. Acta Neuropathol 135:887-906.
Dilokthornsakul P, Valuck RJ, Nair KV, Corboy JR, Allen RR, Campbell JD (2016) Multiple sclerosis prevalence in the United States commercially insured population. Neurology 86:1014-1021.
Dimou L, Simon C, Kirchhoff F, Takebayashi H, Götz M (2008) Progeny of Olig2-expressing progenitors in the gray and white matter of the adult mouse cerebral cortex. J Neurosci 28:10434-10442.
Ding X, Yan Y, Li X, Li K, Ciric B, Yang J, Zhang Y, Wu S, Xu H, Chen W, Lovett-Racke AE, Zhang GX, Rostami A (2015) Silencing IFN-γ binding/signaling in astrocytes versus microglia leads to opposite effects on central nervous system autoimmunity. J Immunol 194:4251-4264.
Dombrowski Y et al. (2017) Regulatory T cells promote myelin regeneration in the central nervous system. Nat Neurosci 20:674-680.
Domingues HS, Falcão AM, Mendes-Pinto I, Salgado AJ, Teixeira FG (2020) Exosome Circuitry During (De)(Re)Myelination of the Central Nervous System. Front Cell Dev Biol 8:483.
Dong Y, Simske JS (2016) Vertebrate Claudin/PMP22/EMP22/MP20 family protein TMEM47 regulates epithelial cell junction maturation and morphogenesis. Dev Dyn 245:653-666.
Drake SS, Mohammadnia A, Heale K, Groh AMR, Hua EM, Zaman A, Hintermayer MA, Zandee S, Gosselin D, Stratton JA, Sinclair DA, Fournier AE (2023) Cellular rejuvenation protects neurons from inflammation mediated cell death. bioRxiv.
Dringen R, Scheiber IF, Mercer JF (2013) Copper metabolism of astrocytes. Front Aging Neurosci 5:9.

Du J, Yi M, Zhou F, He W, Yang A, Qiu M, Huang H (2021) S100B is selectively expressed by gray matter protoplasmic astrocytes and myelinating oligodendrocytes in the developing CNS. Mol Brain 14:154.
Dugas JC, Tai YC, Speed TP, Ngai J, Barres BA (2006) Functional genomic analysis of oligodendrocyte differentiation. J Neurosci 26:10967-10983.
Dulin NO (2020) Calcium-Activated Chloride Channel ANO1/TMEM16A: Regulation of Expression and Signaling. Front Physiol 11:590262.
Duncan GJ, Emery B (2023) End of the road: Astrocyte endfeet regulate OPC migration and myelination. Neuron 111:139-141.
Duncan GJ, Simkins TJ, Emery B (2021) Neuron-Oligodendrocyte Interactions in the Structure and Integrity of Axons. Front Cell Dev Biol 9:653101.
Duncan ID, Marik RL, Broman AT, Heidari M (2017) Thin myelin sheaths as the hallmark of remyelination persist over time and preserve axon function. Proc Natl Acad Sci U S A 114:E9685-E9691.
Durand B, Raff M (2000) A cell-intrinsic timer that operates during oligodendrocyte development. Bioessays 22:64-71.
Dziedzic T, Metz I, Dallenga T, König FB, Müller S, Stadelmann C, Brück W (2010) Wallerian degeneration: a major component of early axonal pathology in multiple sclerosis. Brain Pathol 20:976-985.
Ebrahimi M, Yamamoto Y, Sharifi K, Kida H, Kagawa Y, Yasumoto Y, Islam A, Miyazaki H, Shimamoto C, Maekawa M, Mitsushima D, Yoshikawa T, Owada Y (2016) Astrocyte-expressed FABP7 regulates dendritic morphology and excitatory synaptic function of cortical neurons. Glia 64:48-62.
Edgar JM, McCulloch MC, Montague P, Brown AM, Thilemann S, Pratola L, Gruenenfelder FI, Griffiths IR, Nave KA (2010) Demyelination and axonal preservation in a transgenic mouse model of Pelizaeus-Merzbacher disease. EMBO Mol Med 2:42-50.
Einstein O, Friedman-Levi Y, Grigoriadis N, Ben-Hur T (2009) Transplanted neural precursors enhance host brain-derived myelin regeneration. J Neurosci 29:15694-15702.
Eiraku M, Tohgo A, Ono K, Kaneko M, Fujishima K, Hirano T, Kengaku M (2005) DNER acts as a neuron-specific Notch ligand during Bergmann glial development. Nat Neurosci 8:873-880.
El Waly B, Buttigieg E, Karakus C, Brustlein S, Debarbieux F (2020) Longitudinal Intravital Microscopy Reveals Axon Degeneration Concomitant With Inflammatory Cell Infiltration in an LPC Model of Demyelination. Front Cell Neurosci 14:165.
Elmore MR, Najafi AR, Koike MA, Dagher NN, Spangenberg EE, Rice RA, Kitazawa M, Matusow B, Nguyen H, West BL, Green KN (2014) Colony-stimulating factor 1 receptor signaling is necessary for microglia viability, unmasking a microglia progenitor cell in the adult brain. Neuron 82:380-397.
Engelhardt B, Ransohoff RM (2005) The ins and outs of T-lymphocyte trafficking to the CNS: anatomical sites and molecular mechanisms. Trends Immunol 26:485-495.
Erickson EK, Farris SP, Blednov YA, Mayfield RD, Harris RA (2018) Astrocyte-specific transcriptome responses to chronic ethanol consumption. Pharmacogenomics J 18:578-589.
Escartin C et al. (2021) Reactive astrocyte nomenclature, definitions, and future directions. Nat Neurosci 24:312-325.
Eve M, Gandawijaya J, Yang L, Oguro-Ando A (2022) Neuronal Cell Adhesion Molecules May Mediate Neuroinflammation in Autism Spectrum Disorder. Front Psychiatry 13:842755.
Falcão AM, van Bruggen D, Marques S, Meijer M, Jäkel S, Agirre E, Samudyata, Floriddia EM, Vanichkina DP, Ffrench-Constant C, Williams A, Guerreiro-Cacais AO, Castelo-Branco G (2018) Disease-specific oligodendrocyte lineage cells arise in multiple sclerosis. Nat Med 24:1837-1844.
Fan W, Liu X, Zhang J, Qin L, Du J, Li X, Qian S, Chen H, Qian P (2022) TRIM67 Suppresses TNFalpha-Triggered NF-kB Activation by Competitively Binding Beta-TrCP to IkBa. Front Immunol 13:793147.
Fancy SP, Zhao C, Franklin RJ (2004) Increased expression of Nkx2.2 and Olig2 identifies reactive oligodendrocyte progenitor cells responding to demyelination in the adult CNS. Mol Cell Neurosci 27:247-254.

Fang LP, Bai X (2023) Oligodendrocyte precursor cells: the multitaskers in the brain. Pflugers Arch.
Faust N, Varas F, Kelly LM, Heck S, Graf T (2000) Insertion of enhanced green fluorescent protein into the lysozyme gene creates mice with green fluorescent granulocytes and macrophages. Blood 96:719-726.
Fazakerley JK, Walker R (2003) Virus demyelination. J Neurovirol 9:148-164.
Feil R, Wagner J, Metzger D, Chambon P (1997) Regulation of Cre recombinase activity by mutated estrogen receptor ligand-binding domains. Biochem Biophys Res Commun 237:752-757.
Feil S, Valtcheva N, Feil R (2009) Inducible Cre mice. Methods Mol Biol 530:343-363.
Feng G, Mellor RH, Bernstein M, Keller-Peck C, Nguyen QT, Wallace M, Nerbonne JM, Lichtman JW, Sanes JR (2000) Imaging neuronal subsets in transgenic mice expressing multiple spectral variants of GFP. Neuron 28:41-51.
Fenrich KK, Weber P, Rougon G, Debarbieux F (2013a) Long- and short-term intravital imaging reveals differential spatiotemporal recruitment and function of myelomonocytic cells after spinal cord injury. J Physiol 591:4895-4902.
Fenrich KK, Weber P, Rougon G, Debarbieux F (2013b) Implanting glass spinal cord windows in adult mice with experimental autoimmune encephalomyelitis. J Vis Exp:e50826.
Fex Svenningsen Å, Löring S, Sørensen AL, Huynh HUB, Hjæresen S, Martin N, Moeller JB, Elkjær ML, Holmskov U, Illes Z, Andersson M, Nielsen SB, Benedikz E (2017) Macrophage migration inhibitory factor (MIF) modulates trophic signaling through interaction with serine protease HTRA1. Cell Mol Life Sci 74:4561-4572.
Filippi M, Bar-Or A, Piehl F, Preziosa P, Solari A, Vukusic S, Rocca MA (2018) Multiple sclerosis. Nat Rev Dis Primers 4:43.
Fitzpatrick JM, Anderson RC, McDermott KW (2015) MicroRNA: Key regulators of oligodendrocyte development and pathobiology. Int J Biochem Cell Biol 65:134-138.
Fletcher JM, Lalor SJ, Sweeney CM, Tubridy N, Mills KH (2010) T cells in multiple sclerosis and experimental autoimmune encephalomyelitis. Clin Exp Immunol 162:1-11.
Franklin RJ (2002) Why does remyelination fail in multiple sclerosis? Nat Rev Neurosci 3:705-714.
Franklin RJM, Simons M (2022) CNS remyelination and inflammation: From basic mechanisms to therapeutic opportunities. Neuron 110:3549-3565.
Franssen H, Straver DC (2013) Pathophysiology of immune-mediated demyelinating neuropathies-part I: neuroscience. Muscle Nerve 48:851-864.
Friedrich G, Soriano P (1991) Promoter traps in embryonic stem cells: a genetic screen to identify and mutate developmental genes in mice. Genes Dev 5:1513-1523.
Fröhlich D, Kuo WP, Frühbeis C, Sun JJ, Zehendner CM, Luhmann HJ, Pinto S, Toedling J, Trotter J, Krämer-Albers EM (2014) Multifaceted effects of oligodendroglial exosomes on neurons: impact on neuronal firing rate, signal transduction and gene regulation. Philos Trans R Soc Lond B Biol Sci 369.
Frühbeis C, Kuo-Elsner WP, Müller C, Barth K, Peris L, Tenzer S, Möbius W, Werner HB, Nave KA, Fröhlich D, Krämer-Albers EM (2020) Oligodendrocytes support axonal transport and maintenance via exosome secretion. PLoS Biol 18:e3000621.
Frühbeis C, Fröhlich D, Kuo WP, Amphornrat J, Thilemann S, Saab AS, Kirchhoff F, Möbius W, Goebbels S, Nave KA, Schneider A, Simons M, Klugmann M, Trotter J, Krämer-Albers EM (2013) Neurotransmitter-triggered transfer of exosomes mediates oligodendrocyte-neuron communication. PLoS Biol 11:e1001604.
Fu R, Shen Q, Xu P, Luo JJ, Tang Y (2014) Phagocytosis of microglia in the central nervous system diseases. Mol Neurobiol 49:1422-1434.
Fu Y, Wang H, Huff TB, Shi R, Cheng JX (2007) Coherent anti-Stokes Raman scattering imaging of myelin degradation reveals a calcium-dependent pathway in lyso-PtdCho-induced demyelination. J Neurosci Res 85:2870-2881.
Fuhrmann JC, Kins S, Rostaing P, El Far O, Kirsch J, Sheng M, Triller A, Betz H, Kneussel M (2002) Gephyrin interacts with Dynein light chains 1 and 2, components of motor protein complexes. J Neurosci 22:5393-5402.
Fuller ML, DeChant AK, Rothstein B, Caprariello A, Wang R, Hall AK, Miller RH (2007) Bone morphogenetic proteins promote gliosis in demyelinating spinal cord lesions. Ann Neurol 62:288-300.

Gacem N, Nait-Oumesmar B (2021) Oligodendrocyte Development and Regenerative Therapeutics in Multiple Sclerosis. Life (Basel) 11.
Galloway DA, Blandford SN, Berry T, Williams JB, Stefanelli M, Ploughman M, Moore CS (2019) miR-223 promotes regenerative myeloid cell phenotype and function in the demyelinated central nervous system. Glia 67:857-869.
Gard AL, Williams WC, Burrell MR (1995) Oligodendroblasts distinguished from O-2A glial progenitors by surface phenotype (O4+GalC-) and response to cytokines using signal transducer LIFR beta. Dev Biol 167:596-608.
Garner KM, Amin R, Johnson RW, Scarlett EJ, Burton MD (2018) Microglia priming by interleukin-6 signaling is enhanced in aged mice. J Neuroimmunol 324:90-99.
Gasecka P, Jaouen A, Bioud FZ, B de Aguiar H, Duboisset J, Ferrand P, Rigneault H, Balla NK, Debarbieux F, Brasselet S (2017) Lipid Order Degradation in Autoimmune Demyelination Probed by Polarized Coherent Raman Microscopy. Biophys J 113:1520-1530.
Gaultier A, Wu X, Le Moan N, Takimoto S, Mukandala G, Akassoglou K, Campana WM, Gonias SL (2009) Low-density lipoprotein receptor-related protein 1 is an essential receptor for myelin phagocytosis. J Cell Sci 122:1155-1162.
Gautier HO, Evans KA, Volbracht K, James R, Sitnikov S, Lundgaard I, James F, Lao-Peregrin C, Reynolds R, Franklin RJ, Káradóttir RT (2015) Neuronal activity regulates remyelination via glutamate signalling to oligodendrocyte progenitors. Nat Commun 6:8518.
Ghasemlou N, Jeong SY, Lacroix S, David S (2007) T cells contribute to lysophosphatidylcholine-induced macrophage activation and demyelination in the CNS. Glia 55:294-302.
Ghezzi L, Bollman B, De Feo L, Piccio L, Trapp BD, Schmidt RE, Cross AH (2023) Schwann Cell Remyelination in the Multiple Sclerosis Central Nervous System. Lab Invest 103:100128.
Gilchrist SE, Pennelli GM, Hafizi S (2021) Gas6/TAM Signalling Negatively Regulates Inflammatory Induction of GM-CSF in Mouse Brain Microglia. Cells 10.
Gilson J, Blakemore WF (1993) Failure of remyelination in areas of demyelination produced in the spinal cord of old rats. Neuropathol Appl Neurobiol 19:173-181.
Gimenez MA, Sim JE, Russell JH (2004) TNFR1-dependent VCAM-1 expression by astrocytes exposes the CNS to destructive inflammation. J Neuroimmunol 151:116-125.
Gingrich EC, Case K, Garcia ADR (2022) A subpopulation of astrocyte progenitors defined by Sonic hedgehog signaling. Neural Dev 17:2.
Ginhoux F, Prinz M (2015) Origin of microglia: current concepts and past controversies. Cold Spring Harb Perspect Biol 7:a020537.
Ginhoux F, Greter M, Leboeuf M, Nandi S, See P, Gokhan S, Mehler MF, Conway SJ, Ng LG, Stanley ER, Samokhvalov IM, Merad M (2010) Fate mapping analysis reveals that adult microglia derive from primitive macrophages. Science 330:841-845.
Goddery EN, Fain CE, Lipovsky CG, Ayasoufi K, Yokanovich LT, Malo CS, Khadka RH, Tritz ZP, Jin F, Hansen MJ, Johnson AJ (2021) Microglia and Perivascular Macrophages Act as Antigen Presenting Cells to Promote CD8 T Cell Infiltration of the Brain. Front Immunol 12:726421.
Goldey GJ, Roumis DK, Glickfeld LL, Kerlin AM, Reid RC, Bonin V, Schafer DP, Andermann ML (2014) Removable cranial windows for long-term imaging in awake mice. Nat Protoc 9:2515-2538.
Gorter RP, Baron W (2020) Matrix metalloproteinases shape the oligodendrocyte (niche) during development and upon demyelination. Neurosci Lett 729:134980.
Grabner GF, Eichmann TO, Wagner B, Gao Y, Farzi A, Taschler U, Radner FP, Schweiger M, Lass A, Holzer P, Zinser E, Tschöp MH, Yi CX, Zimmermann R (2016) Deletion of Monoglyceride Lipase in Astrocytes Attenuates Lipopolysaccharide-induced Neuroinflammation. J Biol Chem 291:913-923.
Grajchen E, Wouters E, van de Haterd B, Haidar M, Hardonnière K, Dierckx T, Van Broeckhoven J, Erens C, Hendrix S, Kerdine-Römer S, Hendriks JJA, Bogie JFJ (2020) CD36-mediated uptake of myelin debris by macrophages and microglia reduces neuroinflammation. J Neuroinflammation 17:224.
Granzotto A, Canzoniero LMT, Sensi SL (2020) A Neurotoxic *Ménage-à-trois:* Glutamate, Calcium, and Zinc in the Excitotoxic Cascade. Front Mol Neurosci 13:600089.

Greenberg ML, Weinger JG, Matheu MP, Carbajal KS, Parker I, Macklin WB, Lane TE, Cahalan MD (2014) Two-photon imaging of remyelination of spinal cord axons by engrafted neural precursor cells in a viral model of multiple sclerosis. Proc Natl Acad Sci U S A 111:E2349-2355.

Greenhalgh AD, Zarruk JG, Healy LM, Baskar Jesudasan SJ, Jhelum P, Salmon CK, Formanek A, Russo MV, Antel JP, McGavern DB, McColl BW, David S (2018) Peripherally derived macrophages modulate microglial function to reduce inflammation after CNS injury. PLoS Biol 16:e2005264.

Gregson NA (1989) Lysolipids and membrane damage: lysolecithin and its interaction with myelin. Biochem Soc Trans 17:280-283.

Gregson NA, Hall SM (1973) A quantitative analysis of the effects of the intraneural injection of lysophosphatidyl choline. J Cell Sci 13:257-277.

Griffiths IR, Schneider A, Anderson J, Nave KA (1995) Transgenic and natural mouse models of proteolipid protein (PLP)-related dysmyelination and demyelination. Brain Pathol 5:275-281.

Gu WL, Fu SL, Wang YX, Li Y, Wang XF, Xu XM, Lu PH (2007) Expression and regulation of versican in neural precursor cells and their lineages. Acta Pharmacol Sin 28:1519-1530.

Gude DR, Alvarez SE, Paugh SW, Mitra P, Yu J, Griffiths R, Barbour SE, Milstien S, Spiegel S (2008) Apoptosis induces expression of sphingosine kinase 1 to release sphingosine-1-phosphate as a "come-and-get-me" signal. FASEB J 22:2629-2638.

Gudi V, Moharregh-Khiabani D, Skripuletz T, Koutsoudaki PN, Kotsiari A, Skuljec J, Trebst C, Stangel M (2009) Regional differences between grey and white matter in cuprizone induced demyelination. Brain Res 1283:127-138.

Gulbranson DR, Crisman L, Lee M, Ouyang Y, Menasche BL, Demmitt BA, Wan C, Nomura T, Ye Y, Yu H, Shen J (2019) AAGAB Controls AP2 Adaptor Assembly in Clathrin-Mediated Endocytosis. Dev Cell 50:436-446.e435.

Guo S, Wang Y, Wang A (2020) Identity and lineage fate of proteolipid protein 1 gene (Plp1)-expressing cells in the embryonic murine spinal cord. Dev Dyn 249:946-960.

Guo S, Wang H, Yin Y (2022) Microglia Polarization From M1 to M2 in Neurodegenerative Diseases. Front Aging Neurosci 14:815347.

Guttenplan KA, Stafford BK, El-Danaf RN, Adler DI, Münch AE, Weigel MK, Huberman AD, Liddelow SA (2020) Neurotoxic Reactive Astrocytes Drive Neuronal Death after Retinal Injury. Cell Rep 31:107776.

Guérit S, Fidan E, Macas J, Czupalla CJ, Figueiredo R, Vijikumar A, Yalcin BH, Thom S, Winter P, Gerhardt H, Devraj K, Liebner S (2021) Astrocyte-derived Wnt growth factors are required for endothelial blood-brain barrier maintenance. Prog Neurobiol 199:101937.

Gómez-Nicola D, Fransen NL, Suzzi S, Perry VH (2013) Regulation of microglial proliferation during chronic neurodegeneration. J Neurosci 33:2481-2493.

Hagan N, Kane JL, Grover D, Woodworth L, Madore C, Saleh J, Sancho J, Liu J, Li Y, Proto J, Zelic M, Mahan A, Kothe M, Scholte AA, Fitzgerald M, Gisevius B, Haghikia A, Butovsky O, Ofengeim D (2020) CSF1R signaling is a regulator of pathogenesis in progressive MS. Cell Death Dis 11:904.

Haghayegh Jahromi N, Tardent H, Enzmann G, Deutsch U, Kawakami N, Bittner S, Vestweber D, Zipp F, Stein JV, Engelhardt B (2017) A Novel Cervical Spinal Cord Window Preparation Allows for Two-Photon Imaging of T-Cell Interactions with the Cervical Spinal Cord Microvasculature during Experimental Autoimmune Encephalomyelitis. Front Immunol 8:406.

Haimon Z, Volaski A, Orthgiess J, Boura-Halfon S, Varol D, Shemer A, Yona S, Zuckerman B, David E, Chappell-Maor L, Bechmann I, Gericke M, Ulitsky I, Jung S (2018a) Re-evaluating microglia expression profiles using RiboTag and cell isolation strategies. Nature Immunology 19:636-644.

Haimon Z, Volaski A, Orthgiess J, Boura-Halfon S, Varol D, Shemer A, Yona S, Zuckerman B, David E, Chappell-Maor L, Bechmann I, Gericke M, Ulitsky I, Jung S (2018b) Re-evaluating microglia expression profiles using RiboTag and cell isolation strategies. Nat Immunol 19:636-644.

Haindl MT, Köck U, Zeitelhofer-Adzemovic M, Fazekas F, Hochmeister S (2019) The formation of a glial scar does not prohibit remyelination in an animal model of multiple sclerosis. Glia 67:467-481.
Hall SM (1972) The effect of injections of lysophosphatidyl choline into white matter of the adult mouse spinal cord. J Cell Sci 10:535-546.
Hamilton DL, Abremski K (1984) Site-specific recombination by the bacteriophage P1 lox-Cre system. Cre-mediated synapsis of two lox sites. J Mol Biol 178:481-486.
Hamilton SP, Rome LH (1994) Stimulation of in vitro myelin synthesis by microglia. Glia 11:326-335.
Hammel G, Zivkovic S, Ayazi M, Ren Y (2022) Consequences and mechanisms of myelin debris uptake and processing by cells in the central nervous system. Cell Immunol 380:104591.
Hammond TR, McEllin B, Morton PD, Raymond M, Dupree J, Gallo V (2015) Endothelin-B Receptor Activation in Astrocytes Regulates the Rate of Oligodendrocyte Regeneration during Remyelination. Cell Rep 13:2090-2097.
Hammond TR, Dufort C, Dissing-Olesen L, Giera S, Young A, Wysoker A, Walker AJ, Gergits F, Segel M, Nemesh J, Marsh SE, Saunders A, Macosko E, Ginhoux F, Chen J, Franklin RJM, Piao X, McCarroll SA, Stevens B (2019) Single-Cell RNA Sequencing of Microglia throughout the Mouse Lifespan and in the Injured Brain Reveals Complex Cell-State Changes. Immunity 50:253-271.e256.
Han J, Harris RA, Zhang XM (2017) An updated assessment of microglia depletion: current concepts and future directions. Mol Brain 10:25.
Hao J, Liu R, Piao W, Zhou Q, Vollmer TL, Campagnolo DI, Xiang R, La Cava A, Van Kaer L, Shi FD (2010) Central nervous system (CNS)-resident natural killer cells suppress Th17 responses and CNS autoimmune pathology. J Exp Med 207:1907-1921.
Hariani HN, Ghosh AK, Rosen SM, Tso HY, Kessinger C, Zhang C, Jones WK, Sappington RM, Mitchell CH, Stubbs EB, Rao VR, Kaja S (2024) Lysyl oxidase like-1 deficiency in optic nerve head astrocytes elicits reactive astrocytosis and alters functional effects of astrocyte derived exosomes. Exp Eye Res 240:109813.
Harrington LE, Hatton RD, Mangan PR, Turner H, Murphy TL, Murphy KM, Weaver CT (2005) Interleukin 17-producing CD4+ effector T cells develop via a lineage distinct from the T helper type 1 and 2 lineages. Nat Immunol 6:1123-1132.
Hattori T, Cherepanov SM, Sakaga R, Roboon J, Nguyen DT, Ishii H, Takarada-Iemata M, Nishiuchi T, Kannon T, Hosomichi K, Tajima A, Yamamoto Y, Okamoto H, Sugawara A, Higashida H, Hori O (2023) Postnatal expression of CD38 in astrocytes regulates synapse formation and adult social memory. EMBO J 42:e111247.
Hayakawa K, Esposito E, Wang X, Terasaki Y, Liu Y, Xing C, Ji X, Lo EH (2016) Transfer of mitochondria from astrocytes to neurons after stroke. Nature 535:551-555.
He M, Dong H, Huang Y, Lu S, Zhang S, Qian Y, Jin W (2016) Astrocyte-Derived CCL2 is Associated with M1 Activation and Recruitment of Cultured Microglial Cells. Cell Physiol Biochem 38:859-870.
Hemmerich M, Malorny N, Lewen A, Hollnagel JO, Chausse B, Kann O (2022) Priming of microglia by type II interferon is lasting and resistant to modulation by interleukin-10 in situ. J Neuroimmunol 368:577881.
Hesp ZC, Goldstein EZ, Goldstein EA, Miranda CJ, Kaspar BK, McTigue DM (2015) Chronic oligodendrogenesis and remyelination after spinal cord injury in mice and rats. J Neurosci 35:1274-1290.
Heß K, Starost L, Kieran NW, Thomas C, Vincenten MCJ, Antel J, Martino G, Huitinga I, Healy L, Kuhlmann T (2020) Lesion stage-dependent causes for impaired remyelination in MS. Acta Neuropathol 140:359-375.
Hilton BJ, Bradke F (2017) Can injured adult CNS axons regenerate by recapitulating development? Development 144:3417-3429.
Hirrlinger J, Nave KA (2014) Adapting brain metabolism to myelination and long-range signal transduction. Glia 62:1749-1761.

Hirrlinger PG, Scheller A, Braun C, Hirrlinger J, Kirchhoff F (2006) Temporal control of gene recombination in astrocytes by transgenic expression of the tamoxifen-inducible DNA recombinase variant CreERT2. Glia 54:11-20.
Hirrlinger PG, Scheller A, Braun C, Quintela-Schneider M, Fuss B, Hirrlinger J, Kirchhoff F (2005) Expression of reef coral fluorescent proteins in the central nervous system of transgenic mice. Mol Cell Neurosci 30:291-303.
Hjæresen S, Sejbaek T, Axelsson M, Vinsløv-Jensen H, Mortensen SK, Pihl-Jensen G, Novakova L, Christensen JDR, Pedersen CB, Halle B, Poulsen FR, Lautrup Frederiksen J, Zhang M, Benedikz E, Lycke J, Illes Z, Fex Svenningsen Å (2021) The levels of the serine protease HTRA1 in cerebrospinal fluid correlate with progression and disability in multiple sclerosis. J Neurol 268:3316-3324.
Holmes S, Downs AM, Fosberry A, Hayes PD, Michalovich D, Murdoch P, Moores K, Fox J, Deen K, Pettman G, Wattam T, Lewis C (2002) Sema7A is a potent monocyte stimulator. Scand J Immunol 56:270-275.
Holt LM, Hernandez RD, Pacheco NL, Torres Ceja B, Hossain M, Olsen ML (2019) Astrocyte morphogenesis is dependent on BDNF signaling via astrocytic TrkB.T1. Elife 8.
Holthoff K, Witte OW (2000) Directed spatial potassium redistribution in rat neocortex. Glia 29:288-292.
Hou J, Zhou Y, Cai Z, Terekhova M, Swain A, Andhey PS, Guimaraes RM, Ulezko Antonova A, Qiu T, Sviben S, Strout G, Fitzpatrick JAJ, Chen Y, Gilfillan S, Kim DH, Van Dyken SJ, Artyomov MN, Colonna M (2023a) Transcriptomic atlas and interaction networks of brain cells in mouse CNS demyelination and remyelination. Cell Rep 42:112293.
Hou JY, Zhou XL, Wang XY, Liang J, Xue Q (2023b) Peroxiredoxin-6 Released by Astrocytes Contributes to Neuroapoptosis During Ischemia. Neuroscience 512:59-69.
Hsieh YC, Negri J, He A, Pearse RV, Liu L, Duong DM, Chibnik LB, Bennett DA, Seyfried NT, Young-Pearse TL (2022) Elevated ganglioside GM2 activator (GM2A) in human brain tissue reduces neurite integrity and spontaneous neuronal activity. Mol Neurodegener 17:61.
Hu X, Leak RK, Thomson AW, Yu F, Xia Y, Wechsler LR, Chen J (2018) Promises and limitations of immune cell-based therapies in neurological disorders. Nat Rev Neurol 14:559-568.
Huang DR, Wang J, Kivisakk P, Rollins BJ, Ransohoff RM (2001) Absence of monocyte chemoattractant protein 1 in mice leads to decreased local macrophage recruitment and antigen-specific T helper cell type 1 immune response in experimental autoimmune encephalomyelitis. J Exp Med 193:713-726.
Huang HT, Tzeng SF (2024) Interleukin-33 has the protective effect on oligodendrocytes against impairment induced by cuprizone intoxication. Neurochem Int 172:105645.
Huang J, Vogel G, Yu Z, Almazan G, Richard S (2011) Type II arginine methyltransferase PRMT5 regulates gene expression of inhibitors of differentiation/DNA binding Id2 and Id4 during glial cell differentiation. J Biol Chem 286:44424-44432.
Huang TH, Lin YS, Hsiao CW, Wang LY, Ajibola MI, Abdulmajeed WI, Lin YL, Li YJ, Chen CY, Lien CC, Chiu CD, Cheng IH (2023) Differential expression of $GABA_A$ receptor subunits δ and α6 mediates tonic inhibition in parvalbumin and somatostatin interneurons in the mouse hippocampus. Front Cell Neurosci 17:1146278.
Huang W, Zhao N, Bai X, Karram K, Trotter J, Goebbels S, Scheller A, Kirchhoff F (2014) Novel NG2-CreERT2 knock-in mice demonstrate heterogeneous differentiation potential of NG2 glia during development. Glia 62:896-913.
Huang YS, Cheng SN, Chueh SH, Tsai YL, Liou NH, Guo YW, Liao MH, Shen LH, Chen CC, Liu JC, Ma KH (2009) Effects of interleukin-15 on neuronal differentiation of neural stem cells. Brain Res 1304:38-48.
Hösli L, Zuend M, Bredell G, Zanker HS, Porto de Oliveira CE, Saab AS, Weber B (2022) Direct vascular contact is a hallmark of cerebral astrocytes. Cell Rep 39:110599.
Ikeda O, Murakami M, Ino H, Yamazaki M, Nemoto T, Koda M, Nakayama C, Moriya H (2001) Acute up-regulation of brain-derived neurotrophic factor expression resulting from experimentally induced injury in the rat spinal cord. Acta Neuropathol 102:239-245.
Ishibashi T, Dakin KA, Stevens B, Lee PR, Kozlov SV, Stewart CL, Fields RD (2006) Astrocytes promote myelination in response to electrical impulses. Neuron 49:823-832.

Istiaq A, Umemoto T, Ito N, Suda T, Shimamura K, Ohta K (2022) Tsukushi proteoglycan maintains RNA splicing and developmental signaling network in GFAP-expressing subventricular zone neural stem/progenitor cells. Front Cell Dev Biol 10:994588.
Ito K, Sanosaka T, Igarashi K, Ideta-Otsuka M, Aizawa A, Uosaki Y, Noguchi A, Arakawa H, Nakashima K, Takizawa T (2016) Identification of genes associated with the astrocyte-specific gene Gfap during astrocyte differentiation. Sci Rep 6:23903.
Ito M, Muramatsu R, Kato Y, Sharma B, Uyeda A, Tanabe S, Fujimura H, Kidoya H, Takakura N, Kawahara Y, Takao M, Mochizuki H, Fukamizu A, Yamashita T (2021) Age-dependent decline in remyelination capacity is mediated by apelin-APJ signaling. Nat Aging 1:284-294.
Itoh N, Itoh Y, Tassoni A, Ren E, Kaito M, Ohno A, Ao Y, Farkhondeh V, Johnsonbaugh H, Burda J, Sofroniew MV, Voskuhl RR (2018) Cell-specific and region-specific transcriptomics in the multiple sclerosis model: Focus on astrocytes. Proc Natl Acad Sci U S A 115:E302-E309.
Jahn HM, Kasakow CV, Helfer A, Michely J, Verkhratsky A, Maurer HH, Scheller A, Kirchhoff F (2018) Refined protocols of tamoxifen injection for inducible DNA recombination in mouse astroglia. Sci Rep 8:5913.
Jahn O, Tenzer S, Werner HB (2009) Myelin proteomics: molecular anatomy of an insulating sheath. Mol Neurobiol 40:55-72.
Jang M, Gould E, Xu J, Kim EJ, Kim JH (2019) Oligodendrocytes regulate presynaptic properties and neurotransmission through BDNF signaling in the mouse brainstem. Elife 8.
Jarjour AA, Zhang H, Bauer N, Ffrench-Constant C, Williams A (2012) In vitro modeling of central nervous system myelination and remyelination. Glia 60:1-12.
Jarousse N, Syan S, Martinat C, Brahic M (1998) The neurovirulence of the DA and GDVII strains of Theiler's virus correlates with their ability To infect cultured neurons. J Virol 72:7213-7220.
Jha MK, Morrison BM (2020) Lactate Transporters Mediate Glia-Neuron Metabolic Crosstalk in Homeostasis and Disease. Front Cell Neurosci 14:589582.
Ji-Wei S, Zi-Ying L, Xiang T, Yang Y, Ju-Fen Z, Qing-Hua Z (2022) CNTF induces Clcf1 in astrocytes to promote the differentiation of oligodendrocyte precursor cells. Biochem Biophys Res Commun 636:170-177.
Jia J, Zheng L, Ye L, Chen J, Shu S, Xu S, Bao X, Xia S, Liu R, Xu Y, Zhang M (2023) $CD11c^{+}$ microglia promote white matter repair after ischemic stroke. Cell Death Dis 14:156.
Jin L, Zhang J, Hua X, Xu X, Li J, Wang J, Wang M, Liu H, Qiu H, Chen M, Zhang X, Wang Y, Huang Z (2024) Correction: Astrocytic SARM1 promotes neuroinflammation and axonal demyelination in experimental autoimmune encephalomyelitis through inhibiting GDNF signaling. Cell Death Dis 15:214.
Jourdain P, Rothenfusser K, Ben-Adiba C, Allaman I, Marquet P, Magistretti PJ (2018) Dual action of L-Lactate on the activity of NR2B-containing NMDA receptors: from potentiation to neuroprotection. Sci Rep 8:13472.
Jovanovic DV, Di Battista JA, Martel-Pelletier J, Jolicoeur FC, He Y, Zhang M, Mineau F, Pelletier JP (1998) IL-17 stimulates the production and expression of proinflammatory cytokines, IL-beta and TNF-alpha, by human macrophages. J Immunol 160:3513-3521.
Jung S, Aliberti J, Graemmel P, Sunshine MJ, Kreutzberg GW, Sher A, Littman DR (2000) Analysis of fractalkine receptor CX(3)CR1 function by targeted deletion and green fluorescent protein reporter gene insertion. Mol Cell Biol 20:4106-4114.
Jurga AM, Paleczna M, Kuter KZ (2020) Overview of General and Discriminating Markers of Differential Microglia Phenotypes. Front Cell Neurosci 14:198.
Jäkel S, Agirre E, Mendanha Falcão A, van Bruggen D, Lee KW, Knuesel I, Malhotra D, Ffrench-Constant C, Williams A, Castelo-Branco G (2019) Altered human oligodendrocyte heterogeneity in multiple sclerosis. Nature 566:543-547.
Kabba JA, Xu Y, Christian H, Ruan W, Chenai K, Xiang Y, Zhang L, Saavedra JM, Pang T (2018) Microglia: Housekeeper of the Central Nervous System. Cell Mol Neurobiol 38:53-71.
Kang K, Lee SW, Han JE, Choi JW, Song MR (2014) The complex morphology of reactive astrocytes controlled by fibroblast growth factor signaling. Glia 62:1328-1344.
Kang Z, Altuntas CZ, Gulen MF, Liu C, Giltiay N, Qin H, Liu L, Qian W, Ransohoff RM, Bergmann C, Stohlman S, Tuohy VK, Li X (2010) Astrocyte-restricted ablation of interleukin-17-

induced Act1-mediated signaling ameliorates autoimmune encephalomyelitis. Immunity 32:414-425.
Kann O (2023) Lactate as a supplemental fuel for synaptic transmission and neuronal network oscillations: Potentials and limitations. J Neurochem.
Katdare KA, Kjar A, O'Brown NM, Neal EH, Sorets AG, Shostak A, Romero-Fernandez W, Kwiatkowski AJ, Mlouk K, Kim H, Cowell RP, Schwensen KR, Horner KB, Wilson JT, Schrag MS, Megason SG, Lippmann ES (2024) IQGAP2 regulates blood-brain barrier immune dynamics. bioRxiv.
Kato D, Eto K, Nabekura J, Wake H (2018) Activity-dependent functions of non-electrical glial cells. J Biochem 163:457-464.
Kaur C, Rathnasamy G, Ling EA (2013) Roles of activated microglia in hypoxia induced neuroinflammation in the developing brain and the retina. J Neuroimmune Pharmacol 8:66-78.
Kawai T, Akira S (2007) Signaling to NF-kappaB by Toll-like receptors. Trends Mol Med 13:460-469.
Kelić S, Levy S, Suarez C, Weinstein DE (2001) CD81 regulates neuron-induced astrocyte cell-cycle exit. Mol Cell Neurosci 17:551-560.
Keough MB, Jensen SK, Yong VW (2015) Experimental demyelination and remyelination of murine spinal cord by focal injection of lysolecithin. J Vis Exp.
Kessaris N, Fogarty M, Iannarelli P, Grist M, Wegner M, Richardson WD (2006) Competing waves of oligodendrocytes in the forebrain and postnatal elimination of an embryonic lineage. Nat Neurosci 9:173-179.
Kettenmann H, Hanisch UK, Noda M, Verkhratsky A (2011) Physiology of microglia. Physiol Rev 91:461-553.
Khakh BS, Deneen B (2019) The Emerging Nature of Astrocyte Diversity. Annu Rev Neurosci 42:187-207.
Khan J, Salhotra S, Goswami P, Akhter J, Jahan S, Gupta S, Sharma S, Banerjee BD, Parvez S, Raisuddin S (2019) Bisphenol A triggers axonal injury and myelin degeneration with concomitant neurobehavioral toxicity in C57BL/6J male mice. Toxicology 428:152299.
Khaw YM, Cunningham C, Tierney A, Sivaguru M, Inoue M (2020) Neutrophil-selective deletion of Cxcr2 protects against CNS neurodegeneration in a mouse model of multiple sclerosis. J Neuroinflammation 17:49.
Kieseier BC, Hartung HP (2003) Current disease-modifying therapies in multiple sclerosis. Semin Neurol 23:133-146.
Kieseier BC, Seifert T, Giovannoni G, Hartung HP (1999) Matrix metalloproteinases in inflammatory demyelination: targets for treatment. Neurology 53:20-25.
Kigerl KA, Gensel JC, Ankeny DP, Alexander JK, Donnelly DJ, Popovich PG (2009) Identification of two distinct macrophage subsets with divergent effects causing either neurotoxicity or regeneration in the injured mouse spinal cord. J Neurosci 29:13435-13444.
Kikuchi K, Tatebe T, Sudo Y, Yokoyama M, Kidana K, Chiu YW, Takatori S, Arita M, Hori Y, Tomita T (2021) GPR120 Signaling Controls Amyloid-β Degrading Activity of Matrix Metalloproteinases. J Neurosci 41:6173-6185.
Kim DJ, Kim SH, Lim CS, Choi KY, Park CS, Sung BH, Yeo MG, Chang S, Kim JK, Song WK (2006) Interaction of SPIN90 with the Arp2/3 complex mediates lamellipodia and actin comet tail formation. J Biol Chem 281:617-625.
Kim RY, Hoffman AS, Itoh N, Ao Y, Spence R, Sofroniew MV, Voskuhl RR (2014) Astrocyte CCL2 sustains immune cell infiltration in chronic experimental autoimmune encephalomyelitis. J Neuroimmunol 274:53-61.
Kim W, Cho SB, Jung HY, Yoo DY, Oh JK, Choi GM, Cho TG, Kim DW, Hwang IK, Choi SY, Moon SM (2019) Phosphatidylethanolamine-Binding Protein 1 Ameliorates Ischemia-Induced Inflammation and Neuronal Damage in the Rabbit Spinal Cord. Cells 8.
Kimura I, Dohgu S, Takata F, Matsumoto J, Watanabe T, Iwao T, Yamauchi A, Kataoka Y (2020) Oligodendrocytes upregulate blood-brain barrier function through mechanisms other than the PDGF-BB/PDGFRα pathway in the barrier-tightening effect of oligodendrocyte progenitor cells. Neurosci Lett 715:134594.

Kiryu-Seo S, Ohno N, Kidd GJ, Komuro H, Trapp BD (2010) Demyelination increases axonal stationary mitochondrial size and the speed of axonal mitochondrial transport. J Neurosci 30:6658-6666.
Klistorner A, Klistorner S, You Y, Graham SL, Yiannikas C, Parratt J, Barnett M (2022) Long-term Effect of Permanent Demyelination on Axonal Survival in Multiple Sclerosis. Neurol Neuroimmunol Neuroinflamm 9.
Kolos EA, Korzhevskii DE (2020) Spinal Cord Microglia in Health and Disease. Acta Naturae 12:4-17.
Komiyama Y, Nakae S, Matsuki T, Nambu A, Ishigame H, Kakuta S, Sudo K, Iwakura Y (2006) IL-17 plays an important role in the development of experimental autoimmune encephalomyelitis. J Immunol 177:566-573.
Kondo T, Raff M (2000) Oligodendrocyte precursor cells reprogrammed to become multipotential CNS stem cells. Science 289:1754-1757.
Kong M, Muñoz N, Valdivia A, Alvarez A, Herrera-Molina R, Cárdenas A, Schneider P, Burridge K, Quest AF, Leyton L (2013) Thy-1-mediated cell-cell contact induces astrocyte migration through the engagement of αVβ3 integrin and syndecan-4. Biochim Biophys Acta 1833:1409-1420.
Konishi H, Kobayashi M, Kunisawa T, Imai K, Sayo A, Malissen B, Crocker PR, Sato K, Kiyama H (2017) Siglec-H is a microglia-specific marker that discriminates microglia from CNS-associated macrophages and CNS-infiltrating monocytes. Glia 65:1927-1943.
Konishi H, Okamoto T, Hara Y, Komine O, Tamada H, Maeda M, Osako F, Kobayashi M, Nishiyama A, Kataoka Y, Takai T, Udagawa N, Jung S, Ozato K, Tamura T, Tsuda M, Yamanaka K, Ogi T, Sato K, Kiyama H (2020) Astrocytic phagocytosis is a compensatory mechanism for microglial dysfunction. EMBO J 39:e104464.
Kopper TJ, Gensel JC (2018) Myelin as an inflammatory mediator: Myelin interactions with complement, macrophages, and microglia in spinal cord injury. J Neurosci Res 96:969-977.
Kostic M, Zivkovic N, Stojanovic I (2013) Multiple sclerosis and glutamate excitotoxicity. Rev Neurosci 24:71-88.
Kotter MR, Li WW, Zhao C, Franklin RJ (2006) Myelin impairs CNS remyelination by inhibiting oligodendrocyte precursor cell differentiation. J Neurosci 26:328-332.
Koutsoudaki PN, Skripuletz T, Gudi V, Moharregh-Khiabani D, Hildebrandt H, Trebst C, Stangel M (2009) Demyelination of the hippocampus is prominent in the cuprizone model. Neurosci Lett 451:83-88.
Krasemann S et al. (2017) The TREM2-APOE Pathway Drives the Transcriptional Phenotype of Dysfunctional Microglia in Neurodegenerative Diseases. Immunity 47:566-581.e569.
Krasnow AM, Ford MC, Valdivia LE, Wilson SW, Attwell D (2018) Regulation of developing myelin sheath elongation by oligodendrocyte calcium transients in vivo. Nat Neurosci 21:24-28.
Krumbholz M, Theil D, Derfuss T, Rosenwald A, Schrader F, Monoranu CM, Kalled SL, Hess DM, Serafini B, Aloisi F, Wekerle H, Hohlfeld R, Meinl E (2005) BAFF is produced by astrocytes and up-regulated in multiple sclerosis lesions and primary central nervous system lymphoma. J Exp Med 201:195-200.
Kucukdereli H, Allen NJ, Lee AT, Feng A, Ozlu MI, Conatser LM, Chakraborty C, Workman G, Weaver M, Sage EH, Barres BA, Eroglu C (2011) Control of excitatory CNS synaptogenesis by astrocyte-secreted proteins Hevin and SPARC. Proc Natl Acad Sci U S A 108:E440-449.
Kukurba KR, Montgomery SB (2015) RNA Sequencing and Analysis. Cold Spring Harb Protoc 2015:951-969.
Kuroda M, Muramatsu R, Maedera N, Koyama Y, Hamaguchi M, Fujimura H, Yoshida M, Konishi M, Itoh N, Mochizuki H, Yamashita T (2017) Peripherally derived FGF21 promotes remyelination in the central nervous system. J Clin Invest 127:3496-3509.
Kuypers NJ, James KT, Enzmann GU, Magnuson DS, Whittemore SR (2013) Functional consequences of ethidium bromide demyelination of the mouse ventral spinal cord. Exp Neurol 247:615-622.

Lalive PH, Paglinawan R, Biollaz G, Kappos EA, Leone DP, Malipiero U, Relvas JB, Moransard M, Suter T, Fontana A (2005) TGF-beta-treated microglia induce oligodendrocyte precursor cell chemotaxis through the HGF-c-Met pathway. Eur J Immunol 35:727-737.
Lamers F, van der Ploeg I, Schild L, Ebus ME, Koster J, Hansen BR, Koch T, Versteeg R, Caron HN, Molenaar JJ (2011) Knockdown of survivin (BIRC5) causes apoptosis in neuroblastoma via mitotic catastrophe. Endocr Relat Cancer 18:657-668.
Lampert PW (1978) Autoimmune and virus-induced demyelinating diseases. A review. Am J Pathol 91:176-208.
Lampert PW, Sims JK, Kniazeff AJ (1973) Mechanism of demyelination in JHM virus encephalomyelitis. Electron microscopic studies. Acta Neuropathol 24:76-85.
Lampron A, Larochelle A, Laflamme N, Préfontaine P, Plante MM, Sánchez MG, Yong VW, Stys PK, Tremblay M, Rivest S (2015) Inefficient clearance of myelin debris by microglia impairs remyelinating processes. J Exp Med 212:481-495.
Langley MR, Choi CI, Peclat TR, Guo Y, Simon WL, Yoon H, Kleppe L, Lucchinetti CF, Chini CCS, Chini EN, Scarisbrick IA (2021) Critical Role of Astrocyte NAD(+) Glycohydrolase in Myelin Injury and Regeneration. J Neurosci 41:8644-8667.
Lanz TV et al. (2022) Clonally expanded B cells in multiple sclerosis bind EBV EBNA1 and GlialCAM. Nature 603:321-327.
Larochelle C, Alvarez JI, Prat A (2011) How do immune cells overcome the blood-brain barrier in multiple sclerosis? FEBS Lett 585:3770-3780.
Larson VA, Mironova Y, Vanderpool KG, Waisman A, Rash JE, Agarwal A, Bergles DE (2018) Oligodendrocytes control potassium accumulation in white matter and seizure susceptibility. Elife 7.
Lassmann H, Bartsch U, Montag D, Schachner M (1997) Dying-back oligodendrogliopathy: a late sequel of myelin-associated glycoprotein deficiency. Glia 19:104-110.
Lau LW, Keough MB, Haylock-Jacobs S, Cua R, Döring A, Sloka S, Stirling DP, Rivest S, Yong VW (2012) Chondroitin sulfate proteoglycans in demyelinated lesions impair remyelination. Ann Neurol 72:419-432.
Lazibat I, Rubinić Majdak M, Županić S (2018) Multiple Sclerosis: New Aspects of Immunopathogenesis. Acta Clin Croat 57:352-361.
LeComte MD, Shimada IS, Sherwin C, Spees JL (2015) Notch1-STAT3-ETBR signaling axis controls reactive astrocyte proliferation after brain injury. Proc Natl Acad Sci U S A 112:8726-8731.
Lee SH, Jin WP, Seo NR, Pang KM, Kim B, Kim SM, Lee JH (2017) Recombinant human fibroblast growth factor-2 promotes nerve regeneration and functional recovery after mental nerve crush injury. Neural Regen Res 12:629-636.
Lee Y, Morrison BM, Li Y, Lengacher S, Farah MH, Hoffman PN, Liu Y, Tsingalia A, Jin L, Zhang PW, Pellerin L, Magistretti PJ, Rothstein JD (2012) Oligodendroglia metabolically support axons and contribute to neurodegeneration. Nature 487:443-448.
Lewis ND, Hill JD, Juchem KW, Stefanopoulos DE, Modis LK (2014) RNA sequencing of microglia and monocyte-derived macrophages from mice with experimental autoimmune encephalomyelitis illustrates a changing phenotype with disease course. J Neuroimmunol 277:26-38.
Li J, Miramontes TG, Czopka T, Monk KR (2024a) Synaptic input and Ca 2+ activity in zebrafish oligodendrocyte precursor cells contribute to myelin sheath formation. Nat Neurosci 27:219-231.
Li J, Khankan RR, Caneda C, Godoy MI, Haney MS, Krawczyk MC, Bassik MC, Sloan SA, Zhang Y (2019) Astrocyte-to-astrocyte contact and a positive feedback loop of growth factor signaling regulate astrocyte maturation. Glia 67:1571-1597.
Li Q, Liu S, Zheng T, Li M, Qi B, Zhou L, Liu B, Ma D, Zhao C, Chen Z (2024b) Grafted human-induced pluripotent stem cells-derived oligodendrocyte progenitor cells combined with human umbilical vein endothelial cells contribute to functional recovery following spinal cord injury. Stem Cell Res Ther 15:35.
Li S, Li Y, Yi R, Liu L, Qu J (2020a) Coherent Anti-Stokes Raman Scattering Microscopy and Its Applications. Frontiers in Physics 8.

Li T, Niu J, Yu G, Ezan P, Yi C, Wang X, Koulakoff A, Gao X, Chen X, Sáez JC, Giaume C, Xiao L (2020b) Connexin 43 deletion in astrocytes promotes CNS remyelination by modulating local inflammation. Glia 68:1201-1212.
Li W, Maeda Y, Ming X, Cook S, Chapin J, Husar W, Dowling P (2002) Apoptotic death following Fas activation in human oligodendrocyte hybrid cultures. J Neurosci Res 69:189-196.
Li W, Berlinicke C, Huang Y, Giera S, McGrath AG, Fang W, Chen C, Takaesu F, Chang X, Duan Y, Kumar D, Chang C, Mao HQ, Sheng G, Dodge JC, Ji H, Madden S, Zack DJ, Chamling X (2023a) High-throughput screening for myelination promoting compounds using human stem cell-derived oligodendrocyte progenitor cells. iScience 26:106156.
Li Y, Zhang R, Hou X, Zhang Y, Ding F, Li F, Yao Y, Wang Y (2017) Microglia activation triggers oligodendrocyte precursor cells apoptosis via HSP60. Mol Med Rep 16:603-608.
Li Y, Xie Y, Liu R, Wang Z, Chen P, Wang M, Yu Z, Wang W, Luo X (2023b) Knockout of microglial Hv1 proton channel reduces neurotoxic A1 astrocytes and neuronal damage via the ROS/STAT3 pathway after spinal cord injury. Glia 71:2418-2436.
Liang P, Zhang X, Zhang Y, Wu Y, Song Y, Wang X, Chen T, Liu W, Peng B, Yin J, He F, Fan Y, Han S, He X (2023) Neurotoxic A1 astrocytes promote neuronal ferroptosis via CXCL10/CXCR3 axis in epilepsy. Free Radic Biol Med 195:329-342.
Liang Z, Wang X, Hao Y, Qiu L, Lou Y, Zhang Y, Ma D, Feng J (2020) The Multifaceted Role of Astrocyte Connexin 43 in Ischemic Stroke Through Forming Hemichannels and Gap Junctions. Front Neurol 11:703.
Libbey JE, Fujinami RS (2021) Viral mouse models used to study multiple sclerosis: past and present. Arch Virol 166:1015-1033.
Liddelow SA, Barres BA (2017) Reactive Astrocytes: Production, Function, and Therapeutic Potential. Immunity 46:957-967.
Lim JH, Kang HM, Kim DH, Jeong B, Lee DY, Lee JR, Baek JY, Cho HS, Son MY, Kim DS, Kim NS, Jung CR (2024) ARL6IP1 gene delivery reduces neuroinflammation and neurodegenerative pathology in hereditary spastic paraplegia model. J Exp Med 221.
Lin L, Basu R, Chatterjee D, Templin AT, Flak JN, Johnson TS (2023) Disease-associated astrocytes and microglia markers are upregulated in mice fed high fat diet. Sci Rep 13:12919.
Lin W, Lin Y (2010) Interferon-γ inhibits central nervous system myelination through both STAT1-dependent and STAT1-independent pathways. J Neurosci Res 88:2569-2577.
Lin W, Harding HP, Ron D, Popko B (2005) Endoplasmic reticulum stress modulates the response of myelinating oligodendrocytes to the immune cytokine interferon-gamma. J Cell Biol 169:603-612.
Lindner M, Thümmler K, Arthur A, Brunner S, Elliott C, McElroy D, Mohan H, Williams A, Edgar JM, Schuh C, Stadelmann C, Barnett SC, Lassmann H, Mücklisch S, Mudaliar M, Schaeren-Wiemers N, Meinl E, Linington C (2015) Fibroblast growth factor signalling in multiple sclerosis: inhibition of myelination and induction of pro-inflammatory environment by FGF9. Brain 138:1875-1893.
Lindquist RL, Shakhar G, Dudziak D, Wardemann H, Eisenreich T, Dustin ML, Nussenzweig MC (2004) Visualizing dendritic cell networks in vivo. Nat Immunol 5:1243-1250.
Linnerbauer M, Wheeler MA, Quintana FJ (2020) Astrocyte Crosstalk in CNS Inflammation. Neuron 108:608-622.
Liu D, Liu Y, Xia Z, Dong H, Yi Z (2017) Reactive oxygen species modulator 1 regulates oxidative stress and induces renal and pulmonary fibrosis in a unilateral ureteral obstruction rat model and in HK-2 cells. Mol Med Rep 16:4855-4862.
Liu H, Leak RK, Hu X (2016) Neurotransmitter receptors on microglia. Stroke Vasc Neurol 1:52-58.
Liu J, Magri L, Zhang F, Marsh NO, Albrecht S, Huynh JL, Kaur J, Kuhlmann T, Zhang W, Slesinger PA, Casaccia P (2015) Chromatin landscape defined by repressive histone methylation during oligodendrocyte differentiation. J Neurosci 35:352-365.
Liu K, Aierken A, Liu M, Parhat N, Kong W, Yin X, Liu G, Yu D, Hong J, Ni J, Quan Z, Liu X, Ji S, Mao J, Peng W, Chen C, Yan Y, Qing H (2024a) The decreased astrocyte-microglia interaction reflects the early characteristics of Alzheimer's disease. iScience 27:109281.

Liu L, Belkadi A, Darnall L, Hu T, Drescher C, Cotleur AC, Padovani-Claudio D, He T, Choi K, Lane TE, Miller RH, Ransohoff RM (2010) CXCR2-positive neutrophils are essential for cuprizone-induced demyelination: relevance to multiple sclerosis. Nat Neurosci 13:319-326.
Liu LR, Liu JC, Bao JS, Bai QQ, Wang GQ (2020) Interaction of Microglia and Astrocytes in the Neurovascular Unit. Front Immunol 11:1024.
Liu N, Jiang Y, Chung JY, Li Y, Yu Z, Kim JW, Lok JM, Whalen MJ, Wang X (2019) Annexin A2 Deficiency Exacerbates Neuroinflammation and Long-Term Neurological Deficits after Traumatic Brain Injury in Mice. Int J Mol Sci 20.
Liu Q, Zhou S, Wang X, Gu C, Guo Q, Li X, Zhang C, Zhang N, Zhang L, Huang F (2022) Apelin alleviated neuroinflammation and promoted endogenous neural stem cell proliferation and differentiation after spinal cord injury in rats. J Neuroinflammation 19:160.
Liu SS, Jiang TX, Bu F, Zhao JL, Wang GF, Yang GH, Kong JY, Qie YF, Wen P, Fan LB, Li NN, Gao N, Qiu XB (2024b) Molecular mechanisms underlying the BIRC6-mediated regulation of apoptosis and autophagy. Nat Commun 15:891.
Lloyd AF, Davies CL, Holloway RK, Labrak Y, Ireland G, Carradori D, Dillenburg A, Borger E, Soong D, Richardson JC, Kuhlmann T, Williams A, Pollard JW, des Rieux A, Priller J, Miron VE (2019) Central nervous system regeneration is driven by microglia necroptosis and repopulation. Nat Neurosci 22:1046-1052.
Lloyd-Burton SM, York EM, Anwar MA, Vincent AJ, Roskams AJ (2013) SPARC regulates microgliosis and functional recovery following cortical ischemia. J Neurosci 33:4468-4481.
Lo CH, Skarica M, Mansoor M, Bhandarkar S, Toro S, Pitt D (2021) Astrocyte Heterogeneity in Multiple Sclerosis: Current Understanding and Technical Challenges. Front Cell Neurosci 15:726479.
Locatelli G, Theodorou D, Kendirli A, Jordão MJC, Staszewski O, Phulphagar K, Cantuti-Castelvetri L, Dagkalis A, Bessis A, Simons M, Meissner F, Prinz M, Kerschensteiner M (2018) Mononuclear phagocytes locally specify and adapt their phenotype in a multiple sclerosis model. Nat Neurosci 21:1196-1208.
Lopez JA, Denkova M, Ramanathan S, Dale RC, Brilot F (2021) Pathogenesis of autoimmune demyelination: from multiple sclerosis to neuromyelitis optica spectrum disorders and myelin oligodendrocyte glycoprotein antibody-associated disease. Clin Transl Immunology 10:e1316.
Louie AY, Kim JS, Drnevich J, Dibaeinia P, Koito H, Sinha S, McKim DB, Soto-Diaz K, Nowak RA, Das A, Steelman AJ (2023) Influenza A virus infection disrupts oligodendrocyte homeostasis and alters the myelin lipidome in the adult mouse. J Neuroinflammation 20:190.
Loving BA, Bruce KD (2020) Lipid and Lipoprotein Metabolism in Microglia. Front Physiol 11:393.
Ludwin SK (1980) Chronic demyelination inhibits remyelination in the central nervous system. An analysis of contributing factors. Lab Invest 43:382-387.
Lundgaard I, Osório MJ, Kress BT, Sanggaard S, Nedergaard M (2014) White matter astrocytes in health and disease. Neuroscience 276:161-173.
Lysko DE, Talbot WS (2022) Unmyelinated sensory neurons use Neuregulin signals to promote myelination of interneurons in the CNS. Cell Rep 41:111669.
Ma KH, Svaren J (2018) Epigenetic Control of Schwann Cells. Neuroscientist 24:627-638.
Ma NX, Yin JC, Chen G (2019) Transcriptome Analysis of Small Molecule-Mediated Astrocyte-to-Neuron Reprogramming. Front Cell Dev Biol 7:82.
MacVicar BA, Newman EA (2015) Astrocyte regulation of blood flow in the brain. Cold Spring Harb Perspect Biol 7.
Madisen L, Zwingman TA, Sunkin SM, Oh SW, Zariwala HA, Gu H, Ng LL, Palmiter RD, Hawrylycz MJ, Jones AR, Lein ES, Zeng H (2010) A robust and high-throughput Cre reporting and characterization system for the whole mouse brain. Nat Neurosci 13:133-140.
Mahmoud S, Gharagozloo M, Simard C, Gris D (2019) Astrocytes Maintain Glutamate Homeostasis in the CNS by Controlling the Balance between Glutamate Uptake and Release. Cells 8.
Malo CS, Jin F, Hansen MJ, Fryer JD, Pavelko KD, Johnson AJ (2018) MHC class I expression by microglia is required for generating a complete antigen-specific CD8 T cell response in the CNS. The Journal of Immunology 200:99.97-99.97.

Mancini M, Bassani S, Passafaro M (2020) Right Place at the Right Time: How Changes in Protocadherins Affect Synaptic Connections Contributing to the Etiology of Neurodevelopmental Disorders. Cells 9.
Mantovani A, Sica A, Sozzani S, Allavena P, Vecchi A, Locati M (2004) The chemokine system in diverse forms of macrophage activation and polarization. Trends Immunol 25:677-686.
Manu DR, Slevin M, Barcutean L, Forro T, Boghitoiu T, Balasa R (2023) Astrocyte Involvement in Blood-Brain Barrier Function: A Critical Update Highlighting Novel, Complex, Neurovascular Interactions. Int J Mol Sci 24.
Mao X, Liu J, Chen C, Zhang W, Qian R, Chen X, Lu H, Ge J, Zhao C, Zhang D, Wang Y (2016) PCBP2 Modulates Neural Apoptosis and Astrocyte Proliferation After Spinal Cord Injury. Neurochem Res 41:2401-2414.
Marchetti L, Engelhardt B (2020) Immune cell trafficking across the blood-brain barrier in the absence and presence of neuroinflammation. Vasc Biol 2:H1-H18.
Markoullis K, Sargiannidou I, Schiza N, Roncaroli F, Reynolds R, Kleopa KA (2014) Oligodendrocyte gap junction loss and disconnection from reactive astrocytes in multiple sclerosis gray matter. J Neuropathol Exp Neurol 73:865-879.
Marques RE, Guabiraba R, Russo RC, Teixeira MM (2013) Targeting CCL5 in inflammation. Expert Opin Ther Targets 17:1439-1460.
Mars LT, Saikali P, Liblau RS, Arbour N (2011) Contribution of CD8 T lymphocytes to the immuno-pathogenesis of multiple sclerosis and its animal models. Biochim Biophys Acta 1812:151-161.
Marshall NA, Vickers MA, Barker RN (2003) Regulatory T cells secreting IL-10 dominate the immune response to EBV latent membrane protein 1. J Immunol 170:6183-6189.
Marzan DE, Brügger-Verdon V, West BL, Liddelow S, Samanta J, Salzer JL (2021) Activated microglia drive demyelination via CSF1R signaling. Glia 69:1583-1604.
Matejuk A, Ransohoff RM (2020) Crosstalk Between Astrocytes and Microglia: An Overview. Front Immunol 11:1416.
Matsuzaki M, Hayama T, Kasai H, Ellis-Davies GCR (2010) Two-photon uncaging of gamma-aminobutyric acid in intact brain tissue. Nat Chem Biol 6:255-257.
Matthews AE, Weiss SR, Paterson Y (2002) Murine hepatitis virus--a model for virus-induced CNS demyelination. J Neurovirol 8:76-85.
Matute C, Alberdi E, Domercq M, Pérez-Cerdá F, Pérez-Samartín A, Sánchez-Gómez MV (2001) The link between excitotoxic oligodendroglial death and demyelinating diseases. Trends Neurosci 24:224-230.
Mauch DH, Nägler K, Schumacher S, Göritz C, Müller EC, Otto A, Pfrieger FW (2001) CNS synaptogenesis promoted by glia-derived cholesterol. Science 294:1354-1357.
Mayo L, Quintana FJ, Weiner HL (2012) The innate immune system in demyelinating disease. Immunol Rev 248:170-187.
Mayo L, Trauger SA, Blain M, Nadeau M, Patel B, Alvarez JI, Mascanfroni ID, Yeste A, Kivisäkk P, Kallas K, Ellezam B, Bakshi R, Prat A, Antel JP, Weiner HL, Quintana FJ (2014) Regulation of astrocyte activation by glycolipids drives chronic CNS inflammation. Nat Med 20:1147-1156.
McGavern DB, Murray PD, Rivera-Quiñones C, Schmelzer JD, Low PA, Rodriguez M (2000) Axonal loss results in spinal cord atrophy, electrophysiological abnormalities and neurological deficits following demyelination in a chronic inflammatory model of multiple sclerosis. Brain 123 Pt 3:519-531.
McIntyre LL, Greilach SA, Othy S, Sears-Kraxberger I, Wi B, Ayala-Angulo J, Vu E, Pham Q, Silva J, Dang K, Rezk F, Steward O, Cahalan MD, Lane TE, Walsh CM (2020) Regulatory T cells promote remyelination in the murine experimental autoimmune encephalomyelitis model of multiple sclerosis following human neural stem cell transplant. Neurobiol Dis 140:104868.
McKinnon RD, Piras G, Ida JA, Dubois-Dalcq M (1993) A role for TGF-beta in oligodendrocyte differentiation. J Cell Biol 121:1397-1407.
McMurran CE, Zhao C, Franklin RJM (2019) Toxin-Based Models to Investigate Demyelination and Remyelination. Methods Mol Biol 1936:377-396.

McMurran CE, Jones CA, Fitzgerald DC, Franklin RJ (2016) CNS Remyelination and the Innate Immune System. Front Cell Dev Biol 4:38.
McRae BL, Kennedy MK, Tan LJ, Dal Canto MC, Picha KS, Miller SD (1992) Induction of active and adoptive relapsing experimental autoimmune encephalomyelitis (EAE) using an encephalitogenic epitope of proteolipid protein. J Neuroimmunol 38:229-240.
Melamed E, Palmer JL, Fonken C (2022) Advantages and limitations of experimental autoimmune encephalomyelitis in breaking down the role of the gut microbiome in multiple sclerosis. Front Mol Neurosci 15:1019877.
Mendel I, Kerlero de Rosbo N, Ben-Nun A (1995) A myelin oligodendrocyte glycoprotein peptide induces typical chronic experimental autoimmune encephalomyelitis in H-2b mice: fine specificity and T cell receptor V beta expression of encephalitogenic T cells. Eur J Immunol 25:1951-1959.
Menten P, Wuyts A, Van Damme J (2002) Macrophage inflammatory protein-1. Cytokine Growth Factor Rev 13:455-481.
Merrill JE, Ignarro LJ, Sherman MP, Melinek J, Lane TE (1993) Microglial cell cytotoxicity of oligodendrocytes is mediated through nitric oxide. J Immunol 151:2132-2141.
Mesentier-Louro LA, Rosso P, Carito V, Mendez-Otero R, Santiago MF, Rama P, Lambiase A, Tirassa P (2019) Nerve Growth Factor Role on Retinal Ganglion Cell Survival and Axon Regrowth: Effects of Ocular Administration in Experimental Model of Optic Nerve Injury. Mol Neurobiol 56:1056-1069.
Metzger D, Chambon P (2001) Site- and time-specific gene targeting in the mouse. Methods 24:71-80.
Mezydlo A, Treiber N, Ullrich Gavilanes EM, Eichenseer K, Ancău M, Wens A, Ares Carral C, Schifferer M, Snaidero N, Misgeld T, Kerschensteiner M (2023) Remyelination by surviving oligodendrocytes is inefficient in the inflamed mammalian cortex. Neuron 111:1748-1759.e1748.
Mi S, Miller RH, Lee X, Scott ML, Shulag-Morskaya S, Shao Z, Chang J, Thill G, Levesque M, Zhang M, Hession C, Sah D, Trapp B, He Z, Jung V, McCoy JM, Pepinsky RB (2005) LINGO-1 negatively regulates myelination by oligodendrocytes. Nat Neurosci 8:745-751.
Mi Y, Qi G, Vitali F, Shang Y, Raikes AC, Wang T, Jin Y, Brinton RD, Gu H, Yin F (2023) Loss of fatty acid degradation by astrocytic mitochondria triggers neuroinflammation and neurodegeneration. Nat Metab 5:445-465.
Middeldorp J, Hol EM (2011) GFAP in health and disease. Prog Neurobiol 93:421-443.
Mir WAY, Shrestha DB, Fiumara F, Mohapatra S, Sullivan T, Adhikari A, Verda L (2021) HIV Encephalopathy Mimicking Acute Demyelinating Processes. Cureus 13:e18494.
Miron VE, Franklin RJ (2014) Macrophages and CNS remyelination. J Neurochem 130:165-171.
Miron VE, Boyd A, Zhao JW, Yuen TJ, Ruckh JM, Shadrach JL, van Wijngaarden P, Wagers AJ, Williams A, Franklin RJM, Ffrench-Constant C (2013a) M2 microglia and macrophages drive oligodendrocyte differentiation during CNS remyelination. Nat Neurosci 16:1211-1218.
Miron VE, Boyd A, Zhao JW, Yuen TJ, Ruckh JM, Shadrach JL, van Wijngaarden P, Wagers AJ, Williams A, Franklin RJ, ffrench-Constant C (2013b) M2 microglia and macrophages drive oligodendrocyte differentiation during CNS remyelination. Nat Neurosci 16:1211-1218.
Mishra S, Srinivasan S, Ma C, Zhang N (2021) CD8 + Regulatory T Cell - A Mystery to Be Revealed. Front Immunol 12:708874.
Miyake S, Kim S, Suda W, Oshima K, Nakamura M, Matsuoka T, Chihara N, Tomita A, Sato W, Kim SW, Morita H, Hattori M, Yamamura T (2015) Dysbiosis in the Gut Microbiota of Patients with Multiple Sclerosis, with a Striking Depletion of Species Belonging to Clostridia XIVa and IV Clusters. PLoS One 10:e0137429.
Miyamoto N, Maki T, Shindo A, Liang AC, Maeda M, Egawa N, Itoh K, Lo EK, Lok J, Ihara M, Arai K (2015) Astrocytes Promote Oligodendrogenesis after White Matter Damage via Brain-Derived Neurotrophic Factor. J Neurosci 35:14002-14008.
Mohan H, Friese A, Albrecht S, Krumbholz M, Elliott CL, Arthur A, Menon R, Farina C, Junker A, Stadelmann C, Barnett SC, Huitinga I, Wekerle H, Hohlfeld R, Lassmann H, Kuhlmann T, Linington C, Meinl E (2014) Transcript profiling of different types of multiple sclerosis lesions yields FGF1 as a promoter of remyelination. Acta Neuropathol Commun 2:168.

Molina-Gonzalez I et al. (2023) Astrocyte-oligodendrocyte interaction regulates central nervous system regeneration. Nat Commun 14:3372.
Molofsky AV, Krencik R, Ullian EM, Tsai HH, Deneen B, Richardson WD, Barres BA, Rowitch DH (2012) Astrocytes and disease: a neurodevelopmental perspective. Genes Dev 26:891-907.
Monsma PC, Brown A (2012) FluoroMyelin™ Red is a bright, photostable and non-toxic fluorescent stain for live imaging of myelin. J Neurosci Methods 209:344-350.
Moore Z, Mobilio F, Walker FR, Taylor JM, Crack PJ (2020) Abrogation of type-I interferon signalling alters the microglial response to Aβ. Sci Rep 10:3153.
Morandi B, Bramanti P, Bonaccorsi I, Montalto E, Oliveri D, Pezzino G, Navarra M, Ferlazzo G (2008) Role of natural killer cells in the pathogenesis and progression of multiple sclerosis. Pharmacol Res 57:1-5.
Moyon S, Holloman M, Salzer JL (2023) Neural stem cells and oligodendrocyte progenitor cells compete for remyelination in the corpus callosum. Front Cell Neurosci 17:1114781.
Moyon S, Dubessy AL, Aigrot MS, Trotter M, Huang JK, Dauphinot L, Potier MC, Kerninon C, Melik Parsadaniantz S, Franklin RJ, Lubetzki C (2015) Demyelination causes adult CNS progenitors to revert to an immature state and express immune cues that support their migration. J Neurosci 35:4-20.
Moyon S, Huynh JL, Dutta D, Zhang F, Ma D, Yoo S, Lawrence R, Wegner M, John GR, Emery B, Lubetzki C, Franklin RJ, Fan G, Zhu J, Dupree JL, Casaccia P (2016) Functional Characterization of DNA Methylation in the Oligodendrocyte Lineage. Cell Rep.
Nagashima K, Wege H, Meyermann R, ter Meulen V (1978) Corona virus induced subacute demyelinating encephalomyelitis in rats: a morphological analysis. Acta Neuropathol 44:63-70.
Nait-Oumesmar B, Decker L, Lachapelle F, Avellana-Adalid V, Bachelin C, Baron-Van Evercooren A (1999) Progenitor cells of the adult mouse subventricular zone proliferate, migrate and differentiate into oligodendrocytes after demyelination. Eur J Neurosci 11:4357-4366.
Nakamura TY, Nakao S, Nakajo Y, Takahashi JC, Wakabayashi S, Yanamoto H (2017) Possible Signaling Pathways Mediating Neuronal Calcium Sensor-1-Dependent Spatial Learning and Memory in Mice. PLoS One 12:e0170829.
Nash B, Thomson CE, Linington C, Arthur AT, McClure JD, McBride MW, Barnett SC (2011) Functional duality of astrocytes in myelination. J Neurosci 31:13028-13038.
Nave KA (2010) Myelination and the trophic support of long axons. Nat Rev Neurosci 11:275-283.
Nawaz S, Sánchez P, Schmitt S, Snaidero N, Mitkovski M, Velte C, Brückner BR, Alexopoulos I, Czopka T, Jung SY, Rhee JS, Janshoff A, Witke W, Schaap IAT, Lyons DA, Simons M (2015) Actin filament turnover drives leading edge growth during myelin sheath formation in the central nervous system. Dev Cell 34:139-151.
Neal M, Luo J, Harischandra DS, Gordon R, Sarkar S, Jin H, Anantharam V, Désaubry L, Kanthasamy A (2018) Prokineticin-2 promotes chemotaxis and alternative A2 reactivity of astrocytes. Glia 66:2137-2157.
Neely SA, Williamson JM, Klingseisen A, Zoupi L, Early JJ, Williams A, Lyons DA (2022) New oligodendrocytes exhibit more abundant and accurate myelin regeneration than those that survive demyelination. Nat Neurosci 25:415-420.
Nelson LH, Warden S, Lenz KM (2017) Sex differences in microglial phagocytosis in the neonatal hippocampus. Brain Behav Immun 64:11-22.
Nemes-Baran AD, White DR, DeSilva TM (2020) Fractalkine-Dependent Microglial Pruning of Viable Oligodendrocyte Progenitor Cells Regulates Myelination. Cell Rep 32:108047.
Neumaier EE, Rothhammer V, Linnerbauer M (2023) The role of midkine in health and disease. Front Immunol 14:1310094.
Neumann B, Segel M, Chalut KJ, Franklin RJ (2019) Remyelination and ageing: Reversing the ravages of time. Mult Scler 25:1835-1841.
Nicholas RS, Wing MG, Compston A (2001) Nonactivated microglia promote oligodendrocyte precursor survival and maturation through the transcription factor NF-kappa B. Eur J Neurosci 13:959-967.
Nicholas RS, Stevens S, Wing MG, Compston DA (2002) Microglia-derived IGF-2 prevents TNFalpha induced death of mature oligodendrocytes in vitro. J Neuroimmunol 124:36-44.

Nishiyama A, Chang A, Trapp BD (1999) NG2+ glial cells: a novel glial cell population in the adult brain. J Neuropathol Exp Neurol 58:1113-1124.
Niu J, Tsai HH, Hoi KK, Huang N, Yu G, Kim K, Baranzini SE, Xiao L, Chan JR, Fancy SPJ (2019) Aberrant oligodendroglial-vascular interactions disrupt the blood-brain barrier, triggering CNS inflammation. Nat Neurosci 22:709-718.
Niwa H, Yamamura K, Miyazaki J (1991) Efficient selection for high-expression transfectants with a novel eukaryotic vector. Gene 108:193-199.
Njenga MK, Coenen MJ, DeCuir N, Yeh HY, Rodriguez M (2000) Short-term treatment with interferon-alpha/beta promotes remyelination, whereas long-term treatment aggravates demyelination in a murine model of multiple sclerosis. J Neurosci Res 59:661-670.
Nolan K, Thompson TB (2014) The DAN family: modulators of TGF-β signaling and beyond. Protein Sci 23:999-1012.
Norden DM, Fenn AM, Dugan A, Godbout JP (2014) TGFβ produced by IL-10 redirected astrocytes attenuates microglial activation. Glia 62:881-895.
Noyes K, Weinstock-Guttman B (2013) Impact of diagnosis and early treatment on the course of multiple sclerosis. Am J Manag Care 19:s321-331.
Nygårdas PT, Hinkkanen AE (2002) Up-regulation of MMP-8 and MMP-9 activity in the BALB/c mouse spinal cord correlates with the severity of experimental autoimmune encephalomyelitis. Clin Exp Immunol 128:245-254.
Núñez MT, Hidalgo C (2019) Noxious Iron-Calcium Connections in Neurodegeneration. Front Neurosci 13:48.
O'Sullivan ML, Puñal VM, Kerstein PC, Brzezinski JA, Glaser T, Wright KM, Kay JN (2017) Astrocytes follow ganglion cell axons to establish an angiogenic template during retinal development. Glia 65:1697-1716.
Ohayon D, Escalas N, Cochard P, Glise B, Danesin C, Soula C (2019) Sulfatase 2 promotes generation of a spinal cord astrocyte subtype that stands out through the expression of Olig2. Glia 67:1478-1495.
Ohno N, Chiang H, Mahad DJ, Kidd GJ, Liu L, Ransohoff RM, Sheng ZH, Komuro H, Trapp BD (2014) Mitochondrial immobilization mediated by syntaphilin facilitates survival of demyelinated axons. Proc Natl Acad Sci U S A 111:9953-9958.
Okano H, Temple S (2009) Cell types to order: temporal specification of CNS stem cells. Curr Opin Neurobiol 19:112-119.
Omari KM, John GR, Sealfon SC, Raine CS (2005) CXC chemokine receptors on human oligodendrocytes: implications for multiple sclerosis. Brain 128:1003-1015.
Ono K, Suzuki H, Sawada M (2010) Delayed neural damage is induced by iNOS-expressing microglia in a brain injury model. Neurosci Lett 473:146-150.
Orentas DM, Hayes JE, Dyer KL, Miller RH (1999) Sonic hedgehog signaling is required during the appearance of spinal cord oligodendrocyte precursors. Development 126:2419-2429.
Orihuela R, McPherson CA, Harry GJ (2016) Microglial M1/M2 polarization and metabolic states. Br J Pharmacol 173:649-665.
Owens T (2006) Animal models for multiple sclerosis. Adv Neurol 98:77-89.
Palavicini JP, Wang H, Bianchi E, Xu S, Rao JS, Kang DE, Lakshmana MK (2013) RanBP9 aggravates synaptic damage in the mouse brain and is inversely correlated to spinophilin levels in Alzheimer's brain synaptosomes. Cell Death Dis 4:e667.
Palhol JSC, Balia M, Sánchez-Román Terán F, Labarchède M, Gontier E, Battefeld A (2023) Direct association with the vascular basement membrane is a frequent feature of myelinating oligodendrocytes in the neocortex. Fluids Barriers CNS 20:24.
Pan J, Ma N, Yu B, Zhang W, Wan J (2020) Transcriptomic profiling of microglia and astrocytes throughout aging. J Neuroinflammation 17:97.
Pan W, Wu X, He Y, Hsuchou H, Huang EY, Mishra PK, Kastin AJ (2013) Brain interleukin-15 in neuroinflammation and behavior. Neurosci Biobehav Rev 37:184-192.
Pan Y, Fu Y, Baird PN, Guymer RH, Das T, Iwata T (2023) Exploring the contribution of ARMS2 and HTRA1 genetic risk factors in age-related macular degeneration. Prog Retin Eye Res 97:101159.

Paolicelli RC et al. (2022) Microglia states and nomenclature: A field at its crossroads. Neuron 110:3458-3483.
Park HC, Boyce J, Shin J, Appel B (2005) Oligodendrocyte specification in zebrafish requires notch-regulated cyclin-dependent kinase inhibitor function. J Neurosci 25:6836-6844.
Parkhurst CN, Yang G, Ninan I, Savas JN, Yates JR, Lafaille JJ, Hempstead BL, Littman DR, Gan WB (2013) Microglia promote learning-dependent synapse formation through brain-derived neurotrophic factor. Cell 155:1596-1609.
Paryani F, Kwon JS, Ng CW, Madden N, Ofori K, Tang A, Lu H, Li J, Mahajan A, Davidson SM, Basile A, McHugh C, Vonsattel JP, Hickman R, Zody M, Houseman DE, Goldman JE, Yoo AS, Menon V, Al-Dalahmah O (2023) Multi-OMIC analysis of Huntington disease reveals a neuroprotective astrocyte state. bioRxiv.
Pasquini LA, Calatayud CA, Bertone Uña AL, Millet V, Pasquini JM, Soto EF (2007) The neurotoxic effect of cuprizone on oligodendrocytes depends on the presence of pro-inflammatory cytokines secreted by microglia. Neurochem Res 32:279-292.
Pasquini LA, Millet V, Hoyos HC, Giannoni JP, Croci DO, Marder M, Liu FT, Rabinovich GA, Pasquini JM (2011) Galectin-3 drives oligodendrocyte differentiation to control myelin integrity and function. Cell Death Differ 18:1746-1756.
Patel JR, Williams JL, Muccigrosso MM, Liu L, Sun T, Rubin JB, Klein RS (2012) Astrocyte TNFR2 is required for CXCL12-mediated regulation of oligodendrocyte progenitor proliferation and differentiation within the adult CNS. Acta Neuropathol 124:847-860.
Patel MR, Weaver AM (2021) Astrocyte-derived small extracellular vesicles promote synapse formation via fibulin-2-mediated TGF-β signaling. Cell Rep 34:108829.
Peferoen LA, Gerritsen WH, Breur M, Ummenthum KM, Peferoen-Baert RM, van der Valk P, van Noort JM, Amor S (2015) Small heat shock proteins are induced during multiple sclerosis lesion development in white but not grey matter. Acta Neuropathol Commun 3:87.
Pendleton JC, Shamblott MJ, Gary DS, Belegu V, Hurtado A, Malone ML, McDonald JW (2013) Chondroitin sulfate proteoglycans inhibit oligodendrocyte myelination through PTPσ. Exp Neurol 247:113-121.
Pham LD, Hayakawa K, Seo JH, Nguyen MN, Som AT, Lee BJ, Guo S, Kim KW, Lo EH, Arai K (2012) Crosstalk between oligodendrocytes and cerebral endothelium contributes to vascular remodeling after white matter injury. Glia 60:875-881.
Phares TW, Stohlman SA, Hinton DR, Bergmann CC (2013) Astrocyte-derived CXCL10 drives accumulation of antibody-secreting cells in the central nervous system during viral encephalomyelitis. J Virol 87:3382-3392.
Piaton G, Aigrot MS, Williams A, Moyon S, Tepavcevic V, Moutkine I, Gras J, Matho KS, Schmitt A, Soellner H, Huber AB, Ravassard P, Lubetzki C (2011) Class 3 semaphorins influence oligodendrocyte precursor recruitment and remyelination in adult central nervous system. Brain 134:1156-1167.
Pierson ER, Stromnes IM, Goverman JM (2014) B cells promote induction of experimental autoimmune encephalomyelitis by facilitating reactivation of T cells in the central nervous system. J Immunol 192:929-939.
Plastini MJ, Desu HL, Brambilla R (2020) Dynamic Responses of Microglia in Animal Models of Multiple Sclerosis. Front Cell Neurosci 14:269.
Plemel JR, Michaels NJ, Weishaupt N, Caprariello AV, Keough MB, Rogers JA, Yukseloglu A, Lim J, Patel VV, Rawji KS, Jensen SK, Teo W, Heyne B, Whitehead SN, Stys PK, Yong VW (2018) Mechanisms of lysophosphatidylcholine-induced demyelination: A primary lipid disrupting myelinopathy. Glia 66:327-347.
Plemel JR et al. (2020) Microglia response following acute demyelination is heterogeneous and limits infiltrating macrophage dispersion. Sci Adv 6:eaay6324.
Poduslo SE, Norton WT (1972) Isolation and some chemical properties of oligodendroglia from calf brain. J Neurochem 19:727-736.
Pont-Lezica L, Beumer W, Colasse S, Drexhage H, Versnel M, Bessis A (2014) Microglia shape corpus callosum axon tract fasciculation: functional impact of prenatal inflammation. Eur J Neurosci 39:1551-1557.

Poulen G, Gerber YN, Perez J-C, Oubarrahou K, Lonjon N, Vachiery-Lahaye F, Boukhaddaoui H, Perrin FE (2021) Coherent Anti-Stokes Raman Scattering Microscopy: A Label-Free Method to Compare Spinal Cord Myelin in Different Species. Frontiers in Physics 9.
Prinz M, Mildner A (2011) Microglia in the CNS: immigrants from another world. Glia 59:177-187.
Qi F, Zhang X, Wang L, Ren C, Zhao X, Luo J, Lu D (2022) E3 ubiquitin ligase NEURL3 promotes innate antiviral response through catalyzing K63-linked ubiquitination of IRF7. FASEB J 36:e22409.
Qian D, Li L, Rong Y, Liu W, Wang Q, Zhou Z, Gu C, Huang Y, Zhao X, Chen J, Fan J, Yin G (2019) Blocking Notch signal pathway suppresses the activation of neurotoxic A1 astrocytes after spinal cord injury. Cell Cycle 18:3010-3029.
Qian Y, Liu C, Hartupee J, Altuntas CZ, Gulen MF, Jane-Wit D, Xiao J, Lu Y, Giltiay N, Liu J, Kordula T, Zhang QW, Vallance B, Swaidani S, Aronica M, Tuohy VK, Hamilton T, Li X (2007) The adaptor Act1 is required for interleukin 17-dependent signaling associated with autoimmune and inflammatory disease. Nat Immunol 8:247-256.
Qu J, Zou T, Lin Z (2021) The Roles of the Ubiquitin-Proteasome System in the Endoplasmic Reticulum Stress Pathway. Int J Mol Sci 22.
Quick JD, Silva C, Wong JH, Lim KL, Reynolds R, Barron AM, Zeng J, Lo CH (2023) Lysosomal acidification dysfunction in microglia: an emerging pathogenic mechanism of neuroinflammation and neurodegeneration. J Neuroinflammation 20:185.
Radandish M, Khalilian P, Esmaeil N (2021) The Role of Distinct Subsets of Macrophages in the Pathogenesis of MS and the Impact of Different Therapeutic Agents on These Populations. Front Immunol 12:667705.
Raddassi K, Kent SC, Yang J, Bourcier K, Bradshaw EM, Seyfert-Margolis V, Nepom GT, Kwok WW, Hafler DA (2011) Increased frequencies of myelin oligodendrocyte glycoprotein/MHC class II-binding CD4 cells in patients with multiple sclerosis. J Immunol 187:1039-1046.
Raghavendra V, Tanga FY, DeLeo JA (2004) Complete Freunds adjuvant-induced peripheral inflammation evokes glial activation and proinflammatory cytokine expression in the CNS. Eur J Neurosci 20:467-473.
Rajkovic I, Wong R, Lemarchand E, Rivers-Auty J, Rajkovic O, Garlanda C, Allan SM, Pinteaux E (2018) Pentraxin 3 promotes long-term cerebral blood flow recovery, angiogenesis, and neuronal survival after stroke. J Mol Med (Berl) 96:1319-1332.
Rawji KS, Gonzalez Martinez GA, Sharma A, Franklin RJM (2020) The Role of Astrocytes in Remyelination. Trends Neurosci 43:596-607.
Recasens M, Shrivastava K, Almolda B, González B, Castellano B (2019) Astrocyte-targeted IL-10 production decreases proliferation and induces a downregulation of activated microglia/macrophages after PPT. Glia 67:741-758.
Redwine JM, Armstrong RC (1998) In vivo proliferation of oligodendrocyte progenitors expressing PDGFalphaR during early remyelination. J Neurobiol 37:413-428.
Reichenbach A, Derouiche A, Kirchhoff F (2010) Morphology and dynamics of perisynaptic glia. Brain Research Reviews 63:11-25.
Reichert F, Rotshenker S (2003) Complement-receptor-3 and scavenger-receptor-AI/II mediated myelin phagocytosis in microglia and macrophages. Neurobiol Dis 12:65-72.
Reichert F, Rotshenker S (2019) Galectin-3 (MAC-2) Controls Microglia Phenotype Whether Amoeboid and Phagocytic or Branched and Non-phagocytic by Regulating the Cytoskeleton. Front Cell Neurosci 13:90.
Reijerkerk A, Kooij G, van der Pol SM, Khazen S, Dijkstra CD, de Vries HE (2006) Diapedesis of monocytes is associated with MMP-mediated occludin disappearance in brain endothelial cells. FASEB J 20:2550-2552.
Relucio J, Menezes MJ, Miyagoe-Suzuki Y, Takeda S, Colognato H (2012) Laminin regulates postnatal oligodendrocyte production by promoting oligodendrocyte progenitor survival in the subventricular zone. Glia 60:1451-1467.
Remington LT, Babcock AA, Zehntner SP, Owens T (2007) Microglial recruitment, activation, and proliferation in response to primary demyelination. Am J Pathol 170:1713-1724.

Reynolds AD, Banerjee R, Liu J, Gendelman HE, Mosley RL (2007) Neuroprotective activities of CD4+CD25+ regulatory T cells in an animal model of Parkinson's disease. J Leukoc Biol 82:1083-1094.
Ribeiro TN, Delgado-García LM, Porcionatto MA (2021) Notch1 and Galectin-3 Modulate Cortical Reactive Astrocyte Response After Brain Injury. Front Cell Dev Biol 9:649854.
Richardson WD, Pringle N, Mosley MJ, Westermark B, Dubois-Dalcq M (1988) A role for platelet-derived growth factor in normal gliogenesis in the central nervous system. Cell 53:309-319.
Rigato C, Buckinx R, Le-Corronc H, Rigo JM, Legendre P (2011) Pattern of invasion of the embryonic mouse spinal cord by microglial cells at the time of the onset of functional neuronal networks. Glia 59:675-695.
Rimmerman N et al. (2022) Microglia and their LAG3 checkpoint underlie the antidepressant and neurogenesis-enhancing effects of electroconvulsive stimulation. Mol Psychiatry 27:1120-1135.
Rinaldi M, Thomas L, Mathieu P, Carabias P, Troncoso MF, Pasquini JM, Rabinovich GA, Pasquini LA (2016) Galectin-1 circumvents lysolecithin-induced demyelination through the modulation of microglial polarization/phagocytosis and oligodendroglial differentiation. Neurobiol Dis 96:127-143.
Rinholm JE, Hamilton NB, Kessaris N, Richardson WD, Bergersen LH, Attwell D (2011) Regulation of oligodendrocyte development and myelination by glucose and lactate. J Neurosci 31:538-548.
Ritchie JM (1982) On the relation between fibre diameter and conduction velocity in myelinated nerve fibres. Proc R Soc Lond B Biol Sci 217:29-35.
Rivers LE, Young KM, Rizzi M, Jamen F, Psachoulia K, Wade A, Kessaris N, Richardson WD (2008) PDGFRA/NG2 glia generate myelinating oligodendrocytes and piriform projection neurons in adult mice. Nat Neurosci 11:1392-1401.
Roda RH, FitzGibbon EJ, Boucekkine H, Schindler AB, Blackstone C (2016) Neurologic syndrome associated with homozygous mutation at MAG sialic acid binding site. Ann Clin Transl Neurol 3:650-654.
Rodriguez-Grande B, Varghese L, Molina-Holgado F, Rajkovic O, Garlanda C, Denes A, Pinteaux E (2015) Pentraxin 3 mediates neurogenesis and angiogenesis after cerebral ischaemia. J Neuroinflammation 12:15.
Roncarolo MG, Gregori S, Bacchetta R, Battaglia M, Gagliani N (2018) The Biology of T Regulatory Type 1 Cells and Their Therapeutic Application in Immune-Mediated Diseases. Immunity 49:1004-1019.
Ronzano R, Roux T, Thetiot M, Aigrot MS, Richard L, Lejeune FX, Mazuir E, Vallat JM, Lubetzki C, Desmazières A (2021) Microglia-neuron interaction at nodes of Ranvier depends on neuronal activity through potassium release and contributes to remyelination. Nat Commun 12:5219.
Rose CR, Felix L, Zeug A, Dietrich D, Reiner A, Henneberger C (2017) Astroglial Glutamate Signaling and Uptake in the Hippocampus. Front Mol Neurosci 10:451.
Rothhammer V, Kenison JE, Tjon E, Takenaka MC, de Lima KA, Borucki DM, Chao CC, Wilz A, Blain M, Healy L, Antel J, Quintana FJ (2017) Sphingosine 1-phosphate receptor modulation suppresses pathogenic astrocyte activation and chronic progressive CNS inflammation. Proc Natl Acad Sci U S A 114:2012-2017.
Rowitch DH, Kriegstein AR (2010) Developmental genetics of vertebrate glial-cell specification. Nature 468:214-222.
Ruckh JM, Zhao JW, Shadrach JL, van Wijngaarden P, Rao TN, Wagers AJ, Franklin RJ (2012) Rejuvenation of regeneration in the aging central nervous system. Cell Stem Cell 10:96-103.
Saab AS et al. (2016) Oligodendroglial NMDA Receptors Regulate Glucose Import and Axonal Energy Metabolism. Neuron.
Saadoun S, Bell BA, Verkman AS, Papadopoulos MC (2008) Greatly improved neurological outcome after spinal cord compression injury in AQP4-deficient mice. Brain 131:1087-1098.
Saas P, Boucraut J, Walker PR, Quiquerez AL, Billot M, Desplat-Jego S, Chicheportiche Y, Dietrich PY (2000) TWEAK stimulation of astrocytes and the proinflammatory consequences. Glia 32:102-107.

Saha RN, Pahan K (2006) Regulation of inducible nitric oxide synthase gene in glial cells. Antioxid Redox Signal 8:929-947.
Saher G, Stumpf SK (2015) Cholesterol in myelin biogenesis and hypomyelinating disorders. Biochim Biophys Acta 1851:1083-1094.
Sakry D, Neitz A, Singh J, Frischknecht R, Marongiu D, Binamé F, Perera SS, Endres K, Lutz B, Radyushkin K, Trotter J, Mittmann T (2014) Oligodendrocyte precursor cells modulate the neuronal network by activity-dependent ectodomain cleavage of glial NG2. PLoS Biol 12:e1001993.
Sanmarco LM, Wheeler MA, Gutiérrez-Vázquez C, Polonio CM, Linnerbauer M, Pinho-Ribeiro FA, Li Z, Giovannoni F, Batterman KV, Scalisi G, Zandee SEJ, Heck ES, Alsuwailm M, Rosene DL, Becher B, Chiu IM, Prat A, Quintana FJ (2021) Gut-licensed IFNγ + NK cells drive LAMP1 + TRAIL + anti-inflammatory astrocytes. Nature 590:473-479.
Sanz E, Bean JC, Carey DP, Quintana A, McKnight GS (2019) RiboTag: Ribosomal Tagging Strategy to Analyze Cell-Type-Specific mRNA Expression In Vivo. Curr Protoc Neurosci 88:e77.
Sanz E, Yang L, Su T, Morris DR, McKnight GS, Amieux PS (2009) Cell-type-specific isolation of ribosome-associated mRNA from complex tissues. Proc Natl Acad Sci U S A 106:13939-13944.
Sarkar S, Paidi RK, Biswas SC (2021) Astrocyte-secreted TIMP-1 binds to CD63 and differentially phosphorylates Akt in protecting neurons and promoting cognitive recovery in 5xFAD mice. Alzheimer's & Dementia 17:e052606.
Sasaki-Hamada S, Sanai E, Kanemaru M, Kamanaka G, Oka JI (2022) Long-term exposure to high glucose induces changes in the expression of AMPA receptor subunits and glutamate transmission in primary cultured cortical neurons. Biochem Biophys Res Commun 589:48-54.
Satam H, Joshi K, Mangrolia U, Waghoo S, Zaidi G, Rawool S, Thakare RP, Banday S, Mishra AK, Das G, Malonia SK (2023) Next-Generation Sequencing Technology: Current Trends and Advancements. Biology (Basel) 12.
Sato-Hashimoto M et al. (2019) Microglial SIRPa regulates the emergence of CD11c^{+} microglia and demyelination damage in white matter. Elife 8.
Savarin C, Hinton DR, Valentin-Torres A, Chen Z, Trapp BD, Bergmann CC, Stohlman SA (2015) Astrocyte response to IFN-γ limits IL-6-mediated microglia activation and progressive autoimmune encephalomyelitis. J Neuroinflammation 12:79.
Scaglione A, Patzig J, Liang J, Frawley R, Bok J, Mela A, Yattah C, Zhang J, Teo SX, Zhou T, Chen S, Bernstein E, Canoll P, Guccione E, Casaccia P (2018) PRMT5-mediated regulation of developmental myelination. Nat Commun 9:2840.
Schetters STT, Gomez-Nicola D, Garcia-Vallejo JJ, Van Kooyk Y (2017) Neuroinflammation: Microglia and T Cells Get Ready to Tango. Front Immunol 8:1905.
Schiweck J, Murk K, Ledderose J, Münster-Wandowski A, Ornaghi M, Vida I, Eickholt BJ (2021) Drebrin controls scar formation and astrocyte reactivity upon traumatic brain injury by regulating membrane trafficking. Nat Commun 12:1490.
Schlett JS et al. (2023) NF-κB is a critical mediator of post-mitotic senescence in oligodendrocytes and subsequent white matter loss. Mol Neurodegener 18:24.
Schnädelbach O, Blaschuk OW, Symonds M, Gour BJ, Doherty P, Fawcett JW (2000) N-cadherin influences migration of oligodendrocytes on astrocyte monolayers. Mol Cell Neurosci 15:288-302.
Scholze AR, Foo LC, Mulinyawe S, Barres BA (2014) BMP signaling in astrocytes downregulates EGFR to modulate survival and maturation. PLoS One 9:e110668.
Schonkeren SL, Massen M, van der Horst R, Koch A, Vaes N, Melotte V (2019) Nervous NDRGs: the N-myc downstream-regulated gene family in the central and peripheral nervous system. Neurogenetics 20:173-186.
Schröder LJ, Mulenge F, Pavlou A, Skripuletz T, Stangel M, Gudi V, Kalinke U (2023) Dynamics of reactive astrocytes fosters tissue regeneration after cuprizone-induced demyelination. Glia 71:2573-2590.

Schulz C, Gomez Perdiguero E, Chorro L, Szabo-Rogers H, Cagnard N, Kierdorf K, Prinz M, Wu B, Jacobsen SE, Pollard JW, Frampton J, Liu KJ, Geissmann F (2012a) A lineage of myeloid cells independent of Myb and hematopoietic stem cells. Science 336:86-90.
Schulz K, Kroner A, David S (2012b) Iron efflux from astrocytes plays a role in remyelination. J Neurosci 32:4841-4847.
Schäffner E et al. (2023) Myelin insulation as a risk factor for axonal degeneration in autoimmune demyelinating disease. Nat Neurosci 26:1218-1228.
Sekine Y, Kannan R, Wang X, Strittmatter SM (2022) Rabphilin3A reduces integrin-dependent growth cone signaling to restrict axon regeneration after trauma. Exp Neurol 353:114070.
Selmaj KW, Raine CS (1988) Tumor necrosis factor mediates myelin and oligodendrocyte damage in vitro. Ann Neurol 23:339-346.
Seo H, Lee K (2016) Epac2 contributes to PACAP-induced astrocytic differentiation through calcium ion influx in neural precursor cells. BMB Rep 49:128-133.
Seo JH, Maki T, Maeda M, Miyamoto N, Liang AC, Hayakawa K, Pham LD, Suwa F, Taguchi A, Matsuyama T, Ihara M, Kim KW, Lo EH, Arai K (2014) Oligodendrocyte precursor cells support blood-brain barrier integrity via TGF-β signaling. PLoS One 9:e103174.
Setzu A, Lathia JD, Zhao C, Wells K, Rao MS, Ffrench-Constant C, Franklin RJ (2006) Inflammation stimulates myelination by transplanted oligodendrocyte precursor cells. Glia 54:297-303.
Shahi SK, Yadav M, Ghimire S, Mangalam AK (2022) Role of the gut microbiome in multiple sclerosis: From etiology to therapeutics. Int Rev Neurobiol 167:185-215.
Sherman DL, Tait S, Melrose S, Johnson R, Zonta B, Court FA, Macklin WB, Meek S, Smith AJ, Cottrell DF, Brophy PJ (2005) Neurofascins are required to establish axonal domains for saltatory conduction. Neuron 48:737-742.
Shi K, Li H, Chang T, He W, Kong Y, Qi C, Li R, Huang H, Zhu Z, Zheng P, Ruan Z, Zhou J, Shi FD, Liu Q (2022) Bone marrow hematopoiesis drives multiple sclerosis progression. Cell 185:2234-2247.e2217.
Shi Y, Zhang D, Huff TB, Wang X, Shi R, Xu XM, Cheng JX (2011) Longitudinal in vivo coherent anti-Stokes Raman scattering imaging of demyelination and remyelination in injured spinal cord. J Biomed Opt 16:106012.
Shi Z et al. (2023) Microglia drive transient insult-induced brain injury by chemotactic recruitment of CD8. Neuron 111:696-710.e699.
Shigemoto-Mogami Y, Hoshikawa K, Goldman JE, Sekino Y, Sato K (2014) Microglia enhance neurogenesis and oligodendrogenesis in the early postnatal subventricular zone. J Neurosci 34:2231-2243.
Shiow LR, Favrais G, Schirmer L, Schang AL, Cipriani S, Andres C, Wright JN, Nobuta H, Fleiss B, Gressens P, Rowitch DH (2017) Reactive astrocyte COX2-PGE2 production inhibits oligodendrocyte maturation in neonatal white matter injury. Glia 65:2024-2037.
Sica A, Mantovani A (2012) Macrophage plasticity and polarization: in vivo veritas. J Clin Invest 122:787-795.
Simpson DSA, Oliver PL (2020) ROS Generation in Microglia: Understanding Oxidative Stress and Inflammation in Neurodegenerative Disease. Antioxidants (Basel) 9.
Sinner P, Peckert-Maier K, Mohammadian H, Kuhnt C, Draßner C, Panagiotakopoulou V, Rauber S, Linnerbauer M, Haimon Z, Royzman D, Kronenberg-Versteeg D, Ramming A, Steinkasserer A, Wild AB (2023) Microglial expression of CD83 governs cellular activation and restrains neuroinflammation in experimental autoimmune encephalomyelitis. Nat Commun 14:4601.
Sintzel MB, Rametta M, Reder AT (2018) Vitamin D and Multiple Sclerosis: A Comprehensive Review. Neurol Ther 7:59-85.
Skripuletz T, Hackstette D, Bauer K, Gudi V, Pul R, Voss E, Berger K, Kipp M, Baumgärtner W, Stangel M (2013) Astrocytes regulate myelin clearance through recruitment of microglia during cuprizone-induced demyelination. Brain 136:147-167.
Smith CM, Cooksey E, Duncan ID (2013) Myelin loss does not lead to axonal degeneration in a long-lived model of chronic demyelination. J Neurosci 33:2718-2727.
Smith JA, Das A, Ray SK, Banik NL (2012) Role of pro-inflammatory cytokines released from microglia in neurodegenerative diseases. Brain Res Bull 87:10-20.

Smith KJ (1994) Conduction properties of central demyelinated and remyelinated axons, and their relation to symptom production in demyelinating disorders. Eye (Lond) 8 (Pt 2):224-237.
Sobel RA, Greer JM, Kuchroo VK (1994) Minireview: autoimmune responses to myelin proteolipid protein. Neurochem Res 19:915-921.
Sobottka B, Ziegler U, Kaech A, Becher B, Goebels N (2011) CNS live imaging reveals a new mechanism of myelination: the liquid croissant model. Glia 59:1841-1849.
Sobue A, Komine O, Hara Y, Endo F, Mizoguchi H, Watanabe S, Murayama S, Saito T, Saido TC, Sahara N, Higuchi M, Ogi T, Yamanaka K (2021) Microglial gene signature reveals loss of homeostatic microglia associated with neurodegeneration of Alzheimer's disease. Acta Neuropathol Commun 9:1.
Sofroniew MV, Vinters HV (2010) Astrocytes: biology and pathology. Acta Neuropathol 119:7-35.
Somjen GG (1988) Nervenkitt: notes on the history of the concept of neuroglia. Glia 1:2-9.
Sozmen EG, DiTullio DJ, Rosenzweig S, Hinman JD, Bridges SP, Marin MA, Kawaguchi R, Coppola G, Carmichael ST (2019) White Matter Stroke Induces a Unique Oligo-Astrocyte Niche That Inhibits Recovery. J Neurosci 39:9343-9359.
Stagi M, Dittrich PS, Frank N, Iliev AI, Schwille P, Neumann H (2005) Breakdown of axonal synaptic vesicle precursor transport by microglial nitric oxide. J Neurosci 25:352-362.
Stajano D, Lombino FL, Schweizer M, Glatzel M, Saftig P, Gromova KV, Kneussel M (2023) Tetraspanin 15 depletion impairs extracellular vesicle docking at target neurons. J Extracell Biol 2:e113.
Starossom SC, Mascanfroni ID, Imitola J, Cao L, Raddassi K, Hernandez SF, Bassil R, Croci DO, Cerliani JP, Delacour D, Wang Y, Elyaman W, Khoury SJ, Rabinovich GA (2012) Galectin-1 deactivates classically activated microglia and protects from inflammation-induced neurodegeneration. Immunity 37:249-263.
Sternberg N, Hamilton D (1981) Bacteriophage P1 site-specific recombination. I. Recombination between loxP sites. J Mol Biol 150:467-486.
Stoffels JM, de Jonge JC, Stancic M, Nomden A, van Strien ME, Ma D, Sisková Z, Maier O, Ffrench-Constant C, Franklin RJ, Hoekstra D, Zhao C, Baron W (2013) Fibronectin aggregation in multiple sclerosis lesions impairs remyelination. Brain 136:116-131.
Stolt CC, Lommes P, Sock E, Chaboissier MC, Schedl A, Wegner M (2003) The Sox9 transcription factor determines glial fate choice in the developing spinal cord. Genes Dev 17:1677-1689.
Stys PK (1998) Anoxic and ischemic injury of myelinated axons in CNS white matter: from mechanistic concepts to therapeutics. J Cereb Blood Flow Metab 18:2-25.
Su Y, Wang Y, Zhou Y, Zhu Z, Zhang Q, Zhang X, Wang W, Gu X, Guo A (2017) Macrophage migration inhibitory factor activates inflammatory responses of astrocytes through interaction with CD74 receptor. Oncotarget 8:2719-2730.
Subhramanyam CS, Wang C, Hu Q, Dheen ST (2019) Microglia-mediated neuroinflammation in neurodegenerative diseases. Semin Cell Dev Biol 94:112-120.
Sugimori M, Nagao M, Parras CM, Nakatani H, Lebel M, Guillemot F, Nakafuku M (2008) Ascl1 is required for oligodendrocyte development in the spinal cord. Development 135:1271-1281.
Sung HY, Chen WY, Huang HT, Wang CY, Chang SB, Tzeng SF (2019) Down-regulation of interleukin-33 expression in oligodendrocyte precursor cells impairs oligodendrocyte lineage progression. J Neurochem 150:691-708.
Suzuki H, Imajo Y, Funaba M, Nishida N, Sakamoto T, Sakai T (2021) Current Concepts of Neural Stem/Progenitor Cell Therapy for Chronic Spinal Cord Injury. Front Cell Neurosci 15:794692.
Szczygielski J, Kopańska M, Wysocka A, Oertel J (2021) Cerebral Microcirculation, Perivascular Unit, and Glymphatic System: Role of Aquaporin-4 as the Gatekeeper for Water Homeostasis. Front Neurol 12:767470.
Szebenyi G, Dent EW, Callaway JL, Seys C, Lueth H, Kalil K (2001) Fibroblast growth factor-2 promotes axon branching of cortical neurons by influencing morphology and behavior of the primary growth cone. J Neurosci 21:3932-3941.
Tahir W, Thapa S, Schatzl HM (2022) Astrocyte in prion disease: a double-edged sword. Neural Regen Res 17:1659-1665.

Takahashi S (2021) Neuroprotective Function of High Glycolytic Activity in Astrocytes: Common Roles in Stroke and Neurodegenerative Diseases. Int J Mol Sci 22.
Takano T, Wallace JT, Baldwin KT, Purkey AM, Uezu A, Courtland JL, Soderblom EJ, Shimogori T, Maness PF, Eroglu C, Soderling SH (2020) Chemico-genetic discovery of astrocytic control of inhibition in vivo. Nature 588:296-302.
Takarada-Iemata M, Yoshikawa A, Ta HM, Okitani N, Nishiuchi T, Aida Y, Kamide T, Hattori T, Ishii H, Tamatani T, Le TM, Roboon J, Kitao Y, Matsuyama T, Nakada M, Hori O (2018) N-myc downstream-regulated gene 2 protects blood-brain barrier integrity following cerebral ischemia. Glia 66:1432-1446.
Takeuchi H, Jin S, Suzuki H, Doi Y, Liang J, Kawanokuchi J, Mizuno T, Sawada M, Suzumura A (2008) Blockade of microglial glutamate release protects against ischemic brain injury. Exp Neurol 214:144-146.
Talanki Manjunatha R, Habib S, Sangaraju SL, Yepez D, Grandes XA (2022) Multiple Sclerosis: Therapeutic Strategies on the Horizon. Cureus 14:e24895.
Tambuyzer BR, Ponsaerts P, Nouwen EJ (2009) Microglia: gatekeepers of central nervous system immunology. J Leukoc Biol 85:352-370.
Tan CX, Burrus Lane CJ, Eroglu C (2021) Role of astrocytes in synapse formation and maturation. Curr Top Dev Biol 142:371-407.
Tan CX, Bindu DS, Hardin EJ, Sakers K, Baumert R, Ramirez JJ, Savage JT, Eroglu C (2023) δ-Catenin controls astrocyte morphogenesis via layer-specific astrocyte-neuron cadherin interactions. J Cell Biol 222.
Tan W, Su PP, Leff J, Gao X, Chen J, Guan AK, Kalyanasundaram G, Ma A, Guan Z (2022) Distinct phases of adult microglia proliferation: a Myc-mediated early phase and a Tnfaip3-mediated late phase. Cell Discov 8:34.
Tanaka Y, Arima Y, Higuchi K, Ohki T, Elfeky M, Ota M, Kamimura D, Murakami M (2017) EAE Induction by Passive Transfer of MOG-specific CD4. Bio Protoc 7:e2370.
Tang Y, Le W (2016) Differential Roles of M1 and M2 Microglia in Neurodegenerative Diseases. Mol Neurobiol 53:1181-1194.
Tanuma N, Sakuma H, Sasaki A, Matsumoto Y (2006) Chemokine expression by astrocytes plays a role in microglia/macrophage activation and subsequent neurodegeneration in secondary progressive multiple sclerosis. Acta Neuropathol 112:195-204.
Tatsumi K, Isonishi A, Yamasaki M, Kawabe Y, Morita-Takemura S, Nakahara K, Terada Y, Shinjo T, Okuda H, Tanaka T, Wanaka A (2018) Olig2-Lineage Astrocytes: A Distinct Subtype of Astrocytes That Differs from GFAP Astrocytes. Front Neuroanat 12:8.
Tchieu J, Calder EL, Guttikonda SR, Gutzwiller EM, Aromolaran KA, Steinbeck JA, Goldstein PA, Studer L (2019) NFIA is a gliogenic switch enabling rapid derivation of functional human astrocytes from pluripotent stem cells. Nat Biotechnol 37:267-275.
Thakar S, Wang L, Yu T, Ye M, Onishi K, Scott J, Qi J, Fernandes C, Han X, Yates JR, Berg DK, Zou Y (2017) Evidence for opposing roles of Celsr3 and Vangl2 in glutamatergic synapse formation. Proc Natl Acad Sci U S A 114:E610-E618.
Theer P, Hasan MT, Denk W (2003) Two-photon imaging to a depth of 1000 microm in living brains by use of a Ti:Al2O3 regenerative amplifier. Opt Lett 28:1022-1024.
Thomas RA, Gibon J, Chen CXQ, Chierzi S, Soubannier VG, Baulac S, Séguéla P, Murai K, Barker PA (2018) The Nogo Receptor Ligand LGI1 Regulates Synapse Number and Synaptic Activity in Hippocampal and Cortical Neurons. eNeuro 5.
Tien AC, Tsai HH, Molofsky AV, McMahon M, Foo LC, Kaul A, Dougherty JD, Heintz N, Gutmann DH, Barres BA, Rowitch DH (2012) Regulated temporal-spatial astrocyte precursor cell proliferation involves BRAF signalling in mammalian spinal cord. Development 139:2477-2487.
Timsit S, Martinez S, Allinquant B, Peyron F, Puelles L, Zalc B (1995) Oligodendrocytes originate in a restricted zone of the embryonic ventral neural tube defined by DM-20 mRNA expression. J Neurosci 15:1012-1024.
Todorovic V, Rifkin DB (2012) LTBPs, more than just an escort service. J Cell Biochem 113:410-418.

Tong X, Ao Y, Faas GC, Nwaobi SE, Xu J, Haustein MD, Anderson MA, Mody I, Olsen ML, Sofroniew MV, Khakh BS (2014) Astrocyte Kir4.1 ion channel deficits contribute to neuronal dysfunction in Huntington's disease model mice. Nat Neurosci 17:694-703.
Torkildsen O, Brunborg LA, Myhr KM, Bø L (2008) The cuprizone model for demyelination. Acta Neurol Scand Suppl 188:72-76.
Tournier BB, Bouteldja F, Amossé Q, Nicolaides A, Duarte Azevedo M, Tenenbaum L, Garibotto V, Ceyzériat K, Millet P (2023) 18 kDa Translocator Protein TSPO Is a Mediator of Astrocyte Reactivity. ACS Omega 8:31225-31236.
Traiffort E, Kassoussi A, Zahaf A, Laouarem Y (2020) Astrocytes and Microglia as Major Players of Myelin Production in Normal and Pathological Conditions. Front Cell Neurosci 14:79.
Tripathi RB, Clarke LE, Burzomato V, Kessaris N, Anderson PN, Attwell D, Richardson WD (2011) Dorsally and ventrally derived oligodendrocytes have similar electrical properties but myelinate preferred tracts. J Neurosci 31:6809-6819.
Trotter JH, Dargaei Z, Sclip A, Essayan-Perez S, Liakath-Ali K, Raju K, Nabet A, Liu X, Wöhr M, Südhof TC (2021) Compartment-Specific Neurexin Nanodomains Orchestrate Tripartite Synapse Assembly. bioRxiv:2020.2008.2021.262097.
Truman LA, Ford CA, Pasikowska M, Pound JD, Wilkinson SJ, Dumitriu IE, Melville L, Melrose LA, Ogden CA, Nibbs R, Graham G, Combadiere C, Gregory CD (2008) CX3CL1/fractalkine is released from apoptotic lymphocytes to stimulate macrophage chemotaxis. Blood 112:5026-5036.
Tsai HH, Frost E, To V, Robinson S, Ffrench-Constant C, Geertman R, Ransohoff RM, Miller RH (2002) The chemokine receptor CXCR2 controls positioning of oligodendrocyte precursors in developing spinal cord by arresting their migration. Cell 110:373-383.
Tsai HH, Niu J, Munji R, Davalos D, Chang J, Zhang H, Tien AC, Kuo CJ, Chan JR, Daneman R, Fancy SP (2016) Oligodendrocyte precursors migrate along vasculature in the developing nervous system. Science 351:379-384.
Tsunoda I, Fujinami RS (2002) Inside-Out versus Outside-In models for virus induced demyelination: axonal damage triggering demyelination. Springer Semin Immunopathol 24:105-125.
Tsunoda I, Kuang LQ, Libbey JE, Fujinami RS (2003) Axonal injury heralds virus-induced demyelination. Am J Pathol 162:1259-1269.
Turcotte R, Rutledge DJ, Bélanger E, Dill D, Macklin WB, Côté DC (2016) Intravital assessment of myelin molecular order with polarimetric multiphoton microscopy. Sci Rep 6:31685.
Tzartos JS, Friese MA, Craner MJ, Palace J, Newcombe J, Esiri MM, Fugger L (2008) Interleukin-17 production in central nervous system-infiltrating T cells and glial cells is associated with active disease in multiple sclerosis. Am J Pathol 172:146-155.
Ulivieri C, De Tommaso D, Finetti F, Ortensi B, Pelicci G, D'Elios MM, Ballerini C, Baldari CT (2019) A T Cell Suppressive Circuitry Mediated by CD39 and Regulated by ShcC/Rai Is Induced in Astrocytes by Encephalitogenic T Cells. Front Immunol 10:1041.
Ullrich S, Münch A, Neumann S, Kremmer E, Tatzelt J, Lichtenthaler SF (2010) The novel membrane protein TMEM59 modulates complex glycosylation, cell surface expression, and secretion of the amyloid precursor protein. J Biol Chem 285:20664-20674.
Ulrich F, Carretero-Ortega J, Menéndez J, Narvaez C, Sun B, Lancaster E, Pershad V, Trzaska S, Véliz E, Kamei M, Prendergast A, Kidd KR, Shaw KM, Castranova DA, Pham VN, Lo BD, Martin BL, Raible DW, Weinstein BM, Torres-Vázquez J (2016) Reck enables cerebrovascular development by promoting canonical Wnt signaling. Development 143:147-159.
Upadhya R, Zingg W, Shetty S, Shetty AK (2020) Astrocyte-derived extracellular vesicles: Neuroreparative properties and role in the pathogenesis of neurodegenerative disorders. J Control Release 323:225-239.
Uyeda A, Muramatsu R (2020) Molecular Mechanisms of Central Nervous System Axonal Regeneration and Remyelination: A Review. Int J Mol Sci 21.
Vainchtein ID, Chin G, Cho FS, Kelley KW, Miller JG, Chien EC, Liddelow SA, Nguyen PT, Nakao-Inoue H, Dorman LC, Akil O, Joshita S, Barres BA, Paz JT, Molofsky AB, Molofsky AV (2018) Astrocyte-derived interleukin-33 promotes microglial synapse engulfment and neural circuit development. Science 359:1269-1273.

Valentin-Torres A, Savarin C, Barnett J, Bergmann CC (2018) Blockade of sustained tumor necrosis factor in a transgenic model of progressive autoimmune encephalomyelitis limits oligodendrocyte apoptosis and promotes oligodendrocyte maturation. J Neuroinflammation 15:121.

Vallstedt A, Klos JM, Ericson J (2005) Multiple dorsoventral origins of oligodendrocyte generation in the spinal cord and hindbrain. Neuron 45:55-67.

Van den Berge K, Hembach KM, Soneson C, Tiberi S, Clement L, Love MI, Patro R, Robinson MD (2019) RNA Sequencing Data: Hitchhiker's Guide to Expression Analysis. Annual Review of Biomedical Data Science 2:139-173.

van den Brink SC, Sage F, Vértesy Á, Spanjaard B, Peterson-Maduro J, Baron CS, Robin C, van Oudenaarden A (2017) Single-cell sequencing reveals dissociation-induced gene expression in tissue subpopulations. Nat Methods 14:935-936.

van der Valk P, De Groot CJ (2000) Staging of multiple sclerosis (MS) lesions: pathology of the time frame of MS. Neuropathol Appl Neurobiol 26:2-10.

van Schaik PEM, Zuhorn IS, Baron W (2022) Targeting Fibronectin to Overcome Remyelination Failure in Multiple Sclerosis: The Need for Brain- and Lesion-Targeted Drug Delivery. Int J Mol Sci 23.

VanRyzin JW, Marquardt AE, Argue KJ, Vecchiarelli HA, Ashton SE, Arambula SE, Hill MN, McCarthy MM (2019) Microglial Phagocytosis of Newborn Cells Is Induced by Endocannabinoids and Sculpts Sex Differences in Juvenile Rat Social Play. Neuron 102:435-449.e436.

Vecchiarelli, Simoncicova (2021) Microglial Involvement With Psychiatric Diseases. Psychiatric Times 38:35-38.

Verkhratsky A, Parpura V, Li B, Scuderi C (2021) Astrocytes: The Housekeepers and Guardians of the CNS. Adv Neurobiol 26:21-53.

Viganò F, Schneider S, Cimino M, Bonfanti E, Gelosa P, Sironi L, Abbracchio MP, Dimou L (2016) GPR17 expressing NG2-Glia: Oligodendrocyte progenitors serving as a reserve pool after injury. Glia 64:287-299.

Vogel DY, Vereyken EJ, Glim JE, Heijnen PD, Moeton M, van der Valk P, Amor S, Teunissen CE, van Horssen J, Dijkstra CD (2013) Macrophages in inflammatory multiple sclerosis lesions have an intermediate activation status. J Neuroinflammation 10:35.

Vong KI, Ma TC, Li B, Leung TCN, Nong W, Ngai SM, Hui JHL, Jiang L, Kwan KM (2021) SOX9-COL9A3-dependent regulation of choroid plexus epithelial polarity governs blood-cerebrospinal fluid barrier integrity. Proc Natl Acad Sci U S A 118.

Voskuhl RR, Itoh N, Tassoni A, Matsukawa MA, Ren E, Tse V, Jang E, Suen TT, Itoh Y (2019) Gene expression in oligodendrocytes during remyelination reveals cholesterol homeostasis as a therapeutic target in multiple sclerosis. Proc Natl Acad Sci U S A 116:10130-10139.

Voumvourakis KI, Fragkou PC, Kitsos DK, Foska K, Chondrogianni M, Tsiodras S (2022) Human herpesvirus 6 infection as a trigger of multiple sclerosis: an update of recent literature. BMC Neurol 22:57.

Wan T, Zhu W, Zhao Y, Zhang X, Ye R, Zuo M, Xu P, Huang Z, Zhang C, Xie Y, Liu X (2022) Astrocytic phagocytosis contributes to demyelination after focal cortical ischemia in mice. Nat Commun 13:1134.

Wang C, Kotter MR (2018) Experimental Demyelination and Remyelination of Murine Spinal Cord by Focal Injection of Lysolecithin. Methods Mol Biol 1791:233-241.

Wang H, Fu Y, Zickmund P, Shi R, Cheng JX (2005) Coherent anti-stokes Raman scattering imaging of axonal myelin in live spinal tissues. BiophysJ 89:581-591.

Wang H, Imamura Y, Ishibashi R, Chandana EP, Yamamoto M, Noda M (2010) The Reck tumor suppressor protein alleviates tissue damage and promotes functional recovery after transient cerebral ischemia in mice. J Neurochem 115:385-398.

Wang J, Zhao X, Wan YY (2023) Intricacies of TGF-β signaling in Treg and Th17 cell biology. Cell Mol Immunol 20:1002-1022.

Wang L, Geng J, Qu M, Yuan F, Wang Y, Pan J, Li Y, Ma Y, Zhou P, Zhang Z, Yang GY (2020) Oligodendrocyte precursor cells transplantation protects blood-brain barrier in a mouse model of brain ischemia via Wnt/β-catenin signaling. Cell Death Dis 11:9.

Waring MJ (1965) Complex formation between ethidium bromide and nucleic acids. J Mol Biol 13:269-282.
Waxman SG, Bennett MV (1972) Relative conduction velocities of small myelinated and non-myelinated fibres in the central nervous system. Nat New Biol 238:217-219.
Waxman SG, Ritchie JM (1993) Molecular dissection of the myelinated axon. Ann Neurol 33:121-136.
Weber F, Meinl E, Aloisi F, Nevinny-Stickel C, Albert E, Wekerle H, Hohlfeld R (1994) Human astrocytes are only partially competent antigen presenting cells. Possible implications for lesion development in multiple sclerosis. Brain 117 (Pt 1):59-69.
Wei H, Wu X, Withrow J, Cuevas-Diaz Duran R, Singh S, Chaboub LS, Rakshit J, Mejia J, Rolfe A, Herrera JJ, Horner PJ, Wu JQ (2023) Glial progenitor heterogeneity and key regulators revealed by single-cell RNA sequencing provide insight to regeneration in spinal cord injury. Cell Rep 42:112486.
Wei X, Zhang J, Gu Q, Huang M, Zhang W, Guo J, Zhou X (2017) Reciprocal Expression of IL-35 and IL-10 Defines Two Distinct Effector Treg Subsets that Are Required for Maintenance of Immune Tolerance. Cell Rep 21:1853-1869.
Welsby I, Hutin D, Gueydan C, Kruys V, Rongvaux A, Leo O (2014) PARP12, an interferon-stimulated gene involved in the control of protein translation and inflammation. J Biol Chem 289:26642-26657.
Wendimu MY, Hooks SB (2022) Microglia Phenotypes in Aging and Neurodegenerative Diseases. Cells 11.
Westerlind H, Ramanujam R, Uvehag D, Kuja-Halkola R, Boman M, Bottai M, Lichtenstein P, Hillert J (2014) Modest familial risks for multiple sclerosis: a registry-based study of the population of Sweden. Brain 137:770-778.
Wheeler MA, Jaronen M, Covacu R, Zandee SEJ, Scalisi G, Rothhammer V, Tjon EC, Chao CC, Kenison JE, Blain M, Rao VTS, Hewson P, Barroso A, Gutiérrez-Vázquez C, Prat A, Antel JP, Hauser R, Quintana FJ (2019) Environmental Control of Astrocyte Pathogenic Activities in CNS Inflammation. Cell 176:581-596.e518.
Wheeler MA et al. (2020) MAFG-driven astrocytes promote CNS inflammation. Nature 578:593-599.
White RE, Yin FQ, Jakeman LB (2008) TGF-alpha increases astrocyte invasion and promotes axonal growth into the lesion following spinal cord injury in mice. Exp Neurol 214:10-24.
Wies Mancini VSB, Di Pietro AA, Pasquini LA (2023) Microglia depletion as a therapeutic strategy: friend or foe in multiple sclerosis models? Neural Regen Res 18:267-272.
Wight TN, Kinsella MG, Evanko SP, Potter-Perigo S, Merrilees MJ (2014) Versican and the regulation of cell phenotype in disease. Biochim Biophys Acta 1840:2441-2451.
Williams KA, Deber CM (1993) The structure and function of central nervous system myelin. Crit Rev Clin Lab Sci 30:29-64.
Wlodarczyk A, Løbner M, Cédile O, Owens T (2014) Comparison of microglia and infiltrating CD11c$^+$ cells as antigen presenting cells for T cell proliferation and cytokine response. J Neuroinflammation 11:57.
Wlodarczyk A, Cédile O, Jensen KN, Jasson A, Mony JT, Khorooshi R, Owens T (2015) Pathologic and Protective Roles for Microglial Subsets and Bone Marrow- and Blood-Derived Myeloid Cells in Central Nervous System Inflammation. Front Immunol 6:463.
Wlodarczyk A, Benmamar-Badel A, Cédile O, Jensen KN, Kramer I, Elsborg NB, Owens T (2018) CSF1R Stimulation Promotes Increased Neuroprotection by CD11c+ Microglia in EAE. Front Cell Neurosci 12:523.
Wlodarczyk A, Holtman IR, Krueger M, Yogev N, Bruttger J, Khorooshi R, Benmamar-Badel A, de Boer-Bergsma JJ, Martin NA, Karram K, Kramer I, Boddeke EW, Waisman A, Eggen BJ, Owens T (2017) A novel microglial subset plays a key role in myelinogenesis in developing brain. EMBO J 36:3292-3308.
Woodruff RH, Franklin RJ (1999) Demyelination and remyelination of the caudal cerebellar peduncle of adult rats following stereotaxic injections of lysolecithin, ethidium bromide, and complement/anti-galactocerebroside: a comparative study. Glia 25:216-228.

Wu J, Sabirzhanov B, Stoica BA, Lipinski MM, Zhao Z, Zhao S, Ward N, Yang D, Faden AI (2015) Ablation of the transcription factors E2F1-2 limits neuroinflammation and associated neurological deficits after contusive spinal cord injury. Cell Cycle 14:3698-3712.
Wu YH, Ko TP, Guo RT, Hu SM, Chuang LM, Wang AH (2008) Structural basis for catalytic and inhibitory mechanisms of human prostaglandin reductase PTGR2. Structure 16:1714-1723.
Xu T, Liu C, Deng S, Gan L, Zhang Z, Yang G-Y, Tian H, Tang Y (2023) The roles of microglia and astrocytes in myelin phagocytosis in the central nervous system. Journal of Cerebral Blood Flow & Metabolism 43:325-340.
Yamagata K (2022) Lactate Supply from Astrocytes to Neurons and its Role in Ischemic Stroke-induced Neurodegeneration. Neuroscience 481:219-231.
Yamane K, Mazaki T, Shiozaki Y, Yoshida A, Shinohara K, Nakamura M, Yoshida Y, Zhou D, Kitajima T, Tanaka M, Ito Y, Ozaki T, Matsukawa A (2018) Collagen-Binding Hepatocyte Growth Factor (HGF) alone or with a Gelatin- furfurylamine Hydrogel Enhances Functional Recovery in Mice after Spinal Cord Injury. Sci Rep 8:917.
Yamasaki R et al. (2014) Differential roles of microglia and monocytes in the inflamed central nervous system. J Exp Med 211:1533-1549.
Yan Z, Dai J, Wang J, Feng Q, Wang Y, Han T, Wu C (2023) RNF167-mediated ubiquitination of Tollip inhibits TNF-α-triggered NF-κB and MAPK activation. FASEB J 37:e23089.
Yang F, Beltran-Lobo P, Sung K, Goldrick C, Croft CL, Nishimura A, Hedges E, Mahiddine F, Troakes C, Golde TE, Perez-Nievas BG, Hanger DP, Noble W, Jimenez-Sanchez M (2024) Reactive astrocytes secrete the chaperone HSPB1 to mediate neuroprotection. Sci Adv 10:eadk9884.
Yao LL, Hu JX, Li Q, Lee D, Ren X, Zhang JS, Sun D, Zhang HS, Wang YG, Mei L, Xiong WC (2020) Astrocytic neogenin/netrin-1 pathway promotes blood vessel homeostasis and function in mouse cortex. J Clin Invest 130:6490-6509.
Yeung MSY, Djelloul M, Steiner E, Bernard S, Salehpour M, Possnert G, Brundin L, Frisén J (2019) Dynamics of oligodendrocyte generation in multiple sclerosis. Nature 566:538-542.
Yi S, Jiang X, Tang X, Li Y, Xiao C, Zhang J, Zhou T (2020) IL-4 and IL-10 promotes phagocytic activity of microglia by up-regulation of TREM2. Cytotechnology 72:589-602.
Yona S, Kim KW, Wolf Y, Mildner A, Varol D, Breker M, Strauss-Ayali D, Viukov S, Guilliams M, Misharin A, Hume DA, Perlman H, Malissen B, Zelzer E, Jung S (2013) Fate mapping reveals origins and dynamics of monocytes and tissue macrophages under homeostasis. Immunity 38:79-91.
Yu Z, Sun D, Feng J, Tan W, Fang X, Zhao M, Zhao X, Pu Y, Huang A, Xiang Z, Cao L, He C (2015) MSX3 Switches Microglia Polarization and Protects from Inflammation-Induced Demyelination. J Neurosci 35:6350-6365.
Yuen TJ, Silbereis JC, Griveau A, Chang SM, Daneman R, Fancy SP, Zahed H, Maltepe E, Rowitch DH (2014) Oligodendrocyte-encoded HIF function couples postnatal myelination and white matter angiogenesis. Cell 158:383-396.
Zabala A, Vazquez-Villoldo N, Rissiek B, Gejo J, Martin A, Palomino A, Perez-Samartín A, Pulagam KR, Lukowiak M, Capetillo-Zarate E, Llop J, Magnus T, Koch-Nolte F, Rassendren F, Matute C, Domercq M (2018) P2X4 receptor controls microglia activation and favors remyelination in autoimmune encephalitis. EMBO Mol Med 10.
Zamvil SS, Mitchell DJ, Moore AC, Kitamura K, Steinman L, Rothbard JB (1986) T-cell epitope of the autoantigen myelin basic protein that induces encephalomyelitis. Nature 324:258-260.
Zanna MY, Yasmin AR, Omar AR, Arshad SS, Mariatulqabtiah AR, Nur-Fazila SH, Mahiza MIN (2021) Review of Dendritic Cells, Their Role in Clinical Immunology, and Distribution in Various Animal Species. Int J Mol Sci 22.
Zarei-Kheirabadi M, Vaccaro AR, Rahimi-Movaghar V, Kiani S, Baharvand H (2020) An Overview of Extrinsic and Intrinsic Mechanisms Involved in Astrocyte Development in the Central Nervous System. Stem Cells Dev 29:266-280.
Zarini D, Pasbakhsh P, Mojaverrostami S, Amirizadeh S, Hashemi M, Shabani M, Noshadian M, Kashani IR (2024) Microglia/macrophage polarization regulates spontaneous remyelination in intermittent cuprizone model of demyelination. Biochem Biophys Rep 37:101630.

Zawadzka M, Yeghiazaryan M, Niedziółka S, Miazga K, Kwaśniewska A, Bekisz M, Sławińska U (2022) Forced Remyelination Promotes Axon Regeneration in a Rat Model of Spinal Cord Injury. Int J Mol Sci 24.
Zawadzka M, Rivers LE, Fancy SP, Zhao C, Tripathi R, Jamen F, Young K, Goncharevich A, Pohl H, Rizzi M, Rowitch DH, Kessaris N, Suter U, Richardson WD, Franklin RJ (2010) CNS-resident glial progenitor/stem cells produce Schwann cells as well as oligodendrocytes during repair of CNS demyelination. Cell Stem Cell 6:578-590.
Zeis T, Enz L, Schaeren-Wiemers N (2016) The immunomodulatory oligodendrocyte. Brain Res 1641:139-148.
Zeng J, Wang Y, Luo Z, Chang LC, Yoo JS, Yan H, Choi Y, Xie X, Deverman BE, Gradinaru V, Gupton SL, Zlokovic BV, Zhao Z, Jung JU (2019) TRIM9-Mediated Resolution of Neuroinflammation Confers Neuroprotection upon Ischemic Stroke in Mice. Cell Rep 27:549-560.e546.
Zezula J, Casaccia-Bonnefil P, Ezhevsky SA, Osterhout DJ, Levine JM, Dowdy SF, Chao MV, Koff A (2001) p21cip1 is required for the differentiation of oligodendrocytes independently of cell cycle withdrawal. EMBO Rep 2:27-34.
Zhang S, Kim B, Zhu X, Gui X, Wang Y, Lan Z, Prabhu P, Fond K, Wang A, Guo F (2020) Glial type specific regulation of CNS angiogenesis by HIFα-activated different signaling pathways. Nat Commun 11:2027.
Zhang SZ, Wang QQ, Yang QQ, Gu HY, Yin YQ, Li YD, Hou JC, Chen R, Sun QQ, Sun YF, Hu G, Zhou JW (2019) NG2 glia regulate brain innate immunity via TGF-β2/TGFBR2 axis. BMC Med 17:204.
Zhang T, Pang W, Feng T, Guo J, Wu K, Nunez Santos M, Arthanarisami A, Nana AL, Nguyen Q, Kim PJ, Jankowsky JL, Seeley WW, Hu F (2023) TMEM106B regulates microglial proliferation and survival in response to demyelination. Sci Adv 9:eadd2676.
Zhang X, Bhattacharyya S, Kusumo H, Goodlett CR, Tobacman JK, Guizzetti M (2014) Arylsulfatase B modulates neurite outgrowth via astrocyte chondroitin-4-sulfate: dysregulation by ethanol. Glia 62:259-271.
Zhao X, Wu J, Zheng M, Gao F, Ju G (2012) Specification and maintenance of oligodendrocyte precursor cells from neural progenitor cells: involvement of microRNA-7a. Mol Biol Cell 23:2867-2878.
Zhao Z, Xue J, Zhuo Z, Zhong W, Liu H (2022) The Association of IL7R rs6897932 with Risk of Multiple Sclerosis in Southern Chinese. Neuropsychiatr Dis Treat 18:1855-1859.
Zhong JH, Zhou HJ, Tang T, Cui HJ, Yang AL, Zhang QM, Zhou JH, Zhang Q, Gong X, Zhang ZH, Mei ZG (2018) Activation of the Notch-1 signaling pathway may be involved in intracerebral hemorrhage-induced reactive astrogliosis in rats. J Neurosurg 129:732-739.
Zhou D, Lambert S, Malen PL, Carpenter S, Boland LM, Bennett V (1998) AnkyrinG is required for clustering of voltage-gated Na channels at axon initial segments and for normal action potential firing. J Cell Biol 143:1295-1304.
Zhou X, Spittau B, Krieglstein K (2012) TGFβ signalling plays an important role in IL4-induced alternative activation of microglia. J Neuroinflammation 9:210.
Zhou X, Zhu Y, Gao D, Li M, Lin L, Wang Z, Du H, Xu Y, Liu J, He Y, Guo Y, Wang S, Qiao S, Bao Y, Liu Y, Zhang H (2024) Matrilin-3 supports neuroprotection in ischemic stroke by suppressing astrocyte-mediated neuroinflammation. Cell Rep 43:113980.
Zhu Q, Tan Z, Zhao S, Huang H, Zhao X, Hu X, Zhang Y, Shields CB, Uetani N, Qiu M (2015) Developmental expression and function analysis of protein tyrosine phosphatase receptor type D in oligodendrocyte myelination. Neuroscience 308:106-114.
Zhu Q, Enkhjargal B, Huang L, Zhang T, Sun C, Xie Z, Wu P, Mo J, Tang J, Zhang JH (2018) Aggf1 attenuates neuroinflammation and BBB disruption via PI3K/Akt/NF-κB pathway after subarachnoid hemorrhage in rats. J Neuroinflammation 15:178.
Zhu X, Li H, You W, Yu Z, Wang Z, Shen H, Li X, Yu H, Chen G (2022) Role of Rph3A in brain injury induced by experimental cerebral ischemia-reperfusion model in rats. CNS Neurosci Ther 28:1124-1138.
Zia S, Hammond BP, Zirngibl M, Sizov A, Baaklini CS, Panda SP, Ho MFS, Lee KV, Mainali A, Burr MK, Williams S, Caprariello AV, Power C, Simmen T, Kerr BJ, Plemel JR (2022)

Single-cell microglial transcriptomics during demyelination defines a microglial state required for lytic carcass clearance. Mol Neurodegener 17:82.
Zoecklein LJ, Pavelko KD, Gamez J, Papke L, McGavern DB, Ure DR, Njenga MK, Johnson AJ, Nakane S, Rodriguez M (2003) Direct comparison of demyelinating disease induced by the Daniel's strain and BeAn strain of Theiler's murine encephalomyelitis virus. Brain Pathol 13:291-308.
Zong X, Li Y, Liu C, Qi W, Han D, Tucker L, Dong Y, Hu S, Yan X, Zhang Q (2020) Theta-burst transcranial magnetic stimulation promotes stroke recovery by vascular protection and neovascularization. Theranostics 10:12090-12110.
Zou LH, Shi YJ, He H, Jiang SM, Huo FF, Wang XM, Wu F, Ma L (2019) Effects of FGF2/FGFR1 Pathway on Expression of A1 Astrocytes After Infrasound Exposure. Front Neurosci 13:429.
Zuchero JB, Barres BA (2015) Glia in mammalian development and disease. Development 142:3805-3809.
Zuiderwijk-Sick EA, van der Putten C, Timmerman R, Veth J, Pasini EM, van Straalen L, van der Valk P, Amor S, Bajramovic JJ (2021) Exposure of Microglia to Interleukin-4 Represses NF-κB-Dependent Transcription of Toll-Like Receptor-Induced Cytokines. Front Immunol 12:771453.
Zukor K, Belin S, Wang C, Keelan N, Wang X, He Z (2013) Short hairpin RNA against PTEN enhances regenerative growth of corticospinal tract axons after spinal cord injury. J Neurosci 33:15350-15361.
Zweifel S, Marcy G, Lo Guidice Q, Li D, Heinrich C, Azim K, Raineteau O (2018) HOPX Defines Heterogeneity of Postnatal Subventricular Zone Neural Stem Cells. Stem Cell Reports 11:770-783.

ACKNOWLEDGEMENT

Firstly, I would like to express my gratitude to my both supervisors, Prof. Dr. Frank Kirchhoff and Dr. Franck Debarbieux, for welcoming me into your groups to carry out this exciting PhD project. Your mentorship has been a constant source of challenge and motivation throughout this scientific journey.

I would like to thank the ARSEP foundation (grant agreement No. 1248) for funding this project.

Thank you to all the current and former members of the Kirchhoff group, and those who briefly joined us. I thank as well the former “Imapathiens”, of which I was once a part. You brightened my days in the lab, and I will always cherish the great moments we shared.

I would also express my warm thanks to both of my PhD co-supervisors, Dr. Anja Scheller and Dr. Bilal El Waly. Anja, thank you for your constant support in all situations, your precious advice, and your unwavering availability throughout these years. And to you, Bilal, thank you for sharing and teaching me your knowledge, curiosity, and scientific rigor. Thank you for your friendship, you have been an ally in the face of adversity.

My appreciation goes also to Wenhui Huang and Xianshu Bai for the discussion and help you were always ready to give. Thank you to Qilin Guo for your valuable training at the bench and your assistance whenever I needed it. Thank you to Thomas Hentrich for his collaboration on the sequencing data. Your good vibes and availability were highly appreciated.

Thank you to my colleagues that made my daily life much more pleasant over the years. Lipao Fang, you were a desk’s neighbor always full of positivity (and music!); Liu Qing, to all our late hours in the lab, I'll miss your company and our discussions (and potato salad!); Gebhard Stopper, I won't forget your attentive ear over a coffee, your advice and the help you always offered me (and ginger snacks!); Mariza Bortolanza and Naielly Rodrigues da Silva, thank you for the Brazilian’s mood and all the good times we spent together. Davide and Phillip, thank you for our infernal trio “the Dream team”, all our laughs and discussions, you brought light and joy even on tough days. Your friendship was a blessing throughout this chapter of my life! Florence et Aurélie, merci pour votre soutien constant, les repas du mercredi midi et nos appels en visio. Je suis reconnaissante d'avoir pu vous compter à mes côtés durant cette aventure.

I would also like to thank all the other members of both groups whom I had the chance to know and work with, including Rhea Seth, Frank Rhode, Daniel Schauenburg, Ute Legler, Laura Stopper, Elisa Damo, and Marion Compagnone.

A very special thank you goes my German landlords, Carla and Peter, and their daughters, for welcoming me into your family. Thank you for the tomato spirit, the dinners, the walks and

everything we shared. You took such good care of me, and I will never forget these moments that mean so much to me.

Merci à mes plus proches amis pour votre soutien inestimable durant cette période. Merci à toi, Leif, pour tes visites Toulousaines qui m'auront tant remonté le moral ; à toi, Axelle, merci pour toutes nos discussions quotidiennes et tes encouragements. La vie aura fait de nous bien plus que des amies.

Enfin, j'adresse mes plus chaleureux remerciements à ma famille, pour leur amour et leur indéfectible soutien durant toutes ces années. Merci pour tous vos encouragements, d'avoir toujours été présents dans les bons comme les mauvais moments, et ceux parti trop tôt – Papis, je sais votre fierté à me voir me voir réussir cette folle aventure. A mes parents, pour avoir toujours cru en moi ; papa, merci de m'avoir poussée à persévérer dans la difficulté et de toujours avoir eu un moment à m'accorder pour discuter et me remonter le moral ; maman, merci pour ton amour inconditionnel qui m'aura tant portée, merci de ton abnégation sans borne pour ma réussite, et pour tout ce que tu continues de faire pour moi et ma famille. Tu es mon essentielle.

A toi Christophe, ma paupiette, mon âme-sœur, merci d'avoir traversé tout cela avec moi, de ne jamais avoir lâché ma main, même dans les moments les plus sombres. Merci pour ta résilience et ton amour. Merci d'être l'un des piliers les plus importants de mon existence, merci de m'avoir offert le plus beau rôle de ma vie avec notre fils. Merci pour tout. Je t'aime au-delà des mots.

CURICULUM VITAE AND LIST OF PUBLICATIONS

The curriculum vitae was removed from the electronic version of the doctoral thesis for reasons of data protection.

PUBLICATIONS

D Gobbo, P Rieder, LP Fang, **E Buttigieg**, M Schablowski, E Damo, N Bosche, E Dallorto, P May, X Bai, F Kirchhoff, A Scheller (**2024**). Genetic ablation of $GABA_B$ receptors from oligodendrocyte precursor cells protects against demyelination in the mouse spinal cord. bioRxiv 2024.05.29.596385; doi: https://doi.org/10.1101/2024.05.29.596385

Buttigieg E, Scheller A, El Waly B, Kirchhoff F, Debarbieux F (**2023**). Contribution of Intravital Neuroimaging to Study Animal Models of Multiple Sclerosis. Neurotherapeutics. 20(1):22-38. doi: 10.1007/s13311-022-01324-6. Epub 2023 Jan 18. PMID: 36653665; PMCID: PMC10119369.

El Waly B, **Buttigieg E**, Karakus C, Brustlein S, Debarbieux F. Longitudinal Intravital Microscopy Reveals Axon Degeneration Concomitant With Inflammatory Cell Infiltration in an LPC Model of Demyelination (**2020**). Front Cell Neurosci. 23;14:165. doi: 10.3389/fncel.2020.00165. PMID: 32655371; PMCID: PMC7324938.

Choquet C, Nguyen THM, Sicard P, **Buttigieg E**, Tran TT, Kober F, Varlet I, Sturny R, Costa MW, Harvey RP, Nguyen C, Rihet P, Richard S, Bernard M, Kelly RG, Lalevée N, Miquerol L (**2018**). Correction: Deletion of Nkx2-5 in trabecular myocardium reveals the developmental origins of pathological heterogeneity associated with ventricular non-compaction cardiomyopathy. PLoS Genet. 15;14(8):e1007610. doi: 10.1371/journal.pgen.1007610. Erratum for: PLoS Genet. 6;14(7):e1007502. doi: 10.1371/journal.pgen.1007502. PMID: 30110325; PMCID: PMC6093597.